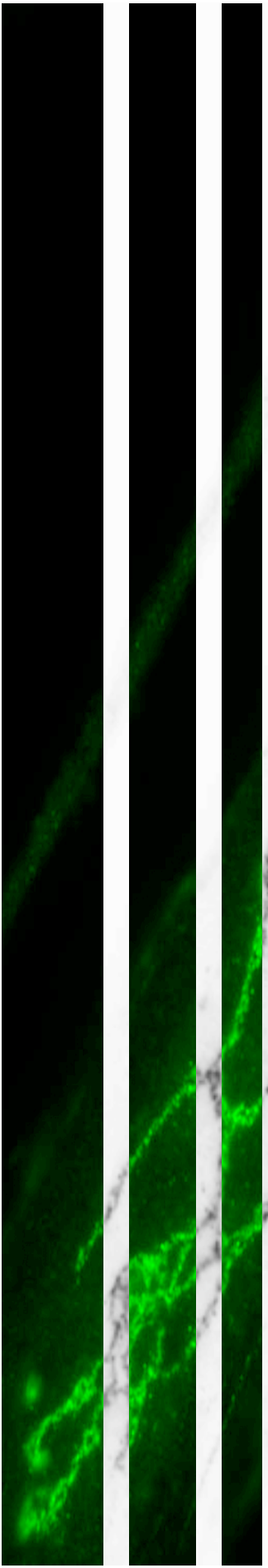

Mário Nôro Laço

Studies on the activity of ataxin-3 and mitochondrial dysfunction in models of Machado-Joseph disease

· U C ·

FMUC FACULDADE DE MEDICINA
UNIVERSIDADE DE COIMBRA

Studies on the activity of ataxin-3 and mitochondrial dysfunction in models of Machado-Joseph disease

Mário Nôro Laço

Universidade de Coimbra

2012

Studies on the activity of ataxin-3 and mitochondrial dysfunction in models of Machado-Joseph disease

Mário Nôro Laço

Dissertation submitted to the Faculty of Medicine of the University of Coimbra, in partial fulfillment of the requirements for the Degree of Doctor in Biomedical Sciences.

Dissertação apresentada à Faculdade de Medicina da Universidade de Coimbra, para prestação de provas de doutoramento em Ciências Biomédicas.

Universidade de Coimbra

2012

Studies on the activity of ataxin-3 and mitochondrial dysfunction in models of Machado-Joseph disease

Mário Nôro Laço

The research and scientific work presented in this thesis was preformed at the Center for Neurosciences and Cell Biology, University of Coimbra, Coimbra, Portugal and at the Paulson Lab, Roy J. and Lucille A. Carver College of Medicine, University of Iowa, Iowa City, Iowa, IA, U.S.A., under the advisorship of Prof. Ana Cristina Rego, Ph.D. and Dr. Henry Paulson, M.D., Ph.D..

A pesquisa e trabalho científicos apresentados neste tese foram efectuados no Centro de Neurociências e Biologia Celular, Universidade de Coimbra, Coimbra, Portugal e no Paulson Lab, Roy J. and Lucille A. Carver College of Medicine, University of Iowa, Iowa City, Iowa, IA, U.S.A., sob a orientação do Professora Doutora Ana Cristina Rego e do Doutor Henry Paulson.

This work was partially funded by the Portuguese Foundation for Science and Technology, under the POCTI program (Ph.D. Fellowship SFRH/BD/17275/2004).

Este trabalho foi parcialmente financiado pela Fundação para a Ciência e a Tecnologia, através do programa POCTI (bolsa de doutoramento com a referência SFRH/BD/17275/2004).

FCT Fundação para a Ciência e a Tecnologia
MINISTÉRIO DA EDUCAÇÃO E CIÊNCIA

POPH
PROGRAMA OPERACIONAL POTENCIAL HUMANO

UNIÃO EUROPEIA
Fundo Social Europeu

Universidade de Coimbra

2012

Cover art:

Fluorescence microscopy image of normal human fibroblasts fixed and immunostained for endogenous ataxin-3, with rabbit polyclonal anti-ataxin-3 primary antibody (MJD; 1:1000) and anti-rabbit Alexa-fluor 488 secondary antibody (1:250; Molecular Probes, USA). The fluorescent signal highlights an intracellular structure, possibly an intracellular organelle (e.g., endoplasmic reticulum), which was not positively identified. A reminder of everything that is still to be discovered about ataxin-3 protein.

To my mother and my father.

À minha mãe e ao meu pai.

“sed etiam si cecidit de genu pugnat”

“but even he fell, he fights on his knees”

“e mesmo que caia, ele combate de joelhos”

(Lucius Annaeus Seneca, De Providentia, II, 6)

Acknowledgements

A work in science rarely results from the action of one individual. This thesis is no exception. During the production of the scientific data presented in this dissertation, I had the privilege to meet, establish relationships and learn with a group of unforgettable people. They will always be remembered for their knowledge, enthusiasm, inspiring drive and dedication to science, but also for their personality, friendship and support. All of them contributed to my personal and scientific growth and directly or indirectly helped me in the conclusion of this important step of my academic career and personal life.

None of this would have even started, if Professor Ana Cristina Rego had not accepted me in her research group and fully supported my project. I want to thank her for her advice, promptitude, interest, constant demand for well-designed, well-planned, robust results, in order to get out the best quality of my scientific work. I also want to acknowledge her for the critical judgment and contribution in the writing and proofreading of this thesis. I will always be thankful for her trust and her personal, scientific and academic support of my work throughout these last years.

An important part of my research was performed in the laboratory of Dr. Henry L. Paulson at the Carver College of Medicine, Iowa City, Iowa, U.S.A.. I want to thank Hank for accepting me in his lab and for the extraordinary welcoming reception I received from him and all the lab personnel, since the first day. The Paulson lab revealed to be an excellent incubator and a cornerstone period for the development and maturation of my scientific and critical judgment. My evolution as a researcher was exponential. I will keep Hank's teachings on how to make and behave in science throughout my scientific and academic progression. I am aware that without this period in Iowa and all I learnt from it, I would have never achieved the same competence as a worker and a thinker in science.

I want to express my gratitude to Professor Catarina Resende de Oliveira for allowing me to develop my work at the institution she presides, the Center for Neurosciences and Cell Biology of Coimbra, but also for being a role model as a researcher and a mode of behavior in science.

I want to acknowledge Professor Ana Luísa Carvalho for her advice and her help in my first steps of my scientific work, specifically in molecular biology techniques.

The best memories are undoubtedly associated with the members of the mitochondrial dysfunction and signaling in neurodegeneration group. Some of them have already left the group and have scattered around the world to pursue their scientific questions, but even so, I want to thank all of them for their friendship, fellowship, scientific discussions, good spirit and support, namely to Sandra Almeida, António Domingues, Ildete Ferreira, Márcio Ribeiro, Tatiana Rosenstock, Sandra Mota, Teresa Oliveira, among many others who have joined and will continue to join our research group to give their first steps in research. Catarina Oliveira, Ana Cristina Silva and Rita Perfeito deserve a special mention, as we have initiated this adventure at the same time and have shared joys, laughs, sadness, demoralization after bad results and supported each other in bad times, to push our work forward without giving up. Thank you for providing the best working environment, and proving that great research and having fun are not incompatible.

I could not left all the members and friends at the Paulson lab with a proper acknowledgement. They received me with open arms, cherished me as if I was a group member, helped me in my research and made me feel at home, when I was thousands of miles away from my departure. Thank you, Tina Knutson, Cynthia Gouvion, Hsiang Wen, Brett Winborn, Ginny Harris, a big kiss to Aislinn Williams and a big hug to Sokol Todi.

Continuing on good friendships in working enviroments, I would like to send big kisses to Luisa Cortes, Isabel Nunes, Isabel Dantas and Teresa Girão, not only for their prompt and ever available technical support, but mainly for their friendship, care, for all the coffees, talks and lunches at the CNC library.

A big thanks and kiss to madames Isabéis, for all the washing, sterilizing, coping with the awful smell of my solutions and for the good spirit and great laughs.

I want to acknowledge Foundation for Science and Technology for providing me the possibility to develop my scientific and academic potential.

Finally, my nuclear core of friends, where those not familiar with lab environment and research fused with the ones sharing the bench with me. To all of them; older friends that Coimbra introduced me very long ago, Sandra, Cristina, Jorge, Raquel; the ones I have added to my life more recently and are outsiders to the world of experiments, Pedro, Armanda, Max, Regina, Magda, Xana, Filipe, André, Yara, Luís, Carlos, Cláudia; among many others that I am certainly and unfairly forgetting to mention; an enormous thank you for putting up with my complains, for listening to my sorrows, for pulling me out of the world of hypothesis and results once in a while, and for keeping me connected to the outside world, from where scientific questions should be raised and to where conclusions should head to. Thank you for your friendship!

My biggest acknowledgement goes to my family, from closer relatives to distant cousins. All have listen to my frustrations, my disappointments at some moment, but they always had a word of comprehension and encouragement, and the patience to hear me in my somewhat long and enthusiastic talks about my work.

To my mother and my father, I owe almost everything. I owe them my origin, growth, development, support, friendship, recognition and pride. I am an extension of themselves and consequently, their contribution is dissipated in every page of this work.

This thesis is dedicated to all of you.

Agradecimentos

Em ciência, raramente uma obra é o resultado da ação de apenas um indivíduo. Esta tese não é exceção. Ao longo dos anos de trabalho de investigação para a preparação desta dissertação, tive o privilégio de contactar, conhecer, aprender e estabelecer relações com pessoas inesquecíveis, quer pelo seu conhecimento, entusiasmo, inspiração e dedicação à ciência, como pela sua personalidade, amizade e apoio. Todas elas contribuíram para a minha evolução científica e pessoal até ao indivíduo que sou hoje e ajudaram, directa ou indirectamente, na conclusão desta etapa da minha carreira académica e da minha vida.

Nada teria início, se a Professora Doutora Ana Cristina Rego não me tivesse aceite no seu grupo de investigação e apostado neste projecto. Quero deixar o meu apreço pela sua orientação, disponibilidade, cuidado, interesse e exigência constantes na obtenção de resultados de qualidade, fidedignos e bem estruturados ao longo de todo o trabalho científico. Agradeço ainda a sua contribuição e juízo crítico ao longo da redação e correção desta tese. Estarei sempre agradecido pela confiança depositada em mim e pelo apoio pessoal, científico e académico prestado ao longo de todos estes anos.

Uma importante parte do trabalho de investigação foi realizado no laboratório do Doutor Henry L. Paulson, no Carver College of Medicine, em Iowa City, Iowa, Estados Unidos da América. Ficarei sempre grato ao Hank por concordar com a minha estadia e pela extraordinária receção demonstrada por todo o pessoal do seu laboratório. O Paulson Lab revelou-se uma incubadora ideal e uma fase fulcral para o desenvolvimento e nutrição do meu juízo crítico e científico. O meu crescimento enquanto investigador foi exponencial durante este período. Os ensinamentos transmitidos pelo Hank sobre como fazer e estar em ciência acompanhar-me-ão ao longo de todo o meu percurso científico e académico. Estou consciente, que sem esta

estadia e com toda a aprendizagem que ela me proporcionou, não teria a mesma qualidade enquanto trabalhador e pensador de ciência.

Um agradecimento especial à Professora Doutora Catarina Resende de Oliveira, não só por permitir o desenvolvimento do meu trabalho científico na instituição que preside, o Centro de Neurociências e Biologia Celular de Coimbra, mas por ser um modelo a seguir enquanto investigador e como forma de estar em ciência.

Quero deixar o meu apreço à Professora Doutora Ana Luísa Carvalho, por me ter orientado e ajudado nas primeiras fases do meu trabalho científico, introduzindo-me às técnicas de biologia molecular.

Contudo, as melhores memórias estão associadas sem dúvida aos elementos do grupo de disfunção mitocondrial e sinalização em neurodegenerescência. Alguns deles já se dispersaram pelo mundo para continuarem a responder às suas questões científicas, mas a todos eles quero agradecer a amizade, o companheirismo, a discussão científica, a boa disposição e a ajuda, especialmente à Sandra Almeida, ao António Domingues, à Ildete Ferreira, ao Márcio Ribeiro, à Tatiana Rosenstock, à Sandra Mota, à Teresa Oliveira, entre muitos outros que passaram e continuam a passar no nosso grupo, dando os primeiros passos em investigação científica. A Catarina Oliveira, a Ana Cristina Silva e a Rita Perfeito merecem uma menção especial por termos enfrentado esta fase das nossas vidas em conjunto, partilhando as alegrias, as gargalhadas, as tristezas, o desânimo dos maus resultados, apoiando-nos uns nos outros para continuar a avançar e nunca desistir. Obrigado por proporcionarem o melhor ambiente de trabalho, mostrando que é possível fazer boa investigação, divertindo-nos.

Não posso deixar de agradecer a todos os colegas e amigos do Paulson Lab. Receberam-me de braços abertos, acarinharam-me como um membro do grupo, ajudaram no meu trabalho e fizeram-me sentir em casa, ainda que a milhares de quilómetros do meu ponto de partida. Um obrigado a Tina Knutson, Cynthia Gouvion, Hsiang Wen, Brett Winborn, Ginny Harris, um beijo especial para Aislinn Williams e um grande abraço para Sokol Todi.

Continuando nas grandes amizades em ambiente de trabalho, não posso deixar de enviar um beijo grande à Luísa Cortes, à Isabel Nunes, à Isabel Dantas e à Teresa Girão, não só pelo apoio técnico, sempre prestável e disponível, mas

principalmente pela amizade, a preocupação, pelos cafés, pelas conversas e pelos almoços na biblioteca.

Um obrigado e um beijo repenicado às donas Isabéis da sala de lavagens, pelas autoclavagens, por suportarem os odores nauseabundos das minhas soluções e mais ainda, pela boa disposição e as risadas fartas.

Um agradecimento à Fundação para a Ciência e a Tecnologia que me proporcionou a possibilidade de expandir o meu potencial académico e científico.

Finalmente, o meu núcleo duro de amigos, alguns fora do ambiente de laboratório e que se fundem com os que partilham as bancadas comigo. A todos vocês; desde os mais antigos, que Coimbra me ofereceu logo desde cedo, Sandra, Cristina, Jorge, Raquel; até aos que partilham a minha vida mais recentemente e fora do mundo das experiências Pedro, Armanda, Max, Regina, Magda, Xana, Filipe, André, Yara, Luís, Carlos, Cláudia; entre muitos outros, que certamente e injustamente me estou a esquecer; um enorme obrigado por aturarem as minhas queixas, por ouvirem os meus lamentos, por me fazerem esquecer o mundo das hipóteses e dos resultados, por me manterem ligado ao mundo exterior donde as questões científicas provêm e para onde as conclusões se devem dirigir. Obrigado pela amizade!

O meu maior agradecimento vai para a minha família, tanto a mais próxima, como a mais afastada. Todos eles ouviram as minhas frustrações, desilusões, com maior ou menor frequência, mas tiveram sempre uma palavra de alento, de compreensão e mostraram paciência para me ouvir, mesmo nos momentos em que falava abundantemente e cheio de entusiasmo.

À minha mãe e ao meu pai, devo quase tudo. Devo-lhes a minha origem, o meu desenvolvimento, o meu crescimento, o apoio, a amizade, o reconhecimento e o orgulho. Sou uma extensão deles e consequentemente, a sua contribuição dissolve-se em cada página deste trabalho.

Esta tese é para todos vós.

Table of contents

Abbreviations

ADP	Adenosine diphosphate
AMP	Adenosine monophosphate
ANOVA	Two-way analysis of variance
Apaf-1	Apoptotic peptidase activating factor 1
Asp	Aspartic acid
ATG	Autophagy-related gene
ATP	Adenosine triphosphate
BDNF	Brain-derived neurotrophic factor
C	Cysteine
Ca^{2+}	Calcium
$CACNA1_A$	Calcium channel, voltage-dependent, P/Q type, alpha 1A subunit
CAG	Cytosine-adenine-guanine
cAMP	Cyclic adenosine monophosphate
cDNA	Complementary deoxyribonucleic acid
CHIP	C-terminus of 70 kDa heat shock protein (Hsp70)-interacting protein
CMA	Chaperone-mediated autophagy
CMV	Cytomegalovirus
CNS	Central Nervous System
CREB	cAMP response element-binding protein
CBP	CREB-binding protein
DCPIP	6,6-dichlorophenolindophenol
DM1	Myotonic dystrophy type 1

DM2	Myotonic dystrophy type 2
DMEM	Dulbecco's modified Eagle's medium
DNA	Deoxyribonucleic acid
DRPLA	Dentatorubral-pallidoluysian atrophy
DTT	1,4-dithiothreitol
DUB	Deubiquitinating enzyme
E4b	Ubiquitin conjugation factor b
EDTA	Ethylenediamine tetraacetic acid
EGFP	Enhanced green fluorescent protein
ER	Endoplasmic reticulum
ERAD	Endoplasmic reticulum associated degradation
FDG	Fluorine-18-fluorodeoxyglucose
18F-Dopa	Fluorine-18-L-dihydroxyphenylalanine
FBS	Fetal bovine serum
FMR	Fragile X mental retardation
FRDA	Friedreich's ataxia
GAPDH	Glyceraldehyde-3-phosphate dehydrogenase
gp78	E3 ubiquitin-protein ligase AMFR
GST	Glutathione-S-transferase
H	Histidine
HD	Huntington's disease
HDAC	Histone deacetylase
HEK	Human embryonic kidney
Hip-1	Huntingtin-interacting protein 1
hHR23A/hHR23B	Human homologs of yeast Rad23 protein
Hrd1	HMG-coA reductase degradation protein 1
HSP	Heat-shock protein
HSP70	Heat-shock protein 70
IP3	Inositol-(1,4,5) triphosphate
JAMM	JAB1/MPN/Mov34 metalloenzyme
K	Lysine

LB	Luria Bertani medium
LDH	Lactate dehydrogenase
MAP	Mitogen-activated protein
MAP-2	Microtubule associated protein 2
MITOL	Mitochondrial ubiquitin ligase
mRNA	Messenger ribonucleic acid
miRNA	Micro ribonucleic acid
MJD	Machado-Joseph disease
MPT	Mitochondrial permeability transition
MRI	Magnetic resonance imaging
MTT	3-[4-5-dimethylthiazol-2-]-2,5-diphenyltetrazolium bromide
N	Asparagine
NADH	Reduced nicotinamide adenine dinucleotide
N-Cor	Nuclear receptor co-repressor
NEDD8	Neural precursor cell expressed developmentally downregulated 8
NES	Nuclear export signal
NGF	Nerve growth factor
NLS	Nuclear localization signal
NMDA	*N*-methyl-D-aspartate
NMR	Nuclear magnetic resonance
3-NP	3-Nitropropionic acid
OTU	Ovarian tumor proteases
PCAF	p300/CBP-associated factor
p53	Tumor protein 53
PAGE	Polyacrilamide gel electrophoresis
PBS	Phosphate buffered solution

PBT	Phosphate-buffered saline plus 0.1% (vol/vol) Triton X-100
PCR	Polymerase chain reaction
PET	Positron emission tomography
PFA	Paraformaldehyde
PGC-1α	Peroxisome proliferator-activated receptor γ coactivator-1
PICK1	Protein interacting with C kinase 1
PML	Promyelocytic leukemia protein
polyQ	Polyglutamine
PPP2R2B	Protein phosphatase 2, regulatory subunit B, beta isoform
PQBP1	Polyubiquitin-binding protein 1
Q	Glutamine
REM	Rapid eye movement
RNA	Ribonucleic acid
RNAi	Ribonucleic acid interference
ROS	Reactive oxygen species
RPMI	Roswell Park Memorial Institute's medium
SBMA	Spinal bulbar muscular atrophy
SCA	Spinocerebellar ataxia
SCA3	Spinocerebellar ataxia type 3
SDS	Sodium dodecyl sulfate
SENP	SUMO-sentrin specific protease
siRNA	Small interfering RNA
Sp1	Specificity protein 1
SPECT	Single-photon emission computed tomography
SUMO	Small ubiquitin-like modifier
TAFII130	TAF4 RNA polymerase II, TBP-associated factor, 135kDa
TBP	TATA box binding protein

TTFA	Thenoyltrifluoroaceton
UBA	Ubiquitin-associated domains
UBL	Ubiquitin-like domain
UCH	Ubiquitin C-terminal hydrolases
UIM	Ubiquitin-interacting motif
ULP	Ubiquitin-like proteases
UPP	Ubiquitin-proteasome pathway
UPS	Ubiquitin-proteasome system
USP/UBP	Ubiquitin-specific processing proteases
VCP/p97	Valosin-containing protein/protein 97
XPC	Xeroderma pigmentosum group C
YAC	Yeast artificial chromosome

Publications

The results presented and discussed in this thesis are all published in peer-reviewed international scientific journals, as follows:

1) Laço M.N., Cortes L., Travis S.M., Paulson H.L., Rego A.C. (2012) Valosin-containing protein (VCP/p97) is an activator of wild-type ataxin-3. *PLoS One* 7(9):e43563.

2) Todi S.V.; Laco M.N.; Winborn B.J.; Travis S.M.; Wen H.M.; Paulson H.L. (2007) Cellular turnover of the polyglutamine disease protein ataxin-3 is regulated by its catalytic activity. *J. Biol. Chem.* 282(40):29348-58.

3) Laço M.N.; Oliveira C.R.; Paulson H.L.; Rego A.C. (2012) Compromised mitochondrial complex II in models of Machado-Joseph disease. *Biochim. Biophys. Acta*. 1822(2):139-149

Summary

Machado-Joseph disease (MJD), also known as spinocerebellar ataxia type 3 (SCA3) is an autosomal, dominant, hereditary neurodegenerative disorder and the most common cause of autosomal inherited ataxia in the world. The first symptoms of MJD usually become apparent in adulthood, around the third or fourth decade of life, although in severe cases, the onset may occur even in childhood. MJD patients exhibit a variety of phenotypes, in a wide combination of motor and non-motor symptoms. Ataxia and gait impairment are the main and primary manifestations of this neurological disorder, associated to a variable degree of oculomotor deficits, dysarthria, pyramidal signs, progressive sensory loss and parkinsonism. Symptoms progressively worsen through the course of the disease until patient's death, 20 or 30 years after the first symptoms.

MJD belongs to the polyglutamine (polyQ) expansion disorders, a group of nine neurological pathologies caused by a dynamic mutation, an expansion in the number of CAG trinucleotide repeats. In MJD, the CAG expansion is present on exon 10 of the MJD1 gene, which codes for the deubiquitinating enzyme, ataxin-3. The onset of MJD symptoms occurs when the CAG expansion extends beyond 52 repeats. The CAG expansion is translated into an expanded polyQ domain within the C-terminus of ataxin-3. A pathological polyQ expansion destabilizes ataxin-3 structure, promotes its misfolding and aggregation and bestows the protein with new toxic properties, which lead to neuronal dysfunction, and consequent neurodegeneration. Although both wild-type and pathological expanded ataxin-3 are expressed throughout all tissues of the body, degeneration occurs only in particular regions of the central nervous system (CNS). Subcortical regions as the pontine nuclei, the dentate nucleus, subthalamic nucleus and the spinal cord are among the most affected. The reasons for

this pattern of neurodegeneration and the specific susceptibility of these neurons to expanded ataxin-3 are still not understood.

Ataxin-3 is a 42kDa intracellular protein with ability to bind and cleave polyubiquitin chains, and currently, it is classified as deubiquitinating enzyme of the Josephin domain proteases class. Ataxin-3 has higher affinity for long ubiquitin chains, with more than four ubiquitin moieties, and a catalytic preference for lysine 63 (K63) mediated linkages between two ubiquitin molecules. Ataxin-3 is regulated by monoubiquitination and phosphorylation events, which determine its activity and intracellular localization. The biological role of ataxin-3 is not entirely clarified. It is suggested that ataxin-3 acts as an ubiquitin chain editing enzyme and it has been implicated in ubiquitin-proteasome pathways, endoplasmic reticulum associated degradation, the cytoprotective response to heat shock stress and in the determination of *Caenorhabditis elegans* longevity. The implication in a multitude of pathways is coupled to a growing number of proteins found to interact with ataxin-3. Recent ataxin-3 interactors have been added to the previously known p97/valosin-containing protein (VCP/p97) and hHR23A/hHR23B (human homologs of yeast Rad23 protein), namely tubulin, microtubule-associated protein 2 (MAP2), dynein, histone deacetylase (HDAC) 6, several transcriptional activators/repressors and parkin. Some interactions are specific of wild-type and are disrupted by the expanded polyQ domain, while others only occur for expanded ataxin-3.

In vitro studies have not found significant differences between the activity of human wild-type and expanded ataxin-3. Therefore, it was a logical step to investigate the role of protein interactions in ataxin-3 activity and how the deubiquitinating activity influences ataxin-3 properties in the cell. Moreover, it was crucial to clarify the contribution of these features and the involvement of mitochondrial dysfunction in the pathogenesis of MJD. To achieve these goals, we performed *in vitro* deubiquitinating studies with wild-type and expanded ataxin-3 in the absence or presence of well-established protein interactors and used several MJD cell and animal models to evaluate expanded ataxin-3 toxicity, particularly focusing on mitochondrial dysfunction, a pathological mechanism shared by several polyQ diseases.

In Chapter 2, the effect of two well-known ataxin-3-interacting proteins, hHR23A and VCP/p97, was investigated over the deubiquitinating activity of ataxin-3. Endogenous hHR23A and endogenous ataxin-3 were predominantly located in the nucleus, whereas endogenous VCP/p97 was more abundant in the cytoplasm. The interactions of VCP/p97 and hHR23A with ataxin-3 were corroborated, despite the differences in intracellular localization and the assembly of a trimolecular complex containing the three endogenous proteins was observed. VCP/p97 and hHR23A interactions with ataxin-3 were also established in *in vitro* conditions. Human recombinant hHR23A, VCP/p97, wild-type and expanded ataxin-3 were purified and subsequently used in *in vitro* deubiquitinating assays to assess the influence of hHR23A and VCP/p97 on ataxin-3 activity. Ataxin-3 exhibited a slow rate of enzymatic activity and a catalytic preference for lysine-63 (K63)-linked polyubiquitin chains. Addition of hHR23A to the *in vitro* assays did not alter ataxin-3 kinetics or substrate preference. On the contrary, the presence of VCP/p97 was able to increase specifically wild-type ataxin-3 performance *in vitro*. Interestingly, this *in vitro* VCP/p97-mediated activation was not detected for expanded ataxin-3.

In Chapter 3, fully active and catalytically inactive ataxin-3 were expressed in cells and used in *in vitro* assays to continue the study of ataxin-3 activity, focused on the influence of catalytic activity over ataxin-3 cellular behavior. Inactive ataxin-3 displayed higher protein levels in comparison to active ataxin-3 due partially to a slower degradation rate of catalytically inactive ataxin-3. Intriguingly, inactive ataxin-3 was more heavily ubiquitinated in the cell than its active counterpart. Despite the higher level of ubiquitination, a slower proteasomal degradation rate for inactive ataxin-3 was determined through *in vitro* studies. The lower proteasomal degradation was correlated with a reduced interaction of catalytically inactive ataxin-3 with VCP/p97, a protein known for shuttling substrates to the proteasome. Ataxin-3 did not interact directly with the proteasome or any of its subunits; however, ataxin-3 and the proteasome were shown to colocalize in discrete subnuclear foci. Interestingly, inactive ataxin-3 exhibited less nuclear colocalization with the proteasome and a diminished localization in the nuclear compartment. Overall, the enzymatic activity of ataxin-3

was shown to modulate its cellular turnover, intracellular localization and the level of ubiquitination.

In Chapter 4, several cell and animal models of MJD were analyzed to evaluate the contribution of mitochondrial dysfunction in MJD pathology. HEK cells transiently transfected with expanded (Q84) enhanced green fluorescent protein (EGFP)-ataxin-3 fusion protein were more susceptible to inhibition of mitochondrial complex II with 3-nitropropionic (3-NP) than HEK cells expressing wild-type (Q28) EGFP-ataxin-3. Similarly, stably transfected rat pheochromocytoma (PC6-3) cell line expressing expanded (Q108) human ataxin-3, in a tetracycline-regulated manner, also displayed a higher susceptibility to 3-NP inhibition than PC6-3 cells expressing the wild-type (Q28) protein. Primary cerebellar granule cells isolated from MJD transgenic mice exhibited the same trend. A higher vulnerability to 3-NP was observed for the transgenic cerebellar granule cells when compared to wild-type cerebellar neurons. Moreover, mitochondria from MJD transgenic mouse brains and lymphoblast cell lines derived from MJD patients showed a tendency towards a reduction in mitochondrial complex II activity. The reduction in complex II activity was even more evident, and statistically significant, in mitochondria of PC6-3 (Q108) cells, stimulated into a neuronal-like phenotype with nerve growth factor (NGF).

In conclusion, a functional ubiquitin protease capability determines more cellular properties of ataxin-3 than exclusively its DUB activity, influencing the turnover and intracellular localization of ataxin-3. Interestingly, catalytically compromised ataxin-3 displays a reduced ability to interact with VCP/p97. On the other way around, VCP/p97 interaction stimulates wild-type ataxin-3 enzymatic activity, suggesting a direct association between VCP/p97 binding and ataxin-3 performance as a DUB. Therefore, this interaction might become a good target not only to modulate ataxin-3 activity but other properties of this protein. More so, as the DUB activity of expanded ataxin-3 was shown to be insensitive to VCP/p97 stimulation, it what might constitute a pathological loss-of-function mechanism. Moreover, the expression of expanded ataxin-3 also exerts mitochondrial dysfunction, through reduction of mitochondrial complex II activity, adding a new pathway in MJD pathogenesis.

Resumo

A doença de Machado-Joseph (MJD, do inglês "Machado-Joseph disease"), também denominada por ataxia espinocerebelosa do tipo 3 (SCA3, do inglês "spinocerebellar ataxia type 3") é uma doença neurodegenerativa, hereditária, autossómica dominante e é a causa mundial mais comum de ataxia hereditária dominante. Os primeiros sintomas de MJD são normalmente percetíveis na idade adulta, durante a terceira ou quarta década de vida, embora em casos severos, a doença possa manifestar-se ainda na infância. Os doentes de MJD exibem uma grande variedade de fenótipos, numa extensa combinação possível de sintomas motores e não-motores. Ataxia e alteração da marcha são os sinais iniciais e principais desta doença neurológica, normalmente associados a um nível variável de défice nos movimentos oculares, disartria, sinais piramidais, perda progressiva de sensibilidade e parkinsonismo. Os sinais e sintomas vão evoluindo para estados mais graves, ao longo da progressão da doença, que culminam na morte dos doentes, 20 a 30 anos após o primeiro sintomas.

MJD pertence ao grupo das doenças de expansões de glutaminas, um grupo constituído por nove doenças neurológicas, causadas por uma mutação dinâmica comum, a expansão do número de repetições de um trinucleotídeo de citosina-adenina-guanina (CAG). Na MJD, a expansão do número de CAGs situa-se no exão 10 do gene MJD1, que codifica para uma enzima deubiquitinizadora, a ataxina-3. A MJD só se estabelece se o número de CAGs na expansão ultrapassar as 52 repetições. A expansão de CAGs é traduzida como um domínio proteico expandido, constituído por sucessivos aminoácidos glutamina, localizado no terminal carboxílico da ataxina-3. Este domínio expandido de poliglutaminas patológico destabiliza a estrutura da ataxina-3, favorece uma conformação errada e a sua consequente agregação, e confere novas propriedades tóxicas à proteína, que induzem disfunção neuronal, e

consequentemente neurodegenerescência. Ambas as formas de ataxina-3, normal e expandida, são expressas em todos os tecidos do corpo, contudo, a degeneração ocorre apenas em determinadas regiões do sistema nervoso central. Regiões subcorticais como os núcleos da ponte, o núcleo dentado, núcleos subtalâmicos e a medula espinhal estão entre as regiões mais afetadas. As razões para este padrão de neurodegeneração e para a suscetibilidade específica destes neurónios para a ataxina-3 expandida não são ainda conhecidas.

A ataxina-3 é uma proteína intracelular com um peso molecular de cerca de 42 kDa, com a capacidade de interagir e clivar cadeias de poliubiquitina, e atualmente, é classificada como uma enzima deubiquitinizadora da classe das proteases com domínio de Josefina. A ataxina-3 apresenta maior afinidade para cadeias longas de ubiquitina, com mais de 4 monómeros de ubiquitina, e uma preferência catalítica por ligações entre duas ubiquitinas através da lisina 63. A ataxina-3 é regulada através de processos de fosforilação e monoubiquitinização, que determinam a sua atividade catalítica e/ou a sua localização intracelular. O papel biológico da ataxina-3 ainda não está totalmente esclarecido. Tem sido proposto que a ataxina-3 atua como uma enzima modificadora de cadeias de ubiquitina e que está envolvida nas vias de ubiquitina-proteassoma, na degradação associada ao retículo endoplasmático, na resposta de defesa celular contra o stresse por choque térmico e na determinação da longevidade de *Caenorhabditis elegans*. A associação da ataxina-3 nesta variedade de vias intracelulares tem sido acompanhada pela descoberta de um número crescente de proteínas que evidenciam afinidade pela ataxina-3. Para além da proteína p97/valosin-containing protein (VCP/p97) e da hHR23A/hHR23B (do inglês, "human homologs of yeast Rad23 protein"), outras proteínas interagem com a ataxina-3, nomeadamente a tubulina, a proteína associada aos microtúbulos 2 (MAP2, do inglês "microtubule-associated protein 2"), a dineína, a deacetilase de histonas 6 (HDAC6, do inglês "histone deacetylase 6"), vários ativadores/repressores da transcrição e a parkina. Algumas destas interações são específicas para a forma normal da ataxina-3, e são abolidas quando o domínio de poliglutaminas expandido está presente, enquanto outras só ocorrem na presença da ataxina-3 expandida.

Estudos *in vitro* demonstraram que não existem diferenças significativas entre as atividades enzimáticas da forma normal e expandida da ataxina-3 humana. Desta forma, investigou-se o papel das interacções inter-proteínas na atividade da ataxina-3 e a influência da atividade deubiquitinizadora influencia no "comportamento" da ataxina-3 na célula. Mais ainda, neste trabalho clarificou-se a contribuição da alteração da atividade da ataxina-3 e o envolvimento da disfunção mitocondrial na patogénese da MJD. Para atingir estes objetivos, foram realizados estudos de deubiquitinização *in vitro* com a ataxina-3 normal e expandida, na ausência ou na presença de proteínas que previamente demonstraram interação com a ataxina-3, e usaram-se vários modelos celulares e animais da MJD para avaliar a toxicidade da ataxina-3 expandida, com principal destaque para a disfunção mitocondrial, um mecanismo patológico cada vez mais transversal das doenças de poliglutaminas.

No Capítulo 2, investigou-se o efeito de duas proteínas, hHR23A e VCP/p97, que previamente demonstraram interagir com a ataxina-3 na atividade deubiquitinizadora da ataxina-3. A hHR23A e a ataxina-3 endógenas foram encontradas predominantemente no núcleo das células, enquanto a VCP/p97 endógena mostrou-se mais abundante no citoplasma. Apesar de existirem diferenças na localização intracelular, as interações da VCP/p97 e da hHR23A com a ataxina-3 foram comprovadas e foi ainda observada a formação de um complexo trimolecular contendo as três proteínas endógenas. As interações da VCP/p97 e hHR23A com a ataxina-3 também foram visualizadas em condições *in vitro*. hHR23A, VCP7p97, ataxina-3 normal e expandida humanas recombinantes foram purificadas e posteriormente utilizadas em ensaios de deubiquitinização *in vitro* para averiguar a influência da hHR23A e da VCP/p97 na atividade enzimática da ataxina-3. A ataxina-3 apresentou uma velocidade baixa de atividade enzimática e uma preferência catalítica por cadeias de poliubiquitina ligadas pela lisina 63. A adição de hHR23A aos ensaios *in vitro* não alterou a cinética ou a preferência de substrato da ataxina-3. Pelo contrário, a presença da VCP/p97 aumentou especificamente a atividade *in vitro* da ataxina-3 normal. Curiosamente, a ativação mediada pela VCP/p97 não foi observada na presença de ataxina-3 expandida.

No Capítulo 3, ataxina-3 enzimaticamente ativa e ataxina-3 cataliticamente inativa foram expressas em células e utilizadas em ensaios *in vitro*, de forma a continuar o estudo da atividade da ataxina-3 e da sua influência nas respostas intracelulares da proteína. A ataxina-3 inativa apresentou níveis proteicos mais elevados em comparação com a ataxina-3 ativa, parcialmente devido à velocidade de degradação mais reduzida da ataxina-3 inativa. A ataxina-3 inativa intracelular mostrou maiores níveis de ubiquitinização do que a forma ativa. Este elevado nível de ubiquitinização foi associado a uma taxa de degradação proteassomal mais reduzida, determinada através de estudos *in vitro*. A redução da degradação da ataxina-3 inativa pelo proteassoma correlacionou-se com uma redução da interação da ataxina-3 inativa com a VCP/p97, proteína que tem a capacidade de entregar substratos ao proteassoma para a sua posterior degradação. Apesar da ataxina-3 e o proteassoma se localizarem em regiões subnucleares bem delimitadas, a ataxina-3 mostrou não interagir diretamente com o proteassoma ou com nenhuma das suas subunidades. Curiosamente, a ataxina-3 inativa exibiu um menor grau de colocalização com o proteassoma e uma menor abundância no compartimento nuclear. Sumariamente, a atividade enzimática da ataxina-3 modula a sua reciclagem celular, a sua localização intracelular e os seus níveis de ubiquitinação.

No Capítulo 4, vários modelos celulares e animais da MJD foram utilizados para avaliar a contribuição da disfunção mitocondrial na patologia da MJD. Células de rim embrionário humano (HEK, do inglês "human embryonic kidney") transfetadas de forma transitória com a proteína de fusão entre ataxina-3 expandida (Q84) e a proteína verde fluorescente (EGFP, do inglês "enhanced green fluorescent protein") mostraram-se mais susceptíveis ao inibidor irreversível do complexo II mitocondrial, o ácido 3-nitropropiónico (3-NP, do inglês "3-nitropropionic acid") do que células HEK que expressavam a proteína de fusão EGFP-ataxina-3 normal (Q28). Igualmente, a linha celular de feocromacitoma de rato (PC6-3) que expressava ataxina-3 humana expandida (Q108) de forma regulada por tetraciclinas, também demonstrou uma maior susceptibilidade para a inibição com 3-NP relativamente às células PC6-3 que espressavam ataxina-3 humana normal (Q28). Culturas primárias de células granulares do cerebelo provenientes de murganhos transgénicos para a MJD exibiram a mesma

tendência, i.e., maior vulnerabilidade para o 3-NP, comparativamente aos neurónios cerebelares de murganhos normais. Mitocôndrias de cérebro de murganhos transgénicos para MJD e de linhas celulares linfoblastóides derivadas de linfócitos de doentes de MJD exibiram uma tendência para uma redução na atividade do complexo II mitocondrial. A redução na atividade do complexo II mitocondrial foi ainda mais evidente, e estatisticamente significativa, em mitocôndrias de células PC6-3 ataxina-3 (Q108) diferenciadas para um fenótipo neuronal após a incubação com NGF (do inglês "nerve growth factor").

Em conclusão, a capacidade ativa de protease de ubiquitina influencia outras propriedades da ataxina-3, para além da sua atividade deubiquitizadora, determinando também a sua reciclagem e localização intracelulares. Curiosamente, a ataxina-3 cataliticamente inativa apresenta uma redução na interação com a proteína VCP/p97. Por outro lado, a interação com a VCP/p97 estimula a atividade enzimática da ataxina-3 normal, sugerindo uma relação direta entre a ligação com a VCP/p97 e a capacidade da ataxina-3 atuar como enzima deubiquitinzadora. Esta interação poderá ser um alvo importante para a modulação da atividade da ataxina-3, assim como, de outras propriedades desta proteína. A interação da ataxina-3 com a VCP/p97 poderá ter uma importância acrescida, uma vez que a atividade da ataxina-3 expandida mostrou-se insensível à estimulação pela VCP/p97, podendo constituir um mecanismo patológico de perda-de-função. Além disso, a expressão de ataxina-3 expandida também induz disfunção mitocondrial, nomeadamente através da redução da atividade do complexo II mitocondrial, revelando uma nova via de patogénese na MJD.

Chapter 1

Introduction

1.1. Trinucleotide repeat disorders

Repetitive deoxyribonucleic acid (DNA) sequences are recurrent in the human genome. They are notably found in telomeres, centromeres and scattered through various DNA regions in the chromosome. Highly repeated DNA is usually arranged in clusters of tandem repeats of a specific sequence. This sequence may be composed of 1 to 10 nucleotides or be more complex and have a motif of hundreds of nucleotides. Three subclasses of tandemly repeated DNA can be defined according to the size of the repetitive cluster: satellite DNA, minisatelitte DNA and microsatellite DNA. Of all the three subclasses, microsatellite DNA is the only that can be found in protein-coding DNA (Strachan and Read, 2004).

Microsatellite DNAs, also known as simple sequence repeats, are relatively small tracts of a repetitive simple DNA sequence composed of up to 10 nucleotides. They are disseminated throughout the human genome and represent 2% of the total DNA. Trinucleotide repeats, repeat sequences made of 3 nucleotides, are relatively rare in comparison to mononucleotide and dinucleotide repeats which account for more than 0.5% of the genome. Trinucleotide repeats are highly polymorphic and have been increasingly used as genetic markers for characterization of populations. Microsatellite DNAs, trinucleotide repeats included, are usually found in intergenic DNA or within the introns of genes. However, there are examples of microsatellite DNA within exons of a coding sequence, some promoting mutations in specific genes, due to their propensity to instability and expansion (Strachan and Read, 2004).

Fragile X syndrome, the most common inherited cause of mental retardation and autism (Todd and Paulson, 2010), was the first disorder to be identified as consequence of a trinucleotide repeat expansion (Kremer et al. 1991; Verkerk et al. 1991). This discovery introduced a new mechanism of disease, a class of dynamic mutations where trinucleotide repeats located in the vicinity or within the coding region of a gene, CGG in the case of Fragile X syndrome, could expand over a determined length and consequently affect gene expression and therefore disease. Since then, trinucleotide repeat expansions have been implicated in a variety of human

diseases, ranging from neurodegenerative disorders to skeletal diseases. Over 40 neurological, neurodegenerative and neuromuscular disorders are most certainly caused by a trinucleotide repeat instability (Pearson et al., 2005).

Trinucleotide repeats can be perfectly stable and be transmitted over generations without altering its length. Normal size trinucleotide repeats can be found in genes coding for enzymes, hormone receptors and in regulatory non-coding sequences of genes without promoting any harm or even being essential for the protein normal function, as as in the case of transcription factors. However, in some cases, the trinucleotide repeat becomes unstable and begins to expand, most probably through a slipped strand mispairing mechanism during DNA replication. Once unstable, the trinucleotide repeats are virtually never transmitted unchanged throughout generations. Expansion and contraction of the repeat can occur depending on the individual disease, the type of trinucleotide repeat or the parental origin of the repeat. However, expansion of the repeat is more common and it is usually more prominent when transmitted through the male lineage. As the size of the expansion is increasing and passed through consecutive generations, it gives rise to asymptomatic individuals, or carriers, and after surpassing a specific length, it starts to produce pathological signs with variable onset, severity and manifestations. The continuous increase in the trinucleotide repeat expansion generally promotes a more severe clinical profile through generations, in a phenomenon known as anticipation (Strachan and Read, 2004).

Trinucleotide repeat expansions associated with human pathologies can be divided in two major classes, according to the size of the expansion and its location relatively to the gene: the untranslated trinucleotide repeat diseases (section 1.2) and the polyglutamine repeat disorders (section 1.3 and beyond) (Everett and Wood, 2004). The first class exhibits very large noncoding repeat expansions of various types of codons (CGG, CCG, CTG, GAA). The large expansions are located in the promoter, untranslated regions or in the introns of the affected gene. The second class is characterized by smaller pathological expansions of a single codon, cytosine-adenine-guanine (CAG), coding for the amino acid glutamine (Q). The CAG repeat expansion

is transcribed and translated, originating an expanded polyglutamine (polyQ) tract in the coded protein.

1.2. RNA-mediated toxicity and untranslated trinucleotide repeat disorders

The ultimate example of an untranslated trinucleotide expansion disorder is the Fragile X syndrome. In this pathology, the trinucleotide expansion exerts its deleterious effect without need of transcription. The expansion of the CGG codon over 200 copies in the 5' untranslated region of FMR1 gene induces abnormal methylation of this regulatory region, which jointly with a decreased histone acetylation promotes FMR1 gene silencing and fragile X mental retardation (FMR) protein knockdown (Coffee et al., 1999). FMR protein is a ribonucleic acid (RNA)-binding protein, regulating transcription and protein synthesis of the messenger ribonucleic acid (mRNA) molecules to which it binds. Therefore, the loss of the FMR protein alters gene expression, which ultimately results in the clinical symptoms of Fragile X syndrome (Orr and Zoghbi, 2007).

On other hand, six neurological or neurodegenerative diseases have been associated with toxicity at the RNA level. These particularly long trinucleotide repeat expansions are located in noncoding regions of specific genes (Li and Bonini, 2010). Since expansions are not inserted in protein-coding regions, the pathology is RNA-mediated. These diseases can be divided into two sub-groups according to the mechanism through which the RNA transcript exerts its deleterious effect. In the first group, which includes myotonic dystrophy type I (DM1) and fragile X-associated tremor ataxia syndrome, the expanded RNA is the primary cause of pathology and has a dominant toxic effect. In others disorders, such as three types of spinocerebellar ataxias (SCAs) (MJD/SCA3, SCA8 and SCA12) and Huntington disease-like 2, the expanded trinucleotide repeat transcript contributes to the development of the disease symptoms, but is not the major player (Li and Bonini, 2010).

Table I – RNA mediated trinucleotide neurological disorders

Disease	Repeat	Gene	Normal repeat	Disease-associated repeat	Antisense transcript	Neurological phenotype
DM1	CTG	3'UTR of dystrophia myotonica protein kinase	5-38	50~1500; or more in congenital DM1	Yes	Adult onset: neuropsychiatric symptoms, executive dysfunction; congenital DM1: mental retardation in >50%
Fragile X tremor ataxia syndrome	CGG	5'UTR of fragile X mental retardation gene 1	20-45	55-200; incomplete penetrance	Yes, possible open reading frame for polyproline	Late onset; cerebellar ataxia, action tremor, dementia parkinsonism; neuropsychiatric symptoms in females
MJD/ SCA3	CAG	Exon 10 of ataxin-3	Up to 44	~45-51: reduced penetrance; ~52-86: full penetrance	Unknown	Ataxia; parkinsonism, dystonia; dementia uncommon
SCA 8	CTG	5'UTR of Kelch-like 1	15-50	~71-1300; incomplete penetrance	Yes, possible open reading frame for polyQ	Cerebellar ataxia; dementia uncommon
SCA 12	CAG	5'UTR/promoter of PPP2R2B	Up to 32	51-78	Unknown	Action tremor; cerebellar ataxia; dementia uncommon
HD-like 2	CTG	3'UTR of junctophilin 3	6-28	>41	Yes, possible open reading frame for polyQ	Clinically similar to HD

Adapted from Todd and Paulson (2010).

One mechanism through which a trinucleotide repeat expansion in a mRNA molecule can have a dominant toxic effect is the promotion of aberrant RNA-protein

interactions. The expanded-repeat RNA sequence attracts RNA-binding proteins and promotes the establishment of unusually stable RNA-protein interactions, sequestering the RNA-binding proteins, and so, reducing their activity (Figure 1.1.). This seems to be the case of DM1. Many RNA-binding proteins are regulators of mRNA maturation pathways, and their unavailability to the cell results in the incorrect splicing of various mRNAs, escalating the toxic effect of the trinucleotide expansion to other gene transcripts. Moreover, anomalous interactions between proteins and expanded-repeat RNA molecules may promote stabilization of the proteins, inducing protein accumulation and the formation of inclusions (Figure 1.1.). Furthermore, these inclusions can activate chaperones, protein quality control proteins, proteasome components and ubiquitin, hallmarks of many of these disorders (Todd and Paulson, 2010).

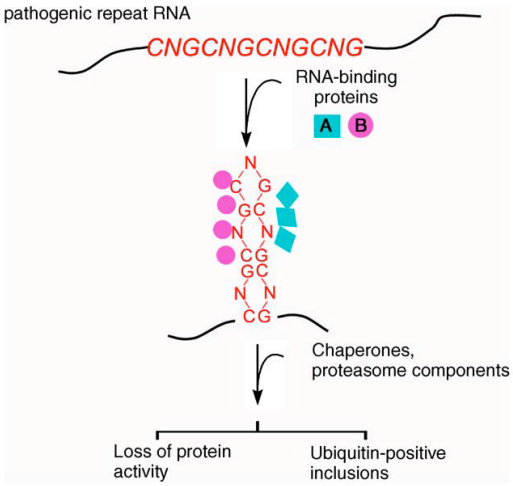

Figure 1.1. - Dominant effects of a pathogenic repeat RNA on protein functions. Expansion of a trinucleotide repeat within a RNA can cause aberrant RNA–protein interactions. Sequestration of RNA-binding proteins (A and B in the figure), might lead to their depletion and loss of normal function. This binding could also lead to abnormal RNA–protein complexes, leading to the formation of inclusions, and could also affect protein quality-control pathways, for example, inducing mislocalization of chaperone and proteasome components. Adapted from Li and Bonini (2010).

Expanded-repeat mRNA can also induce toxic effects through the activation of phosphorylarion signaling pathways, altering the phosphorylated state of regulatory proteins, as occurs for DM1, where protein kinase C seems to be overactivated (Kuyumcu-Martinez et al., 2007). Gene expression may also be altered by RNA-mediated toxicity, since an expanded trinucleotide repeat in the untranslated regions of the mRNA molecule may disrupt the normal binding of proteins and micro ribonucleic acid (miRNA) to their regulatory sites, altering the expression levels of the expanded gene. Some genes associated with trinucleotide repeat expansion diseases have shown to be regulated by miRNAs. Ataxin-1 gene, the mutated gene in SCA1, is one example and a strong candidate to this kind of pathological mechanism (Lee et al., 2008).

More complex outcomes may occur from expanded-repeat RNAs. In SCA8, evidences exist that both sense and antisense are transcribed, producing not only a CAG expanded-repeat RNA further translated to a polyQ peptide, but also a CUG expanded-repeat RNA (Moseley et al., 2006). Therefore, SCA8 symptoms might result from a combination of toxic effects of a polyQ peptide and a CUG-expanded RNA molecule. The production of both sense and antisense transcripts might originate double-strand RNA molecules, which could subsequently be recognized and processed by the ribonucleic acid interference (RNAi) machinery, inducing RNAi-downregulation of several genes and affecting gene expression in a broad range (Figure 1.2.). Morever, recent data collected from a fly-model of MJD/SCA3 have raised the possibility of a role for RNA toxicity in some polyQ diseases, which were previously thought to be caused exclusively by the presence of a polyQ peptide (Li et al., 2008). All trinucleotide repeat expansion disorders may have toxic contributions of both the mutated protein and the expanded RNA transcript, with each of these two components adopting more or less relevance in the pathological mechanism, depending on the particular trinucleotide repeat disease.

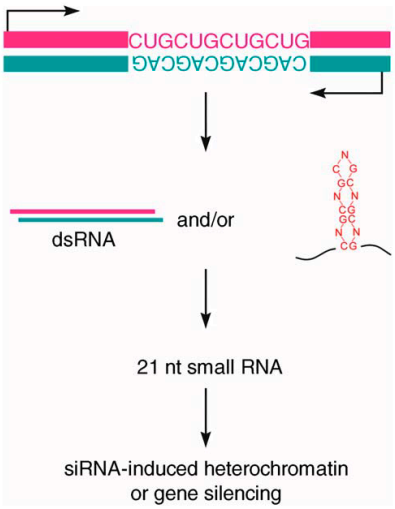

Figure 1.2. - Expanded trinucleotide repeat RNA could induce dominant effects through the generation of small RNAs. In disease loci where antisense RNA that contains the repeats is generated, interactions between sense and antisense transcripts could form double-stranded RNA, providing a substrate for the RNAi pathway and for processing into small RNAs. The expanded-repeat RNA hairpin itself can be processed into small RNAs. Small RNAs generated could target the expression of other genes with sequence homology and cause silencing or chromatin silencing. Adapted from Li and Bonini (2010).

1.3. Polyglutamine disorders

In 1991, another mechanism through which trinucleotide expansion repeats could produce toxicity was discovered. The X-linked spinal bulbar muscular atrophy (SBMA), a progressive motor neuron disease, was described as being caused by CAG expansion in the gene coding for the androgen receptor (La Spada et al., 1991). This new mechanism involved the transcription and translation of the expanded CAG triplet into an elongated polyQ tracts in the protein coded by the mutated gene. Over the following two decades, at least eight other disorders have been classified as polyglutamine disorders (Table II). The collection of pathologies includes SBMA, Huntington's disease (HD), six types of SCAs and dentatorubral-pallidoluysian atrophy (DRPLA). PolyQ diseases are late-onset inherited neurodegenerative disorders and

with one exception, SBMA, which is linked to chromosome X segregation, they are all transmitted through successive generations in an autosomal dominant manner (Williams and Paulson, 2008). Anticipation is also a shared feature, with longer expansions promoting earlier onset and more severe symptoms. Anticipation is due to the instability of the CAG repeat which tends to expand, specially when transmitted through the male lineage. This instability promotes the appearance of longer expansions throughout generations. The onset of the first symptoms inversely correlate with the number of CAGs present in the mutated gene. In the longer CAG expansions, this relation is so tight that it is possible to predict the age of onset with a minimal margin of error, based on the number of CAGs carried by the patient. Even so, variability in the age of onset has also been reported without an increase in the number of CAG codons, suggesting that CAG repeat length may not be the only determinant for the age of onset.

PolyQ disease proteins are not evolutionarily or physiologically related and besides a common mutation, there are no other similarities. In general, polyQ proteins have a glutamine tract of 10 to 30 residues in their normal isoform. PolyQ-induced neurodegeneration is usually associated with a polyQ domain longer than 35-40 glutamines (Morfini et al., 2005). In all pathologies, the polyQ/CAG expansions exhibit a dominant toxic effect, being the presence of one expanded allele sufficient to cause disease. The existence of a shared mutation between polyQ disorders and similarity in the range of the polyQ length associated with toxicity are suggestive of a common pathogenic mechanism. However, protein context surrounding the expanded polyQ tract influences its biochemical properties, and thus, its toxic effect. Furthermore, specific cellular environment and protein interactions involving each unique expanded polyQ protein are the most probable responsible for the distinctive phenotypes and specificity in the degenerating areas for each polyQ disorder. One intriguing feature of polyQ disorders is the preferential degeneration of distinctive neuronal populations, in a typical and discriminating pattern for each disease, despite the widespread expression of the mutated proteins through different cell types and tissues. The higher susceptibility of neurons to polyQ toxicity in comparison to other cell types is still not fully understood.

Table II – Polyglutamine disorders.

Disease	Gene product	Normal repeat	Expanded repeat	Neurological phenotype
HD	Huntingtin	6-34	36-121	Chorea, dystonia, cognitive deficits, psychiatric problems
SCA1	Ataxin-1	6-44	39-82	Ataxia, slurred speech, spasticity, cognitive impairments
SCA2	Ataxin-2	15-24	32-200	Ataxia, polyneuropathy, decreased reflexes, infantile variant with retinopathy
MJD/SCA3	Ataxin-3	13-36	55-87	Ataxia, parkinsonism, spasticity
SCA6	$CACNA1_A$	4-19	10-33	Ataxia, dysarthria, nystagmus, tremors
SCA7	Ataxin-7	4-35	37-306	Ataxia, blindness, cardiac failure in infantile form
SCA17	TBP	25-42	47-63	Ataxia, cognitive decline, seizures, and psychiatric problems
SBMA	Androgen receptor	9-36	38-62	Motor weakness, swallowing, gynecomastia, decreased fertility
DRPLA	Atrophin	7-34	49-88	Ataxia, seizures, choreoathetosis, dementia

Adapted from Orr and Zoghbi (2007).

1.4. Pathological mechanisms in polyglutamine disorders

Whether polyQ toxicity derives from new harmful properties or the disruption of protein's normal activity is still a matter of ongoing discussion.

SBMA is a good paradigm of the gain-of-function/loss-of-function dychotomy of polyQ proteins. The expanded polyQ tract is essential for neurodegeneration to occur in all polyQ disorders, but in the case of SBMA, there is a strong indication that the presence of an expanded polyQ domain produces a gain-of-function in the affected

protein, the androgen receptor. Indeed, mutations leading to the loss-of-function of the androgen receptor cause testicular feminization but do not promote motor neuron degeneration (Pinsky et al., 1992). Neurodegeneration seems to be driven from a new toxic property provided by the presence of an elongated polyQ domain in the androgen receptor. On the other hand, the activation of the androgen receptor by its ligand can increase the severity of the phenotype; thus, normal activity of androgen receptor modulates polyQ toxicity (Katsuno et al., 2002). Most likely, both gain-of-function/loss-of-function phenomena do take place and play a part in pathogenesis, each having a smaller or greater importance depending on each particular polyQ disorder.

1.4.1. Aggregation

In the last two decades, several studies demonstrated that proteins containing long polyQ tracts were bestowed with a propensity to misfold and accumulate into large intracellular aggregates (Figure 1.3.). Detection of expanded protein accumulation into intracellular inclusions in specific brain regions were reported for all polyQ disorders, and *in vitro* experiments revealed that the protein aggregation was mediated by the polyQ stretch (Cummings and Zoghbi, 2000). Furthermore, aggregates were found in the degenerating areas of patients' brains, establishing a connection between polyQ aggregation and neurodegeneration. The long and slow process of protein accumulation inside neurons is also a very appealing explanation for the late-onset and progressive worsening of symptoms in polyQ diseases. All these findings led to the hypothesis that polyQ protein aggregation, and consequently intracellular inclusions, were responsible for neurodegeneration. This hypothetic pathogenic mechanism led to the insertion of polyQ disorders in a broader group of neurodegenerative diseases comprising Alzheimer's and Parkinson's diseases, in which aggregation of specific proteins is a generalized hallmark. Aggregation can occur outside and inside the cell, sometimes, in patterns characteristic of each neurological disorder. In Alzheimer's disease, amyloid beta peptide deposits primarily outside the cell, on the other hand, aggregates of polyQ disorders are generally intracellular, with a

more prevalent cytoplasmic, nuclear or perinuclear localization, depending on the expanded protein and respective disease.

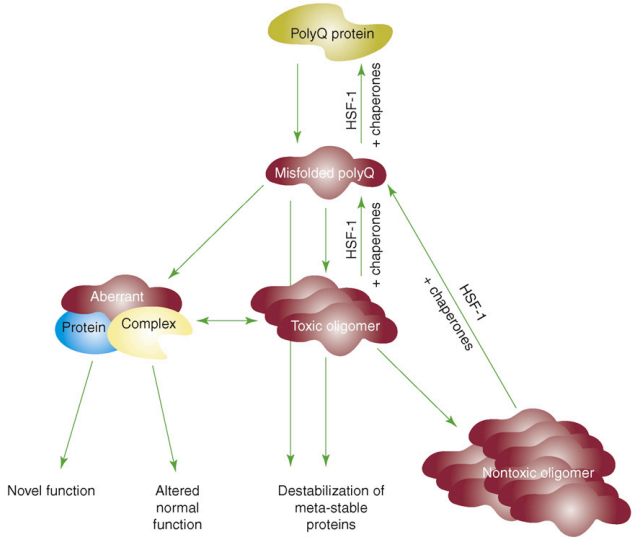

Figure 1.3. - Possible cellular process of expanded polyQ protein misfolding. PolyQ proteins, when expanded, are prone to misfold. A cellular response can be triggered through the expression of certain chaperones, including Hsp70 and Hsp40, which help refold misfolded polyQ proteins. Chaperones can help to dissociate oligomers into polyQ monomers. Misfolded monomers can also form complexes with other proteins. These heteroprotein complexes can involve (i) animbalance in the levels of normally occurring protein complexes, or (ii) the generation of novel complexes. Oligomers of polyQ protein also can interact with cellular proteins, resulting in altered function. Adapted from Williams and Paulson (2008).

More recently, however, intracellular macromolecular inclusions have shown not to be the major toxic players; instead, intermediate and less complex aggregated species, such as smaller aggregates or oligomers, have been defined as the harmful forms of the polyQ-expanded proteins (Klement et al., 1998; Saudou et al., 1998; Arrasate et al., 2004; Slow et al., 2005). In this updated hypothesis, oligomers would be produced by interaction and stabilization of polyQ peptides, which over a certain threshold, would self-associate through hydrogen bonds into hydrogen-bonded polar zippers (Perutz et al., 1994). Non-covalent interactions with other proteins and peptide cross-linkage through transglutaminase activity were also hypothesized to have a role in

polyQ oligomer production (Green et al., 1993; Kahlem et al., 1996). Similarly to Alzheimer's disease, oligomerization may also result from the formation of β-sheet amyloid-like structures organized in fibrillar and non-fibrillar aggregates (Tanaka et al., 2001; Perutz et al., 2002). Expanded polyQ β-strand/β-turn structure was related to aggregation and neuronal toxicity (Poirier et al., 2005). As previously mention, the protein sequences flanking the polyQ domain modulate its biochemical properties, including polyQ-mediated aggregation (Masino et al., 2004; de Chiara et al., 2005; Ellisdon et al., 2006; Thakur et al., 2009). Therefore, depending on the specific protein, aggregation may occur through different mechanisms and result in variable aggregated structures with different cell toxicity effects. Currently, large inclusions are seen as by-products resulting from continuous protein accumulation or even as a cellular defense response to bring oligomers, the pathogenic species, "out of solution" (Figure 1.3.). Indeed, the direct correlation between aggregates and neurodegeneration was disputed since early on. In 1999, studies in brains of HD patients reported aggregate formation mainly in unaffected interneurons, with few or no aggregates detected in degenerated cells, supporting the hypothesis that aggregation is a cytoprotective mechanism against polyQ neurotoxicity rather than a sign of cell death (Kuemmerle et al., 1999). A more careful and discriminative evaluation of the toxic effect of each stage of the progressive process of protein aggregation is mandatory, to clarify which are the primary pathogenic species in polyQ diseases. This will further help to clarify the role of specific forms of protein aggregates in other neurodegenerative diseases.

1.4.2. Proteolytic cleavage

Post-translational modifications of the expanded polyQ protein have shown to modulate the mechanism of disease. Proteolytic cleavage of polyQ proteins, in particular, have been extensively studied. The pathological mechanism in some polyQ diseases, namely HD, Machado-Joseph disease/Spinocerebellar ataxia type 3 (MJD/SCA3) and SBMA, seems to integrate proteolytic steps of the affected proteins (Figure 1.4.). Inclusions found in HD patient brains have shown to be enriched in N-terminal fragments containing the extended polyQ tract (DiFiglia et al., 1997; Sieradzan et al., 1998). However, for some disorders, spinocerebellar ataxia type 1

(SCA1) as an example, there are no evidences of production of cleavage fragments. The expanded polyQ induces alterations in protein conformation, leading to mysfolding and to the consequent exposure of protein domains more susceptible to protease cleavage (Paulson et al., 1999; Lunkes et al., 2002). The proteolysis of expanded proteins releases smaller peptides containing the polyQ tract, which usually exhibit a higher tendency for aggregation and toxicity, in comparison to the full-length protein (Ikeda et al., 1996; Cooper et al., 1998; Ellerby et al., 1999). Cleavage of the sequences flanking the polyQ domain abolishes their modulating effect over polyQ toxicity. Furthermore, the resulting polyQ-containing fragment mimics more closely the characteristics of a pure polyQ stretch. Several proteases have been found to cleave polyQ proteins, but caspases and calpains have been the most studied due to their association with programmed cell death pathways. Caspase cleaving sites have been identified or predicted in HD, SBMA, DRPLA and MJD/SCA3 affected proteins (Wellington et al., 1998). Proteolytic fragments might even result from the action of a myriad of proteases with little specificity or coordination. Proteolytic cleavage is accepted to be an initial event in some polyQ pathologies and independently of the proteolytic path, the smaller polyQ-containing peptides seem to be important initiators of the aggregation process leading to the formation of toxic species, either the oligomers or the intracellular inclusions (Bauer et al., 2009). There is a subsequent recruitment and sequestration of longer fragments, the full-length protein and house-keeping proteins, into the larger aggregates. Moreover, for some polyQ proteins, the cleavage process increases their translocation to the nucleus, enhancing their toxic effect (Hackam et al., 1999).

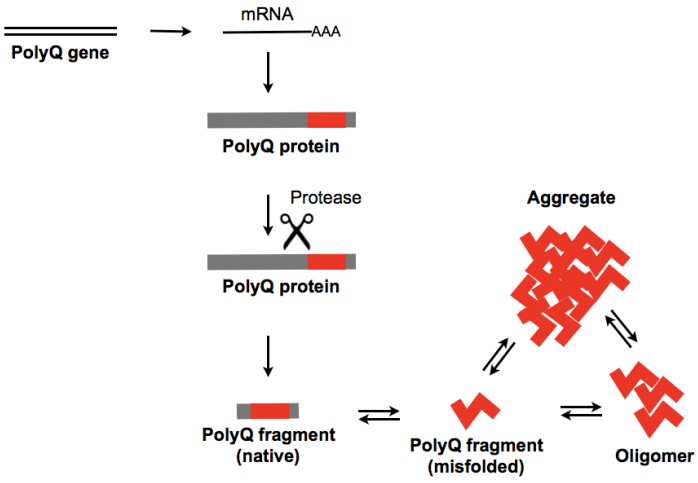

Figure 1.4. – Proteolytic cleavage in the pathogenesis of polyglutamine diseases. Many polyglutamine diseases appear to be initiated by proteolytic cleavage to generate a toxic fragment. The expanded polyglutamine tract allows transition into an altered conformation that may cause toxicity through several mechanisms. The peptide may exert toxicity as a monomer or it may self-associate to form toxic oligomers. The oligomers can assemble into larger aggregated species and ultimately are deposited in macromolecular intracellular inclusions.

1.4.3. Nuclear import and gene expression deregulation

Aggregation of expanded polyQ proteins inside the nuclear compartment has been observed in several polyQ disorders, and for some pathologies, SCA1 and SBMA, the presence of the expanded protein inside the nucleus is essential for the development of neurotoxicity and disease symptoms (Brooks et al., 1995; Klement et al., 1998; Saudou et al., 1998; Peters et al., 1999; Orr et al., 2001; Katsuno et al., 2002). The presence of expanded polyQ domains in the nucleus seems to disrupt nuclear organization and normal function, affecting gene expression and transcription through various pathways (Sun et al., 2007; Zoghbi and Orr). Putative nuclear localization signals (NLS) have been discovered in a subset of polyQ proteins, which could justify

their translocation to the nuclear compartment (Trottier et al., 1998; Kaytor et al., 1999; Schilling et al., 1999). The presence of NLS is not surprising for some of these proteins, because the nucleus is the site of their normal activity; ataxin-7 is a good example of this. However, the majority of the polyQ proteins have a preferential cytoplasmic distribution and only after a proteolytic cleavage, the resulting fragments have facilitated access to the nucleus. Once inside the nucleus, expanded proteins or fragments disturb gene expression mainly by interacting with transcription factors (Okazawa et al., 2003). These interactions can involve soluble polyQ protein, initial stages of aggregation, as monomers or oligomers, or even, sequestration into large intranuclear aggregates. cAMP (cyclic adenosine monophosphate) response element-binding protein (CREB)-binding protein (CBP), p300/CBP-associated factor (PCAF), p53, specificity protein 1 (Sp1), TAF4 RNA polymerase II, TATA box binding protein (TBP)-associated factor, 135kDa (TAFII130), polyubiquitin-binding protein 1 (PQBP1) are a few of the transcription factors or cofactors known to establish aberrant interactions with expanded polyQ proteins. Some of them have been found to bind to more than one protein affected in polyQ diseases, while others show specificity to one expanded polyQ protein. CBP, in particular, has been highly associated with polyQ-induced gene repression and found to be sequestered in intranuclear inclusions of several expanded polyQ proteins (McCampbell et al., 2000; Nucifora et al., 2001; Stenoien et a., 2002). On the other hand, Sp1 interacts directly with soluble expanded huntingtin, the polyQ protein affected in HD, in a polyQ-dependent manner (Dunah et al., 2002; Li et al., 2002). In any case, the aberrant interactions with the mutant proteins keep these transcription factors from performing their normal activity, repressing gene expression under their regulation (Chan et al., 2002; Luthi-Carter et al., 2002; Kotliarova et al., 2005; Kuhn et al., 2007). Alterations in gene expression are one of the main mechanisms through which neurodegeneration can be triggered and might be partly responsible for the neuron-specific degeneration.

1.4.4. Phosphorylation and Sumoylation

The biochemical properties and cytotoxicity of expanded polyQ peptides have shown to be modulated into some extent by post-translational modifications.

Phosphorylation of polyQ proteins was observed to alter proteolytic cleavage, the initial conversion into pathological entities and nuclear transport of these disease-associated proteins (Warby et al., 2009). In particular, phosphorylation of huntingtin at serine 421 was shown to be neuroprotective, decreasing the accumulation of huntingtin and huntingtin fragments in the nucleus (Hubert et al., 2002; Humbert et al., 2002; Rangone et al., 2004). Moreover, phosphorylation in another residue, serine 434, diminished proteolytic cleavage of huntingtin mediated by caspase-3, which was associated to a reduction in polyQ aggregation and cytotoxicity (Luo et al., 2005). A decrease in aggregation and cytotoxicity of mutant huntingtin have also been described to be linked to phosphorylation at serine 536. Similarly to serine 434, this site seems to prevent huntingtin cleavage when phosphorylated, but this time, by preventing proteolysis activity of calpains as well (Gafni et al., 2004). However, phosphorylation of polyQ-expanded proteins is not always protective. Phosphorylation of ataxin-1, the affected protein in SCA1, favors its interaction with 14-3-3 protein, which leads to ataxin-1 accumulation and neurodegeneration. An expanded polyQ tract in androgen receptor seems to augment its propensity to phosphorylation, which has been shown to be related to an increase in mutant androgen receptor toxicity. The development of drugs capable of modulating the phosphorylated/dephosphosrylated state of polyQ proteins has been seen as a promising strategy to overcome proteotoxicity in polyQ diseases.

Another post-translational modification of proteins is the addition of a small peptide, small ubiquitin-like modifier (SUMO), to specific lysines of target proteins. Sumoylation is not as well studied as phosphorylation pathways, but recent and growing data suggests that sumoylation regulates protein localization in the cell, protein-protein interactions and transactivation of transcription factors (Sarge and Park-Sarge, 2009). SUMO is a small protein similar to ubiquitin and, in fact, it has been proposed that sumoylation and ubiquitination have opposite effects. Elevated levels of SUMO1 have been found in degenerating neurons of different polyQ diseases patients (Ueda et al., 2002). In some polyQ diseases, such as HD and DRPLA, sumoylation of the affected proteins, huntingtin and atrophin-1, respectively, seems to enhance their neurotoxicity, although through opposite mechanisms. Sumoylation of

mutant huntingtin increases its stability and prevents its accumulation into large aggregates, resulting in a build-up of intermediate oligomeric species, which seem to be more toxic (Steffan et al., 2004). On the other hand, sumoylation of polyQ-expanded atrophin-1 increases its propensity for aggregation, accelerating aggregate formation and cell death (Terashima et al., 2002). In opposition to this, sumoylation of mutant androgen receptor and mutant ataxin-1, the mutated proteins in SBMA and SCA1, respectively, appears to reduce their aggregation and to be neuroprotective (Terashima et al., 2002; Riley et al., 2005). These opposite and confusing effects over different polyQ proteins demonstrate that more data needs to be collected in order to clarify the role of sumoylation in neurodegeneration.

1.4.5. Alterations in heat shock response

The expression of expanded polyQ domains with subsequent protein misfolding and aggregation represent a proteotoxic stress stimuli for the cell, which triggers a stress response mechanism involving heat-shock proteins (HSPs) as major participants. HSPs were initially described as proteins that would have their expression increased after a heat shock stimulus, as part of a physiological cellular response to heat-induced alterations in proteins. HSPs recognize misfolded proteins, stabilize them and promote their normal and native conformation (Muchowski et al., 2000). In response to polyQ expression, HSPs behave in two different phases (Bauer and Nukina, 2009). Initially, an increase in HSPs expression is detected as a part of the regular stress response to a proteotoxic stimuli; this initial up-regulation is followed by a second step of progressive reduction in the levels of HSPs, generally occurring at later stages of neurodegeneration (Hay et al., 2004; Huen et al., 2005). In more advanced neurodegeneration, it has been reported that HSPs are recruited to aggregation sites, becoming trapped and sequestered inside the inclusion, and thus, compromising their availability and normal activity in the cell (Wyttenbach et al., 2000; Wyttenbach et al., 2001; Hay et al., 2004). Consequently, the cell can not initiate normal stress responses and what starts as a cell response to polyQ toxicity, evolves into a facilitating mechanism to polyQ-mediated pathogenesis through reduction in HSPs activity and consequent build-up of aberrant proteins. HSPs have been described to recognize

expanded polyQ proteins and prevent their aggregation by stabilization of their monomeric conformation (Muchowski et al., 2000). Indeed, several types of HSPs have been shown to co-localize with nuclear aggregates in brains of transgenic mice, and even, in human brains from patients of several polyQ disorders (Cummings et al., 1998; Yvert et al., 2000; Zander et al., 2001; Schmidt et al., 2002). Moreover, over-expression of HSPs, specifically HSP40 and HSP70 family members, have shown to be efficient at diminishing the number of inclusions in cell and *in vivo* models of polyQ diseases, and even more successful at abolishing cell death (Stenoien et al., 1999; Jana et al., 2000; Kazemi-Esfarjani and Benzer, 2000; Kobayashi et al., 2000). Reduced formation of intracellular inclusions following over-expression of HSPs supports the hypothesis that HSPs are able to keep the expanded polyQ-containing proteins in a soluble form, most certainly to promote their handling by the protein degradation pathways. Recognition of the mutant proteins by HSPs may even prevent the deleterious interactions with important cellular targets essential for disease progression, hence, reducing polyQ toxic effect (Muchowski et al., 2002).

1.4.6. Dysfunction of protein degradation pathways

The primary protein degradation pathway of the cell for short-lived and aberrant proteins is the ubiquitin-proteasome pathway (UPP) (Goldberg, 2003), making the UPP one of the most important proteolytic pathways in the eukaryotic cell. The UPP directly regulates the cellular levels of a variety of proteins, placing the UPP in the center of many biological and physiological processes. A role for UPP has been described in cell division, cell differentiation, signal transduction, intracellular transport and obviously in the protein quality control (Glickman and Ciechanover, 2002; Ciechanover, 2003; Welchman et al., 2005).

The degradation of proteins by the UPP is a two-step process: the attachment of an ubiquitin signal, usually several ubiquitin molecules, and the degradation of the polyubiquitinated protein by the 26S proteasome complex (Pickart, 2001; Glickman and Ciechanover, 2002). The 26S proteasome complex is composed of two main parts: a regulatory cap, 19S, and the catalytic core, 20S. The polyubiquitin chains are recognized by the 19S cap of the proteasome complex and the substrate protein is

unfolded, deubiquitinated and inserted through a pore into the catalytic core of the 20S particle. The proteolysis takes place in the 20S core of the proteasome complex, which contains trypsin-, chymotrypsin- and peptidyl-glutamyl peptide-hydrolyzing activities, releasing small peptides into the cytoplasm, where they can be further degraded to free amino acids by cytosolic peptidases (Glickman and Ciechanover, 2002; Pickart and Cohen, 2004). Initially described solely as a protein degradation pathway, it is currently known that the UPP influence extends beyond the regulation of protein levels and its importance is reflected in the growing number of diseases associated to UPP dysfunction.

Indeed, UPP impairment is very deleterious to the cell due to deregulation of cellular signaling pathways and decrease in protein turnover, with a consequent accumulation of malfunctioning or damaged proteins. Therefore, disruption of UPP normal activity has been implicated in a broad range of human diseases, including neurological diseases such as Alzheimer's disease, Parkinson's disease, Huntington's disease, among others (Dawson and Dawson, 2003; Hope et al., 2003; Huang and Figueiredo-Pereira, 2010). UPP impairment mediated by expanded polyQ proteins has been reported, although there is still some debate regarding these evidences (Bence et al., 2001; Jana et al., 2001; Khan et al., 2007; Bennett et al., 2007). Many polyQ proteins have shown to be ubiquitinated in their soluble and specially in their aggregated state (Ross and Poirier, 2004). Ubiquitinated inclusions have been observed in brain samples of patients of polyQ diseases and proteasomal subunits have been found to be retained inside intracellular inclusions (Paulson et al. 1997; Holmberg et al., 1998; Chai et al., 1999; Koyano et al., 1999). These data corroborate the involvement of UPP activity in the pathological mechanism of these neurological diseases, although its precise role is still not fully understood. Ubiquitination of polyQ inclusions is suggestive of a cellular attempt to clear out the toxic proteins through the UPP. The same cell defense mechanism also justifies the recruitment of proteasome complexes to the vicinity of intracellular inclusions, in order to favour the degradation of aberrant proteins. Indeed, the inhibition of ubiquitination of expanded ataxin-1, the mutated protein in SCA1, resulted in increased cellular toxicity, suggesting that ubiquitination modulates the clearance of the expanded protein and has an important

detoxifying effect. The impairment of UPP by polyQ proteins is most likely mediated through two mechanisms. The first involves the sequestration of proteasome components into intracellular inclusions, altering proteasome cellular distribution. The second may involve the direct blockage of the proteasome catalytic core by the polyQ tract, which than inhibit protein degradation of other substrates (Doi et al., 2004; Davies et al., 2007). Both mechanisms culminate in UPP dysfunction through reduction of proteasome activity, which translates into an increase of proteotoxic stress for the cell. An alternative mechanism for reduction in UPP activity may underlie a caspase-dependent cleavage of proteasome components in a apoptotic scenario triggered by polyQ aggregation (Sun et al., 2004).

The cell possesses other degradation mechanisms besides the UPP to cope with polyQ proteins, namely the autophagy process (Figure 1.5.). Currently, it is accepted that the UPP has an important initial role in the clearance of soluble misfolded polyQ proteins, while autophagy plays the major role at the degradation of aggregated proteins and mature aggregates (Rubinsztein et al., 2007; Wong and Cuervo, 2010b). The autophagy-lysosomal pathway is a complex mechanism, conserved throughout evolution, combining the action of autophagic and non-autophagic proteins. Three types of autophagy have been described according to the feeding mechanism of cargo into lysosomes: chaperone-mediated autophagy, microautophagy and macroautophagy. Macroautophagy is the most important degradation pathway of long-lived proteins and intracelular organelles. It is characterized by the assembly of doubled-membrane autophagic vacuoles around the cargo, the autophagosomes, which later fuse with lysosomes containing the proteolytic enzymes responsible for the degradation, forming the autophagolysosome (Levine and Klionsky, 2004; Mizushima et al., 2008).

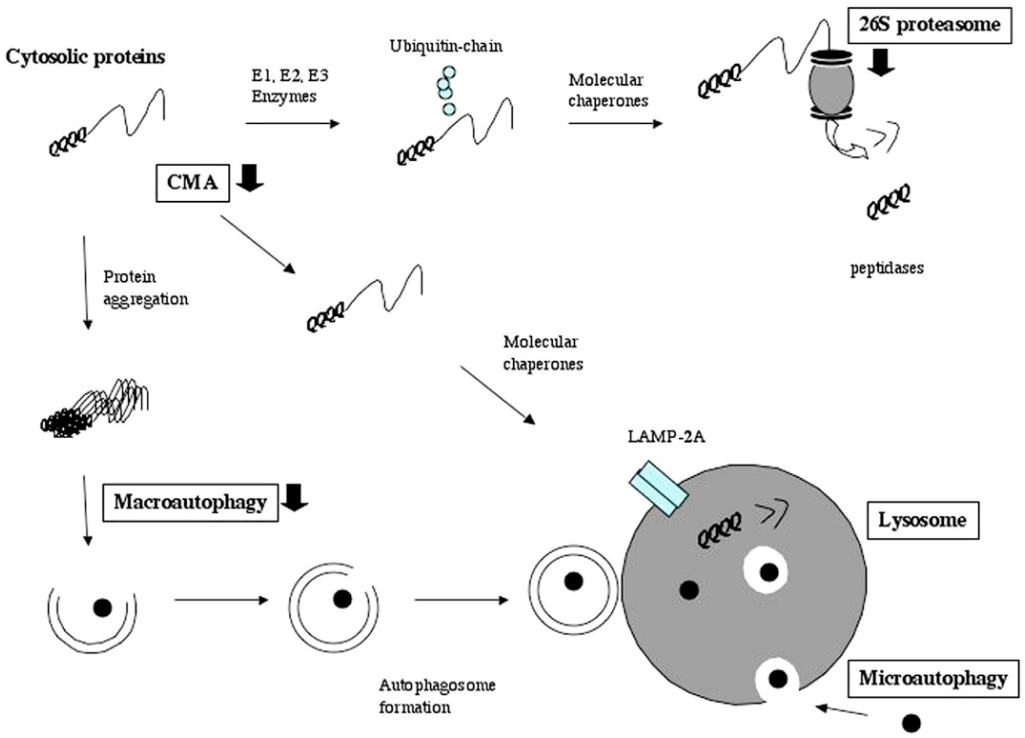

Figure 1.5. - Shortlived proteins are degraded by the ubiquitin–proteasome pathway (UPP) while long-lived proteins are more likely degraded by autophagic processes. The UPP is highly regulated by ubiquitin-activating (E1), -conjugating (E2) and -ligating (E3) enzymes ensuring that a specific substrate is tagged by polyubiquitin chains for destruction by the 26S proteasome. Proteins can also be degraded by chaperone-mediated autophagy (CMA) or macroautophagy. Macroautophagy normally degrades various cellular structures (e.g. mitochondria) and is hypothesised to eliminate toxic aggregated protein species. Macroautophagy, CMA and UPP decline during normal ageing process (filled arrows), which might favor the progression of age-related diseases. Adapted from Hands et al. (2008)

Presently, there is an increasing interest over the role of autophagy in the Central Nervous System (CNS) and several evidences have implicated autophagy in neurogedenerative disorders, including polyQ diseases. The major breakthrough was provided by D. Rubinsztein and colleagues, in 2002, by being able to clear polyQ aggregates in cells, fly and mouse models of HD, using a chemical inductor of autophagy, rapamycin (Ravikumar et al., 2002; 2004). Moreover, blockage of expanded polyQ proteins expression in conditional animal models or gene silencing of

the expanded genes was followed by a rapid clearance of the polyQ proteins and their aggregates, through pathways which seemed to be UPP-independent (Regulier et al., 2003; Xia et al., 2004; Yamamoto et al., 2000). This effective clearance of expanded polyQ proteins was associated with an improvement in disease phenotype. Blockage of UPP could even be counterbalanced by stimulating autophagy (Li et al., 2008; Pandey et al., 2007). Accumulation of autophagosomes has also been found in brains of animal models and patients of HD (Kegel et al., 2000; Sapp et al., 1997). This accumulation of autophagosomes seems to be a consequence of an impaired fusion with lysosomes, compromising the subsequent degradation, rather than a sign of excessive autophagy, which was previously suggested to occur in neurodegenerative disorders. (Boland et al., 2008; Cuervo 2004; Levine and Kroemer, 2009; Wong and Cuervo, 2010a). Inhibition of autophagy through knockdown of the autophagy-related (ATG) gene in *Caenorhabditis elegans* also produced an increment in polyQ aggregates, associated with an increase in polyQ toxicity (Jia et al., 2007). Apparently, the polyQ proteins disrupt several independent protein degradation pathways, and the UPS jointly the autophagy-lysosomal pathway seem to coordinate their actions in attempt to cope with the proteotoxicity of these expanded proteins.

1.4.7. Impairment of axonal transport

Neurons are highly differentiated cells comprising a cell body and several cellular extensions specialized in stimuli input, the dendrites, and one cellular projection for output, the axon. Most often, these cellular projections constitute more than 99% of the total volume and surface area of the neuron. These extensive area and volume, which in some motor neurons are a meter away from the cell body, have to be maintained functional at the expense of an active and efficient intracellular transport system. A group of molecular motor-proteins, kinesin and dynein families, is responsible for moving the required cargos, both from the cell body to the neuronal extremities (anterograde transport) and *vice-versa* (retrograde transport) (Morfini et al., 2005). The intracellular transport is tightly regulated and assures that molecules, proteins, intracellular organeles or other cellular components reach their precise and specific intracellular site (Morfini et al., 2001). Without these mechanisms, neurons

would not be able to receive, transmit and integrate stimuli and information. Due to their architecture, neurons are very susceptible to disturbances in intracellular transport, both anterograde and retrograde. Inhibition of fast axonal transport, more associated with membrane-bound organelles, results in neuronal dysfunction and neuronal death (Sickles et al., 1996) (Figure 1.6.). Mutations in motor proteins also progress into neuronal dysfunction in humans and animal models, and moreover, changes in the regulation of fast axonal transport have been implicated in neurodegeneration (Reid et al., 2002; Hafezparast et al., 2003; Pigino et al., 2003). Several indications of alterations in fast axonal transport in polyQ-expansion disorders have been found, most notably in HD. The mutated protein in HD, huntingtin, is a vesicle-associated protein and seems to have a large role in neuronal intracellular transport (DiFiglia et al., 1995). Degeneration of neurites and vesicle accumulation were observed in HD patient brains and cultured striatal neurons expressing expanded huntingtin (Li et al., 2001; Trettel et al., 2000). In addition, expression of mutant huntingtin reduced the transport rate of vesicles containing brain-derived neurotrophic factor (BDNF) in cellular models (Gauthier et al., 2004). Mammalian neurons are extremely sensitive to reductions in the transport of neurotrophic factors, since they require a continuous delivery of surviving signals to prevent a programmed cell death (Figure 1.6.). Therefore, alterations in axonal transport in the brain can directly promote neurodegeneration through apoptosis. Accumulation of cargo-containing vesicles is not exclusive of HD and it was reported to occur in other polyQ diseases, and in most cases, prior to any sign of apoptosis or cell death, suggesting that early neuropathology stems from fast axonal transport dysfunction. Interestingly, a cytoplasmic localization of the polyQ peptides is required for the manifestation of deleterious effects over axonal transport. Mutated proteins engineered to exclusively locate in the nucleus do not disrupt intracellular transport (Arrasate et al., 2004). Moreover, there is no requirement of aggregates, oligomers or any other intermediate aggregation step (Szebenyi et al., 2003). The soluble polyQ-containing protein is efficient at inhibiting fast axonal transport, although large intracellular inclusions also represent a physical barrier to vesicular transport. Four mechanisms explaining how polyQ-expanded proteins can alter fast axonal transport have been proposed: i) steric

interference - related to the presence of large inclusions and to the spatial barrier their size represent to the transport of large materials throughout the cytoplasm; ii) sequestration of motor proteins - also dependent on the presence of intracellular aggregates which would restrain these motor protein inside the inclusion; iii) loss of function - some polyQ proteins are functionally associated to axonal transport, such as huntingtin; and iv) an enzymatic mechanism - where polyQ proteins modify the phosphorylated and dephosphorylated states of regulatory proteins, thus, altering the axonal transport (Morfini et al., 2005). This last mechanism is more consistent with the fact that low concentrations of expanded proteins are sufficient to disrupt intracellular transport. Altogether, there are strong indications that polyQ disorders are a group of neurodegenerative diseases in which alterations in axonal transport play an important role.

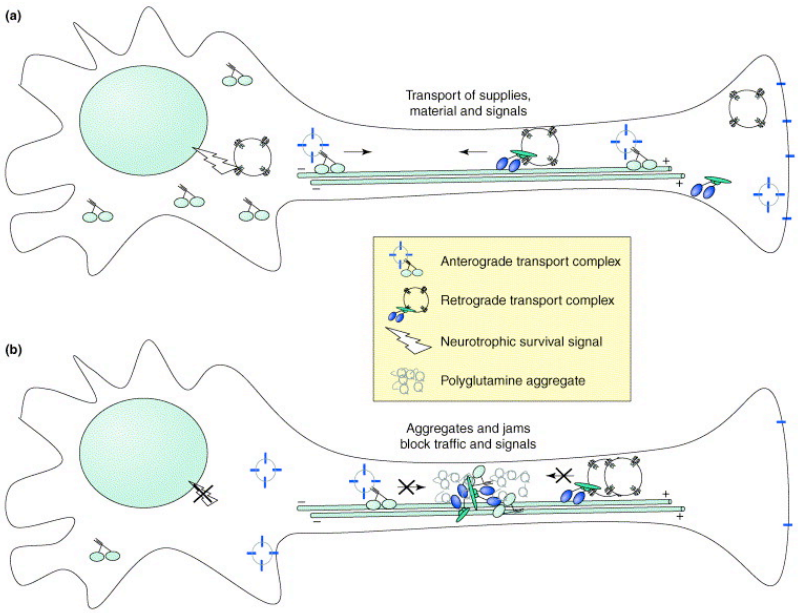

Figure 1.6. – Axonal transport in normal and diseased neurons. (**a**) Microtubule-dependent transport in healthy neurons. Anterograde and retrograde axonal transport complexes proceed along uniformly oriented microtubule tracks. Anterograde transport complexes include cargoes crucial to the function of the axon and synapse. Retrograde transport includes the transmission of neurotrophic survival signals to the cell body, influencing nuclear gene expression. (**b**) In diseased cells, aggregates and jams block traffic and signals. The formation of polyglutamine aggregates could cause transport dysfunction via the physical

blockage of transport by aggregates, or the titration of available motor protein levels, resulting in decreased transport efficiency, or a combination of these, or other mechanisms. The impairment in transport could then promote disease through decreased levels of anterograde cargoes vital for axonal or synaptic function. Furthermore, the inhibition of retrograde transport may result in reduction of neurotrophic survival signals to the cell body. Adapted from Guzik and Goldstein (2004)

1.4.8. Mitochondrial dysfunction

Mitochondria are intracellular organelles specialized in the production of energy readily available to the cell, through the synthesis of adenosine triphosphate (ATP). Because many redox and electron transference reactions are required for ATP production in mitochondria, these organelles are also major sites of reactive oxygen species (ROS) production in the cell, due to electron leakage from the respiratory chain. ROS production leads to oxidation and damage of biological macromolecules including DNA, proteins and lipids. A number of endogenous antioxidants are specialized in reversing this oxidative damage, however over a certain level the damage is irreversible and have toxic effects. Neurons are metabolically very active cells, producing and consuming great amounts of oxygen to maintain a constant energy productions required for unceasing regulation of ionic gradients and electric excitability.

Mitochondrial dysfunction has increasingly gained a central role in polyQ-induced pathogenesis. Impairment of the respiratory chain, stress-induced mitochondrial depolarization, free radical production followed by oxidative stress and disrupted metabolic pathways are examples of processes occurring during mitochondrial dysfunction in polyQ diseases (Grunewald and Beal, 1999; Panov et al., 2002; Browne and Beal, 2006). Most of the evidences of mitochondrial impairment in polyQ disorders come from HD. Indications of metabolic alterations in HD were suggested through the early observation that HD patients exhibited weight loss despite sustained caloric intake. Later on, positron emission tomography (PET) scans revealed a significant reduction in glucose metabolism in the striatum (the most affected brain area in HD) in HD patients prior to any notorious brain degeneration (Browne and Beal, 2004; Browne et al., 2008). Meanwhile, other studies have reported a decrease

around 50% in mitochondrial complex II activity in the caudate nucleus (which is part of the striatum) of HD brains, and administration of complex II inhibitors, 3-nitropropionic acid or malonate, in animal and cell models mimicked the HD phenotype (Beal et al., 1993; Brouillet et al., 1995; Gu et al., 1996). Besides having a primary role in energy production, mitochondria are also intracellular calcium (Ca^{2+}) reservoirs of great importance. High concentrations of intracellular Ca^{2+} are rapidly brought to basal levels due to transport and sequestration of the excessive Ca^{2+} into these intracellular reservoirs. Mitochondrial accumulation of Ca^{2+} in the matrix is driven by the high mitochondrial transmembrane potential, and so, very high concentrations of Ca^{2+} can promote the decrease in mitochondrial potential. Ca^{2+} loading capacity of mitochondria is also affected in polyQ disorders, namely, in cell models of HD (Milakovic and Johnson, 2005; Milakovic et al., 2006; Oliveira et al., 2006). Cells expressing the expanded polyQ protein showed reduced mitochondrial Ca^{2+} uptake capacity. Studies using isolated mitochondria incubated with polyQ proteins also revealed an increase in ROS production and a reduction in Ca^{2+} storage capacity, as a consequence of direct effects of polyQ proteins on mitochondria (Puranam et al., 2006). Indeed, expanded huntingtin has been found to be associated to neuronal mitochondrial membranes (Panov et al., 2002). Moreover, direct interaction of mutant huntingtin with mitochondria has been shown to induce mitochondrial permeability transition (MPT) pore opening, through decrease of the Ca^{2+} threshold, which triggers MPT pore opening. Mitochondria isolated from animal models of HD showed lower capacities and rates of mitochondrial Ca^{2+} transport, a decreased stability of the mitochondrial potential in response to Ca^{2+} transport, which translated into a decreased Ca^{2+} threshold for MPT pore opening (Gellerich et al., 2008). After MPT pore opening, cytochrome C is released from the mitochondria, initiating apoptotic events (Coo et al., 2004). Moreover, mitochondria from lymphoblasts of HD patients exhibited a lower mitochondrial potential and disruption of this potential at lower Ca^{2+} loads (Panov et al., 2002). These findings indicate that mitochondria exposed to polyQ proteins, particularly in HD, acquire calcium handling defects and increased sensitivity to depolarization mediated by Ca^{2+} transport (Quintanilla and Johnson, 2009). Reduction of mitochondrial Ca^{2+} buffering capacity has been strongly

linked to excitotoxicity involving the overactivation of *N*-methyl-D-aspartate (NMDA) receptors, a subtype of ionotropic glutamate receptors. Increased activation of NMDA receptors associated to a lower Ca^{2+} handling by mitochondria promote high cytoplasmatic Ca^{2+} concentrations during longer periods (Oliveira et al., 2007), which may be responsible for NMDA-induced apoptosis observed in HD brains. Other physiological processes of mitochondria are altered by the over-expression of mutant huntingtin. Normal fusion and fission dynamics of mitochondria seems to be diminished in *Caenorhabditis elegans* and other animal HD models, which compromises normal mitochondrial ATP synthesis (Wang et al., 2009; Song et al., 2011). Expanded huntingtin also affects mitochondria indirectly through other pathological mechanisms. Abnormal interactions with transcription co-activators like peroxisome proliferator-activated receptor ɣ coactivator-1 (PGC-1α), which is involved in mitochondrial biogenesis and regulates mitochondrial response to oxidative stress, interferes with co-activator´s normal function, reducing mitochondrial defenses to oxidative damage and establishing an indirect link between mutant huntingtin, mitochondrial dysfunction and oxidative stress in HD (St-Pierre et al., 2006; Weydt et al., 2006). Importantly, the brain is very susceptible to oxidative stress due to their high oxygen consumption and relatively weak antioxidant defense systems (Hands et al. 2008). Moreover, the transcription of PGC-1α is also altered by the presence of expanded huntingtin due to the interference on CREB-regulated gene expression (Cui et al., 2006), as previously discussed. Indications of mitochondrial failures have also been found in other polyQ diseases besides HD. Various expanded polyQ proteins were shown to disrupt axonal transport of mitochondria, which may lead to an abnormal distribution and to the accumulation of old and defective mitochondria in the cell (Orr et al., 2008). Moreover, expression of expanded polyQ androgen receptor decreased the number of mitochondria and impaired mitochondrial potential, followed by an increase in ROS production. Downregulation of important genes for mitochondrial function and antioxidant defense mechanisms have also been reported in SBMA (Ranganathan et al., 2009). All these data suggest that mitochondrial dysfunction may be a common and central feature in the pathogenic mechanisms of polyQ diseases.

1.4.9. Apoptosis

Degeneration of specific populations of neurons is the ultimate outcome of expression of polyQ-expanded proteins. Neuronal death in polyQ disorders occurs through a complex array of different mechanisms and pathways. Most of the pathological mechanisms triggered in the presence of toxic polyQ peptides promote the malfunction of cellular systems required for proper cell maintenance, as previously described, and lead to the activation of cell death pathways. One of these polyQ pathological mechanisms, mitochondrial dysfunction, is closely associated to cell death pathways, establishing a link between polyQ toxicity and direct activation of cell death. For this reason, enhancers of mitochondrial dysfunction, such as excitotoxicity, metabolic stress, and generation of ROS are strong inducers of cell death. Apoptosis is one of the most studied cell death pathways and is characterized by a variety of programmed cell death processes, all highly regulated and energy-dependent. A cell undergoing apoptosis exhibits a typical shrinkage of the nucleus, associated with chromatin condensation and cleavage of DNA. Later on, the nucleus breaks up into smaller particles, immediately followed by a reduction in cell volume and cell fragmentation into membrane-enclosed bodies, the apoptotic bodies. The apoptotic events are performed by the action of a group of effector proteases, the caspases. These are cysteine proteases that cleave selectively protein sequences after an aspartic acid (Asp) residue, hence, their designation of caspases. These enzymes are synthesized in the cell as inactive precursors, and are posteriorly activated by proteolytic cleavage, most often by other caspases. In their active state, caspases cleave several protein-substrates in the cell, thus the characteristic apoptotic features and ultimately cell death, are outcomes of proteolytic activity of caspases over their substrates. Caspases have been found to be activated in polyQ disorders and were even found in intracellular inclusions (Wang et al., 1999; Sanchez et al., 1999). Cytochrome C release has been reported in cells expressing expanded polyQ proteins (Li et al., 2000). The release of cytochrome C out of mitochondria is a triggering signal for the activation of apoptosis through the intrinsic pathway. Cytosolic cytochrome C brings two initiator

proteins, apoptotic peptidase activating factor 1 (Apaf-1) and procaspase 9, together into a complex, the apoptosome, which promotes procaspase 9 autocleavage in the presence of deoxyATP into its active form, caspase 9. This caspase 9 triggers the proteolysis of other inactive procaspases, initiating a caspase cascade that activates downstream effector caspases, such as caspase 3. Indeed, caspase 3, along with other effector caspases like caspase 6, has been shown to be activated in animal and cell models of polyQ disorders and their inhibition have a neuroprotective effect (Graham et al., 2006; Warby et al., 2008). Ca^{2+} has also a major role in triggering apoptosis since high intracellular concentrations of this ion increases mitochondrial membrane permeability, inducing the release not only of cytochrome C, but also of other proapoptotic proteins into the cytoplasm. Hence, any mechanisms leading to high and prolonged cytosolic Ca^{2+} concentrations are inducers of apoptosis. Excessive intracellular Ca^{2+} entry through abnormal activation of NMDA receptors and increased Ca^{2+} release from the endoplasmic reticulum through inositol-(1,4,5) triphosphate (IP3) receptor type 1 have been associated to the presence of mutated polyQ proteins (Bezprozvanny and Hayden, 2004). Altered intracellular signaling not only leads to mitochondrial-mediated activation of caspases, but also directly stimulates the activity of other intracellular cysteine proteases sensitive to high concentrations of Ca^{2+}, such as calpains, in a combined and synergistic effect of distinct proteolytic pathways (Tang et al., 2003; Chen et al., 2008). Due to its ultimate consequences, apoptosis is under a tight management of a collection of proteins, some being facilitators of its activation (pro-apoptotic), while others prevent the initiation of cell death pathways (anti-apoptotic). At normal conditions, the balance between these two kinds of proteins favors the anti-apoptotic proteins, hence, cell survival. However, a cytotoxic stimulus may increase the expression of pro-apoptotic proteins or release them from anti-apoptotic inhibition, disrupting the pro-survival balance and setting off apoptotic events. Expanded polyQ proteins can push the cell towards apoptosis by disruption in the balance of the intracellular levels of pro-apoptotic and anti-apoptotic proteins. Moreover, expression of expanded polyQ proteins have been reported to be at the basis of an up-regulation of pro-apoptotic Bax protein and a down-regulation of anti-apoptotic proteins, such as Bcl-xL (Tsai et al., 2004; Chou et al., 2006; Wang et

al., 2006a). Protein unfolding, loss of expanded polyQ proteins normal activity and sequestration of active house-keeping proteins in intracellular aggregates may also contribute to apoptosis. The presence of an expanded polyQ domain in huntingtin decreases its affinity for huntingtin-interacting protein 1 (Hip-1), increasing the amount of unbound Hip-1 in the cytoplasm and promoting the formation of Hip-1 dimers, which can activate caspase-8 (Hackam et al., 2000). Other mechanisms induced by mutant polyQ proteins have been discovered where intracellular organeles, such as endoplasmic reticulum (ER) may associate with mitochondria in the central role of apoptosis activation. In SCA2, disruption of Golgi apparatus, probably due to loss of normal ataxin-2 function, seems to have a crucial role in caspase-3 activation and ER stress which may be a common phenomenon observed in the presence of polyQ-expanded proteins (Nishitoh et al., 2002; Huyhn et al., 2003).

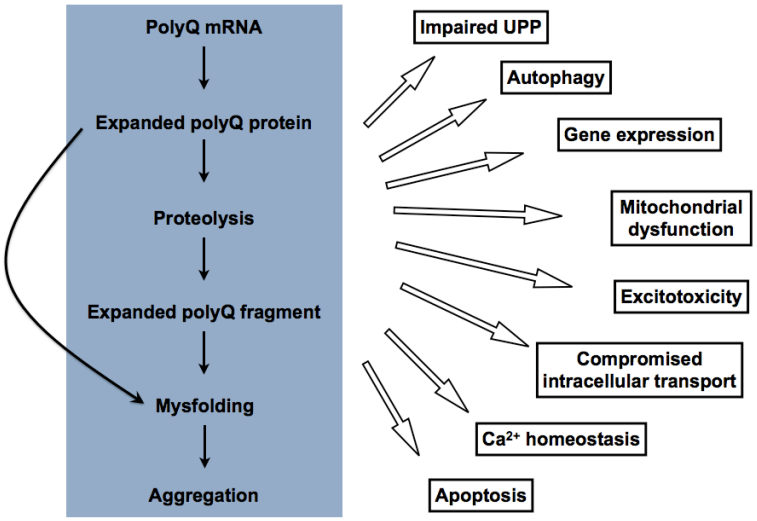

Figure 1.7. - Summary of potential pathological mechanisms involved in the pathogenesis of polyglutamine diseases. The processing of polyQ proteins is highlighted in blue background.

1.5. Spinocerebellar ataxias

Ataxia is described as a neurological sign or symptom of loss of coordination, particularly in walking movements. Therefore, a characteristic ataxic individual exhibits gait imbalance, limb incoordination and incapacities in performing gross and fine motor skills (Paulson, 2009). As a disease, ataxias comprise a large range of progressive disorders with incoordination of gait as the hallmark symptom. In most of these disorders, the movement incoordination derives from the degeneration of the cerebellar cortex and its afferent or efferent connections. Ataxia may have an acquired or a genetic origin. To identify and correctly diagnose an individual with ataxia is not always clear, since there is a phenotypic overlap between several diseases. The timing of onset of the first symptoms and family history are crucial information to distinguish between a non-hereditary disorder or a probable genetic cause, but specific biochemical and genetic testing are the major references to achieve the final diagnosis. Ataxic disorders are most often classified into non-hereditary and hereditary ataxias. The non-hereditary ataxias are separated into acquired ataxias and sporadic degenerative ataxias (Klockgether, 2007). Alcoholic cerebellar degeneration, more prevalent in heavy consumers of alcohol, and paraneoplastic cerebellar degeneration, an immune-response mediated degeneration mainly associated to malignant tumors, are two examples of acquired ataxias (Shams'ili et al., 2003). The etiology of sporadic degenerative ataxias, such as multiple system atrophy or sporadic adult onset ataxia, is still largely unknown (Gilman et al., 1999; Abele et al., 2007). The hereditary ataxias include the autosomal recessive ataxias and the dominantly inherited SCAs. Patients with a disease onset as early as 25 years old and no reports of such disorder in other generations, autosomal recessive ataxias should be proposed, with Friedreich's ataxia (FRDA) being the most common (Ribai et al., 2007). On the other hand, if one of the parents had a similar pathology, SCA is most likely. Moreover, since 20% of patients diagnosed with sporadic adult-onset ataxia turn out to exhibit a pathogenic genetic mutation regardless of a negative family history, molecular testing for FRDA and SCAs

should be advised if no evidences for an acquired ataxia or multiple system atrophy are present (Klockgether, 2008).

Table III – Genes and mutations that cause autosomal dominant cerebellar ataxias.

Disease	Gene	Mutation	Key symptom in addition to cerebellar ataxia
Polyglutamine expansion SCAs			
SCA1	*ATXN1*	CAG repeat	Early swallowing and respiratory signs
SCA2	*ATXN2*	CAG repeat	Slow eye movements
SCA3	*ATXN3*	CAG repeat	..
SCA6	*CACNA1A*	CAG repeat	..
SCA7	*ATX7*	CAG repeat	Visual loss
SCA17	*TBP*	CAG repeat	Dementia
DRPLA	*ATN1*	CAG repeat	Epilepsy
Non-coding expansion SCAs			
SCA8	*ATXN8* and *ATXN80S*	CTG repeat	..
SCA10	*ATXN10*	ATTCT	..
SCA12	*PPP2R2B*	CAG repeat	..
SCA31	*BEAN-TK2*	TGGAA repeat	..
SCA36	*NOP56*	GGCCTG repeat	..
Conventional mutations SCAs			
SCA5	*SPTBN2*	Missense, in-frame deletion	..
SCA11	*TTBK2*	Frameshift	..
SCA13	*KCNC3*	Missense	Mental retardation
SCA14	*PRKCG*	Missense	Myoclonus
SCA15/16	*ITPR1*	Missense, deletion	..
SCA20	..	Duplication	Dysphonia
SCA27	*RGR14*	Missense, frameshift	..
SCA28	*AFG3L2*	Missense	Ptosis
SCA35	*TGM6*	Point mutation	Ocular dysmetria
Loci (test unavailable)			
SCA4	..	..	Sensory neuropathy
SCA18	..	..	Sensory neuropathy
SCA19	..	..	..
SCA21	..	..	Mental retardation
SCA22	Allelic to SCA19?	..	Mental retardation
SCA23	..	..	..
SCA25	..	..	Sensory neuropathy
SCA26	..	..	..
SCA30	..	..	..
SCA32	..	..	Mental retardation
SCA34	..	..	Sensory neuropathy

Adapted from Durr (2010). (.. – unknown)

SCAs are autosomal dominant inherited disorders that are very different in terms of symptoms and genetic causes. In these progressive neurological pathologies, the cerebellum slowly degenerates, often accompanied by alterations in the brainstem and other regions of the CNS and more rarely in the peripheral nervous system (Taroni and DiDonato, 2004). Traditionally, SCAs were classified according to the characteristic pattern of the affected brain regions in each disorder: olivopontocerebellar atrophy, spinopontine atrophy, cortical cerebellar atrophy, as examples. However, this terminology has proven to be ineffective as variations in brain areas showing degeneration are common within the same disease, between different individuals, and even in the same family. These differences in the affected areas are also associated to heterogenous clinical manifestations (Paulson, 2009). The continuous discovery in the past decades of the genes mutated in some of these SCAs, the most prevalent at least, have facilitated the comprehension and the diagnosis of these disorders through molecular testing. Nowadays, SCAs are named and ordered according to the discovery of the disease-related gene, in a total of at least 30 disorders (Paulson, 2009) (Table III). Despite the variety in phenotype, cerebellar impairment is a common trade for SCAs. Some SCAs are purely cerebellar affecting all layers of cerebellar cortex (molecular, Purkinje cell, and granule cell layers) and major deep nuclei of the cerebellum. For example, SCA6 is a cerebellar ataxia with specific degeneration of one neuronal population, the Purkinje cells. Other SCAs have clearly a wider extracerebellar brain component, being common among SCAs the damage in the basal ganglia, spinal cord and peripheral nerves. The involvement of particular extracerebellar brain regions and the manifestations of individual clinical features may even be distinctive hallmarks of some SCAs (Figure 1.8.), contributing to the identification of a specific disorder: the cortical involvement in SCA17, the retinal degeneration in SCA7 and epilepsy in SCA10. Autosomal dominant ataxias are divided in three groups based on the type of mutation that is responsible for the disease onset: ataxias caused by conventional mutations; non–protein coding repeat expansion ataxias; and expanded CAG/polyQ ataxias (Paulson, 2009).

Ataxias caused by conventional mutations are the most recent category of SCAs and comprise all the hereditary autosomal dominant ataxias deriving from

deletions, insertions, missense mutations, nonsense mutations and splice site mutations in particular genes or affecting particular genomic sequences. Disorders included in this classification are: SCAs 5, 11, 13, 14, 15/16, 20, and 27. However, more examples are expected to be added as technological progress and genome screening will improve our knowledge on genetic defects behind the rare neurological diseases. The genes or genomic sequences affected in this group of SCAs is very wide and no single biological link or pathway can be established between them, indicating that degeneration of cerebellum and brainstem may be a common outcome of dysfunction in distinct cellular pathways (Paulson, 2009). The onset of these SCAs occurs characteristically early in life, most often in childhood, but symptoms are not as severe as observed for the juvenile forms of SCAs of other classes. In fact, these diseases progress little in adulthood and patients have a normal life expectancy. Pathologically, conventional mutation SCAs are usually "pure" cerebellar disorders with the neurodegeneration confined to the cerebellum, letting the brainstem undamaged (Dürr, 2010).

Non–protein coding repeat expansion ataxias are autosomal hereditary ataxias caused by DNA repeat (tri- or pentanucleotide) expansions in specific genes, although these expansions are not inserted in protein-coding sequences. Therefore, the expanded DNA repeats are not translated into an aberrant amino acid sequence in disease-associated protein. It is not entirely clear how these expansions promote neurodegeneration even so, the proposed pathological mechanism for these disorders implies an accumulation and gain of function by RNA transcripts containing the expanded repeats (Todd and Paulson, 2010). As previously discussed for untranslated trinucleotide expansion disorders, the accumulation of these expanded transcripts in the cell sequester RNA-binding proteins and disrupt normal RNA splicing machinery, altering a great number of other unrelated transcripts, which culminate in the pathological symptoms. SCAs 8, 10 and 12 are the ataxias included in this group, although discussion is still open on the pathological mechanism occurring in SCA8 (Moseley et al., 2006). Evidences have been gathered supporting the translation of the DNA repeat expansions into protein in SCA8 pathology.

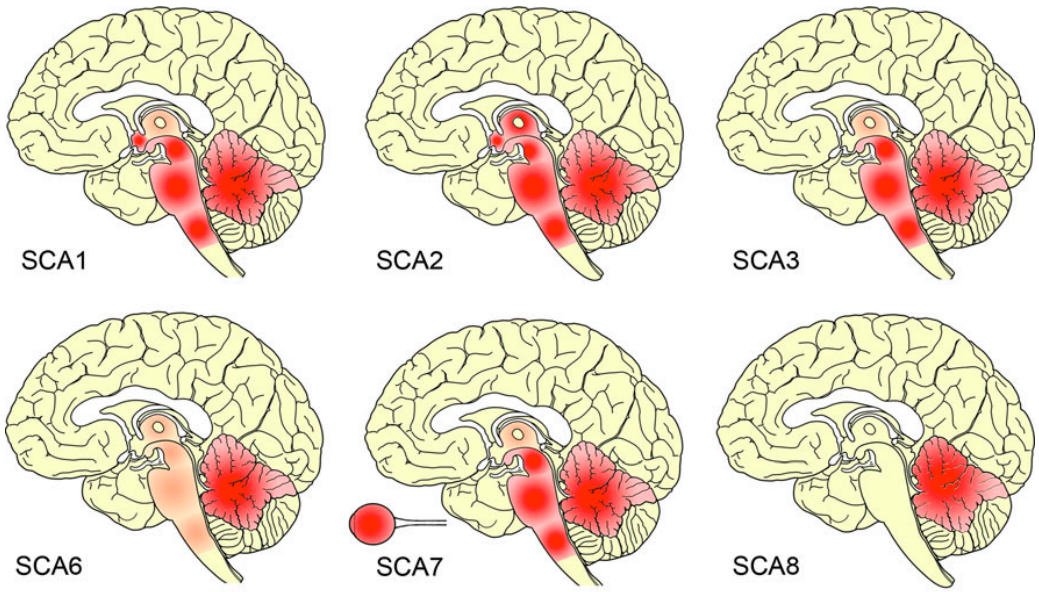

Figure 1.8. - Distribution of neuronal loss in the brain of patients with SCA 1, 2, 3, 6, 7 and 8. Diagram representation of midsagittal sections through the cerebrum, cerebellum and brainstem of the human brain. The degree of neuronal loss in the cerebral cortex, basal forebrain, thalamus, cerebellum and brainstem is indicated by red (severe) or light red (marked). Adapted from Seidel et al. (2012)

The expanded CAG/polyQ ataxias are the best studied category of all the autosomal dominant ataxias. SCA 1, 2, 3, 6, 7, 17 and DRPLA are the pathologies included in this group. As the name implies, these SCAs are caused by CAG repeat expansions in coding regions of distinctive genes for each disease. The CAG expansion is later translated as an expanded polyQ tract in the affected protein, and for this reason, these disorders are also known as polyQ ataxias and members of the polyglutamine diseases. Gait impairment is the characteristic first symptom with onset usually in adulthood, in the 3rd or 4th decade of life (Globas et al., 2008). For some polyQ SCAs, there is an inverse correlation between the CAG length and the disease onset (Schols et al., 2004). Although ataxia is the classical symptom, patients with polyQ SCAs exhibit clinical manifestations of extracerebellar involvement (Guerrini et

al., 2004; Schulz et al., 2010). Neurological dysfunction and neurodegeneration are more diffuse than in other classes of SCAs. Diplopia, dysarthria, impaired handwriting, and episodic vertigo can even precede ataxia as first symptoms (Globas et al., 2008). As disease progresses, the clinical manifestations worsen and become increasingly complex, culminating in death due to brainstem failure (Dürr, 2010). Clinical manifestations are also dependent on the CAG repeat length. A wide range of abnormal eye movements are also commonly observed in polyQ SCAs. Genetic anticipation is registered for some polyQ SCAs with younger generations exhibiting increased severity of symptoms and sooner disease onset. Most of the times, anticipation is associated with an increase in CAG expansion through sucessive generations. Anticipation is considered to be a hallmark of polyQ SCAs (Stevanin et al., 2000; Dürr, 2010).

1.6. Machado-Joseph disease/Spinocerebellar ataxia type 3

Machado-Joseph disease (MJD; MIM #109150), or spinocerebellar ataxia type 3 (MJD/SCA3), is a dominantly inherited autosomal neurodegenerative disorder, belonging to the expanded CAG/polyQ ataxias (Bettencourt and Lima, 2011). Initially designated as Machado disease, MJD first diagnosis was made in a family (Machado) of Portuguese immigrants in Massachussets, United States of America (Nakano et al., 1972). It was described as an hereditary ataxia, starting around the 4th decade of life, with gait impairment and ataxia as initial symptoms, most often associated with endgaze nystagmus, mild dysarthria, hyporeflexia and distal muscle atrophy. After its first description in 1972, this progressive neurodegenerative disorder was diagnosed in other families, some of Azorean descent (Thomas and Joseph), as being independent clinical entities and bearing different terminologies: nigro-spinodentatal degeneration with nuclear ophthalmoplegia, autosomal dominant striatonigral degeneration and Azorean disease of the nervous system (Woods and Schaumburg, 1972; Rosenberg et al., 1976; Romanul et al., 1977). The subsequent diagnosis of all forms of manifestations of this pathology in Portuguese families living in Portugal (Azores islands and mainland) led to the congregation of the different clinical syndromes under one

designation, Machado-Joseph disease (Coutinho and Andrade, 1978). Later on, in 1993 and 1994, respectively, the genes associated with MJD and SCA3, two distinct disorders at the time, were mapped to the same chromosomal region 14q32.1, and thereon, they were recognized as one single clinical entity (Takiyama et al., 1993; Kawaguchi et al., 1994; Haberhausen et al., 1995). For this reason, MJD and SCA3 are currently the most common nominations for this hereditary ataxia and are used interchangeably.

1.6.1. Clinical manifestations and prevalence

MJD is the most common inherited autosomal dominant ataxia in several populations and it is usually considered the most frequent SCA in the world (Riess et al., 2008). Even so, MJD is a rare disorder with a prevalence of 1:100000 in continental Portugal. However, due to its dominantly autosomal manner of inheritance and to founder effect, MJD exhibits higher levels of prevalence in specific areas of the world, most notably in the Azores Islands, where its highest expression is registered (1/239, in Flores Island) (Bettencourt et al., 2008). Initially, MJD was thought to be associated to a Portuguese background and that its worldwide distribution was a consequence of the Portuguese discoveries in the 15th and 16th centuries (Schöls et al., 2004). The development of molecular testing for MJD has altered this preconception. Since then, MJD has been diagnosed in patients of different ethnic backgrounds and unrelated geographically to portuguese diaspora. The frequency of MJD among other SCAs varies between populations. It is very high in Brazil, where it can account for 92% of all cases of SCA, Portugal (58-74%), China (48-49%), Germany (42%) and Japan (as high as 63%). MJD is less frequent in Canada (24%) and United States of America (21%) and considered to be rare in South Africa (4%) and in the Italian (1%) population (Bettencourt and Lima, 2011).

MJD is clinically a very heterogenous neurodegenerative disorder and phenotypically is associated to a wide spectrum of motor and non-motor symptoms. This heterogeneity is a consequence of the multitude of neuroanatomical systems affected in MJD, most notably the cerebellar, pyramidal, extra-pyramidal, motor neuron and oculomotor systems (D'Abreu et al., 2010). Ataxia is the typical first

symptom observed in MJD, although some patients complain of diplopia, before any impairment in movement coordination (Coutinho, 1994). Gait instability usually sets around the 4th decade of life, but the onset of the disease might vary between 4 and 70 years old. MJD is a fatal disease with a mean survival of 21 years after onset, although it can span from 7 to 29 years (Kieling et al., 2007). Progressive cerebellar ataxia is the major neurological sign, not rarely associated with limb incoordination. Intentional tremor is visible in some patients, and as disease progresses, dysarthria and dysphagia are observed in MJD. Pyramidal involvement is also a common feature of MJD, with the lower limbs being predominantly more affected than the upper limbs. Spasticity may be a prominent sign in some patients and even cases of spastic paraplegia have been reported (Sakai and Kawakami, 1996). Dystonia, fasciculation of facial and lingual muscles and parkinsonism, in form of bradykinesia and rigidity, are also frequently associated with MJD (Rosenberg, 1992; Jardim et al., 2001). Degeneration of motor fibers might even induce muscle atrophy, usually with more expression distally, producing foot drop. Alterations in eye movements are significative and important signs in MJD diagnosis: gaze-evoked nystagmus, altered saccadic movements, decrease smooth pursuit gain, impaired vestibulo-ocular reflex, supranuclear vertical gaze palsy, and even, external progressive ophtalmoplegia (Gordon et al., 2003). Another distinctive feature more prevalent in MJD than in other SCAs is the "bulging eyes appearance", which is due to the conjugation of eyelid retraction and reduced blinking (Coutinho, 1994). Sensory fibers are also heavily affected, compromising tactile and proprioceptive sensibility in wide areas of the body and originating neuropathic pain. MJD patients also complain of nocturia, urinary incontinence, intolerance to low temperatures and hypohidrosis as result of alterations in the autonomic system, namely the genitourinary and sudomotor systems (Yeh et al., 2005). Recently, non-motor symptoms have been related to MJD with specially attention being given to sleep related disorders. Problems with sleeping and daytime sleepiness have been reported in a large percentage of MJD patients and two specific conditions have been associated to MJD: restless legs syndrome and rapid eye movement (REM) sleep behaviour disorder (Friedman et al., 2003). Insomnia is also a common complain (D'Abreu et al., 2009). Dementia is not usually observed in MJD,

although minor deficits in cognitive functions, changes in normal behaviour and reduction of verbal and visual memory do occur. Chronic pain, fatigue and ultimately depression due to loss of independence and quality of life are also usual trend in MJD patients (Cecchin et al., 2007; Franca et al., 2007).

MJD is a very heterogenous disorder, exhibiting not only a wide range of neurological signs and other clinical manifestations, but also a great variability in the age of onset. The high level of pleomorphism in different MJD patients was observed already at the first descriptions and it is a constant characteristic throughout the history of the disease. In an attempt to classify this diversity in phenotypes, Coutinho and Andrade developed a system in 1978, where MJD was divided in 3 subtypes in accordance with clinical manifestations observed in affected individuals. Almost every patient exhibits cerebellar signs, external progressive ophtalmoplegia and some degree of pyramidal sign. The distinction between clinical types is based on the presence or absence of particular extrapyramidal and peripheral signs. In type 1 ("type Joseph" - 13% of patients), the disease has an early onset (mean of 24.3 years), symptoms progress rapidly, with marked spasticity, rigidity, bradykinesia, dystonia and relatively little cerebellar ataxia. Type 2 ("type Thomas" - the most common 57%) disease is characterized by classical cerebellar ataxia and ophtalmoplegia with presence or absence of pyramidal (upper motor neuron) signs. Extrapyramidal signs are absent or have reduced expression. First symptoms occur at middle age (mean of 40.5 years) and the progression of the disease is slow, or after 5 to 10 years, alters to another clinical type by expression of additional neurological signs. Type 3 ("type Machado" - 30%) exhibits the later onset (mean of 46.8 years) and it is distinguished by the presence of peripheral polyneuropathy over a characteristic profile of cerebellar ataxia and external progressive ophtalmoplegia (Bettencourt and Lima, 2011). Later on, other authors have described a type 4 to include patients showing signs of dopa-responsive parkinsonism, and even a type 5 has recently been proposed, after the description of two patients exhibiting spastic paraplegia with no cerebellar ataxia (Suite et al., 1986; Sakai and Kawakami, 1996). Although the clinical types are an attempt to simplify MJD heterogeneity, they are of relative small value in clinical practice. There is a considerable overlap between different MJD types and some patients exhibit symptoms

of more than one clinical type. Moreover, one patient might even change of MJD clinical type during the progression of the disease (Fowler, 1984).

1.6.2. Neuropathology

MJD is a neurodegenerative disorder affecting primarily the CNS. In general, brains from MJD patients have a lower weight in comparison to brains from healthy individuals with no psychiatric or neurological history (Rüb et al., 2008; Horimoto et al., 2011). Degeneration of the cerebellum, pons, medulla oblongata, all cranial nerves except the olfactory and optical nerves, are a constant trademark of MJD brains, as well as the depigmentation of the substantia nigra (Rüb et al., 2002; 2003b) (Figure 1.9.). Besides the cerebellum and the brainstem, magnetic resonance imaging (MRI) of MJD patients have also shown a reduction in volume of the caudate and putamen nuclei (Klockgether et al., 1998).

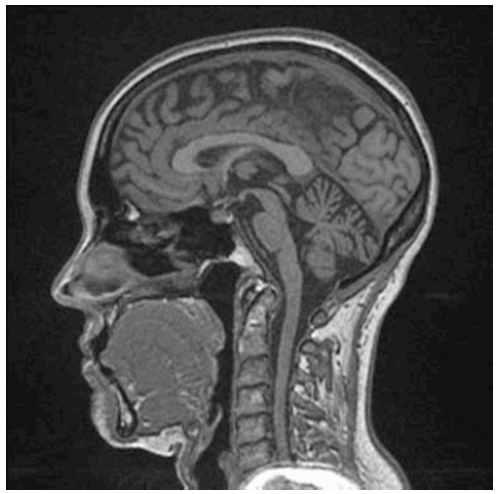

Figure 1.9. - Sagittal, T1-weighted MRI of a 54-year old SCA3 patient with 70 CAG repeats and symptoms for 5 years demonstrating moderate atrophy of the cerebellar vermis and enlargement of the fourth ventricle as well as mild pontine shrinkage. Adapted from (Riess et al., 2008).

The recent developments in imaging technologies have increased our knowledge regarding neurodegeneration in MJD and added a vast and wide list of

nuclei and other gray matter structures, which are known today to be altered in this disorder. The motor cerebellothalamocortical pathway (i.e., cerebellar dentate nucleus, pontine nuclei, thalamic ventral lateral nucleus), nuclei of the basal ganglia-thalamocortical tract, the substantia nigra, ventral tegmental area, non-motor thalamic nuclei (lateral geniculate body, pulvinar), subcortical nuclei of somatosensory pathways (e.g., ventral posterior lateral and ventral posterior medial thalamic nuclei, cuneate and gracile nuclei, Clarke's column), the vestibular nuclei, eye movement-related (e.g., oculomotor, trochlear, abducens, reticulotegmental nucleus of the pons) and ingestion-related (i.e., trigeminal, facial, ambiguus, dorsal motor vagal, solitary nuclei and reticular formation) brainstem nuclei, among other midbrain and brainstem nuclei (e.g., red, arcuate prepositus hypoglossal, inferior olive) exhibit alterations in MJD patients (Rüb et al., 2005; Rüb et al., 2006a; Rüb et al., 2006b; Riess et al., 2008). Single-photon emission computed tomography (SPECT) studies of MJD brains have even shown alterations in blood perfusion of the parietal, frontal, temporal lobes and the basal ganglia in addition to the vermis and hemispheres of the cerebellum (Etchebehere et al., 2001). A decrease in Fluorine-18-L-dihydroxyphenylalanine (18F-Dopa) uptake was also observed in brain areas not traditionally altered in terms of morphology in MJD pathology, such as the cerebral cortex and the striatum (Taniwaki et al., 1997). Nowadays, MJD is no longer seen as a neurodegenerative disorder with an olivopontocerebellar pattern as in its first descriptions; moreover, a degeneration spread over more regions of the CNS might even explain the diversity in symptoms and the heterogeneity of the disease. Although the chronological evolution of neurodegeneration in MJD is not well established, the progression of atrophy is not the same for all brain regions. The cerebellar dentate nucleus, the substantia nigra, the vestibular nuclei, eye movement-related nuclei, red and reticular nuclei are usually the first areas to show alterations in MJD progression. The thalamus, ingestion-related nuclei, cranial nerves and other pontine nuclei along with the inferior olive are affected later on in disease development (Iwabuchi et al., 1999; Rüb et al., 2005). The degeneration of pons and midbrain seems to be age-dependent, whereas the duration of the disease has been correlated to temporal or occipital lobe and globus pallidus atrophy (Onodera et al., 1998). PET scans of asymptomatic MJD patients using

fluorine-18-fluorodeoxyglucose (FDG) has uncovered a decrease in radioactively labelled glucose consumption in cerebellar hemispheres, brainstem and occipital, parietal and temporal cortices, suggesting that MJD pathological alterations might begin prior to any neurological sign (Soong and Liu; 1998). The wide distribution of affected gray matter rivals with the relatively minor involvement of white matter in MJD neuropathology. Alterations in white matter associated with MJD are the degeneration of peripheral and cranial nerves, atrophy of vestibulospinal tract, spinocerebellar tract, cuneate and gracile fascicles and alterations in cerebellar peduncles and trapezoid body (Iwabuchi et al., 1999; Rüb et al., 2007; Riess et al., 2008). MRI has indicated axonal dysfunction even in the absence of measurable anatomical alterations in white matter (D'Abreu et al., 2009).

1.6.3. Genetics of Machado-Joseph disease

MJD is an inherited genetic disease transmitted in an autosomal dominant pattern with full penetrance. It was only in 1993 that MJD locus was mapped in the long arm of chromosome 14, in the region 14q24.3-q32 (Takiyama et al., 1993). A dynamic mutation, an expansion in the number of a CAG trinucleotide motif, located in the same chromosomic region (14q32.1) was found to be present in every MJD patient of a studied family (Kawaguchi et al., 1994). At the time, this unknown gene was named *MJD1*, although nowadays the official denomination is *ATXN3* gene. Further investigation revealed that *ATXN3* gene is the only gene associated with MJD and it extends through 48kb, containing a total of 11 exons (Ichikawa et al., 2001). The CAG tract susceptible to mutation is located on exon 10 (Figure 1.10.). More recently, two additional exons 6a and 9a, were proposed (Bettencourt et al., 2010). Thus, in terms of molecular genetics, MJD is a CAG/polyQ SCA sharing a common pathological mutation with SCA1, 2, 6, 7, 17, SBMA, HD and DRPLA, an expansion of CAG repeats.

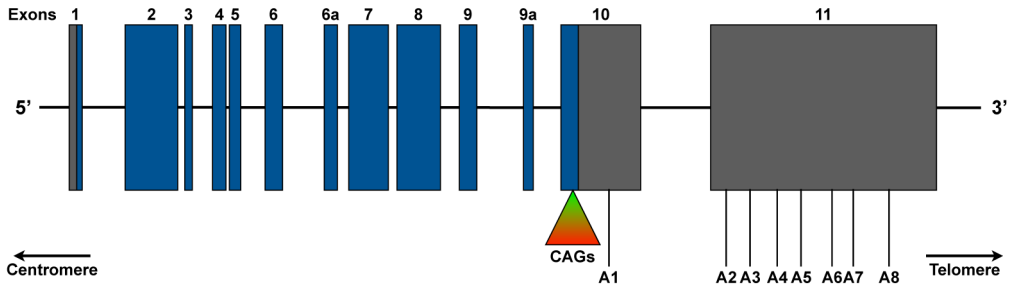

Figure 1. 10. - Schematic representation of the *ATXN3* gene structure. Exons are numbered from 1 to 11 and are represented as boxes. Blue boxes indicate the coding regions, grey boxes represent the untranslated regions (UTRs). The CAG tract is located on exon 10. Polyadenylation consensus sequences are marked from A1 to A8.

MJD is a polyQ disorder and a number of previously described features of this group of diseases are also found in MJD. Normal individuals have a CAG tract in their exon 10 of *ATXN3* gene, however in these individuals the number of repeats is confined between 12 and 44. CAG repeats well established with pathology span from 55 to 87 repeats (Maciel et al., 2001) (Table II). As in other polyQ diseases, although rare for MJD, there is an intermediate range of alleles from 45 to 54 CAG repeats that exhibit incomplete penetrance, 45 CAG repeats being the shortest record associated to MJD and 51 CAG repeats the longest tract found in a healthy individual (Maciel et al., 2001; van Alfen et al., 2001; Padiath et al., 2005). Another rare event in MJD is homozygosity for expanded alleles, which seems to be accompanied by worsen clinical manifestations, severe progression and earlier onset, than those observed in heterozygous patients (Sobue et al., 1996; Carvalho et al., 2008). Genetic and haplotype studies have identified four independent MJD haplotypes, although two of them represent 94% of all MJD families analysed, indicating a reduced mutational rate (Gaspar et al., 2001). Therefore, two mutational events and their founder effects explain almost the entire worldwide distribution of MJD. These two mutational events occurred at different times. The first and oldest event (5,774 ± 1,116 years old) is associated with an Asian origin, contradicting the usual idea of Portuguese/Azorean origin. The distribution of the latest mutational event (1,416 ± 434 years old) is linked

to recent Portuguese emigration (Gaspar et al., 2001; Martins et al., 2007).

As in other polyQ diseases, there is an inverse correlation between the number of CAG repeats in the expanded allele and the appearance of first symptoms. Longer CAG tracts are associated with younger ages of onset (Maciel et al., 1995; Maruyama et al., 1995). The same pattern of inverse correlation is also observed for the mRNA levels of *ATXN3* gene transcripts (Bettencourt et al., 2010). Besides earlier age of onset, longer expanded CAG tracts have also been correlated to the manifestation of clinical symptoms as pseudoexophthalmos and pyramidal signs (Takiyama et al., 1995). Anticipation is another phenomenon characteristic of polyQ disorders and also present in MJD. Normal CAG-range alleles are transmitted unchanged, however expanded alleles are prone to further extension in the number of trinucleotide repeats over generations (Igarashi et al., 1996; Tsuji et al., 1997). Anticipation is fed on the intergenerational germinal instability observed for the CAG tract and successive generations of an affected MJD family progressively exhibit earlier ages of onset and severe phenotypes. In MJD, intergenerational instability has greater expression when transmitted through male lineage, therefore, increasing the risk of earlier onset in offspring from affected fathers (Igarashi et al., 1996). Polymorphisms interrupting a pure CAG stretch have been found both in normal and expanded alleles (CAA, in third and sixth position; AGG, in 4th position of the CAG tract) (Kawaguchi et al., 1994). Interestingly, CGG/GGG polymorphisms were found at the 3'-end of the CAG tract and the CGG variation is characteristically found only in alleles with more than 20 CAGs, suggesting that this variant might be associated with CAG instability (Limprasert et al., 1996). Expanded CAG repeat instability is not exclusive of MJD; it is a shared feature with other polyQ disorders and even to other non-CAG triplet repeat pathological conditions. The mechanism behind the elongation of the CAG tract into a dynamic mutation is not fully understood. Studies on the distribution and frequency in the population of different CAG repeat lengths in the *ATXN3* locus support an elongation mechanism containing multiple steps, most probably based on gene conversion and DNA slippage during DNA replication (Martins et al., 2006). A common misconception is to regard the intermediate size alleles as the origin of new pathological expanded mutations through additional expansion of CAG repeats.

Surprisingly, the source of new mutated alleles seems to be the smaller CAG tract-containing alleles (Lima et al., 2005). Variations in the instability of CAG tracts between different regions of MJD brains, somatic mosaicism, have also been reported. In this respect, the cerebellar cortex displayed shorter expanded repeat sizes than other parts of the brain (Lopes-Cendes et al., 1996; Hashida et al., 1997). Other factors besides the CAG expansion size seem to influence MJD onset and progression. Variability within MJD families is lower than variability between different MJD-affected families, suggesting that other genetic factors might have a major contribution in the disease, although environmental factors can not be ruled out (DeStefano et al., 1996). Search for additional genes with modifier activity on the course of MJD is still ongoing, however a few correlations have already been discovered. The size of CAG repeat of other SCA-associated gene, namely SCA2 - *ATXN2* gene was previously correlated with the severity of fasciculations observed in MJD patients, suggesting an interplay between these two CAG/polyQ disease-related genes (Jardim et al., 2003). Moreover, it has been observed that women have later onset of the disease in comparison with brothers with the same CAG repeat length (Kawakami et al., 1995). However, a sex effect is still not confirmed for MJD (Dürr et al., 1995).

1.6.4. *ATXN3* gene transcripts

The *ATXN3* gene is ubiquitously expressed with all adult tissues tested exhibiting detectable levels of *ATXN3* mRNA (Ichikawa et al., 2001). The *ATXN3* gene codes for a protein with an estimated molecular size of 42 kDa, ataxin-3. In the brain, *ATXN3* transcription is detected both in neurons and glial cells, although neurons exhibit higher levels of expression (Nishiyama et al., 1996). Different isoforms of *ATXN3* mRNA transcripts have been proposed and identified based on alternative splicing variants and alternative polyadenylation sites. Northern blot analysis allowed to set the size of four of these different *ATXN3* gene transcripts approximately around 1.4, 1.8, 4.5 and 7.5 kb (Ichikawa et al., 2001). *MJD1a* was the first description of an *ATXN3* gene product, in 1994 (Kawagushi et al., 1994). Afterwards, three other transcripts (*pMJD1-1*; *pMJD2-1*; *pMJD5*) were reported and all differed from the original *MJD1a* transcript by different C-terminals (Goto et al., 1997). *MJD1a*

comprises the first 10 of the 11 exons present in the *ATXN3* gene. The later and longer variants contained exon 11 in its structure. A fifth variant, named *H2*, was described in 2001 and is characterized by a similar amino acid sequence to transcript *pMJD1-1* but lacking exon 2, due to alternative splicing (Ichikawa et al., 2001) (Figure 1.10.). Most recently, about 56 splicing variants for the *ATXN3* gene were reported as outcome of individual or combined contributions of four independent splicing mechanisms (Bettencourt et al., 2010). Thus, alternative splicing events is adopting an increasing importance in the overall diversity and variability of the *ATXN3* gene expression. In the multitude of splicing variants, more relevance have been given to two *ATXN3* gene products that vary in the presence or absence of exon 11 in their C-terminus. Recent data has concluded that the longer exon 11-containing variant is the most widely expressed and the most common and abundant isoform in the brain. The translated amino acid sequence of each of these two splicing variants (presense/absence of exon 11) were found to have different biochemical properties, when a CAG-expanded allele is present and expressed, which might be relevant to the pathogenic mechanism of MJD (Harris et al., 2010).

1.7. Ataxin-3

Ataxin-3 is the protein coded by the MJD-associated gene, *ATXN3*. Initially, it was described as a peptide containing 339 amino acids and an additional variable stretch of glutamines. Since then, several isoforms of the protein have been observed or suggested with some modifications to the original described structure. It is a relatively well conserved protein throughout species, having been identified in unicellular eukaryotes, plants, fungi and animals, including arthropods, platyhelminthes, nematodes and vertebrates. In humans, ataxin-3 has a molecular weight of approximately 42 kDa in healthy individuals, depending on the isoform, and it is ubiquitously expressed throughout the body, being present in different tissues and cell types. The same wide spread expression is also found in the brain, although the expression levels differ throughout different brain regions. Intracellularly, ataxin-3 has been found both in the cytoplasm and in the nucleus of different cell types, although in

neurons it has a predominantly cytoplasmic distribution (Paulson et al., 1997; Schmidt et al., 1998; Trottier et al., 1998; Ichikawa et al., 2001).

Ataxin-3 is arranged in a globular well-structured N-terminal domain (the first 182 amino acid residues), the Josephin domain, together with a more loose and flexible C-terminal, containing 2 or 3 ubiquitin-interacting motifs (UIMs) (depending on the isoform) and a variable polyQ tract (Masino et al., 2003) (Figure 1.11.). The Josephin domain has a papain-like structure with a globular catalytic domain and a helical hairpin and is responsible for the enzymatic activity of ataxin-3. The presence of specific and highly conserved residues in Josephin amino acid sequence and the study of its nuclear magnetic resonance (NMR) spectroscopy structure suggested a similarity to deubiquitinating cysteine proteases (Burnett et al., 2003; Mao et al., 2005; Nicastro et al., 2005). Indeed, the presence of triad of amino acid, cysteine (C14), histidine (H119) and a asparagine (N134), in the catalytic pocket is characteristic of cysteine proteases and reminiscent of ubiquitin C-terminal hydrolases (UCH) and ubiquitin-specific processing proteases (USP/UBP) (Albrecht et al., 2004). Another amino acid residue in the N-terminal of Josephin, glutamine (Q9), is also necessary for optimal activity. Additionally, the Josephin domain contains also two ubiquitin binding sites: one, inside the catalytic cleft, and a second, on the surface opposite to the catalytic site (Nicastro et al., 2009). The ubiquitin protease activity (i.e. cleavage of isopeptide bonds between two ubiquitin moieties) of ataxin-3 was initially predicted through integrative bioinformatics studies; since then, ataxin-3 ability to cleave ubiquitin chains has been well established through biochemical studies (Burnett et al., 2003; Scheel et al., 2003; Berke et al., 2005; Winborn et al., 2008). Nowadays, ataxin-3 and other Josephin domain-containing proteins are considered part of an independent superfamily of cysteine deubiquitinating enzymes (DUBs) (Tzvetkov and Breuer, 2007). Interestingly, a deneddylase activity has also been described for ataxin-3. Neural precursor cell expressed developmentally downregulated 8 (NEDD8) is an ubiquitin-like molecule and it can be conjugated to specific proteins in a process resembling ubiquitination. The importance of neddylation to protein's function is still in debate however, ataxin-3 has shown to be able to interact and cleave this ubiquitin-like motif from substrates, indicating a possible role in NEDD8-dependent pathways (Ferro et al., 2007).

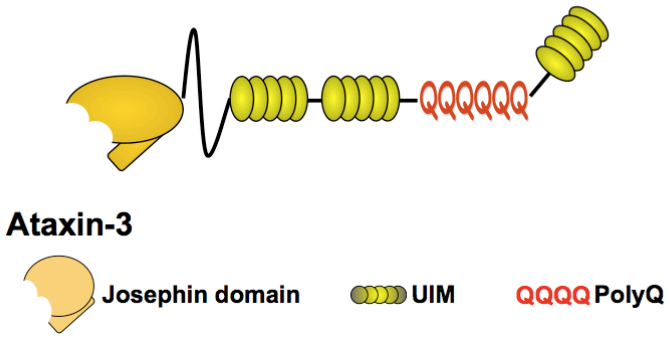

Figure 1.11. – Schematic representation of human ataxin-3 protein. It is depicted the globular catalytic domain (Josephin) is located in the N-terminal of the protein, follow by two or three ubiquitin-interacting motifs (UIMs), depending on the isoform. The polyQ tract is located in the C-terminal, after de second UIM.

The UIMs are folded into alpha helix (α-helix) secondary structures and interact with ubiquitin moieties. Ataxin-3 might have 2 or 3 UIMs in its constitution, depending on the isoform. The first two UIMs are aligned one next to the other, separated by a short linker, just prior to the polyQ domain (Donaldson et al., 2003; Chai et al., 2004). The first two UIMs cooperate synergistically in the binding of ubiquitin molecules (Song et al., 2010). In the isoforms containing a third UIM, this is located in the C-terminal of ataxin-3, after the polyQ domain. The third UIM is not essential for an efficient ubiquitin binding and its function is not completely understood (Burnett et al., 2003; Donaldson et al., 2003; Chai et al., 2004). Interestingly, 3 UIMs ataxin-3 is the most common isoform in the human brain (Harris et al., 2010).

The polyQ domain is localized closer to the C-terminus of the protein. It is of variable length, according to the number of CAG repeats on the *ATXN3* allele, and when over 54 glutamine residues is associated with MJD. In its expanded and disease-associated form, the polyQ domain is thought to endow ataxin-3 with a new neurotoxic function, inducing neuronal cell death in selective brain regions (Bevivino and Loll, 2001), as previously described for other polyQ proteins.

1.7.1. Ubiquitination and deubiquitination

Owing to the fact that ataxin-3 is both an ubiquitin-binding protein and a deubiquitinating enzyme, the following two sections describe the intricate processes of ubiquitination and deubiquitination.

1.7.1.1. Ubiquitination

Ubiquitination is the covalent attachment of ubiquitin to another protein. It is a post-translational modification that might influence the function, stability and cellular localization of the ubiquitinated protein (Hershko and Ciechanover, 1998; Pickart and Eddins, 2004; Pickart and Fushman, 2004). Ubiquitin is a small peptide composed of 76 amino acids. It is the most highly conserved protein in eukaryotes, with only three amino acid substitutions between yeast and human (Ozkaynak et al., 1984). Ubiquitin signals the substrate protein and alters its cellular fate. The process of attaching an ubiquitin moiety to a target protein, or ubiquitination, depends on sequential steps catalyzed by three types of enzymes: an ubiquitin activating enzyme, E1; a ubiquitin conjugating enzyme, E2; and an ubiquitin ligase, E3 (Pickart, 2001; Fang and Weissman 2004; Pickart and Fushman, 2004). E1 enzymes are responsible by the activation of ubiquitin through the formation of a thiol ester bond between the C-terminus of ubiquitin and the catalytically active cysteine of E1, in an ATP-dependent reaction. Afterwards, the activated ubiquitin is transferred from the E1 to a cysteine in the active site of an ubiquitin conjugating enzyme, E2. The E2 is generally associated with an ubiquitin ligase, E3, which helps in the final transfer of the ubiquitin motif to a lysine in the substrate protein. The E3 is responsible for substrate specificity, assuring that the correct target protein is ubiquitinated. In some cases, the ubiquitin moiety is transferred from the E2 to the E3 enzyme before being attached to the target protein (Figure 1.12.). The ubiquitin signal can modify the cellular fate of the ubiquitinated protein, and so, this last step is highly regulated. These sequential steps may be repeated several times, with new ubiquitin monomers being linked to the ubiquitin previously attached to the target protein, originating a chain of ubiquitin motifs (Pickart, 1997; Lam et al., 2002).

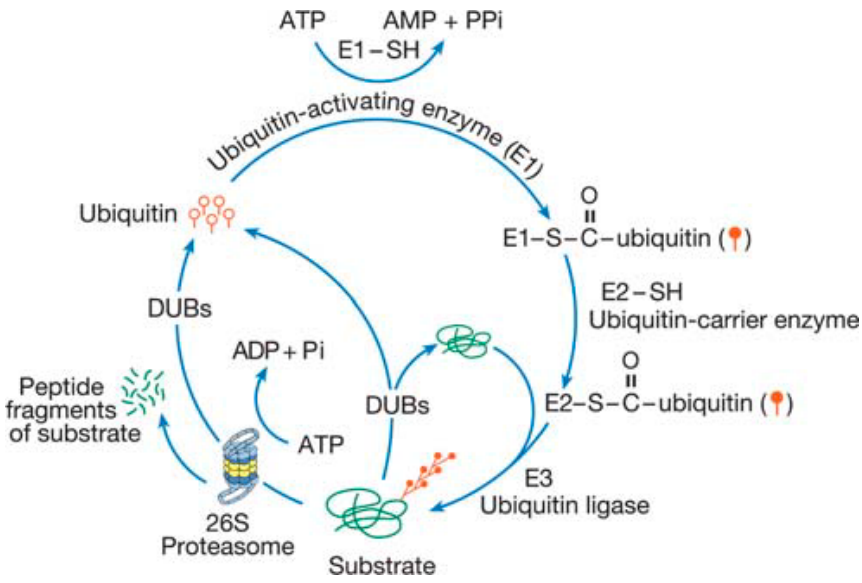

Figure 1.12. - The ubiquitin-proteasome pathway (UPP). Ubiquitin is selectively and covalently linked to the substrate through an enzymatic process involving three different classes of enzymes, E1, E2, and E3. First, ubiquitin is activated by E1 to form an ubiquitin-AMP intermediate. Activated ubiquitin is passed on to E2 (ubiquitin carrier enzymes). E2s transfers ubiquitin to an E3 (ubiquitin ligase), which ligates the activated ubiquitin to the substrate. Another ubiquitin then attaches to the ubiquitin, that is linked to a substrate, and thus, through successive linkages of ubiquitin, a polyubiquitin chain is formed. Polyubiquitinated substrates are degraded by a proteolytic complex called the 26S proteasome in an ATP-dependent reaction. Ubiquitin is not degraded but the polyubiquitin chain is disassembled by deubiquitinating enzymes (DUBs) and ubiquitin is recycled. DUBs can disassemble the polyubiquitin chain if a substrate is ubiquitinated erroneously and prevent the degradation of the substrate. Adapted from Hegde (2010).

A new ubiquitin molecule can be linked to another ubiquitin monomer through any of the seven available lysines (K) in the ubiquitin sequence (K6, K11, K27, K29, K33, K48, K63). These different options of linkages originate a diversity in ubiquitin chains, and subsequently a diversity in ubiquitin signals, depending on their length, type of linkage and different architecture (Pickart and Fushman, 2004; Kim et al., 2007; Ikeda and Dikic, 2008). Polyubiquitin chains linked through K48 are the best studied ubiquitin signal. It is well established as a sign for proteasomal degradation of the targeted proteins (Glickman and Ciechanover, 2002; Pickart and Fushman, 2004). K63 polyubiquitin chains are traditionally not seen as a degradation signal and have

shown to be involved in different events, such as DNA repair, signal transduction and receptor endocytosis (Pickart and Fushman, 2004; Chen and Sun, 2009). However, *in vitro* experiments have also revealed the proteasomal degradation of proteins tagged with K63 ubiquitin chains (Saeki et al., 2009). There is less information regarding the cellular role of the other ubiquitin linkages. K6- and K11-linkages may also be associated with proteasomal degradation; K11-linked ubiquitin chains might even have a role in the endoplasmic reticulum-associated degradation (ERAD) (Kirkpatrick et al., 2006; Xu et al., 2009). K6-linkages may regulate DNA repair, K27- and K33-linkages may be assembled during stress responses and K29-linked chains may be important in ubiquitin fusion degradation pathway (Johnson et al., 1995; Hatakeyama et al., 2001; Nishikawa et al., 2004).

1.7.1.2. Deubiquitination and deubiquitinating enzymes

DUBs are enzymes that catalyze the cleavage of ubiquitin or ubiquitin-like moieties from pro-proteins or ubiquitin/ubiquitin-like modified proteins. DUBs are involved in all parts of the ubiquitin pathway (Wilkinson, 1997). They are responsible for the maintenance of a cytoplasmic pool of free ubiquitin through cleavage of ubiquitin precursor proteins. Ubiquitin is expressed as a polyubiquitin peptide or fused to ribosomal proteins. The polyubiquitin peptide consists of multiple ubiquitin copies that have to be proteolytically processed by DUBs to release free monomeric ubiquitin. The released ubiquitin has to suffer further proteolysis at its C-terminus to assume its fully mature form. The ubiquitin-fused ribosomal proteins have also to be deubiquitinated to originate mono-ubiquitin (Wiborg et al., 1985; Baker and Board, 1987; Ozkaynak et al. 1987). Besides providing new monomers to the ubiquitin cellular pool, DUBs also recycle ubiquitin molecules previously used in ubiquitination of target proteins (Wilkinson, 1997; Nijman et al., 2005). In this way, DUBs resemble phosphatases in the kinase/phosphatase pathways, reverting the ubiquitin signal, and therefore, altering the cellular role of these target proteins. DUBs also cleave free unattached polyubiquitin chains, previously released from target proteins by other DUBs or derived from *de novo* synthesis by ubiquitin conjugating enzymes, into monomeric ubiquitin (Wilkinson et al., 1995; Piotrowski et al., 1997). Finally, DUBs

release ubiquitin monomers trapped in random and uncontrolled side-reactions of small cellular nucleophiles with the thiol ester intermediates involved in protein ubiquitination (Pickart and Rose, 1985). Through studies of the human genome, there are around 100 putative DUBs in humans with specificity for ubiquitin signals and they are classified into five different families (Nijman et al., 2005). They are the UCH, the USP/UBP (both previously identified in section 1.7), the ovarian tumor (OTU), the Josephin domain proteases and the JAB1/MPN/Mov34 metalloenzyme (JAMM) domain zinc-dependent metalloprotease family. There are other known families of DUBs, but their specificity for ubiquitin is low or they are specialized in ubiquitin-like proteins SUMO or NEDD8, namely the Adenain family of cysteine proteases: the ubiquitin-like proteases (ULP or SENPs in humans).

Although few substrates of DUBs and their physiological role have been described, the necessity of such a large number of families and enzymes involved in deubiquitination may reflect a high degree of substrate specificity. This specificity of DUBs would be a good mechanism to control the ubiquitin signal in an overwhelming number of target proteins. If each DUB acts on a limit number of substrate proteins, only a fraction of the total target proteins have their ubiquitin signal modified, leaving the others intact. Similarly to other cellular proteases, accurate regulation of DUB activity is essential to prevent the deubiquitination and alterations in the ubiquitin signal of inappropriate proteins (Liz and Sousa, 2005). Thus, DUBs are post-translationally modified by phosphorylation, ubiquitination, sumoylation, which may alter their activity, cellular distribution and degradation, defining the timing and the cellular localization of substrate cleavage (Reyes-Turcu et al., 2009). Interestingly, DUB activity is usually cryptic, meaning that the energy resulting from the association with the correct substrate or scaffolding protein is often required for the rearrangement into the catalytically active conformation, adding another level of regulation on DUB activity (Liz and Sousa, 2005). Additional domains in DUBs, apart from the catalytic domain, determine protein interactions and substrate specificity. The interaction of a DUB with its substrate might even be less stable than with its associated scaffolding-protein, as the enzyme should be able to release its products after proteolytic cleavage of ubiquitin (Reyes-Turcu et al., 2009). The accessory domains are essential for the

correct physiological role of DUBs. They modulate the binding to ubiquitin, the preference of specific ubiquitin chain linkages, cellular localization of the enzyme and establish the interaction with other proteins (substrate adapters, scaffold proteins and inhibitors) involved in substrate recognition (Reyes-Turcu and Wilkinson, 2009). These domains acquire a particular importance in individual DUBs that can recognize and cleave multiple substrates. A great number of DUBs do not work as free enzymes; instead they associate into multi-protein complexes to exert their normal cellular role. These complexes facilitate the co-localization between DUBs and their specific substrate but also permit sequential cycles of ubiquitination and deubiquitination, allowing the unidirectionality of pathways dependent on proper ubiquitin signals (Reyes-Turcu et al., 2009). Recent attention as been drawn to DUBs associated with E3 ligases in one same multi-protein complex, which regulate negatively the ubiquitin conjugation (Ventii and Wilkinson, 2008).

The importance of the ubiquitin signal on cellular functions explains why DUBs and deubiquitination are so highly regulated. Indeed, the activity of DUBs is involved in cell cycle regulation, transcription, gene expression, DNA repair, kinase activation, microbial pathogenesis and proteasomal or lysosomal protein degradation (Guterman and Glickman, 2004; Schmidt et al., 2005; Adhikari et al., 2007; Lindner, 2007; Komada, 2008; Song and Rape, 2008). Moreover, mutations in several DUBs have been associated to a broad range of pathological conditions, from cancer to neurological diseases (Fischer, 2003; Jiang and Beaudet, 2004; Shanmugham and Ovaa, 2008). The importance of these enzymes in the regulation of almost every cellular function is growing, as more knowledge about DUBs is being gathered. Therefore, DUBs are currently gaining more interest as potential pharmacological targets and may prove to be in the center of therapeutic approaches to treat various diseases, in a near future.

1.7.2. Enzymatic activity of ataxin-3

A great number of recent enzymatic and biochemical studies support the involvement of ataxin-3 in ubiquitin metabolism (Doss-Pepe et al., 2003). The presence of several domains known to be involved in ubiquitin binding, UIMs, and a catalytic

domain with an ubiquitin protease activity, Josephin domain, strongly corroborate this hypothesis (Masino et al., 2003). Moreover, reduction of ataxin-3 levels in the cell promotes the accumulation of ubiquitinated proteins, suggesting a role for ataxin-3 in degradation pathways and protein turnover, namely in the UPP (Doss-Pepe et al., 2003). Similar accumulation of highly ubiquitinated proteins was found in knockout mice for ataxin-3 (Schmitt et al., 2007). Surprisingly, these mice do not exhibit any major anatomical, physiological or behavioral alterations. Thus, ataxin-3 expression is not obligatory to cell survival, suggesting that other enzymes (e.g. other DUBs) can substitute ataxin-3 biological function in the cell.

As described in section 1.7., the deubiquitinating activity of ataxin-3 is conferred by the Josephin domain. This globular N-terminal domain is able to bind and cleave ubiquitin chains, releasing free ubiquitin monomers and since its description in ataxin-3, this domain has been found in other DUBs (Masino et al., 2003). Josephin domain has two ubiquitin-interacting sites in its structure: site 1, close to the catalytic site, important for catalytic activity and proper positioning of the ubiquitin moieties relatively to the catalytic triad of amino acid; and site 2, independent from the enzymatic activity, but relevant for the preference of specific ubiquitin chain linkages and the interaction with other proteins containing ubiquitin-like domains (Nicastro et al., 2009). The Josephin domain is able to cleave ubiquitin chain of different linkages, although an increased efficiency at deubiquitinating K48-linked in comparison to K63-linked ubiquitin chains has been reported (Nicastro et al., 2010). Interestingly, when the whole protein is present, the opposite linkage preference is verified, with ataxin-3 cleaving K63-linked ubiquitin chains more efficiently (Winborn et al., 2008; Nicastro et al., 2010). Regardless of ubiquitin chain preference, ataxin-3 is a very slow enzyme with reduced deubiquitinating activity *in vitro* (Chow et al., 2004b). Much is still unknown regarding ataxin-3 requirements for proper deubiquitinating activity and the lack of a biological substrate and optimal conditions might justify the poor performance of ataxin-3 *in vitro*. It is not uncommon within DUBs to only engage into the active catalytic structure after presentation of its complementary substrate (Reyes-Turcu et al., 2009).

As mentioned previously, ataxin-3 has 2 or 3 UIMs depending on the isoform,

located at the C-terminus of the protein. The UIMs domains are specialized in the interaction with ubiquitin domains and are responsible for the ataxin-3 binding properties to ubiquitin chains (Burnett et al., 2003; Berke et al., 2005). Ataxin-3 binds to ubiquitin chains of different linkages (K48- and K63-linked) with similar affinities; however a minimum of 4 ubiquitin moieties in an ubiquitin chain are required for ataxin-3 binding (Burnett et al., 2003; Chai et al., 2004; Winborn et al., 2008). Interestingly, K48-linked ubiquitin chain composed of 4 ubiquitin monomers is the minimal signal for protein degradation through the UPP (Burnett et al., 2003; Schmitt et al., 2007; Winborn et al., 2008). The first two UIMs located prior to the polyQ region in the ataxin-3 structure collaborate synergistically in the binding of ubiquitin chain and are important for the K63-linkage preference observed for ataxin-3 activity (Song et al., 2010). These two UIMs may be responsible for substrate presentation and correct positioning of the ubiquitin chain in the catalytic cleft of the Josephin domain, thus determining which linkage will be preferentially cleaved (Berke et al., 2005). In a mechanistic view, the UIMs recognize and bind the ubiquitin chains, present them to the Josephin domain, which through its own ubiquitin interacting sites, positions the isopeptide bond between two ubiquitin moieties in the adequate configuration in the catalytic site, allowing cleavage to occur (Mao et al., 2005; Winborn et al., 2008). The three UIM-containing isoform has a similar deubiquitinating activity to the two UIM variant, suggesting that the third UIM does not contribute for ataxin-3 deubiquitinating activity. In fact, the function of the third UIM is not completely understood (Harris et al. 2010).

In contrast to other DUBs, ataxin-3 does not cleave ubiquitin chains to complete digestion into free monomers. Instead, ataxin-3 is currently viewed as an "editing DUB" that modifies the architecture of ubiquitin chains attached to protein substrates, through detailed trimming of these chains. The enzymatic activity of ataxin-3 may thus change the ubiquitin signal attached to a given protein and alter its cellular fate (Winborn et al. 2008). In fact, evidences of slower protein degradation after ataxin-3 deubiquitination have been gathered, suggesting that ataxin-3 may work in the UPP. However, the biological role of ataxin-3 is still not completely understood and due to its cleavage preference for K63 linkages, ataxin-3 may be associated in DNA repair, gene

expression, endocytosis and intracellular transport, all mechanisms where K63-linked ubiquitin signals seem to be highly relevant (Weissman, 2001; Winborn et al. 2008).

Most DUBs are under a tight control in the cell, because their activity may have great repercussions in the levels and quality of their substrates (Reyes-Turcu et al., 2009). Similar control may be applied to ataxin-3 and cellular regulation of its activity is plausible. Many DUBs have shown to be regulated through post-translational modifications (described in section 1.7.1.2.) and several sites of possible phosphorylation, ubiquitination and proteolytic cleavage have also been described for ataxin-3 (Goti et al., 2004; Haacke et al., 2007; Mueller et al., 2009; Todi et al., 2009). These modifications might affect ataxin-3 directly, inhibiting or enhancing its activity, or indirectly, through modulation of protein-protein interactions or translocation to a different subcellular compartment. The interaction with another protein, the presence of a co-factor, the shift to an appropriate cellular environment might influence the enzymatic rate or the substrate preference of ataxin-3. Other DUBs have been shown to be activated by protein-protein interactions and substrate-induced structural alterations (Reyes-Turcu et al., 2009). One such post-translational modification of ataxin-3, monoubiquitination at lysine 117, in proximity to the catalytic site in the Josephin domain, has proven to enhance ataxin-3 activity. Indeed, monoubiquitination of ataxin-3 alone was able to increase the deubiquitinating activity without any other additional factor (Todi et al., 2009). Interestingly, protein-induced stress up-regulate ataxin-3 ubiquitination, which promotes an increased deubiquitinating activity in what is suggested to be a positive feedback mechanism of coping with these sort of cellular aggressions. Moreover, proteotoxic stresses have been shown to alter ataxin-3 localization in the cell, inducing its translocation to the nucleus (Reina et al., 2010). In fact, phosphorylation of serines 340 and 352 by casein kinase 2, an active nuclear localization signal (NLS) and two described and possibly functional nuclear export signals (NES) in ataxin-3 structure have suggested that ataxin-3 levels in the nuclear compartment might be under the control of distinct and well-coordinated mechanisms (Antony et al., 2009; Macedo-Ribeiro et al., 2009; Muller et al. 2009; Reina et al. 2010). Such a tight regulation of ataxin-3 nuclear localization has been interpreted as an indication for a particular role of ataxin-3 inside the nucleus or that the nuclear

compartment might gather the optimal conditions for its deubiquitinating activity.

1.7.3. Cellular role of ataxin-3

Ataxin-3 has been implicated in several distinct pathways and cellular mechanisms. Due to its deubiquitinating activity, ataxin-3 was immediately associated to protein turnover and protein homeostasis pathways (Doss-Pepe et al., 2003). A function in transcriptional regulation was also initially proposed (Li et al., 2002; Evert et al., 2003). However, recent evidences have suggested a role in cytoskeleton organization and other mechanisms dependent on the correct assembly of cytoskeleton elements as aggresome formation and myogenesis (Burnett and Pittman, 2005; Mazzucchelli et al., 2009; Rodrigues et al., 2010).

The ability to bind to ubiquitin chains and the ubiquitin protease activity indicates that ataxin-3 might have a role in UPP. Moreover, two of the first protein interactions described for ataxin-3, p97/valosin-containing protein (VCP/p97) and hHR23A/hHR23B (human homologs of yeast Rad23 protein, a UV excision repair protein) supported this hypothesis, as both proteins were directly or indirectly involved in ubiquitin pathways (Wang et al., 2000; Boeddrich et al., 2006). VCP/p97 is a 97 kDa AAA ATPase, composed of 3 domains: D1, D2 with ATPase activity and an N-terminal domain involved in protein interaction, including with ataxin-3. VCP/p97 is a very abundant intracellular protein and assembles into homomeric hexamers with a ring-like structure (Wang et al., 2004; Madsen et al., 2009). VCP/p97 has been associated with several cellular functions and systems, including ERAD (Zhong and Pittman, 2006). ERAD is the cellular mechanism through which misfolded or aberrant proteins or protein complexes of the secretory pathway are identified and addressed to proteasomal degradation through initial ubiquitination, followed by its export to the cytoplasm and delivery to the proteasome (Wang et al., 2006b). Ataxin-3 interacts with VCP/p97 through its C-terminus, in a specific region proximal to the polyQ domain, and the length of the polyQ stretch has an influence on the interaction (Boeddrich et al., 2006). VCP/p97 and ataxin-3 work together in the ERAD, on the translocation of ubiquitinated substrates out of the ER, sending them to proteasomal degradation (Zhong and Pittman, 2006). However, it is not clear if ataxin-3 has an enhanced or

inhibitory action in this pathway. More recently, roles for the interaction between VCP/p97 and ataxin-3 have been proposed in cellular stress responses and in the determination of *Caenorhabditis elegans* longevity (Kuhlbrodt et al., 2011). These effects were dependent on ataxin-3 deubiquitinating activity and were mediated through the insulin/insulin-like growth factor pathway. The involvement of ataxin-3 in stress responses has been suggested in other studies. Ataxin-3 was shown to rise its levels in the nucleus after a proteotoxic stress, and to be increasingly ubiquitinated, and therefore, more active after the same type of cellular stress (Mueller et al., 2009; Todi et al., 2009; Reina et al., 2010). Stress stimuli might increase the levels of misfolded proteins, challenging stress response pathways and likely demanding an increased ataxin-3 activity. Interestingly, it has been found that ataxin-3 can reduce polyQ toxicity in fly models of polyQ diseases, including MJD (Warrick et al., 2005). This effect was dependent on active ataxin-3, both its deubiquitinating and ubiquitin-binding activities, and the presence of functional proteasomes, linking the polyQ protective role of ataxin-3 to protein quality control pathways.

Human homologs of yeast Rad23 protein A and B (hHR23A/hHR23B) were initially associated to the nucleotide excision repair machinery; later on, a broader action of these proteins was proposed, involving the delivery of protein substrates to the proteasome (Chen and Madura, 2006; Dantuma et al., 2009). hHR23A and hHR23B have a ubiquitin-like domain, through which they interact with the Josephin domain of ataxin-3, and two ubiquitin-associated domains for recognition of ubiquitin motifs (Wang et al., 2000; Nicastro et al., 2005). Therefore, the interaction between ataxin-3 and hHR23A/hHR23B further supports the involvement of ataxin-3 in protein quality control systems or even a possible role on DNA repair mechanisms. The possibility of direct interaction between ataxin-3 and the proteasome itself have also been reported, although this association is not clearly established (Doss-Pepe et al., 2003). A number of other important members of the UPP, the ubiquitin ligases, have also been found to interact with ataxin-3. The currently examples are ubiquitin conjugation factor b (E4b), parkin, C-terminus of 70 kDa heat shock protein (Hsp70)- interacting protein (CHIP), HMG-coA reductase degradation protein 1 (Hrd1), E3 ubiquitin-protein ligase AMFR (gp78) and mitochondrial ubiquitin ligase (MITOL) (Matsumoto et al., 2004; Jana et

al., 2005; Ying et al., 2009; Sugiura et al., 2010; Durcan et al., 2011). Although some of these ubiquitin ligases may act on ubiquitinated substrates together with ataxin-3, most of them have shown to recognize ataxin-3 as a suitable protein substrate for ubiquitination, and therefore, promoting its degradation. Thus, these enzymes might control ataxin-3 activity, and ultimately its substrates, through regulation of the intracellular levels of ataxin-3. As part of the UPP and in conjunction with its interactors, ataxin-3 may edit ubiquitin chains attached to specific protein substrates, hence, determining their cellular fate, their degradation rate, their translocation into a subcellular compartment, or even their interaction with other proteins. Acting as a DUB, ataxin-3 may regulate the levels of unrelated proteins, and consequently, exert influence a variety of cellular pathways (Reyes-Turcu et al., 2009; Todi et al., 2009).

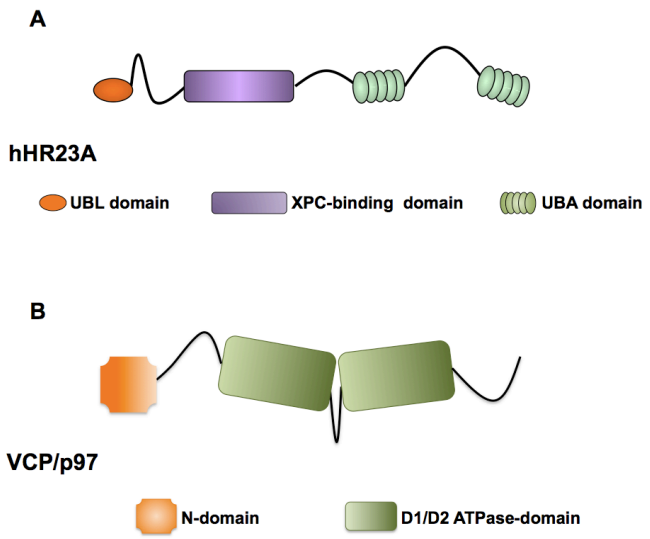

Figure 1.13. – Schematic representation of human hHR23A and VCP/p97 proteins. (**A**) hHR23A is composed of a N-terminal ubiquitin-like domain (UBL), a xeroderma pigmentosum group C (XPC)-binding domain and two ubiquitin-associated domains (UBA). Interaction with human ataxin-3 is established through the UBL domain. (**B**) VCP/p97 has two ATPase domains (D1, D2) and a protein-interacting domain in its N-terminal, through which VCP/p97 interacts with human ataxin-3.

Most recently, increasing evidences have been found of ataxin-3 association to

cytoskeleton components. Ataxin-3 was shown to interact with tubulin, microtubule-associated protein 2 (MAP2) and dynein, suggesting an active role in the assembling of the cytoskeleton (Mazzucchelli et al., 2009). Indeed, knock-down of ataxin-3 expression has been associated to disorganization of microtubules, microfilaments and intermediate filaments, promoting morphologic alterations in cells and the rupture of cell adhesions (do Carmo Costa et al., 2010; Rodrigues et al., 2010). The interaction with these proteins has also implicated ataxin-3 in a role linking the cytoskeleton and protein quality control systems, namely the formation of aggresomes (Burnett and Pittman, 2005). Aggresomes are intracellular collections of misfolded protein that are unable to be degraded by the UPP due to proteasome inhibition or substrate resistance to proteasomal enzymatic activity. The misfolded proteins accumulate at the microtubule-organizing center and are further targeted for lysosomal degradation, in a attempt to relieve the cell of the proteotoxic burden (Markossian and Kurganov, 2004). Ataxin-3 has been shown to have a preponderant role in the formation and maturation of aggresomes, and even to co-localize with these structures in the cell (Burnett and Pittman, 2005). Moreover, ataxin-3 is known to interact with dynein and histone deacetylase (HDAC) 6, two proteins associated to the translocation of misfolded proteins to the microtubule-organizing center, favoring the aggresome progression (Burnett and Pittman, 2005).

Although unrelated to protein homeostasis, the first studies regarding the biological function of ataxin-3 gathered results implying a possible role on transcription regulation. It was observed that the expression of ataxin-3 alters the expression of a significant number of unrelated genes (Evert et al., 2001; Evert et al., 2003). Moreover, knock-down of ataxin-3 expression also changes the expression profile of numerous genes (Rodrigues et al., 2007). Ataxin-3 is known to interact with many regulators of gene expression. Both transcriptional activators - CBP, p300 and PCAF - and two transcriptional repressors - HDAC3 and nuclear receptor co-repressor (N-Cor) - have been confirmed to associate with ataxin-3 (Li et al., 2002; Evert et al., 2006a). Indeed, interaction of ataxin-3 with histones, independent of the polyQ domain has been also reported (Li et al., 2002). This multitude of interactions places ataxin-3 in several regulatory pathways of transcriptional regulation, through which it can influence the

expression of a large number of genes.

Despite the diversity in the intracellular mechanisms that ataxin-3 seems to be associated, a common origin for all the biological roles of ataxin-3 is conceivable, centered around its ubiquitin protease activity and its interaction with the UPP. Through the UPP, ataxin-3 may regulate the levels of a great number of proteins with distinct cellular roles, affecting a broad spectrum of intracellular pathways, thus, amplifying the effects of ataxin-3 deubiquitinating activity in the cell.

1.8. Expanded ataxin-3

Similarly to other polyQ diseases, the pathological mechanism through which a CAG expansion in the *ATXN3* gene evolves to manifestation of clinical and pathological signs and neurodegeneration characteristic of MJD is not completely understood. Even so, it is generally accepted that the unstable expanded CAG tract has a central and initiating role in all the proposed pathways of pathogenesis (Williams and Paulson, 2008) (Figure 1.14.). The expanded polyQ domain seems to endow ataxin-3 with new biochemical and biophysical properties. One of the most evident is the higher propensity to misfold, and consequently, to aggregate (Bevinino and Loll, 2001; Chow et al., 2004c; Williams and Paulson, 2008). The aggregates of expanded ataxin-3 are enriched in β-sheet fibrillar structures, similar to the amyloid aggregates described for Alzheimer's disease and other protein misfolding diseases (Bevinino and Loll, 2001; Chen et al., 2002). As in these diseases, the amyloid-like structures promote the alteration in conformation from soluble proteins to monomeric species that can self-assemble into multimeric aggregates (Uversky, 2010). The process of expanded ataxin-3 aggregation seems to be composed of a two-step mechanism, starting with conformational changes and self-association of monomers through regions other than the polyQ stretch. An expanded polyQ-dependent second step follows where further conformational arrangements occur, originating higher stability sodium dodecyl sulfate (SDS)-insoluble aggregates (Ellisdon et al., 2006; Ellisdon et al., 2007). Increasing evidences suggest that other regions in the protein, apart from the expanded polyQ domain, have an active influence over the structural and biochemical properties of

ataxin-3 (Chow et al., 2004a; Masino et al., 2004; Gales et al., 2005). These other domains may modulate the characteristics of expanded ataxin-3 in terms of pathological entity, which ultimately might be translated into distinct aspects of MJD pathology. Interestingly, it has been found that the Josephin domain has a primal role over the conformational state of ataxin-3, determining the initial alterations in its structure, during the first step of aggregation (Gales et al., 2005; Ellisdon et al., 2006; Masino et al. 2004). The cellular context (e.g. protein interactions, subcellular localization) might also determine the cellular toxicity induced by expanded ataxin-3, since cell degeneration in MJD is only observed in neurons of selective regions in the brain, despite the ubiquitously expression of the mutated protein.

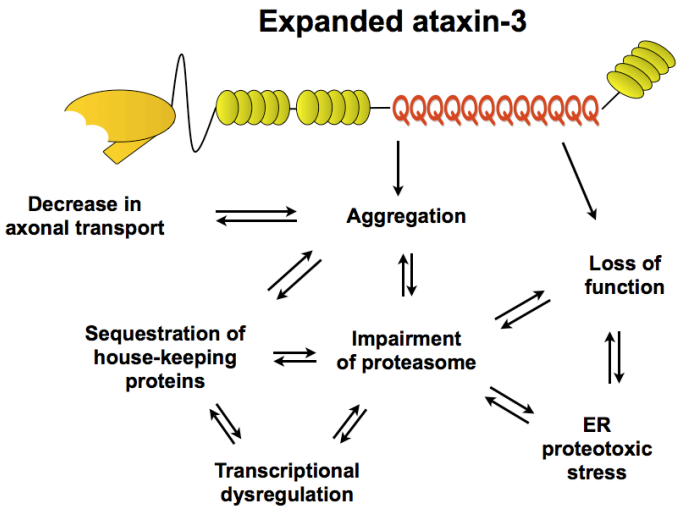

Figure 1.14. – Schematic representation of human expanded ataxin-3 and a summary of some the pathological mechanisms associated with expanded ataxin-3 toxicity.

Intracellular and intranuclear inclusions of aggregated proteins in neuronal cells are an hallmark of all polyQ diseases and it has also been observed in MJD patients, as well as in transgenic animals and cell models expressing ataxin-3 with expanded polyQ domains (Paulson et al., 1997; Schmidt et al., 1998; Chai et al., 1999;

Cemal et al., 2002; Schmidt et al., 2002; Goti et al., 2004; Chou et al., 2008; Seidel et al., 2010; Teixeira-Castro et al., 2011). After its discovery, expanded ataxin-3 aggregates were soon placed in the center of several proposed mechanisms of cell toxicity induced by polyQ expanded proteins (Paulson et al., 1997; Chai et al., 1999; Warrick et al., 1999; McCampbell et al., 2000; Chai et al., 2002; Schmidt et al., 2002; Gunawardena et al., 2003). However, intracellular inclusions positive for ataxin-3 were found both in highly degenerated brain areas and in unaffected regions of the CNS of MJD patients (Paulson et al., 1997; Trottier et al., 1998; Yamada et al., 2000; Ross and Poirier, 2004; Evert et al., 2006b). Thus, and as described before in this thesis, intracellular aggregation have recently been interpreted not as a pathological phenomenon, but instead as a cellular defense mechanism to cope with expanded, misfolded and proteolytic-resistant proteins, which may have greater deleterious effects to the cell if left in their soluble form (Arrasate et al., 2004; Slow et al., 2005). In this view, the possible toxic species would be dimers, oligomers or small aggregates instead of the fully matured inclusions. The lack of correlation between intracellular inclusions and the neurodegenerated areas in MJD led also to the hypothesis that the distribution of intracellular inclusions through the different CNS regions is, in fact, dependent on the individual characteristics of each MJD patient, such as CAG repeat length, age of onset and SCA3 progression, instead of being a common trait of the disease (Schöls et al., 1995; Rüb et al., 2006). Moreover, some authors suggested that the intracellular inclusions of expanded ataxin-3 do not have any role on MJD pathological mechanism, neither a toxic or a protective effect, and thus, do not determine the future cellular fate of neurons (Iwabuchi et al., 1999; Rüb et al., 2006). Therefore, although the association of intracellular inclusions and MJD condition has long been established, it is still in debate the true role of the aggregates in MJD pathogenesis, as in other polyQ diseases and, in general, in the several neurodegenerative diseases.

The inclusions are not exclusively constituted of expanded ataxin-3. Transcription factors, such as TATA-binding protein (TBP) and CBP, proteasomal subunits, ubiquitin, molecular chaperones and even non-expanded ataxin-3 have also been found to co-localize with these inclusions (Paulson et al. 1997; Perez et al., 1998; Chai et al. 1999; Warrick et al., 1999; Chai et al., 2002; Schmidt et al. 2002;

Donaldson et al., 2003). The sequestration of important house-keeping proteins inside the aggregates are one of the mechanisms suggested to explain transcriptional dysregulation and the impairment of proteasome and the quality control pathways in polyQ diseases, including MJD. This way, even if the process of aggregation is a defense mechanism against the polyQ-expanded protein, the later recruitment and sequestration of key proteins may turn a physiological response into an auto-sufficient pathological mechanism, continuously depleting the cell of house-keeping proteins. Interestingly, non-expanded ataxin-3 is also found in the aggregates of expanded ataxin-3 (Takahashi et al., 2001; Uchihara et al., 2001; Warrick et al., 2005). The sequestration and depletion of non-expanded ataxin-3 from the cell might enhance the pathogenesis of expanded ataxin-3, due to reduction of active non-expanded ataxin-3 and its proposed protective effect against polyQ toxicity.

Similarly to other polyQ proteins, aggregation of expanded ataxin-3 is intensified if shorter fragments of the protein are produced. Cell lines expressing expanded polyQ-containing C-terminal fragments of ataxin-3 show increased aggregation and cell death (Paulson et al., 1997; Haacke et al., 2006; Breuer et al., 2010). Proteolytic cleavage of expanded ataxin-3 has been reported in MJD models and in brains of MJD patients. Expanded ataxin-3 fragments were even found to be more abundant in the affected areas of MJD brains (Goti et al., 2004; Colomer Gold et al., 2007; Haacke et al., 2007; Jung et al., 2009). Caspases and calcium-dependent calpain proteases were shown to cleave expanded ataxin-3 and this proteolytic processing was associated with increased aggregation (Berke et al., 2004; Haacke et al., 2007; Jung et al., 2009). Moreover, mutation of caspase cleaving sites in expanded ataxin-3 reduces the levels of proteolytic fragments and neuronal toxicity (Jung et al., 2009).

Another pathological mechanism of expanded ataxin-3 is the interference with axonal transport. As previously described in section 1.4.7, due to its long cytoplasmic extensions, neurons are highly dependent on the transport of intracellular organeles and molecules along the neurites. Aggregates deposited in the axon or the dendrites of neurons may represent a physical obstacle to axonal transport of such cargo, blocking its movement down the neurites, promoting cell dysfunction and ultimately cell death

(Gunawardena et al., 2003).

Besides promoting aggregation, the expanded polyQ domain may interfere, at the monomeric level, with the function, the protein interactions and the cellular localization of ataxin-3. From this point of view, MJD pathology would have a contribution from a possible loss of function of ataxin-3. Knock-out mice and *C. elegans* for ataxin-3 do not manifest any major phenotype due to loss of normal ataxin-3, suggesting that ataxin-3 activity in a healthy animal context is not essential for survival (Rodrigues et al., 2007; Schmitt et al., 2007). Moreover, *in vitro* studies comparing normal and expanded ataxin-3 have not found relevant differences in their deubiquitinating activities (Berke et al. 2004; Burnett et al., 2003; Winborn et al., 2008). More recently, however, expanded ataxin-3 exhibited an increased activity towards ubiquitinated parkin, in comparison to the non-expanded form (Durcan et al., 2011), which supposedly promotes parkin turnover through autophagic degradation (Durcan and Fon, 2011). On the other hand, an accumulation of highly ubiquitinated substrates has been observed in cells, following the overexpression of expanded ataxin-3, suggesting an association between polyQ expansion and a dysfunction in normal ubiquitin protease activity of ataxin-3 (Winborn et al. 2008).

Another possibility is the proposed gain-of-function hypothesis, where the expanded polyQ domain would promote new and abnormal protein interactions, which would mediate expanded ataxin-3 toxic effects. Due to its higher propensity for aggregation, it has been proposed that polyQ-expanded ataxin-3 might establish stronger interactions with its biological substrates, sequestering them in the aggregates and removing them from normal degradation pathways, and hence, leading to an accumulation of ubiquitinated proteins in the cell (Burnett et al., 2003; Burnett and Pittman, 2005). This accumulation may even increase during the normal process of aging, due to physiological deterioration of protein quality control pathways associated with age, which may exacerbate the expanded ataxin-3 effect and justify the middle-age onset of MJD. The expanded polyQ tract does not disturb the interaction of ataxin-3 with two of its best known interactors, hHR23A and hHR23B. However, hHR23A is also found in expanded ataxin-3 aggregates (Wang et al., 2000). On the contrary, the polyQ expansion alters ataxin-3 binding to VCP/p97, stabilizing it

(Boeddrich et al., 2006). Expanded ataxin-3 establishes a stronger interaction with VCP/p97, which may explain the co-localization of VCP/p97 with intracellular inclusions in MJD (Boeddrich et al., 2006). The increased extent of this interaction was proposed as the mechanism through which expanded ataxin-3 impairs ERAD and promotes the accumulation of ubiquitinated substrates in the ER, activating ER proteotoxic stress responses that may contribute to cell death and neuronal degeneration (Wang et al., 2006b; Zhong and Pittman, 2006). Transcription factors (CBP, p300 and PCAF) are another class of proteins showing increased binding for both non-expanded and expanded ataxin-3 (Li et al., 2002). A reduction in the availability of these factors to the cell might have a role in the transcriptional dysregulation described for several genes in a MJD context (Chou et al., 2006; Evert et al., 2006b; Chou et al., 2008). In accordance, nuclear localization of expanded ataxin-3 seems to exacerbate the pathological phenotype (Bichelmeier et al., 2007). Expanded ataxin-3 has been suggested to induce transcriptional dysregulation though decrease in histone acetylation, which is ameliorated with the administration of histone deacetylase (HDAC) inhibitors (Chou et al., 2010). However, this pathological mechanism is not entirely clear, as histone acetylation seems to be increased in some cellular models and in brains of MJD patients (Evert et al., 2006a).

1.9. Models of Machado-Joseph disease

The study of MJD soon demanded for reliable model systems to study the pathological mechanisms and to test new therapeutic approaches. In fact, since the first description of the *ATXN3* gene by Kawaguchi and collaborators, in 1994, several models of MJD have been developed, in attempt to faithfully replicate the pathophysiology of this neurological disease.

Most of our current knowledge regarding expanded ataxin-3 aggregation, co-localization with other proteins and aggregation-induced toxicity was collected from cell models. Primary cell cultures, neuronal or neuronal-like and non-neuronal immortal cell lines have all been used in MJD studies. Studies of ataxin-3 aggregation through overexpression of full-length or truncated versions of expanded ataxin-3

complementary DNAs (cDNAs) were mainly conducted in cell lines (Ikeda et al., 1996; Paulson et al., 1997; Perez et al., 1998; Chai et al., 1999a; Chai et al. 1999b; Evert et al., 1999; Evert et al., 2001;Yoshizawa et al., 2001; Wen et al., 2003; Tsai et al., 2004; Jeub et al., 2006; Chang et al., 2009), while signal transduction and apoptotic pathways triggered by expanded ataxin-3 were mostly analyzed in primary cell cultures (Chou et al., 2006; Chen et al., 2008; Hu et al., 2009; Chou et al., 2011). Taken together, MJD cell models have shown that: i) expanded ataxin-3 has a higher tendency for aggregation; ii) truncated polyQ-containing ataxin-3 peptides are more toxic and aggregation-prone; iii) pathological ataxin-3 aggregates can have nuclear and cytoplasmic localization; iv) wild-type ataxin-3 is recruited into expanded ataxin-3 aggregates; v) molecular chaperones, proteasome subunits and transcription factors co-localize with ataxin-3 aggregates; vi) overexpression of molecular chaperones is protective against pathological ataxin-3-induced cell death; vii) expanded ataxin-3 decreases anti-apoptotic Bcl-2 protein, up-regulates Bax, increases cytochrome C release and activates caspase-3 and 9, inducing or sensitizing cells to apoptosis; and viii) pathological ataxin-3 promotes alterations in transcriptional activity of p53, disturbances in calcium signaling and modifications in electrophysiological properties of neuronal-like cells.

The lack of an integrated view of the disease, the absence of interplay between the different types of cells of the nervous tissue and the loss of the highly stratified architecture of the CNS are limitations associated with the sole usage of cell models in Neuroscience. To overcome these disadvantages, several animal models of MJD have been created. Although ataxin-3 is relatively conserved throughout evolution and ataxin-3 homologues are found in numerous species, apart from humans, there is no report of MJD or similar disease in other animals, as in other neurodegenerative diseases. Thus, all current animal models of MJD were genetically engineered to express full-length or fragments of expanded human ataxin-3. Invertebrate animal models are specially appealing for large screening studies due to their short lifespan, reduced complexity and low cost. Invertebrate animal models of MJD have been generated for *Drosophila melanogaster* and *Caenorhabditis elegans*.

The first *C. elegans* model of MJD was generated though expression of full-

length or truncated ataxin-3 under a pan-neuronal promoter, unc-119 (Khan et al., 2006). The range of polyQ length in these animals varied from normal to highly pathological range animals both for full-length and truncated forms of ataxin-3. Perinuclear aggregation was observed in all pathological polyQ length truncated constructs expressing animals and in older animals expressing full-length protein with the highest polyQ length (130Q). In this model, higher polyQ length was associated with earlier aggregation, higher toxicity, interruption of normal synaptic transmission, behaviour defects, neuronal dysfunction, neuronal swelling and abnormal branching of neurites. Moreover, some research has been developed using *C. elegans* ataxin-3 orthologue, namely in the laboratory of P. Maciel (University of Minho, Portugal), in order to study the biological function and protein interactions of ataxin-3 (Rodrigues et al., 2009, 2011). Most recently, the same lab developed a new *C. elegans* model of MJD retaining some degree of neuron-specific aggregation and neuronal dysfunction towards expanded ataxin-3, emphasizing the importance of the sequences flanking the expanded polyQ domain for the specificity of MJD pathogenesis (Teixeira-Castro et al., 2011). Furthermore, the authors observed an age-dependent modulator effect over expanded ataxin-3-induced phenotypes and a protective role of insulin/insulin growth factor-1-like and heat shock factor-1 pathways against expanded ataxin-3 pathogenesis (Teixeira-Castro et al., 2011).

Another invertebrate species frequently developed as an animal model of MJD, particularly by the laboratory of N. Bonini, is the *Drosophila melanogaster*. The first fly model of MJD was developed in 1998 and expressed a truncated form of pathogenic ataxin-3 containing the expanded polyQ domain (Warrick et al.,1998). Formation of characteristic nuclear inclusions and late-onset cell degeneration were observed, with neurons and pigment cells of the eye exhibiting a higher susceptibility after the expression of an expanded polyQ tract. Subsequently, neurodegeneration was shown to be suppressed by the overexpression of Hsp70, a molecular chaperone, although this effect over polyQ toxicity was not associated with a reduction in nuclear inclusions (Warrick et al., 1999). Later on, an independent group, using the same animal model, described locomotor dysfunction and abnormal olfactory behavior in flies expressing the expanded polyQ domain, establishing a link between these motor defects and the

ataxic movements of MJD patients (Kim et al., 2004). In 2005, N. Bonini and collaborators generated a new *Drosophila* model of MJD, expressing the full-length human protein (Warrick et al., 2005). Surprisingly, in this model, wild-type human ataxin-3 has shown to be a powerful suppressor of expanded polyQ toxicity. Moreover, the protection against neurodegeneration provided by wild-type ataxin-3 required its ubiquitin protease and ubiquitin binding capacities and was dependent on proteasome function. Later on, flies expressing truncated and full-length expanded ataxin-3 were applied in a genetic screen for modifiers of ataxin-3-induced neurodegeneration (Bilen and Bonini, 2007). The selected modifiers affected protein misfolding and interfered with protein accumulation through one of two mechanisms: a proteasome-dependent manner or autophagy. Following studies in these same *Drosophila* MJD models have suggested a component of RNA-based toxicity in polyQ neurodegeration and polyQ diseases in general (Bilen et al., 2006). *Drosophila* models expressing human expanded ataxin-3 mutated for specific caspase-sites have shown a reduction in the neuronal loss dependent on expanded ataxin-3 cleavage, which might be partially mediated by caspases (Jung et al., 2009). More recently, fly models of MJD have implicated a role for ion homeostasis in MJD pathogenesis, through the discovery of the suppressor activity of protein interacting with C kinase 1 (PICK1, a regulatory protein of trafficking of ion channel subunits to and from the plasma membrane) following expanded ataxin-3-mediated neurodegeneration (McGurk et al., 2011).

Interestingly, the first animal model of MJD was generated in a mammalian species, the mouse. In 1996, a japanese group designed two lines of transgenic mice expressing full-length or a fragment of human ataxin-3, both containing an expanded polyQ tract (Q79), and both directed for selective expression in the cerebellar Purkinje cells (Ikeda et al. 1996). Although these cells are not the primary target in MJD, the animals expressing the expanded polyQ (Q79) truncated form developed a severe phenotype with early onset (1-2 months of age), exhibiting ataxia and a marked cerebellar degeneration.

Cemal and colleagues generated a second mouse model of MJD (C57BL/6J strain) in 2002 (Cemal et al., 2002). In this model, the whole human *ATXN3* gene, together with its regulatory sequences were cloned into a yeast artificial chromosome

(YAC). Expanded human ataxin-3 was expressed in most tissues and organs; however, degeneration was restricted to pontine and cerebellar nuclei, resembling the neurodegeneration pattern of MJD. Moreover, these mice developed ubiquitinated intranuclear inclusions in brain regions similar to those detected in postmortem human MJD brains. This animal model even replicated many of the symptoms and characteristic signs of MJD. They displayed mild and progressive motor disabilities, gait problems, tremor, along with a reduction in weight. In subsequent studies, this MJD model displayed several metabolic alterations in cerebrum and cerebellum, an increase in glutamine, a decrease in phosphocholine and myo-inositol, and a higher sensitization of the type 1 IP_3 receptor to its ligand, leading to abnormalities in Ca^{2+}-dependent signaling (Chen et al. 2008).

In 2004, a third mouse model of MJD (C57BL/6J strain) was described, also expressing an expanded (Q71) full-length human ataxin-3 (*MJD1a* isoform), but in this model, the transgene expression was under the control of the mouse prion promoter (Goti et al., 2004). This promoter ensures a robust expression of Q71 human ataxin-3 in the CNS. These animals exhibited a severe phenotype, at an earlier age (2-4 months of age), an advantage in comparison to the YAC mouse model. However, the pathological phenotype was restricted to the transgenic homozygous mice. These mice displayed ataxia, postural abnormalities, kyphosis, weight loss and premature death. Neuropathologically, this model did not show any obvious neurodegeneration, although intranuclear inclusions were observed in a few neuronal populations, namely in the deep cerebellar and pontine nuclei, substantia nigra and spinal cord. A fragment of ataxin-3 containing the polyQ tract, resulting from a proposed caspase-mediated cleavage, was also found in brains of symptomatic mice.

Another MJD mouse model (C57BL/6J strain) was generated in 2007 by Bichelmeier and colleagues, using the mouse prion promoter as regulator of transgene expression. In this model human ataxin-3 (*MJD1a* isoform) with 15, 70 or 148 glutamines was expressed. Similarly to Goti et al. (2004) model, the expanded ataxin-3-expressing mice displayed a strong and progressive phenotype, with severe symptoms associated to the expression of expanded ataxin-3 and polyQ length, though an absence of major neurodegeneration. Mice with larger polyQ repeats (Q148)

developed more pronounced neurological signs and at an earlier age, in comparison to Q70-ataxin-3 mice. In opposition to Goti's model, heterozygous mice also developed pathological symptoms. Moreover, intranuclear inclusions were more abundant, present in all brain areas with exception of the Purkinje cells in cerebellum. In the same study, the authors also developed equivalent transgenic mouse lines expressing human ataxin-3 fused to a NLS or a NES, in order to evaluate the importance of nuclear localization of expanded ataxin-3 for the pathology of MJD. The NES and the consequent absence of expanded ataxin-3 from the nucleus were associated with milder symptoms, whereas the presence of NLS worsened the pathological phenotype.

The hypothesis that neuronal dysfunction in MJD was the main cause of the clinical symptoms and occurred before any signs of neurodegeneration led to the development of another MJD mouse model, once more expressing human expanded (Q79) ataxin-3 under the regulation of mouse prion promoter, but this time, in a different mouse strain, FVB/N (Chou et al., 2008). This fifth mouse model of MJD exhibited motor incoordination, inability to return to normal body posture, ataxic gait and weight loss, starting at 5-6 months of age and progressively worsening through mice lifespan. Intranuclear inclusions were present in the dentate nucleus of the cerebellum, pontine nuclei and substantia nigra. Chou and colleagues (2008) reported a cerebellar transcription dysregulation in the transgenic mice expressing expanded ataxin-3, including transcripts for proteins involved in glutamatergic and GABAergic neurotransmission, neuronal survival and differentiation, intracellular Ca^{2+} signaling, mitogen-activated protein (MAP) kinase pathways and heat shock proteins. Most notably, some of these transcripts have their levels altered even before the manifestation of any symptoms. Afterwards, the same authors were able to delay the onset of symptoms in this MJD mouse model, through stimulation of DNA transcription using sodium butyrate, a HDAC inhibitor, supporting the idea that polyQ proteins alter gene transcription before the establishment of clinical symptoms or any irreversible damage (Chou et al. 2011).

The existence of a therapeutical window, early in MJD progression, more responsive to treatments and where total recovery from pathological symptoms could be reached, found further support in the first conditional MJD mouse model

(C57BL/6J strain) generated in 2009 (Boy et al., 2009). These mice expressed full-length human expanded (Q77) ataxin-3 complementary DNA (cDNA) under the control of prion promoter, but regulated through a tetracycline-dependent (Tet-Off) system, as the administration of tetracycline antibiotics in the transgenic mice diet blocked the expression of the polyQ expanded protein. Once more, the prion promoter ensured an expression directed to the brain. However, the expression of expanded ataxin-3 in the cerebellum of these transgenic mice appeared to be mainly centered in glial cells and neurodegeneration was mostly restricted to the Purkinje cells, two cell types that do not recapitulate the human MJD neuropathology. Even so, these animals developed hyperactivity, reduced anxiety at 6 months of age, followed by a reduction in rotarod performance at 9 months and ataxic movements at 20 months of age. In addition to the progressive neurological phenotype, a reduction in body weight was also reported in these transgenic animals. Interestingly, the turning off of the expanded ataxin-3 expression at an early stage in disease progression reverted the pathological phenotype, and after 5 months the transgenic animals performed similarly to control mice. Therefore, and despite the limitations over cell-specificity expression, this mouse model clearly demonstrated that MJD symptoms can be reverted through elimination of the expanded protein.

In 2010, the same authors generated a different MJD mouse model (C57BL/6J strain) expressing human expanded ataxin-3 with a longer polyQ stretch (Q148) under the control of rat huntingtin promoter (Boy et al., 2010). This model displayed low levels of transgene expression, which are distributed evenly and ubiquitously throughout the mouse brain. The reduced level of expression was associated with a mild phenotype, with slow disease progression; indeed, intranuclear inclusions were only observed in homozygous transgenic mice and later in life, at 18 months of age. The onset of symptoms began at 4-6 months of age through hyperactivity, but motor deficits were only detectable at 12 -14 months. Interestingly, motor symptoms became apparent before the deposition of intranuclear inclusions or any signs of neurodegeneration, further supporting the hypothesis that MJD is a neuronal dysfunction based-disease and not an outcome of neuronal loss. This model was later crossbred with the mouse models developed by Bichelmeier and collaborators (2007) to

further pursuit and clarify the proposed protective effect of wild-type ataxin-3 over polyQ toxicity (Hubener and Riess, 2010). However, this study was unable to replicate the positive results previously observed in *Drosophila* MJD models; thus, an increase in wild-type ataxin-3 levels did not ameliorate expanded ataxin-3 induced-phenotype (Warrick et al., 2005).

Finally, the group of P. Maciel generated the most recent transgenic MJD mouse model (FVB/N backcrossed with C57BL/6J strain), which expresses human expanded (83 or 94 glutamines) ataxin-3 under the control of cytomegalovirus (CMV) promoter (Silva-Fernandes et al., 2010). The expression of expanded ataxin-3 was disseminated through all tissues and organs, however selective degeneration of cerebellum, pontine nuclei, thalamus and substantia nigra was observed. Moreover, this neurodegeneration was progressive and correlated with the exacerbation of the pathological phenotype overtime. The transgenic mice manifested motor incoordination at early age, but no intranuclear inclusions were detected at any age, favoring the idea that these two phenomena are not related. Interestingly, this animal model exhibited instability in the number of CAG repeats throughout generations, a characteristic previously found in another MJD mouse model. Moreover, the generational instability induced an increase in the number of CAGs, with longer CAG repeats being associated with severe phenotypes, mimicking what is observed in human MJD families. Somatic mosaicism was also found in these transgenic mice, although longer CAG repeats were not related with the degenerated areas of the brain (Silva-Fernandes et al., 2010). This is indeed, another similarity to the human MJD brains.

The rat has been also used to develop an animal model of MJD. Differently from the mouse models, the rat MJD models developed by Alves and colleagues (2008) had a localized expression of expanded ataxin-3 to restricted regions of the brain (Alves et al., 2008a). The selective distribution of human ataxin-3 expression was achieved through stereotaxic delivery of lentiviral vectors coding for the polyQ expanded protein into living rat brains. The lentiviral vectors were injected in the striatum and the substantia nigra, separately. Through this approach, the authors could assess the individual contribution of these two brain regions to the clinical symptoms and pathogenesis of MJD. Although the transgene was not present since birth, the human

expanded ataxin-3 was expressed in high levels and ubiquitinated intraneuronal inclusions were relatively abundant. Neuronal death was also demonstrated through the decreased levels of neuronal markers and irreversible condensation of chromatin, karyopyknosis. Moderate motor deficits were also reported when viral transduction was targeted to the substantia nigra (Alves et al. 2008b) Further studies using this same model have concluded that the overexpression of wild-type ataxin-3 do not protect against expanded ataxin-3 toxicity, as previously observed in *Drosophila* MJD models. The studies continued, demonstrating that knocking down endogenous ataxin-3 in the rat brain is not toxic and does not aggravate the MJD symptoms of this animal model (Alves et al. 2010).

1.10. Treatment of Machado-Joseph disease

So far, as in other polyQ and neurodegenerative diseases, there is no known etiological treatment for the progressive neurodegeneration in MJD. The therapeutics applied to MJD patients aim to reduce the severe and incapacitating symptoms and to provide the best possible quality of life. A few clinical trials with the combination of antibiotics sulfamethoxazole and trimethoprim have initially shown encouraging results (Mello and Abbott, 1988; Azulay et al., 1994; Correia et al., 1995; Sakai et al., 1995). Patients exhibited a reduction in spasticity, together with an improvement in gait, in hyperreflexia of patellar reflex, in vision (contrast sensitivity) and benefits in movement coordination. Trimethoprim-sulfamethoxazole ameliorated the clinical symptoms supposedly via an increase in biopterin and homovanillic acid levels, which were found to be reduced in the cereberospinal fluid of MJD patients. However, a broader trial with a larger number of MJD patients did not corroborate any of these findings for trimethoprim-sulfamethoxazole therapy (Schulte et al., 2001). Fluoxetine, a selective serotonin reuptake inhibitor, have also proven to be ineffective in improving motor deficits of MJD patients (Monte et al., 2003). On the other hand, MJD patients subjected to treatment with the partial agonist of the serotonin 5-HT_{1A} receptor, tandospirone, showed reduction in ataxia, relief in leg pain and benefits in their sleep disturbances and depressive mood (Takei et al., 2004). Lamotrigine, an anticonvulsant

drug shown to effectively reduce the levels of expanded ataxin-3 in MJD lymphoblastoid cell lines through a still unknown mechanism, have also shown encouraging results on gait improvement in MJD patients (Liu et al., 2005).

Even so, the current treatment given to MJD patients is designed only to ameliorate or reduce the incapacitating symptoms associated with this disease. Amantadine, a weak antagonist of NMDA glutamate receptors which increases dopamine release and blocks dopamine uptake, is prescribed for bradykinesia and dystonia (Woods and Schaumburg, 1972). Botulinum toxin is also used for dystonia, although under caution due to the risk of increasing the muscle atrophy already prevalent in some MJD patients, while dopamine agonists and levodopa are very effective for parkinsonism (Tuite et al., 1995; Buhmann et al., 2003). Taltirelin hydrate, an analog of thyrotropin-releasing hormone with the same physiological actions as the hypothalamic hormone, is beneficial for speech articulation, and the disabling muscle cramps commonly affecting MJD patients are treated with magnesium, chinine, mexiletine and carbazepine, due to their antiarrhythmic and anti-excitatory actions (Kanai et al., 2003; Shirasaki et al., 2003). The symptoms of restless legs symptoms, also very present in MJD, respond well to dopaminergic therapy and tilidine (Schöls et al., 1998).

In addition to the pharmacological therapy, MJD patients cope better with ataxia and associated motor disabilities when under a combined program of physiotherapy and daily training of gait and body posture (D'Abreu et al., 2010). Moreover, physical exercise improves self-esteem, prevents depression and exercises techniques to overcome patients' disabilities. Later on in the progression of the disease, strollers and wheelchairs become mandatory to prevent falls and major fractures that would cause permanent immobilization. Speech therapy may be implemented against dysarthria and dysphagia, in attempt to keep oral communication and control of ingestion for as long as possible, as well as a preventive measure against pneumonia from food aspiration (D'Abreu et al., 2010). Diplopia in MJD can not be treated by eye surgery, and thus, the prescription of prism glasses are the usual solution for the visual problems of these patients (Riess et al., 2008).

The advances in MJD genetics and the growing information about expression

profiles and polymorphisms of *ATXN3* gene have increased the interest in gene therapy as a possible treatment for MJD. Recent studies using small interfering RNA (siRNA) have shown some promising results in downregulating specifically the expanded ataxin-3 gene in a rat model of MJD (Alves et al., 2008a). The downregulation of expanded ataxin-3 was associated with an improvement in phenotype. The selectivity for the expanded ataxin-3 allele was achieved by directing the siRNAs to an intragenic single nucleotide polymorphism, G987GG/C987GG, situated just after the CAG tract. The C987GG polymorphism is present in more than 70% of the expanded alleles found in worldwide population of MJD patients (Gaspar et al., 2001; Martins et al., 2007). Taking advantage of this difference, the authors specifically designed siRNAs for the C987GG polymorphism and successfully discriminated the normal from the expanded allele. A second strategy to silence specifically an expanded allele, based on the different number of CAG repeats, was also accomplished in cell lines expressing both non-expanded and expanded forms of ataxin-3 (Hu et al., 2009). The side effects of ataxin-3 knockout in humans are still unknown, thus, a similar strategy of distinction between normal and expanded alleles would be mandatory in a siRNA therapeutic approach for MJD patients, in order to maintain the expression and function of non-expanded ataxin-3. However, much has still to be done to apply these gene therapy methodologies to the actual treatment of MJD patients.

1.11. Objectives

The scientific work developed and presented in this thesis was focused on three main aims:

Aim 1. - To study the modulatory effect of VCP/p97 and hHR23A interactions over the deubiquitinating activity of ataxin-3.

Ataxin was previously shown to possess the ability of binding and cleaving long polyubiquitin chains into smaller fragments. Preceding studies have revealed a substrate preference of ataxin-3 for K63-linked polyubiquitin chains. Still, even in the presence of this preferred substrate, ataxin-3 has a very slow kinetics in comparison to other DUBs. Efforts have been made in attempt to discover post-translational regulatory mechanisms that could enhance ataxin-3 activity. Monoubiquitination of ataxin-3 was reported to be such a mechanism and shown to be successful at increasing the deubiquitination rate of ataxin-3. However, other regulatory pathways might have a role in ataxin-3 activity, resembling what is observed for other DUBs. The study of ataxin-3 regulation has become more relevant, since a loss-of-function phenomenon was proposed as a hypothesis for MJD pathogenesis. In this work, we investigated if protein-protein interactions could modulate the deubiquitinating activity of ataxin-3. VCP/p97 and hHR23A were chosen among all other known ataxin-3 interactors, because both proteins are involved in protein degradation pathways and their interaction sites with ataxin-3 are well established. This study intended to better characterize ataxin-3 activity and its regulatory pathways and ultimately, to understand if a loss-of-function mechanism may contribute for the toxicity of expanded ataxin-3. Expanded ataxin-3 has shown similar enzymatic properties to wild-type ataxin-3. Therefore, loss-of-function is not due to a reduced reaction rate at basal state, but instead it might stem from the absence of a positive enhancer stimulus of expanded ataxin-3 deubiquitinating activity. Therefore, the effects of VCP/p97 and hHR23A interactions were also studied for expanded ataxin-3. Any difference regarding the

modulation of wild-type *versus* expanded ataxin-3 activities might hereafter be exploited as a possible pharmacological target for MJD therapy.

Aim 2. - To assess the influence of a functional deubiquitinating capacity in the intracellular and biological properties of ataxin-3.

Many cellular pathways are regulated by ubiquitination and deubiquitination processes. DUBs play a major role in these pathways by feeding the intracellular pool of free ubiquitin and by removing or altering the ubiquitin signal attached to protein-substrates. Due to their central function in various cellular mechanisms, DUBs are highly regulated proteins. Although, a lot is still unknown regarding the regulation of DUBs, DUB activity is usually cryptic in which the interaction with a substrate or another interacting protein is necessary to promote enzyme's active state. Therefore, the presence of a fully functional catalytic domain might alter and modulate the overall properties of a DUB. Taking this into account, in this part of the work, we aimed to determine the influence of a functional Josephin domain for the cellular properties of the entire ataxin-3 protein, using a catalytic inactive ataxin-3. Inactivity was obtained through the mutation of a specific cysteine residue, present in the Josephin catalytic cleft and essential for catalysis. The catalytic inactive mutant proteins were used in comparison to active ataxin-3 proteins, to determine the contribution of a functional Josephin domain in the protein levels, ubiquitination pattern and intracellular distribution of ataxin-3. Further investigation of these regulatory processes might discover intracellular pathways, susceptible to modulation, which may reveal to be useful to improve cell's ability to cope with toxic expanded ataxin-3.

Aim 3. – To evaluate the mitochondrial dysfunction in MJD pathogenesis

Previous studies have reported several levels of mitochondrial dysfunction in different polyQ disorders. Alterations in mitochondrial architecture, mitochondria fusion and fission processes, intracellular transport of mitochondria, mitochondrial

Ca^{2+} handling and buffer capacity, along with deregulation of mitochondrial complexes activities and activation of apoptotic mitochondrial pathways, have all been associated with polyQ pathogenesis. Most studies have been carried out in HD cell and animal models, although other polyQ diseases have also been assessed for mitochondrial dysfunction. Even so, the contribution of mitochondrial dysfunction in MJD pathogenesis is still not clearly investigated. This part of the work intended to address this topic by measuring the cell susceptibility to selective mitochondrial inhibitors, under the expression of wild-type or expanded human ataxin-3. The comparison of cell viability under mitochondrial inhibition in the presence of wild-type or expanded ataxin-3 discloses the deleterious effect of expanded ataxin-3 in mitochondrial function. Moreover, the analysis of the activity of each individual mitochondrial complex in several cell and animal models of MJD discriminates the crucial step of the mitochondrial respiratory chain that may be selectively deregulated by expanded ataxin-3. Usage of various models of MJD further corroborates that mitochondrial dysfunction might be a hallmark of MJD pathogenesis.

Chapter 2

Valosin-containing protein (VCP/p97) is an activator of wild-type ataxin-3

2.1. Abstract

Alterations in the ubiquitin-proteasome system (UPS) have been reported in several neurodegenerative disorders characterized by protein misfolding and aggregation, including the polylgutamine diseases. Machado-Joseph disease (MJD) or Spinocerebellar Ataxia type 3 is caused by a polyglutamine-encoding CAG expansion in the *ATXN3* gene, which encodes a 42 kDa deubiquitinating enzyme (DUB), ataxin-3. We investigated ataxin-3 deubiquitinating activity and the functional relevance of ataxin-3 interactions with two proteins previously described to interact with ataxin-3, hHR23A and valosin-containing protein (VCP/p97). We confirmed ataxin-3 affinity for both hHR23A and VCP/p97. hHR23A and ataxin-3 were shown to colocalize in discrete nuclear foci, while VCP/p97 was primarily cytoplasmic. hHR23A and VCP/p97 recombinant proteins were added, separately or together, to normal and expanded ataxin-3 in *in vitro* deubiquitination assays to evaluate their influence on ataxin-3 activity. VCP/p97 was shown to be an activator specifically of wild-type ataxin-3, exhibiting no effect on expanded ataxin-3, In contrast, we observed no significant alterations in ataxin-3 enzyme kinetics or substrate preference in the presence of hHR23A alone or in combination with VCP/p97. Based on our results we propose a model where ataxin-3 normally functions with its interactors to specify the cellular fate of ubiquitinated proteins.

2.2. Introduction

Ataxin-3 is a 42 kDa intracellular protein capable of binding and hydrolysing ubiquitin chains (Burnett et al, 2003; Berke et al., 2005; Winborn et al., 2008). Ataxin-3 was first recognized as the protein implicated in Machado-Joseph disease (MJD), also known as spinocerebellar ataxia type 3 (Riess et al., 2008). MJD is a polyglutamine disorder, one of a group of nine neurodegenerative diseases that share a common genetic cause: an expansion of a CAG trinucleotide repeat in the coding region of the respective disease genes (Paulson, 2007; Bauer and Nukina, 2009; Hands and Wyttenbach, 2010). In the case of MJD, the pathogenic expansion occurs in the *ATXN3* gene, which encodes a deubiquitinating enzyme (DUB), ataxin-3. When expanded the CAG repeat encodes an abnormally long polyglutamine (polyQ) track near the C-terminus of ataxin-3 (Dürr et al., 1996; Paulson et al., 1997b). The polyQ expansion destabilizes ataxin-3 structure, increasing its propensity to misfold and form large intracellular aggregates (Bevinino and Loll, 2001; Ellisdon et al., 2007). Through its aggregation, expanded ataxin-3 sequesters house-keeping proteins that are essential for cell homeostasis inside intracellular aggregates (Paulson et al., 1997a; Perez et al., 1998; Haacke et al., 2006). Although these aggregates were initially speculated to cause neurodegeneration, more recent studies suggest that their formation represents a cellular defense mechanism against smaller toxic oligomers of the mutant protein (Gales et al., 2005; Ellisdon et al., 2006).

The polyQ expansion alone can not account for all the specific characteristics and selective neuronal loss in MJD. The protein context in which the polyQ is expressed is a crucial determinant of the pathological mechanisms triggered by expanded ataxin-3 (Nozaki et al., 2001; Ellisdon et al., 2006; Bichelmeier et al., 2007; Fei et al., 2007; Saunders et al., 2009). Many recent studies have focused on wild-type ataxin-3 function. Ataxin-3 has shown to be a DUB with an N-terminal catalytic "Josephin" domain with ubiquitin hydrolase activity, and two or three ubiquitin-interacting motifs (UIM) depending on the splice isoform, responsible for the interaction with ubiquitin chains (Burnett et al, 2003; Berke et al., 2005). Ataxin-3

possesses higher affinity for longer ubiquitin chains, containing at least four molecules of ubiquitin, and preferentially cleaves linkages between ubiquitin molecules established through lysine 63 (K63) (Winborn et al., 2008). These characteristics suggest that ataxin-3 is an ubiquitin chain editing enzyme.

As an enzyme, ataxin-3 is regulated at multiple levels in the cell. Mono-ubiquitination of ataxin-3, which is enhanced by proteotoxic stress, increases its ubiquitin hydrolase activity (Todi et al., 2009). Ataxin-3's translocation between the nucleus and the cytosol is regulated by nuclear import and export signals in association with specific phosphorylation and dephosphorylation events (Macedo-Ribeiro et al., 2009; Mueller et al., 2009). The high degree of regulation sustains a central role for ataxin-3 in the protein quality control of the cell. Ataxin-3 has been implicated in ubiquitin-proteasome pathways (Schmitt et al., 2007), endoplasmic reticulum associated degradation (ERAD) (Zhong and Pittman, 2006) and the cytoprotective response to heat shock stress (Reina et al., 2010).

The study of ataxin-3 enzymatic activity, its nuclear-cytoplasm translocation, and the colocalization of other cellular proteins to intracellular aggregates formed by expanded ataxin-3 have spurred the search for ataxin-3 interactors. A growing number of interactors have been identified that are diverse in structure and function, reflecting the wide range of biological activities associated with ataxin-3 (Wang et al., 2000; Boeddrich et al., 2006; Evert et al., 2006; Mazzucchelli et al., 2009). Some of these protein interactions occur independently of the polyQ expansion and likely relate to normal ataxin-3 function. In the current study, we have focused on two of these interactors, hHR23A and valosin-containing protein (VCP/p97). hHR23A and hHR23B, the human homologs of RAD23 yeast protein, are involved in DNA repair pathways and the delivery of ubiquitinated substrates to the proteasome for degradation (Dantuma et al., 2009). hHR23A has two ubiquitin-associated (UBA) domains which recognize and bind ubiquitin motifs, and an ubiquitin-like domain which interacts with the globular catalytic domain of ataxin-3 (Raasi et al., 2004). VCP/p97 protein is a 97 kDa AAA ATPase involved in several cellular pathways, including the extraction of ubiquitinated proteins from the endoplasmic reticulum for degradation by ERAD (Zhong and Pittman, 2006). VCP/p97 is an abundant cellular

protein that has numerous interactions with other proteins (Madsen et al., 2009). An extensive study has uncovered the region in ataxin-3 crucial to the interaction with VCP/p97, which is situated after the second UIM, just prior to the polyQ domain (Boeddrich et al., 2006).

In previous reports, ataxin-3 was shown to be a DUB with rather slow kinetics (Winborn et al., 2008). However, a post-translational modification of ataxin-3, ubiquitination, was highly effective at enhancing ubiquitin hydrolase activity of ataxin-3 (Todi et al., 2009). Here, we sought to investigate whether VCP/p97 or hHR23A, both of which are involved in protein degradation pathways, also enhanced ataxin-3 activity through direct interactions. Modulation of ataxin-3 activity through protein-protein interactions might represent an additional level of regulation over its DUB activity and cellular roles. Moreover, a better understanding of how ataxin-3 is regulated may lead to the identification of pathological targets underlying neurodegeneration in MJD.

2.3. Material and methods

2.3.1. Cell line culture

COS 7 cells (ATCC®, UK) were cultured in Dulbecco's modified Eagle's medium (DMEM) supplemented with 10% fetal bovine serum (FBS) (Invitrogen, UK) and 1% streptomycin/penicillin (Gibco, UK), at 37ºC and under a 95% air and 5% CO_2 controlled atmosphere.

2.3.2. Immunocytochemistry and microscopy

Confluent cultures of COS-7 cells (ATCC®, UK) were split and cells were plated over 13 mm glass coverslips without coating. In the next day, the cells were washed 2 times with phosphate buffered solution (PBS, in mM: 137 NaCl, 2.7 KCl, 1.4 K_2HPO_4, 4.3 Na_2HPO_4, pH 7.4) before being fixed in 4% paraformaldehyde (PFA) in PBS for 15 minutes. Thereafter, the cells were rinsed 3 times with PBS and opsonized with 5% goat serum in PBT (PBS plus 0.1% Triton X-100) for 1 hour at room temperature. Cells were incubated with primary antibodies: mouse monoclonal anti-ataxin-3 1H9 (1:1000; Chemicon, USA), rabbit polyclonal anti-hHR23A (1:50; ProteinTech Group, USA), rabbit polyclonal anti-VCP/p97 (1:200; Cell Signaling, USA) diluted in 5% goat serum in PBT for 1 hour at room temperature, then the coverslips were washed 2 times with PBS and immersed in a diluted solution of secondary antibodies: anti-mouse Alexa-fluor 594 (1:250; Molecular Probes, USA) and anti-rabbit Alexa-fluor 488 (1:250; Molecular Probes, USA) in 5% goat serum in PBT for another hour at room temperature. Finally, cells were stained with Hoechst 33342 (1 μg/μl; Molecular Probes, USA) in PBS for 5 minutes, before mounting the coverslips in DAKO solution. Confocal images were taken in a LSM 510 Meta confocal microscope (Carl Zeiss, Germany) with a EC-PlanNeofluar (40x magnification) and a Plan-ApoChromat (63x magnification) using a Diode 405-30 (405 nm), Argon/2 (488 nm) and DPSS 561-10 (561 nm) lasers.

2.3.3. Plasmids

The construction of pGEX-6P1 vectors expressing wild-type (Q22) ataxin-3, catalytically inactive (C14A) ataxin-3 mutant and expanded (Q80) ataxin-3 was previously described (Winborn et al., 2008). hHR23A and human VCP/p97 plasmids were generated by digesting the corresponding pcDNA3-hHR23A and pET28-VCP/p97-wt with BamHI and NotI, followed by insertion of the released fragments into pGEX-6P1 vector. ^{282}RKRR-HNHH (Q22) and (Q80) ataxin-3 constructs were generated through mutation of the respective pGEX-6P1-(Q22), -(Q80) ataxin-3 plasmids with forward primer 5'-CTTACTTCAGAAGAGCTTCATAACCATCA and reverse primer 5'-GCTGCTGTTTTTCAAAGTAGGCTTCATGA by polymerase chain reaction (PCR).

2.3.4. Recombinant protein purification

Glutathione-S-transferase (GST) fusion proteins were purified as previously described (Todi et al., 2007). Briefly, pGEX-6P1 plasmids encoding GST-Atx-3 (Q22), GST-Atx-3 (Q22) ^{282}RKRR-HNHH, GST-Atx-3 (Q80), GST-Atx-3 (Q80) ^{282}RKRR-HNHH, GST-hHR23A and GST-VCP/p97 were transformed into BL21 E. coli cells (GE Healthcare, UK) and individual colonies were obtained by selective growth in solid Luria Bertani medium (LB) plus ampicillin at 37°C overnight. In the following day, 1 ml of the overnight growth was used to inoculate 100 ml of liquid LB for additional growth at 37°C until reaching an optical density = 0.4. GST-fusion proteins expression was induced with 1 mM isopropyl-1-thio-D-galactopyranoside for 5 h at 30°C. After this expression period, the cells were centrifuged at 4000 rpm for 15 min at 4ºC and resuspended in ice-cold lysis buffer (150 mM NaCl, 50 mM NaH_2PO_4, 10% glycerol, 0.5 mM ethylenediamine tetraacetic acid (EDTA), 1 mM 1,4-dithiothreitol (DTT)), sonicated, and centrifuged for an additional 10 min to remove debris. The supernatants were incubated with glutathione-Sepharose beads (GE Healthcare, UK) in ice, for 30 min, with gentle agitation and the beads were rinsed 4 times with PreScission protease cleavage buffer (50 mM Tris-HCl, 150 mM NaCl, 10 mM EDTA, 1 mM DTT, pH 8.0, 20% glycerol), before being incubated with PreScission protease (80 units/ml, GW Healthcare, UK) in cleavage buffer overnight, with gentle agitation.

The next day, beads were centrifuged in Spin-X centrifuge tube filter columns (Corning Costar, USA) and the supernatant containing the recombinant protein free of the GST domain was collected and stored at - 80ºC.

2.3.5. Immunoprecipitation

For the immunoprecipitation of endogenous proteins, COS-7 cells (ATCC®, UK) were lysed in FLAG lysis buffer (50 mM Tris, 150 mM NaCl, 1 mM EDTA, 1% Triton X-100, pH 7.4) supplemented with 1 µg/ml protease inhibitor cocktail (chymostatin, pepstatin A, leupeptin, and antipain). For the immunoprecipitation from *in vitro* samples, 100 nM of both recombinant proteins were incubated in deubiquitination buffer (50 mM HEPES, 0.5 mM EDTA, 0.1 µg/µl ovalbumine , 1mM DTT, 1 µg/ml protease inhibitor cocktail, at 37° C for 5 hours. Cell lysates and *in vitro* samples were washed with Protein A Sepharose beads (GE Healthcare, UK) to reduce nonspecific binding to the beads, before the incubation with mouse monoclonal (1H9; 1:1000) or rabbit polyclonal (MJD; 1:1000) anti-ataxin-3 antibodies overnight, at 4 °C with gentle agitation. Beads were then precipitated by centrifugation at 500 x g, 4ºC for 5 min, washed six times with FLAG lysis buffer, and the protein was eluted with Laemmli buffer at room temperature. The eluted immunoprecipitates were collected in Spin-X centrifuge tube filter columns by centrifugation and stored at - 80ºC and resolved by SDS-PAGE followed by western blotting.

2.3.6. Pull-down experiments

Recombinant GST-VCP/p97 fusion protein or GST protein alone were expressed in BL-21 cells (GE Healthcare, UK) as described in the recombinant protein purification section. The cells were sonicated and centrifuged to discard cell debris. The lysates were poured into columns containing glutathione-Sepharose beads (GE Healthcare, UK) and incubated for 30 min on ice with occasional agitation. Beads were washed 6 times with FLAG lysis buffer before being added to COS-7 total extracts in FLAG Lysis buffer, which had been previously incubated with glutathione beads for 1 hour to reduce unspecific interactions with the beads. COS-7 total extracts were in contact with the beads for 2 hours, at 4ºC in constant agitation. Beads were

washed another 4 times with FLAG lysis buffer supplemented with protease inhibitors and resuspended in Laemmli buffer for 15 min, at room temperature. Beads were centrifuged a last time for 5 min, at 500 x g and the elutants were stored at - 80 ºC.

2.3.7. Protease assays

100 nM human recombinant wild-type (Q22) or expanded (Q80) ataxin-3 was incubated with 250 nM K63 or K48 linked hexa-ubiquitin chains (Boston Biochem, USA) in the absence or presence of 100 nM recombinant VCP/p97, 100nM recombinant hHR23A, or both. The protease assay was performed in *in vitro* deubiquitination buffer, at 37°C for up to 20 hours. Samples from the reaction mixture were collected at 0, 2, 5 and 20 hours. Reactions were stopped with loading buffer at room temperature.

2.3.8. SDS-PAGE and immunoblotting

Total extracts from COS-7 cells (ATCC®, UK), ubiquitin protease assay and immunoprecipitation samples were collected and separated by SDS-PAGE using 10% polyacrylamide gels. Afterwards, the proteins were transferred onto polyvinylidene difluoride membranes (Hybond-P, GE Healthcare, UK) which were further blocked in a 5% non-fat milk solution for 60 minutes. Membranes were incubated with a mouse monoclonal anti-ataxin-3 (1H9, 1:1000, Chemicon), a rabbit polyclonal anti-hHR23A (1:1000; ProteinTech Group, USA), a rabbit polyclonal anti-VCP/p97 (1:1000, Cell Signaling, USA) or a rabbit polyclonal anti-ubiquitin (1:1000, Dako, Denmark) antibodies overnight, at 4ºC with agitation. After being washed, the blots were incubated with alcaline phosphatase conjugated anti-mouse secondary antibody (GE Healthcare, UK) and developed with enhanced chemifluorecence. The membranes were visualized in a Biorad VersaDoc Imaging System Model 3000.

2.3.9. Statistical analysis

Data were expressed as mean ± SEM of the number of experiments indicated in the figure legends. Comparisons between two conditions were performed by two-tailed unpaired t-test. Significance was defined at $p<0.05$.

2.4. Results

2.4.1. VCP/p97 and hHR23A interact directly with ataxin-3

It was previously shown that ataxin-3 can bind and cleave ubiquitin chains (Burnett et al, 2003; Berke et al., 2005; Winborn et al., 2008). Since protein-protein interactions are known to modulate enzymatic activity, we hypothesized that hHR23A and/or VCP/p97 could modify the ubiquitin hydrolase activity of ataxin-3 through direct interaction. To test this hypothesis we investigated the interaction between these three proteins *in vitro* and in cells.

Immunostaining for hHR23A and ataxin-3 in COS-7 cells revealed a strong spatial correlation (Figure 2.1.A). Endogenous hHR23A and ataxin-3 were both more prevalent in the nucleus. Within this organelle, hHR23A and ataxin-3 exhibited a punctate pattern with additional diffuse distribution throughout the nucleoplasm, excluding the nucleolus. Ataxin-3 and hHR23A were often present in the same nuclear puncta, although the proteins did not perfectly co-localized through the entire cell. The presence of both proteins in specific subnuclear regions may indicate the compartmentalization of nuclear areas dedicated to protein degradation. Immunoprecipitation of endogenous ataxin-3 from COS-7 cell extracts co-precipitated endogenous hHR23A, suggesting that these co-localized proteins also interact in the cell (Figure 2.1.B). As previously reported (Wang et al. 2000; Chen and Madura, 2006), immunoprecipitation of recombinant ataxin-3 co-precipitated recombinant hHR23A, demonstrating that hHR23A and ataxin-3 directly interact *in vitro* (Figure 2.1.C).

VCP/p97 is an abundant cellular protein that is homogeneous distributed throughout the cytosol of immunostained COS-7 cells, as shown in Figure 2.1.D. Unlike ataxin-3 and hHR23A, VCP/p97 was not enriched in the nucleus. Nevertheless, recombinant GST-VCP/p97 fusion protein bound to GSH-beads was able to pull-down endogenous ataxin-3 from COS-7 cell extracts (Figure 2.1.E), indicating a significant interaction between the two proteins. Recombinant human

wild-type (Q22) ataxin-3 also co-immunoprecipitated recombinant VCP/p97 *in vitro* (Figure 2.1.F), supporting a direct interaction between ataxin-3 and VCP/p97.

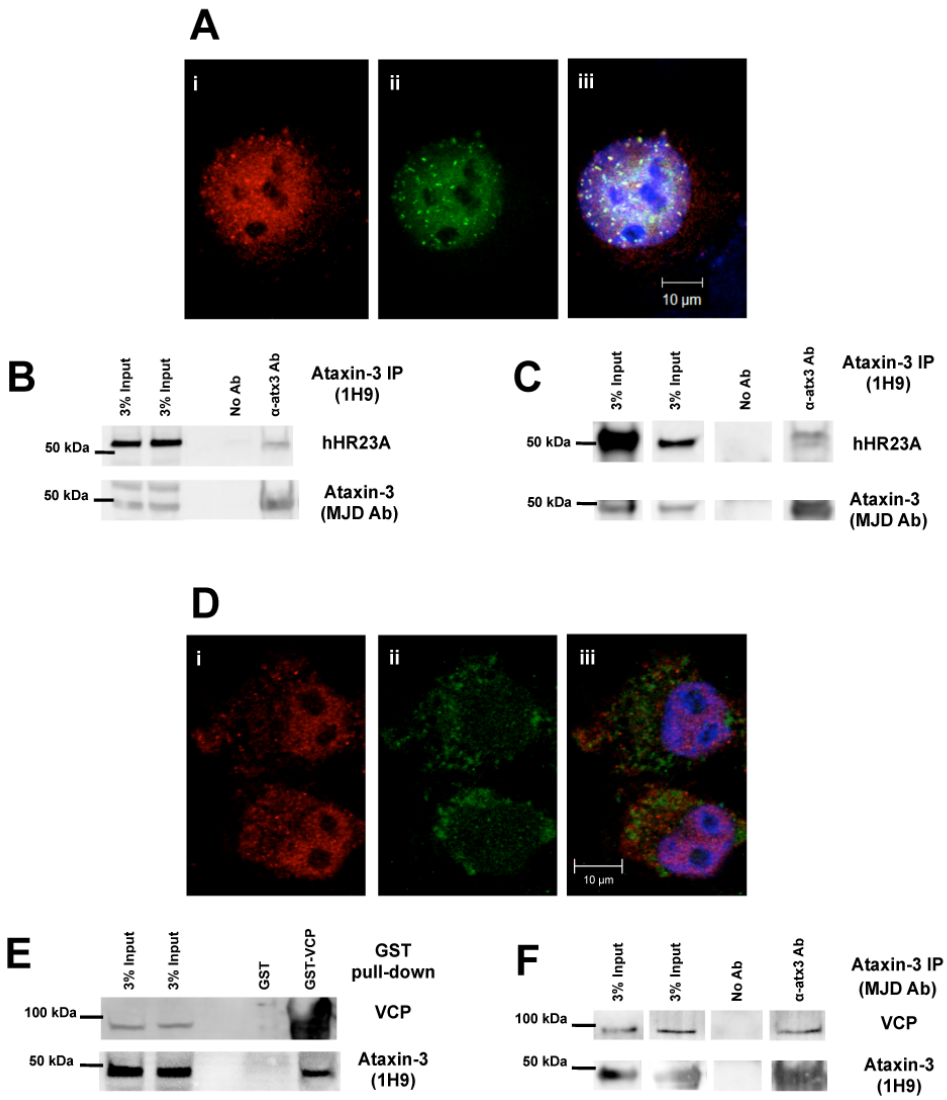

Figure 2.1. - Ataxin-3 interacts directly with hHR23A and VCP/p97. (**A**) Confocal microscopy images of COS-7 cells fixed and immunostained for endogenous ataxin-3 (i-red) and hHR23A (ii-green). DNA was stained with Hoescht 33342 (blue) in the merged image (iii). (**B**) Endogenous ataxin-3 was immunoprecipitated from COS-7 cell extracts and co-immunoprecipitation of endogenous hHR23A was determined by western blotting. (**C**) Recombinant human ataxin-3 and recombinant human hHR23A were incubated under the same conditions applied in the *in vitro* protease assays, for 5 hours at 37ºC. Recombinant ataxin-3 was precipitated using anti-ataxin-3 (1H9) antibody and hHR23A co-

immunoprecipitation was analyzed by western blotting. (**D**) Visualization of endogenous ataxin-3 (i-red) and VCP/p97 (ii-green) through confocal microscopy in fixed COS-7 cells using specific antibodies. Nuclei were stained Hoescht 33342 dye (blue) for merged images. (**E**) Recombinant GST-VCP/p97 fusion protein was used to pull-down endogenous ataxin-3 from COS-7 total extracts. Endogenous ataxin-3 and recombinant VCP/p97 were detected by western blotting. (**F**) Recombinant human VCP/p97 and recombinant human (Q22) ataxin-3 were added to a buffered solution at 37ºC for 5 hours. These samples were used to immunoprecipitate ataxin-3 and co-immunoprecipitation of VCP/p97 was assessed by western blotting.

2.4.2. VCP/p97 enhances wild-type ataxin-3 activity *in vitro*

Ataxin-3 interacts with VCP/p97 through a region near the polyQ domain and far from the Josephin domain (Boeddrich et al., 2006). The interaction with VCP/p97 may position ataxin-3 in close proximity to polyubiquitinated protein substrates in the cell, as implied by its regulatory effect of the ERAD pathway (Zhong and Pittman, 2006). To determine whether VCP/p97 can alter ataxin-3 activity, we performed *in vitro* deubiquitination experiments in which recombinant human VCP/p97 was added to the reaction. Ataxin-3 enzymatic activity was assessed through *in vitro* deubiquitination assays as in Burnett et al. (2003) and Winborn et al. (2008). Ataxin-3 acts on longer ubiquitin chains and exhibits preference for ubiquitin chains with ubiquitin molecules linked through K63 (Winborn et al. 2008). Thus, an ubiquitin chain containing six ubiquitin molecules linked through K63 was used as an optimal substrate to evaluate the influence of hHR23A in ataxin-3 deubiquitinating activity. Ataxin-3 (Q22) incubated with K63 linked hexa-ubiquitin chains generated lower molecular weight reaction products, resulting from the cleavage of ubiquitin linkages (Figure 2.2.A). When VCP/p97 was added to the reaction employing K63-linked chain, an increase in the accumulation of reaction products was observed (Figures 2.2.A and 2.2.B). In contrast, VCP/p97 did not enhance significantly the cleavage of K48-linked chains by ataxin-3 (Figures 2.2.C and 2.2.D). Increased cleavage of K63-linked chains in the presence of VCP/p97 was not due to ataxin-3 stabilization, because there were no differences in ataxin-3 levels through the reaction course, in the presence or absence of VCP/p97 (Figure 2.2.A). To rule out the possibility that the

enhanced K63-linked chain cleavage reflected a direct activity of VCP/p97 on ubiquitin chains, we incubated catalytically inactive ataxin-3 mutant (C14A) with VCP/p97 under the same reaction conditions.

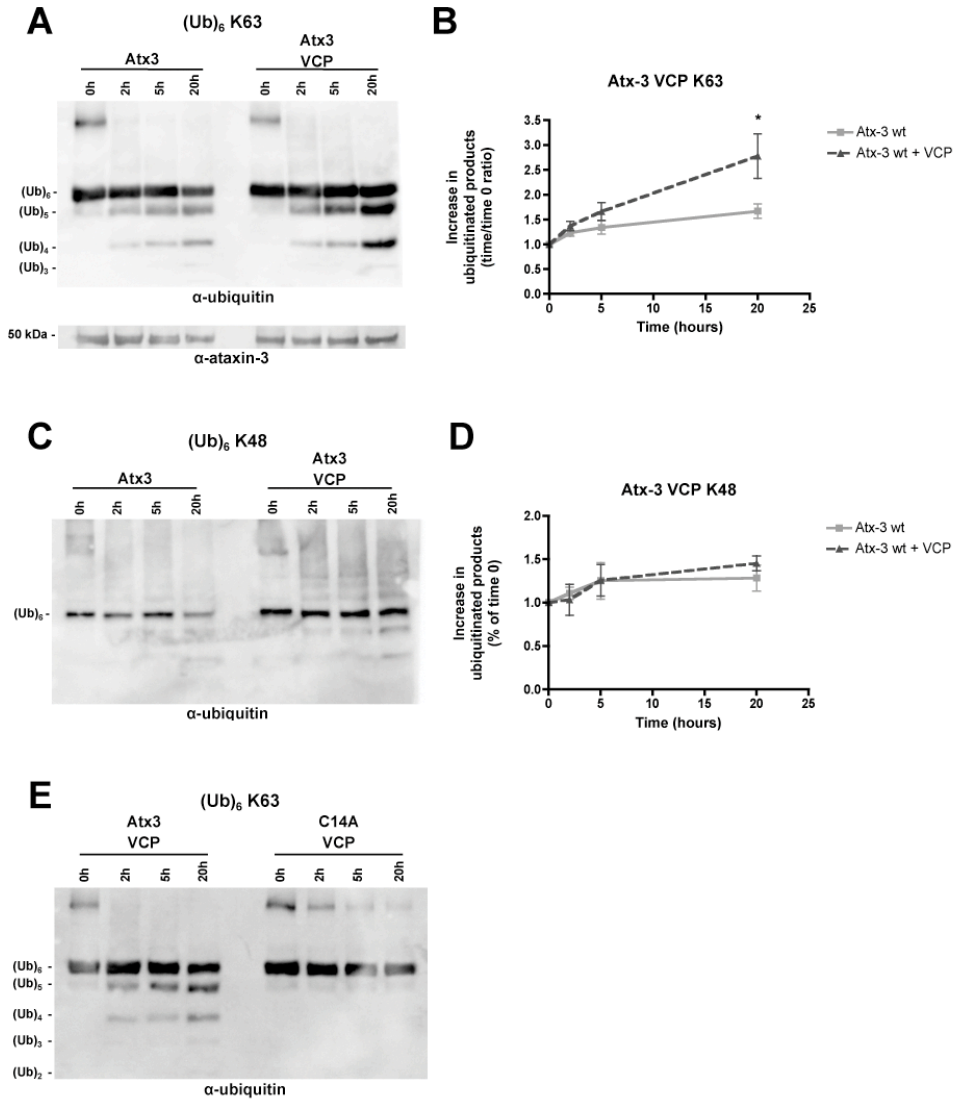

Figure 2.2. - VCP/p97 enhances deubiquitinase activity of ataxin-3 *in vitro*. K63-linked (**A**) and K48-linked (**C**) hexa-ubiquitin chains (250 nM) were incubated with recombinant human (Q22) ataxin-3 (100 nM) with or without recombinant human VCP/p97 (100 nM) for 20 hours at 37°C. Samples collected at 0, 2, 5 and 20 hours were submitted to SDS-PAGE analysis and reaction products were detected by

immunoblotting with an anti-ubiquitin antibody. The graphs summarize the mean ± SEM of the increase in reaction products over time resulting from the hydrolysis of K63-linked (**B**) and K48-linked (**D**) hexa-ubiquitin chains by ataxin-3 in the absence (light grey squares) or presence (dark grey triangles) of VCP/p97 in 3 - 5 independent experiments. Statistical analysis: * $p<0.05$, compared to recombinant human wild-type ataxin-3 alone at 20 hours. (**E**) K63-linked hexa-ubiquitin chains (250 nM) were incubated with recombinant wild-type or catalytically inactive (C14A) ataxin-3 (100 nM) in the presence of VCP/p97 (100 nM) for 20 hours at 37ºC. The 0, 2, 5 and 20 hours time-points were analysed by western blotting with an anti-ubiquitin antibody.

As shown in Figure 2.2.E, no reaction products were detected, demonstrating that VCP/p97 enhances ataxin-3 enzymatic activity rather than act directly on ubiquitin chains.

2.4.3. VCP/p97 does not enhance ubiquitin hydrolase activity of expanded ataxin-3

Previous *in vitro* studies of ataxin-3 activity have not identified any differences in substrate preference or reaction kinetics between wild-type (Q22) and expanded (Q80)

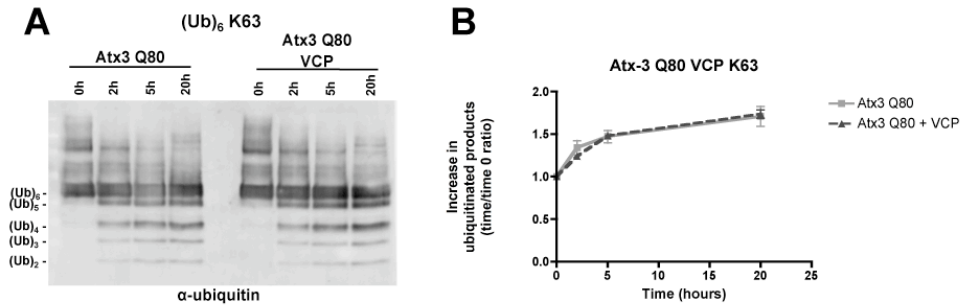

Figure 2.3. - VCP/p97 does not enhance expanded ataxin-3 activity *in vitro*. (**A**) Recombinant human expanded (Q80) ataxin-3 (100 nM) was incubated with K63-linked hexa-ubiquitin chains (250 nM) in the absence or presence of recombinant human VCP/p97 (100 nM), for 20 hours at 37ºC. Samples of 0, 2, 5 and 20 hours time-points were separated by SDS-PAGE and immunoblotted for ubiquitin. (**B**) The graph shows the mean ± SEM of the increase in reaction products over time resulting from the deubiquitinase activity of expanded ataxin-3 over K63-linked hexa-ubiquitin chains in the absence (light grey squares) or presence (dark grey triangles) of VCP/p97 in 4 independent experiments

ataxin-3 (Winborn et al., 2008). Nevertheless, we sought to investigate whether VCP/p97 similarly stimulated the protease activity of expanded ataxin-3. To test this, we expressed and purified human recombinant ataxin-3 with 80 glutamines (Q80). We assayed recombinant human expanded ataxin-3 (Q80) in the same reaction conditions used for nonpathogenic ataxin-3, in the absence or presence of VCP/p97. Unexpectedly, VCP/p97 did not alter expanded ataxin-3 activity towards K63-linked ubiquitin chains (Figures 2.3.A and 2.3.B). This result validates the direct VCP/p97 stimulation of wild-type ataxin-3. An indirect effect of VCP/p97 over ataxin-3 activity (e.g. increased accessibility to the ubiquitin chains) would produce a similar effect in both wild-type and expanded proteins.

2.4.4. Blockade of VCP/p97-ataxin-3 protein interaction abolishes VCP/p97 stimulation of ataxin-3 protease activity

The region of ataxin-3 that mediates the interaction with VCP/p97 is located between the first two ubiquitin-interacting motifs (UIM)s, near the polyQ track (Boeddrich et al., 2006). A sequence of four amino acids in ataxin-3 is crucial for this interaction, the basic amino acids ^{282}RKRR (arginine/lysine-rich motif), which also constitute part of a nuclear localization signal (Trottier et al., 1998; Antony et al., 2009; Macedo-Ribeiro et al., 2009). A four amino acid substitution (^{282}RKRR to HNHH) has been shown to block the interaction between ataxin-3 and VCP/p97 *in vitro*. We substituted these four amino acids in wild-type (Q22) and expanded (Q80) ataxin-3 constructs in order to block the interaction between ataxin-3 and VCP/p97. Recombinant ataxin-3 mutants were incubated with human recombinant VCP/p97 under the same experimental conditions of *in vitro* deubiquitination assays, followed by immunoprecipitation of ataxin-3. As expected, the ^{282}RKRR - HNHH amino acids substitution effectively reduced the interaction of ataxin-3 mutants with VCP/p97 *in vitro* (Figure 2.4.A). Whereas VCP/p97 was co-immunoprecipitated with wild-type (Q22) and expanded (Q80) ataxin-3, almost no VCP/p97 co-immunoprecipitated with the wild-type (Q22) and expanded (Q80) (^{282}RKRR-HNHH ataxin-3 variants).

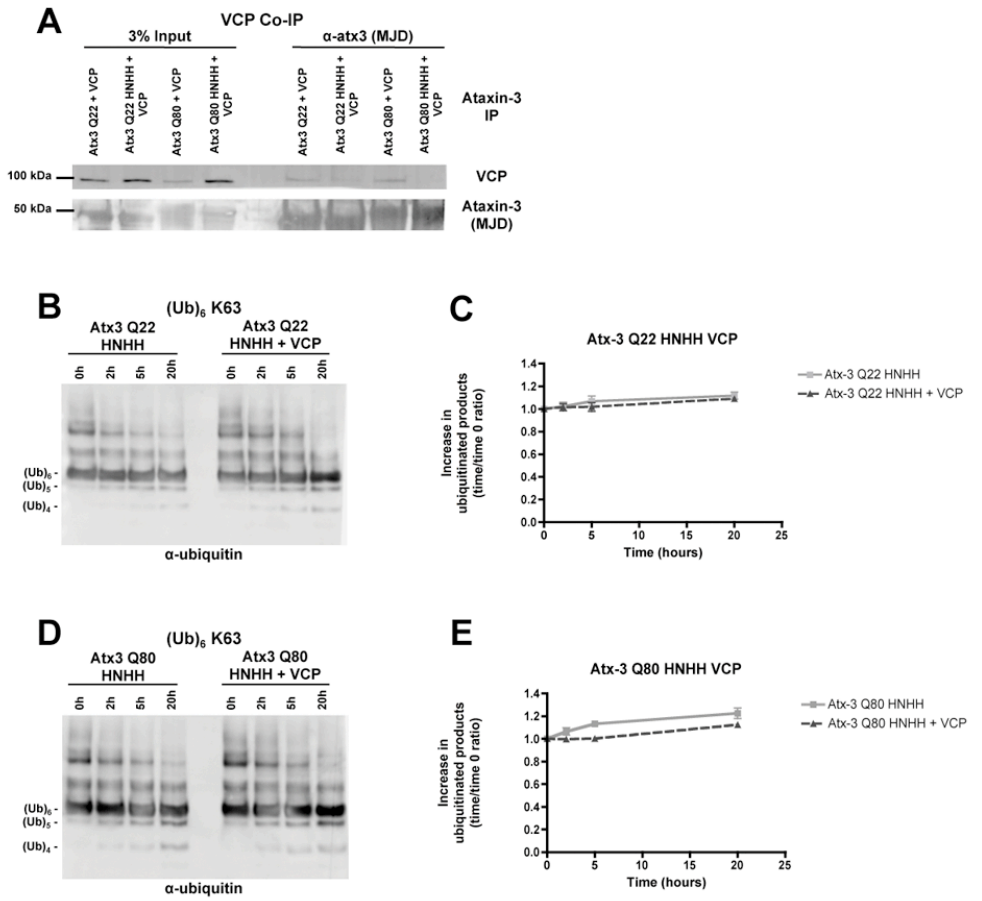

Figure 2.4. - VCP/p97 enhancement of wild-type ataxin-3 activity is mediated through a direct protein-protein interaction. (**A**) Co-immunoprecipitation of recombinant human VCP/p97 (100 nM) with ataxin-3 (100 nM) with 22 or 80 glutamines in its wild-type or (^{282}RKRR-HNHH) mutant form, after a pre-incubation of 5 hours at 37ºC in a buffered solution. Ataxin-3 forms were precipitated with an anti-ataxin-3 polyclonal antibody (αMJD) and co-immunoprecipitation was assessed by western blotting using anti-VCP/p97 polyclonal antibody. (**B**) Ubiquitin protease assay for Q22 and Q80 (^{282}RKRR-HNHH) ataxin-3 mutants (100 nM) in the absence or presence of recombinant human VCP/p97 (100 nM), using K63-linked hexa-ubiquitin chains (250 nM) as substrate. Samples were collected at times 0, 2, 5 and 20 hours and analyzed by western blotting using an anti-ubiquitin antibody. Graphs express the mean ± SEM of the increase in reaction products over time resulting from the hydrolysis of K63-linked hexa-ubiquitin chains by Q22 (**C**) and Q80 (**D**) (^{282}RKRR-HNHH) ataxin-3 mutants in the absence (light grey squares) or presence (dark grey triangles) of VCP/p97 from 3 independent experiments.

We then tested the ubiquitin hydrolase activity of the ^{282}RKRR-HNHH ataxin-3 mutants *in vitro*. Wild-type (Q22) and expanded (Q80) ^{282}RKRR-HNHH mutants were both catalytically active, however the protease activity of these mutants was slightly reduced compared to normal Q22 and Q80 ataxin-3 (Figure 2.5.), registering a decrease in the total amount and in the rate of production of low molecular weight ubiquitin chains (Figures 2.4.B and 2.4.D).

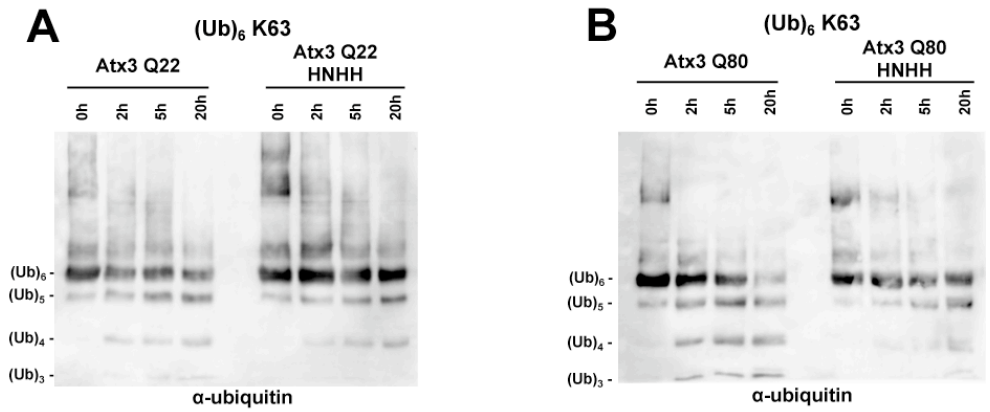

Figure 2.5. - (^{282}RKRR-HNHH) ataxin-3 VCP/p97-binding mutants exhibit a small reduction in their protease activity. Ubiquitin protease assay for (**A**) wild-type (Q22) normal and (^{282}RKRR-HNHH) ataxin-3 mutant and (**B**) expanded (Q80) and (^{282}RKRR-HNHH) ataxin-3 mutant, using K63-linked hexa-ubiquitin chains as substrate. Samples were collected at times 0, 2, 5 and 20 hours and analyzed by western blotting using an anti-ubiquitin antibody.

Moreover, adding VCP/p97 to the reaction system did not increase the ubiquitin hydrolase activity of either ^{282}RKRR-HNHH mutant (Figures 2.4.C and 2.4.E). These results demonstrate that VCP/p97 stimulation of wild-type (Q22) ataxin-3 protease activity is mediated through a direct interaction with the enzyme.

2.4.5. hHR23A does not change the kinetics or the substrate preference of ataxin-3

hHR23A can simultaneously bind ubiquitin chains and ataxin-3 (Wang et al., 2000; Raasi et al., 2004; Nicastro et al., 2005).

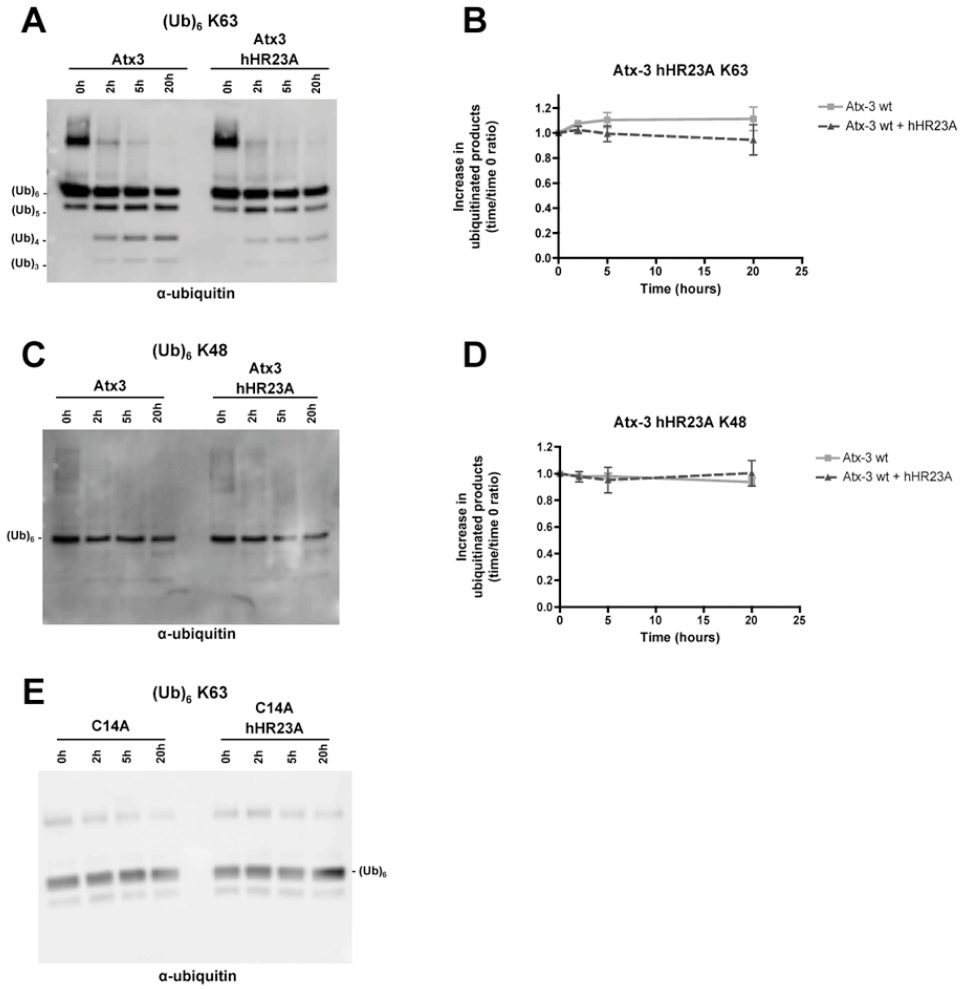

Figure 2.6. - hHR23A has no effect over the ubiquitin hydrolase activity of ataxin-3. Recombinant human (Q22) wild-type (**A, C**) or catalytic inactive (C14A) (**E**) ataxin-3 (100 nM) was incubated alone or together with recombinant hHR23A (100 nM) in a buffered solution containing hexa-ubiquitin chains (250 nM) with K63 (**A, E**) or K48 (**C**) linkages for 20 hours at 37ºC. Samples were collected at 0, 2, 5 and 20 hours and analyzed by immunoblotting. The reaction products were detected using an antibody against ubiquitin (**A, C, E**). The appearance of reaction products resulting from the cleavage of K63-linked (**B**) or

K48-linked (**D**) hexa-ubiquitin chains by ataxin-3 in the absence (light grey squares) or presence (dark grey triangles) of hHR23A was quantified; the mean ± SEM of 4 independent experiments was plotted in graphs.

In our co-localization studies, hHR23A and ataxin-3 revealed a high homology in their nuclear distributions. For these reasons, hHR23A emerged as a strong candidate for a direct modulator of the ubiquitin hydrolase activity of ataxin-3. To test this model, we quantified the enzymatic activity of recombinant human wild-type ataxin-3 (Q22) in the absence or presence of recombinant hHR23A (Figure 2.6.). As reported previously, ataxin-3 (Q22) deubiquitinates K63-linked ubiquitin chains and promotes the appearance of smaller ubiquitin chains over time. No enhancement in the rate of accumulation of reaction products was observed in the presence of hHR23A (Figures 2.6.A and 2.6.B); rather, there was a trend towards decreased accumulation of reaction products. hHR23A did not alter the substrate preference of ataxin-3 either, as ataxin-3 continued to cleave K63-linked chains more robustly than K48-linked ubiquitin chains (Figures 2.6.C and 2.6.D). Hence, hHR23A does not alter ataxin-3 activity, at least in these *in vitro* assays. Our data is in accordance with a recent report also showing no alteration in the ability of ataxin-3 to cleave ubiquitin chains in the presence of hHR23A (Nicastro et al., 2010). As expected, catalytically inactive ataxin-3 mutant (C14A) failed to generate reaction products (Figure 2.6.E).

2.4.6. hHR23A blocks the VCP/p97 stimulation of ataxin-3 ubiquitin hydrolase activity

hHR23A and VCP/p97 are both involved in protein quality control through their connections with protein degradation and the ubiquitin-proteasome system (Dantuma et al., 2009; Madsen et al., 2009). Recent studies have established ataxin-3 as an important contributor to ubiquitin-dependent protein quality control (Zhong and Pittman, 2006; Reina et al., 2010). *Caenorhabditis elegans* homologues for hHR23A, VCP/p97 and ataxin-3 have been previously found to assemble in a trimolecular complex (Rodrigues et al., 2009). To assess if these proteins could establish a similar trimolecular complex in our cellular system, endogenous hHR23A was

immunoprecipitated from COS-7 cells and co-immunoprecipitation of endogenous VCP/p97 and endogenous ataxin-3 was assessed through western blotting. Accordingly, both endogenous VCP/p97 and endogenous ataxin-3 were co-immunoprecipitated with hHR23A (Figure 2.7.A). Since ataxin-3, hHR23A and VCP/p97 are linked to the same cellular pathways, we assessed whether ataxin-3 enzymatic activity is altered when exposed to two protein interactions with different effects regarding ataxin-3 stimulation.

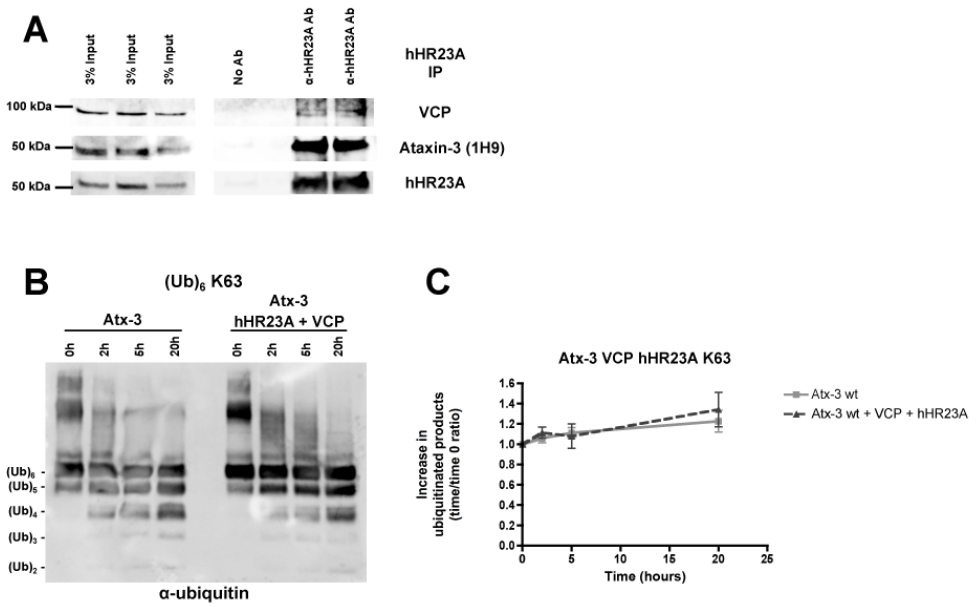

Figure 2.7. - hHR23A blocks the VCP/p97 enhancement of ataxin-3 activity *in vitro*. (**A**) Endogenous hHR23A was immunoprecipitated from COS-7 cell extracts and the co-immunoprecipitation of endogenous ataxin-3 and endogenous VCP/p97 was determined by western blotting. (**B**) *In vitro* deubiquitination assay of K63-linked hexa-ubiquitin chains (250 nM) by wild-type (Q22) ataxin-3 (100 nM) alone or in the presence of both hHR23A (100 nM) and VCP/p97 (100 nM). Western blotting was performed for samples collected after 0, 2, 5 and 20 hours of reaction and anti-ubiquitin reactivity was assessed. (**C**) Quantification of the increase in reaction products over time (time = 0 hours as control) resulting from the hydrolysis of K63-linked hexa-ubiquitin chains by wild-type (Q22) ataxin-3 alone (light grey squares) or in the presence (dark grey triangles) of hHR23A and VCP/p97 was plotted as the mean ± SEM of 4 independent experiments.

In vitro deubiquitination assays were performed with wild-type (Q22) ataxin-3 in the absence or presence of hHR23A and VCP/p97 simultaneously, using K63-linked hexa-ubiquitin chains in the reaction (Figures 2.7.B and 2.7.C). In both conditions wild-type ataxin-3 was able to cleave ubiquitin chains. However, when hHR23A and VCP/p97 were both added to the reaction solution, we did not observe an increase in wild-type ataxin-3 activity (Figures 2.7.B and 2.7.C), as we have previously observed with VCP/p97 alone. Interestingly, ataxin-3 in conjunction with hHR23A and VCP/p97 had similar activity to ataxin-3 alone, displaying neither the increase in activity caused by VCP/p97, nor the trend to reduced activity observed with hHR23A. Taken together, these results suggest that, at least in *in vitro* reactions, hHR23A and VCP/p97 counter the effect of each other on ataxin-3 DUB activity.

2.5. Discussion

In this study, we demonstrate that hHR23A and human VCP/p97 are able to directly interact with human ataxin-3; indeed, we confirm the association of endogenous ataxin-3 with endogenous hHR23A and VCP/p97 (Trottier et al., 1998; Nicastro et al., 2005; Schmitt et al., 2007; Antomy et al., 2009; Macedo-Ribeiro et al., 2009). In our work, VCP/p97 revealed to be a selective activator of wild-type ataxin-3. VCP/p97 stimulation of DUB activity was observed for wild-type ataxin-3, but not for the toxic expanded form. These data suggest the existence of a loss of function component on MJD pathology.

Ataxin-3 binds and cleaves poly-ubiquitin chains (Burnett and Pittman, 2003; Berke et al., 2005). With respect to ubiquitin hydrolase activity, ataxin-3 displays clear substrate preference: ataxin-3 preferentially cleaves K63-linked over K48-linked ubiquitin chains, and longer over shorter chains (Winborn et al., 2008). Even with its preferred substrates, the reaction kinetics of ataxin-3 *in vitro* is slower than those of other well-studied deubiquitinating enzymes (Nicastro et al., 2010). Recent studies have shown that mono-ubiquitination of ataxin-3 itself is a strong activator of ataxin-3 activity (Todi et al., 2009), but in cells under basal conditions the amount of mono-ubiquitinated ataxin-3 is minor. Therefore, we investigated whether two well known ataxin-3 interactors could modulate ataxin-3 protease activity.

VCP/p97 is an abundant protein, comprising approximately one percent of total protein in some cells (Dalal and Hanson, 2001; Mori-Konya et al., 2009). Though it is distributed throughout the nucleus and cytoplasm of COS-7 cells, VCP/p97 is more abundant in the cytosol, in contrast with ataxin-3, which is predominantly nuclear in these cells. Despite this difference in localization, we established both a cellular and a direct *in vitro* interaction between ataxin-3 and VCP/p97 in our experiments, confirming previously published results (Doss-Pepe et al., 2003; Zhong and Pittman, 2006; Boeddrich et al., 2006). Importantly, VCP/p97 proved to be an activator of wild-type ataxin-3 ubiquitin hydrolase activity *in vitro*, nearly doubling the accumulation of lower molecular weight ubiquitin chain reaction products. Activation

has also been reported for other deubiquitinating enzymes (Yao et al., 2006; Cohn et al., 2007) and most recently, a synergistic cooperation between ataxin-3 and CDC-48 (*C. elegans* orthologue of VCP/p97) was found to have a role in ageing regulation and ubiquitin-mediated proteolysis in *C. elegans* (Kuhlbrodt et al., 2011). VCP/p97 did not appear to alter ataxin-3 substrate preference, as K63-linked hexa-ubiquitin chains were still cleaved more extensively than K48-linked hexa-ubiquitin chains. VCP/p97 also had no effect on the activity of mutant (i.e. expanded) ataxin-3. The region of ataxin-3 essential for VCP/p97 interaction is situated just amino-terminal to the polyQ region, so it is conceivable that polyQ repeat length may affect the interaction between the two proteins. Previous studies have reported an increased interaction between VCP/p97 and polyQ-expanded ataxin-3 (Boeddrich et al., 2006) and our own *in vitro* co-immunoprecipitation studies are consistent with this observation. Even so, this interaction is apparently not sufficient to stimulate the activity of expanded ataxin-3. Although the changes in ataxin-3 structure induced by the expanded polyQ domain seem to promote a stronger association with VCP/p97, the same conformational alterations might abrogate any allosteric effect in favor of catalytic activation. It is important to recall that VCP/p97 normally is organized as a ring-like hexamer rather than as a monomer (Beuron et al., 2006). A single VCP/p97 hexamer might engage differentially with normal and expanded ataxin-3 polypeptides in a manner that permits activation only of normal ataxin-3 molecules. Additional conformational and structural studies of both proteins in this interaction will be needed to define the mechanism.

Our results confirm that the ^{282}RKRR sequence of ataxin-3 mediates binding to VCP/p97 (Boeddrch et al., 2006) and establish that this region is essential for the activation of ataxin-3 activity by VCP/p97. The ^{282}RKRR-HNHH substitution disrupts the interaction of VCP/p97 with wild-type and expanded ataxin-3, and blocks VCP/p97-activation of ataxin-3 DUB activity. We thus conclude that VCP/p97-mediated enhancement of ataxin-3 DUB activity is dependent on direct VCP/p97 interaction with ataxin-3. A competent protein-protein interaction with VCP/p97 is mandatory to induce a significant increase in wild-type ataxin-3 activity. Therefore, a

more restrained protein-protein interaction might also justify the ineffectiveness of VCP/p97 in increasing expanded ataxin-3 ubiquitin hydrolase activity.

Ataxin-3 resides in the nucleus, cytosol and possibly mitochondria (Tait et al., 1998; Trottier et al., 1998; Pozzi et al., 2008). In some types of cells, ataxin-3 is predominantly nuclear while in other cells it is largely cytoplasmic. In COS-7 cells, we observed a primarily nuclear distribution of ataxin-3, similar to what we have observed in human fibroblasts and in mouse cerebellar granule cells (Laço et al., unpublished data). Ataxin-3 exhibits the capacity to shuttle in and out of the nucleus, presumably responding to specific stimuli (Chai et al., 2002; Macedo-Ribeiro et al., 2009; Reina et al., 2010). In the nuclear compartment, ataxin-3 exhibits a punctate pattern with a superimposed, lighter homogeneous distribution throughout the nucleoplasm that spares the nucleolus. This nuclear pattern is very similar to that of hHR23A; indeed, we observed a high degree of co-localization of these two proteins, to the subnuclear foci. Interestingly, the 20S and 19S subunits of the proteasome also exhibit a punctate nuclear distribution in COS-7 cells and several other tested cell types (Rockel et al., 2005; Scharf et al., 2007). These proteasome-enriched nuclear foci are in close association with the ataxin-3 containing-nuclear foci (not shown). The discrete distribution of ataxin-3 and hHR23A into specific nuclear regions, might represent specialized nuclear compartments dedicated to protein quality control and protein degradation.

Interestingly, and despite the tight relation in nuclear distribution and a clear interaction in cellular assays and *in vitro* between ataxin-3 and hHR23A, we found that hHR23A does not influence the ubiquitin hydrolase activity of ataxin-3. hHR23A did not increase ataxin-3 DUB activity or change its substrate preference, in accordance with recent data by Nicastro and colleagues (2010). On the contrary, ataxin-3 actually displayed a non-significant trend towards decreased activity when hHR23A was added to the reaction system. Both ataxin-3 and hHR23A are able to bind ubiquitin chains (Kang et al., 2007), therefore the decrease in ataxin-3 activity might reflect competition for the ubiquitin chains by the two proteins. Ataxin-3 would be left with less free non-hHR23A bound ubiquitin chains to work on, reducing the quantity of end products of deubiquitination. hHR23A was first proposed to be part of the DNA repair machinery

(Hsieh et al., 2005); while other studies have shown an influence of ataxin-3 in nuclear gene expression (Evert et al.,2001; 2003; 2006). The close association to proteasome-enriched nuclear areas and the influence in expression of specific factors and nuclear proteins levels may link various physiological roles of ataxin-3 and hHR23A to protein degradation.

Recent studies have expanded the number of proteins known to interact with ataxin-3 (Evert et al., 2006; Ferro et al., 2007; Tao et al., 2008; Mazzucchelli et al., 2009; Durcan et al., 2011). In a cellular context, ataxin-3 likely does not function alone (Zhong and Pittman, 2006; Wang et al. 2008), since protein-protein interactions are established continuously and dynamically in the cell. New protein-protein interactions involving ataxin-3 may be established along with its deubiquitination activity over protein-substrates. Indeed, distinct protein interactions may differently modulate ataxin-3 ubiquitin hydrolase activity, as observed in our study regarding the role of hHR23A and VCP/p97. We exposed ataxin-3 to both hHR23A and VCP/p97 in an attempt to better understand how ataxin-3 activity may be regulated in the cell. Interestingly, the presence of hHR23A negated the activation induced by VCP/p97. Competition between hHR23A and VCP/p97 for a common binding site on ataxin-3 seems unlikely since the described areas of interaction for these two proteins are in different regions of ataxin-3 (Boeddrich et al., 2006; Nicastro et al., 2005). Nevertheless, interaction with hHR23A could change the affinity of ataxin-3 for VCP/p97 and thus impair VCP/p97-induced activation of ataxin-3. Also, competition for hexa-ubiquitin chains between hHR23A and ataxin-3 might reduce substrate availability for ataxin-3 when hHR23A and VCP/p97 are added, thereby reducing ataxin-3 DUB activity. On the other hand, ataxin-3 is probably deubiquitinating faster the available ubiquitin chains due to VCP/p97 activation. VCP/p97 stimulation of ataxin-3 activity might compensate the lack of substrate and the slight inhibitory effect of hHR23A, originating similar total amounts of reaction products. These interesting data demonstrate that ataxin-3 activity in the cell might be highly regulated and the repercussions of ataxin-3 enzymatic action might derive from the equilibrium of all the various inputs coming from the different interactions ataxin-3 is establishing at a specific moment.

Taken together with previously published studies, our results favor the view that ataxin-3 engages in multiple protein-protein interactions that influence its DUB activity within the cell (Zhong and Pittman, 2006; Mazzucchelli et al., 2009; Rodrigues et al., 2009; Durcan et al., 2011). Such interactions might influence the selection of ubiquitinated proteins on which ataxin-3 would act. Ataxin-3 is an interesting DUB in part because it can discriminate between different ubiquitin chain conformations (Winborn et al., 2008). Resembling the phosphorylation and dephosphorylation procedures, different ubiquitin signals made of different ubiquitin chains with different arrangements and topologies will almost certainly trigger different cellular outcomes. The selective activity of ataxin-3 over some ubiquitin linkages may alter the ubiquitin signal on the ubiquitinated substrates and consequently determine their future cellular role. In this way, ataxin-3 may represent an important checkpoint on the future fate of ubiquitinated proteins in the cell and its interactions may play a major role in modulating this event (Kuhlbrodt et al., 2011).

Our results and previous published data on VCP/p97 and hHR23A lead us to propose a model in which these proteins interact with ataxin-3 at different points of the processing of ubiquitinated protein-substrates (Figure 2.8.). VCP/p97 and ataxin-3 have been described to work together in the retrotranslocation of ubiquitinated substrates from the endoplasmic reticulum in the ERAD (Zhong and Pittman, 2006). Recently, it has been shown that ataxin-3 deubiquitinates C-terminus of Hsp70-interacting protein (CHIP) and parkin (Winborn et al., 2008; Durcan et al., 2011). VCP/p97 may bind to ubiquitinated CHIP, parkin or other protein-substrates, present them to ataxin-3 and activate the enzyme. Ataxin-3 would cleave preferentially K63 linkages out of the ubiquitin chains, releasing a K48-linkage enriched ubiquitin chain. The interaction with VCP/p97 would facilitate the ataxin-3 editing of ubiquitin chains on its substrates. hHR23A would easily recognize the K48-linkage enriched ubiquitin chain left attached to the protein-substrates, since hHR23A has higher affinity for K48 linkages (Raasi et al., 2004; Varadan et al., 2005). Finally, hHR23A would take the ubiquitinated substrate out of the catalytic pocket of ataxin-3 and would transfer it to the proteasome or other alternative cellular destination, as depicted in Figure 2.8..

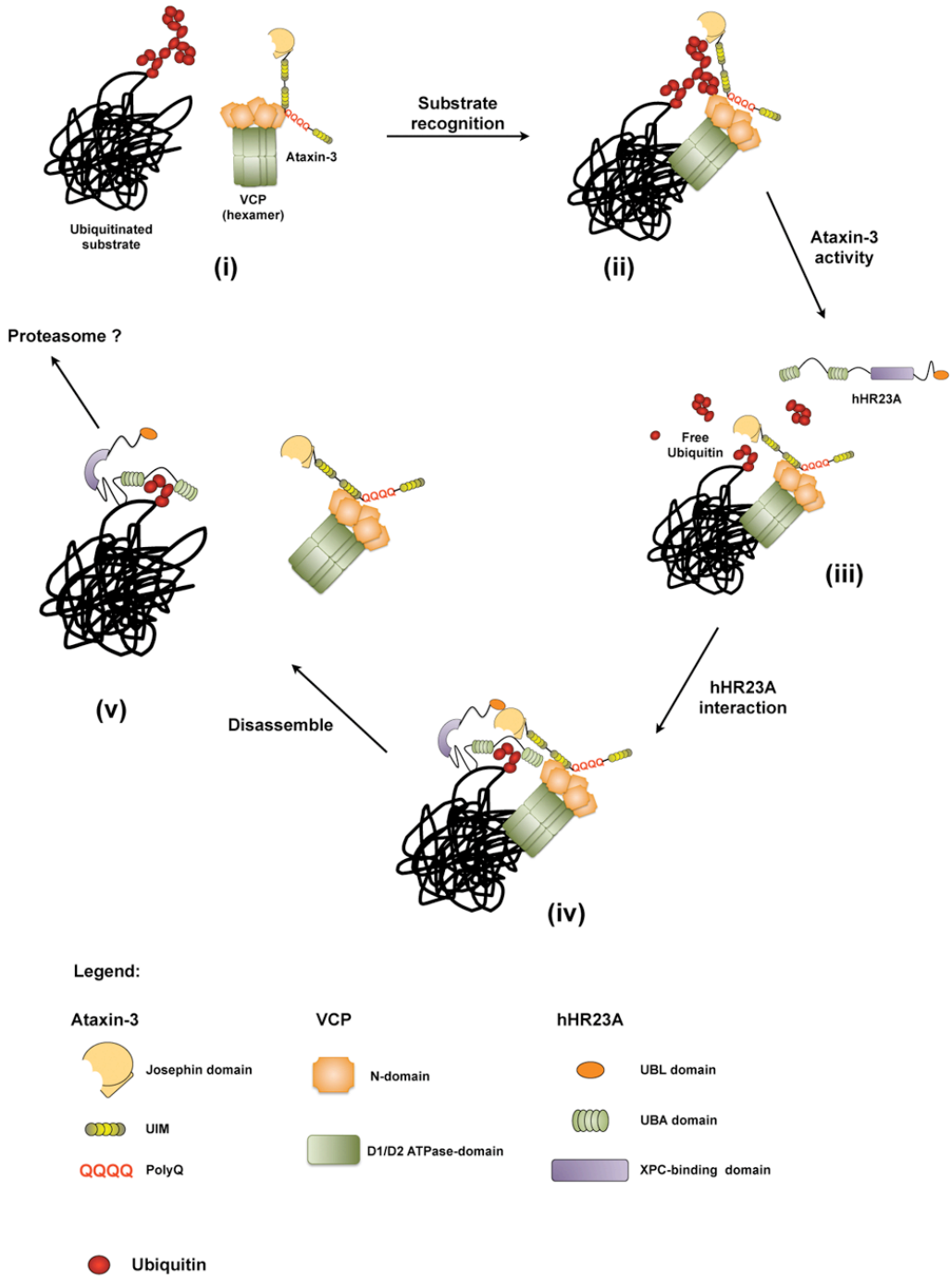

Figure 2.8. - Proposed model of sequential events during the interaction between ataxin-3, VCP/p97 and hHR23A. (i) Ataxin-3 interacts with a monomer of the VCP/p97 hexamer through its ^{282}RKRR region, assembling in a complex capable of recognizing the ubiquitinated substrate. (ii) Ataxin-3 acts on

the branched ubiquitin chains attached to the ubiquitinated protein, originating a clear and perceptible ubiquitin signal. (iii) Due to its K63-linkage preference, ataxin-3 leaves an all K48-linkage ubiquitin chain on the surface of the protein. (iv) The ubiquitin signal released by ataxin-3 is recognized by hHR23A and interpreted as a degradation signal. (v) hHR23A delivers the ubiquitinated protein to the proteasome for degradation.

Taking this model into account, the absence of stimulation of expanded ataxin-3 by VCP/p97 may have strong implications in MJD pathology. We may hypothesize that without the activation of VCP/p97, expanded ataxin-3 would work less efficiently as a DUB, leading to an accumulation of ubiquitinated proteins in the cell. Such a reduction in ubiquitin chain processing by expanded ataxin-3 not only would favor the accumulation, and possibly aggregation, of ubiquitinated proteins in the cell, but also might perturb the delivery of ubiquitinated substrates to their appropriate cellular destination. Thus, the disturbance of normal cellular pathways of ubiquitin signaling would add up to other cellular stresses promoted by the expression of a pathogenic polyQ fragment. The presence of a polyQ expansion in ataxin-3 may impair protein homeostasis through direct inhibition of the proteasome (Venkatraman et al., 2004; Díaz-Hernández et al., 2006) and thus promote the formation of expanded ataxin-3 aggregates. In addition, the polyQ expansion in ataxin-3 protein may compromise its ubiquitin chain editing activity over ubiquitinated substrates. The buildup of protein malfunction and misleading signals in the cell together with expanded ataxin-3's intrinsic propensity to aggregate, may initiate a chronic cascade of events, culminating in neuronal dysfunction and cell death.

Chapter 3

Cellular turnover of the polyglutamine disease protein ataxin-3 is regulated by its catalytic activity

3.1. Abstract

Ataxin-3, a deubiquitinating enzyme, is the disease protein in spinocerebellar ataxia type 3, one of many neurodegenerative disorders caused by polyglutamine expansion. Little is known about the cellular regulation of ataxin-3. This is an important issue, since growing evidence links disease protein context to pathogenesis in polyglutamine disorders. Expanded ataxin-3, for example, is more neurotoxic in fruit fly models when its active site cysteine is mutated (Warrick et al., 2005). We therefore sought to determine the influence of ataxin-3 enzymatic activity on various cellular properties. Here we present evidence that the catalytic activity of ataxin-3 regulates its cellular turnover, ubiquitination, and subcellular distribution. Cellular protein levels of catalytically inactive ataxin-3 were much higher than those of active ataxin-3, in part reflecting slower degradation. *In vitro* studies revealed that inactive ataxin-3 was more slowly degraded by the proteasome and that this degradation occurred independent of ubiquitination. Slower degradation of inactive ataxin-3 correlated with reduced interaction with the proteasome shuttle protein, VCP/p97. Enzymatically active ataxin-3 also showed a greater tendency to concentrate in the nucleus, where it colocalized with the proteasome in subnuclear foci. Taken together, these and other findings suggest that the catalytic activity of this disease-linked deubiquitinating enzyme regulates several of its cellular properties, which in turn may influence disease pathogenesis.

3.2. Introduction

Ataxin-3, a deubiquitinating enzyme (DUB), is the disease protein in the polyglutamine disorder Machado-Joseph disease/Spinocerebellar ataxia type 3 (MJD/SCA3) (Kawaguchi et al., 1994; Stevanin et al., 1995a; 1995b). MJD/SCA3 is one of nine known neurodegenerative diseases, including Huntington's disease and various spinocerebellar ataxias, which are caused by CAG repeat expansions that encode abnormally long polyglutamine (polyQ) tracts in otherwise dissimilar proteins (Cummings and Zoghbi, 2000; Paulson et al., 2000; Zoghbi and Orr, 2000; Koeppen, 2005). All nine are age-related, progressive disorders that typically cause initial symptoms in midlife, leading to death 15–30 years later.

PolyQ diseases manifest different clinical and neuropathological features despite their similar polyQ expansions, indicating that disease protein context contributes to the range and degree of neurodegeneration in each disease. Indeed, identifying normal functions and interactions of specific polyQ disease proteins has helped to define disease pathogenesis. In several polyQ disease proteins, domains far removed from the polyQ tract contribute to pathogenesis. For example, in SBMA, caused by an expansion in the androgen receptor, testosterone is required for neuronal degeneration, although the hormone-binding domain of the androgen receptor is distant from the polyQ region (Katsuno et al., 2002; Schmidt et al., 2002; Katsuno et al., 2006).

Ataxin-3 contains an N-terminal ubiquitin protease (Josephin) domain, two or three C-terminal ubiquitin interaction motifs (UIMs) depending on splice variant, and a polyQ tract that resides between the second and third UIMs. This polyQ tract normally contains ~ 12–40 glutamine residues, which become expanded in disease to ~ 50–84 repeats. Ataxin-3 functions as a DUB, binding ubiquitin chains through its UIMs and cleaving them through the Josephin domain. Its protease activity is lost when the catalytic cysteine at position 14 is mutated to alanine (C14A) (Burnett et al., 2003; Chai et al., 2004; Mao et al., 2005).

Evidence increasingly suggests that ataxin-3 functions in protein quality

control. A common pathological feature of polyQ diseases is the accumulation of intracellular inclusions containing the disease protein. Ataxin-3 is unique among polyQ diseases, however, in that the nonpathogenic (i.e. nonexpanded) form of the protein also localizes to aggregates in other disorders (Fujigasaki, et al., 2000; Takahashi et al., 2001; Seilhean et al., 2004; Donaldson et al., 2003). In addition, individuals homozygous for expanded *MJD1* present with more severe symptoms and earlier onset of MJD/SCA3 than heterozygous individuals (Lerer et al., 1996; Sakai and Kawakami, 1996), suggesting a dosage effect in MJD/SCA3. In *Drosophila*, ataxin-3 serves a DUB-dependent neuroprotective role against expanded polyQ proteins (Warrick et al., 2005). Recent evidence also suggests that ataxin-3 regulates endoplasmic reticulum-associated protein degradation by adjusting the rate of extraction of endoplasmic reticulum-associated protein degradation substrates through its interaction with VCP/p97 (Zhong and Pittman, 2006). Together, these reports indicate that ataxin-3 functions in protein quality control.

Deubiquitinating enzymes, through their ubiquitin precursor processing and protein deubiquitinating activities, play central roles in many cellular processes from DNA repair and cell cycle regulation to cell-cell interactions (Amerik and Hochstrasser, 2004; Nijman et al., 2005). Their importance to cellular homeostasis is highlighted by their involvement in hereditary diseases, including neurodegeneration and certain types of cancer. The significance of DUBs notwithstanding, little is known about their regulation in the cell. Given the importance of protein context in polyQ disease pathogenesis and the fact that ataxin-3 functions as a DUB, we investigated whether ataxin-3 catalytic activity alters its cellular properties. Here we provide evidence that the catalytic activity of ataxin-3 influences its steady state levels, ubiquitination pattern, and subcellular localization.

3.3. Material and methods

3.3.1. Cell culture maintenance and transfections

Cells were maintained and transfected as described previously (Berke et al., 2005).

3.3.2. FLP-in 293 cell lines

Approximately 5 x 10^6 FLP-in 293 cells were transfected with 5.4 μg of pOG44 and 0.6 μg of pcDNA/FRT targeting vector. Selection medium (Dulbecco's modified Eagle's medium with 10% fetal bovine serum, 1% penicillin/streptomycin, and 200 μg/ml hygromycin) was added to the cells 48 h later. Selected cells were then grown in growth medium (Dulbecco's modified Eagle's medium with 10% fetal bovine serum, 1% penicillin/streptomycin, and 50 μg/ml hygromycin).

3.3.3. Constructs

Ataxin-3 constructs were maintained in the following vectors: FLAG-AT3Q25(FL), FLAG-AT3Q22(C14A), FLAG-AT3Q80(FL), and FLAG-AT3Q80(C14A) in pVETL-Cmcs; FLAG-AT3Q22(FL) and FLAG-AT3Q22(SA) in pFLAG; and Myc-AT3Q22(FL) and Myc-AT3Q22(C14A) in pcDNA3. HA-tagged ubiquitin was in pRK5 and was a generous gift from Dr. Ted Dawson.

3.3.4. Protein immunoprecipitation from cells

Cells were lysed in one of the following ice-cold buffers supplemented with Complete Mini Protease Inhibitor tablets (Roche Applied Science), depending on the experiment: RIPA (50mMTris, 150mMNaCl, 0.1% SDS, 0.5% deoxycholic acid, 1% Nonidet P-40, pH 7.4), Nonidet P-40 buffer (150 mM NaCl, 20 mM HEPES, 1 mM EDTA, 1% Nonidet P-40, pH 7.4), FLAG lysis buffer (50 mM Tris, 150 mM NaCl, 1 mM EDTA, 1% Triton X-100, pH 7.4), or Buffer A (20mM HEPES, 120mM NaCl,

10% glycerol, 1% Triton X-100, pH 7.4). Lysates were incubated with anti-FLAG M2 affinity beads (Sigma) for 2 h at 4 °C. Beads were washed four times, and protein was eluted with 3xFLAG peptide (Sigma) at 4 °C or with 6% SDS at room temperature. For experiments studying ataxin-3 ubiquitination, cell lysates were denatured with 1% SDS (30 min at room temperature) and then renatured with 4.5% Triton X-100 (30 min at room temperature) prior to immunoprecipitation in RIPA buffer. For ataxin-3 immunopurified from cells for use in *in vitro* assays, bead-bound proteins were rinsed five times with RIPA and twice with Buffer B (50 mM HEPES, 0.5mM EDTA, 1mM dithiothreitol, and 0.1 mg/ml ovalbumin, pH 7.5) and eluted with 3xFLAG peptide. For experiments where the proteasome was inhibited before cell lysis, we used MG-132 (Calbiochem) or lactacystin (Boston Biochem) in growth media at a final concentration of 10 μM.

3.3.5. Quantitative real time PCR

COS-7 cells were transfected with Lipofectamine Plus (Invitrogen) per the manufacturer's instructions. Messenger RNA (mRNA) was collected 48 h later using TRIZOL reagent (Invitrogen), following the manufacturer's protocol. cDNA of the extracted mRNA was obtained in a reverse transcription reaction, and it was further used for quantitative real time PCR in an ABI PRISM 7700 sequence detection system (Applied Biosystems), using SYBR Green I (Applied Biosystems) as the reporter dye. c-Myc quantification was used for endogenous control reactions. The primer sequences used were the following: for ataxin-3, forward (5'-TTC TAT ATT TGT CGT TAA GGG TGA TCT G-3') and reverse (5'-GCA TCT GTT GGA CCC TAA TCA TC-3'); for c-Myc, forward (5'-TCA AGA GGT GCC ACG TCT CC-3') and reverse (5'-TCT TGG CAG CTG GAT AGT CCT T-3').

3.3.6. GST fusion protein purification

pGEX-6P1 plasmids encoding GST or GST-ataxin-3 were transformed into BL21 E. coli cells. Individual colonies were grown at 37 °C overnight in LB plus ampicillin, and then 5 ml was used to inoculate 100 ml of LB for additional growth at 37 °C for an additional 3 h. Fusion protein expression was induced with 1mM

isopropyl-1-thio-β- D-galactopyranoside for 2 h at 37 °C. Cells were centrifuged and resuspended in ice-cold phosphate-buffered saline, lysed by sonication, and centrifuged for 10 min to remove debris. Lysates were frozen in liquid nitrogen and stored at -80 °C.

3.3.7. GST pull-down experiments

GST or GST-ataxin-3 (between 100 and 300 nM concentration) was incubated with 50 µl of glutathione-Sepharose beads (GST Microspin columns; GE Healthcare), 26 S proteasomal fractions (between 1 and 10 nM; Boston Biochem), ATPγS (4 mM; Sigma), MgCl2 (10 mM), and proteasome inhibitors (lactacystin (Boston Biochem) or MG-132 (Calbiochem), used at 100 –150 nM) at room temperature for 5–10 min in FLAG lysis buffer, Nonidet P-40 buffer, or Buffer A. Beads were rinsed three or four times with the same buffer. Protein was eluted using 10 mM reduced glutathione in Buffer B (15 min at room temperature).

3.3.8. Antibodies and western blotting

Proteins were electrophoresed on SDS-PAGE Ready Gels (Bio-Rad) and transferred to polyvinylidene difluoride membrane. Membranes were blocked for 20 min in blocking buffer (TBS-Tween with 5% dry milk powder). Primary antibodies were diluted in blocking buffer and incubated with membranes for 1 h at room temperature or overnight at 4 °C. Secondary antibodies were incubated with membranes for 1 h. The following primary antibodies were used: anti-ataxin-3 mouse monoclonal antibody (mAb) (1:2000; 1H9; Chemicon), anti-ataxin-3 rabbit polyclonal antibody (pAb) (1:20,000; MJD), anti-HA rabbit pAb (1:1000; Y11; Santa Cruz Biotechnology, Inc., Santa Cruz, CA), anti-ubiquitin mouse mAb (1:10,000; P4D1; Santa Cruz Biotechnology), anti-tubulin mouse mAb (1:50,000; Sigma), anti-FLAG rabbit pAb (1:1000; Sigma), anti-ubiquitin rabbit pAb (1:1000; Dako), anti-glyceraldehyde-3-phosphate dehydrogenase mouse mAb (1:500; Chemicon). Primary antibodies for 26 S proteasomal subunits (from Affiniti unless otherwise noted) were the following: anti-20 S rabbit pAb (1:500; Zymed Laboratories Inc.), anti-20 S rabbit pAb (1:500), anti-RPT2 rabbit pAb (1:500), anti-RPN2 mouse (mAb) (1:5000), anti-RPT3

mouse mAb (1:1000), anti-RPT5 mouse mAb (1:1000), anti-RPT6 mouse mAb (1:1000), anti-RPT4 mouse mAb (1:2500), anti-RPT1 mouse mAb (1:5000), anti-RPN10 mouse mAb (1:500). Goat anti-mouse and anti-rabbit peroxidase-conjugated secondary antibodies from Jackson Laboratories were used at 1:15,000.

3.3.9. Immunofluorescence

Cells were fixed in 4% paraformaldehyde in phosphate-buffered saline for 20 min, rinsed three times with PBT (phosphate-buffered saline plus 0.1% Triton X-100), and blocked for 1 h in 5%normal goat serum in PBT. Cells were stained overnight in primary antibody (anti-20 S rabbit polyclonal (1:500; Affiniti) and anti-FLAG mouse monoclonal (1:500; Sigma)). Fluorescent secondary antibodies were used at 1:1000 (Jackson Laboratories) for 2 h. Fluorescence was visualized with a Bio-Rad krypton/argon mixed gas confocal laser microscope, based on a Nikon Eclipse upright microscope providing excitation wavelengths of 488, 568, and 647 nm. Images were collected at a x100 magnification factor and compiled using ImageJ (National Institutes of Health).

3.3.10. *In vitro* 26S degradation and DUB assay

GST-ataxin-3 (0.35 μM) was incubated with 10 nM rabbit 26 S fractions (Boston Biochem), 10 mM MgCl2, and a 1x ATP regeneration system (ERS; Boston Biochem) in Buffer B at 37 °C. At specific time points, aliquots were taken from each tube, and the reaction was stopped by the addition of 6% SDS. For ataxin-3 deubiquitination, ubiquitin-aldehyde (Boston Biochem) was used at a 4 μM concentration. Reaction was stopped by the addition of 6% SDS.

3.3.11. *In vitro* deubiquitination assay

FLAG-AT3Q22(C14A) that was coexpressed in COS-7 cells with HA-ubiquitin constructs was immunopurified using anti-FLAG antibody beads (Sigma) with an additional, stringent, denature/renature step (see "Protein immunoprecipitation from cells"). FLAG-AT3Q22(C14A) (ranging between 0.1 and 1 μM concentration) was eluted in Buffer B using 3x FLAG peptide (Sigma) and

incubated with GST-AT3Q22(FL) or GSTQ22(C14A) (used between 4 and 8 μM) in Buffer B and protease inhibitor mixture P8340 (Sigma) at 37 °C. Aliquots were taken at specific time points, and the reaction was stopped by the addition of 6% SDS. As a positive control, we used Lys-63 linked hexaubiquitin chains (Boston Biochem) at 250 nM concentration.

3.3.12. Pulse-chase analysis

COS-7 cells were transfected with FLAG-AT3Q25(FL) or FLAG-AT3Q22(C14A) DNA to yield comparable protein levels. 48 h later, cells were starved for 30 min with methionine/cysteine-free Dulbecco's modified Eagle's medium plus 5% dialyzed fetal bovine serum (Invitrogen) and pulsed for 40 min with [^{35}S]methionine medium (12 μCi/μl; PerkinElmer Life Sciences). Following the pulse, cells were washed twice with phosphate-buffered saline and chased in Dulbecco's modified Eagle's medium, fetal calf serum, 2 mM methionine, 2 mM cysteine for 0–24 h. RIPA buffer cell lysates were immediately frozen in liquid nitrogen and maintained at -80 °C until time of immunopurification. FLAG-AT3 was immunoprecipitated as described above.

3.3.13. Densitometry and statistical analysis

Immunoblots were scanned using a Canon LiDE 60 flatbed scanner. Images were collected in Adobe Photoshop 7.0. Densitometry was measured using identically sized regions with ImageJ, and data were analyzed using Microsoft Excel. Student's *t* test was used to determine statistical differences between experimental or control groups. Prior to analysis, recorded intensities were corrected for background intensity and normalized to loading control lanes.

3.4. Results

3.4.1. Ataxin-3 catalytic activity affects its steady state levels in cells

Ataxin-3 can be rendered catalytically inactive by mutating its active site cysteine at position 14 (cysteine to alanine; C14A). In transfected cells, we noticed that ataxin-3(C14A) is consistently expressed at much higher levels than fully functional ataxin-3. As shown in Figure 3.1.A, expression of equal amounts of plasmids encoding epitope-tagged, normal ataxin-3 (FLAG-AT3Q25(FL)) or catalytically inactive ataxin-3 (FLAG-AT3Q22(C14A)) led to markedly different levels of ataxin-3 protein. The higher levels of catalytically inactive ataxin-3 were observed whether ataxin-3(C14A) had a normal repeat (Q22) or a pathogenic, expanded repeat (Q80; Figures 3.1.A, left and middle panels; 3.2 and 3.3). This phenomenon was observed both in COS-7 cells (Figure 3.1.A) and in HEK293 cells (data not shown). Moreover, ataxin-3 that had been mutated elsewhere in the protein did not show this same effect. For example, ataxin-3 with mutations in each UIM (AT3Q22(SA)), which does not bind polyubiquitin chains but retains catalytic activity (Winborn et al., 2008), did not display increased steady state levels (Figures 3.1.A, right; 3.3.). Parallel experiments employing enhanced green fluorescent protein and ataxin-3 cotransfection confirmed that the difference in protein levels between active and inactive ataxin-3 was not due to variable transfection efficiency (data not shown). These results suggest that the much higher ataxin-3 (C14A) protein levels are functionally linked to loss of protease activity.

Intriguingly, co-expression of wild type ataxin-3 noticeably reduced the levels of inactive ataxin-3 (Figure 3.1.B). Normal (Q25) and expanded (Q80) ataxin-3 were able to suppress the levels of coexpressed, inactive ataxin-3 whether it had an expanded (Q80) or normal (Q22) repeat (Figure 3.1.B). These results suggest both that the catalytic site of ataxin-3 modulates steady state levels and that ataxin-3 may act in trans to regulate the cellular fate of other ataxin-3 proteins.

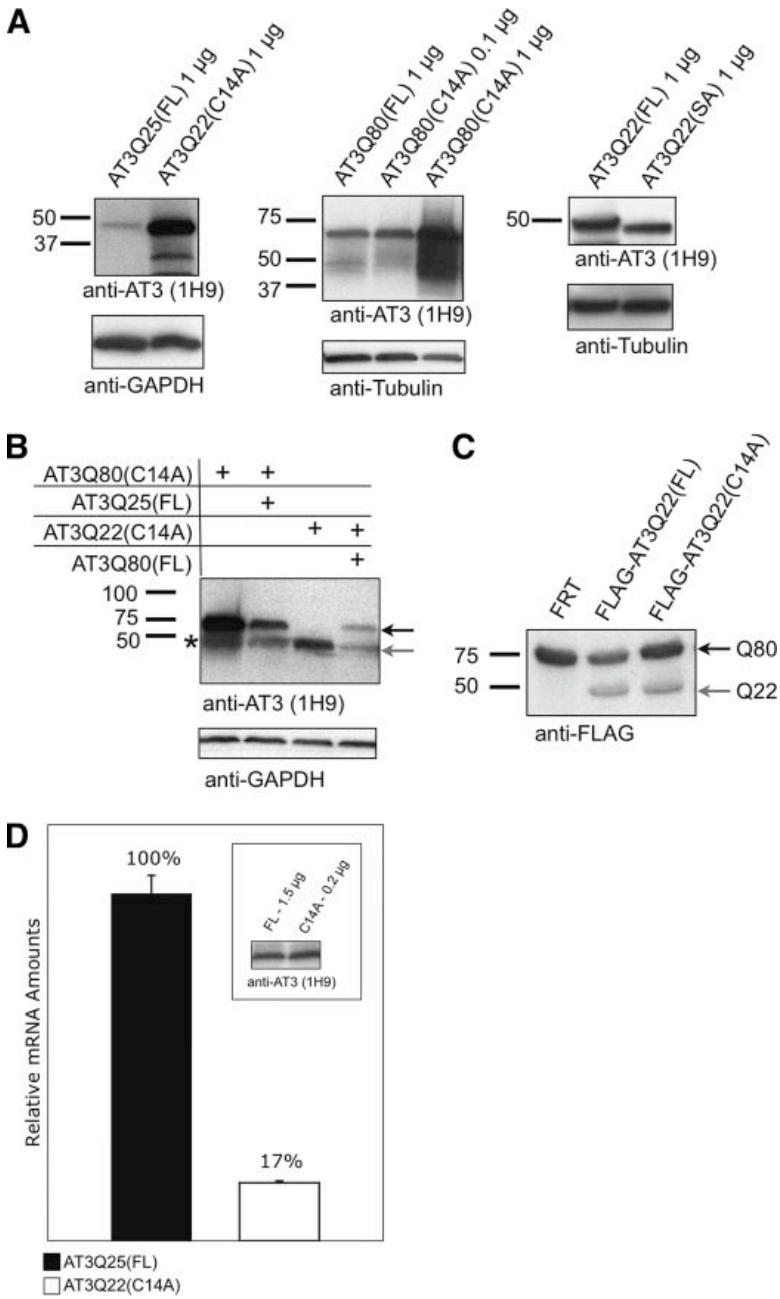

Figure 3.1. - Ataxin-3 catalytic activity affects its steady state levels in cells. (**A)** COS-7 cells were transiently transfected with the indicated constructs, harvested 48 h later, and probed on Western blot with the indicated antibodies. Transfection of equal amounts of FLAG-AT3Q25(FL) or FLAG-AT3Q22(C14A) plasmid DNA results in markedly higher levels of catalytically inactive ataxin-3 protein compared with

normal ataxin-3 (left). Similar increased levels are observed for poly(Q)-expanded, catalytically inactive ataxin-3 (middle). In fact, comparing the first two lanes, note that about one-tenth the DNA amount of inactive ataxin-3 needs to be transfected compared with active ataxin-3 to yield similar protein levels. Mutating the ubiquitin-binding motifs of ataxin-3 (FLAG-AT3Q22(SA)) does not lead to increased levels of ataxin-3 (right). Loading controls were glyceraldehyde-3-phosphate dehydrogenase (GAPDH) and tubulin. Each group of cells received the same total amount of DNA by using a combination of empty vector and ataxin-3 DNA. (**B**) Steady state levels of FLAG-AT3Q80(C14A) or FLAG-AT3Q22(C14A) are reduced by cotransfection of catalytically active FLAG-AT3 containing repeats of 25 or 80 polyQ. Ataxin-3 with 25Q migrates at 50 kDa (gray arrow). Ataxin-3 with 80Q migrates at 75 kDa (black arrow). Loading control was GAPDH. Each group of COS-7 cells received the same total amount of DNA by using a combination of empty vector and ataxin-3 DNA. The asterisk next to the first lane denotes a by-product of AT3Q80(C14A), which migrates at the same area as AT3Q25(FL). (**C**) Transient coexpression of AT3Q80(C14A) (all lanes, black arrow) in FLP-in cell lines stably expressing empty vector (FRT), AT3Q22(FL), or AT3Q22(C14A) recapitulates the modulatory effect that functional ataxin-3 (middle lane, gray arrow) has on catalytically inactive AT3Q80(C14A). Equal protein loaded (30 µg). (**D**) Quantitative real time PCR analysis of ataxin-3 mRNA levels in COS-7 cells transiently transfected with the indicated amounts of FLAG-AT3Q25(FL) or FLAG-AT3Q22(C14A) DNA to yield comparable cellular protein levels (inset). Shown are means ± S.D. (n = 3). Each group of cells received the same total amount of DNA by using a combination of empty vector and ataxin-3 DNA.

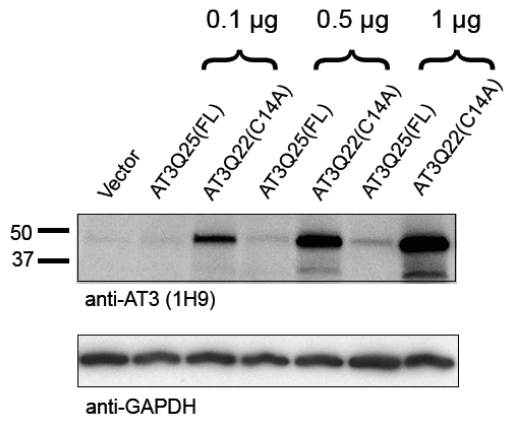

Figure 3.2. - Western blot of the experiment described in Figure 3.1.A, left panel, showing that the difference in protein levels between AT3Q25(FL) and AT3Q22(C14A) is observable over a range of plasmid DNA levels.

We confirmed the modulatory effect of functional ataxin-3 on catalytically inactive ataxin-3 protein levels in stably transfected cell lines. The FLP-in 293 cell line was used to generate pooled, transfected cells that stably express various forms of ataxin-3. Levels of catalytically inactive, expanded FLAG-AT3Q80(C14A) were lowered only in the presence of stably expressed, active FLAG-AT3Q22(FL) (Figure 3.1.C).

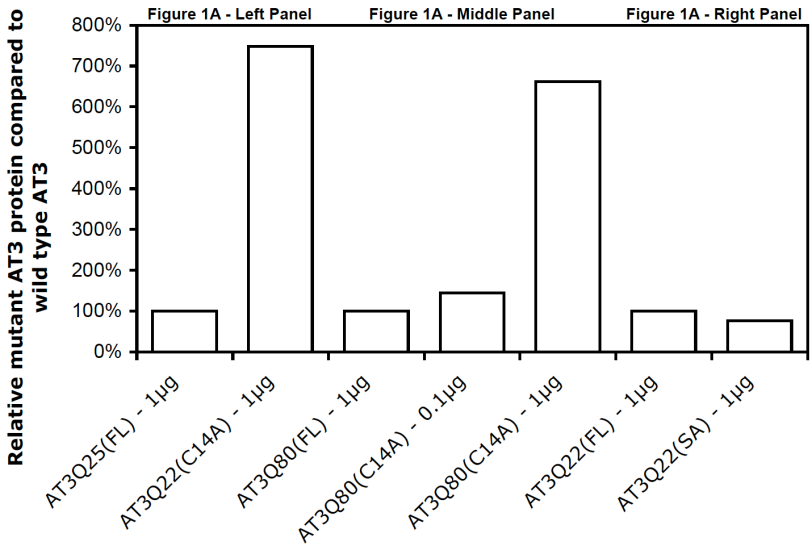

Figure 3.3. - Densitometry measurements of the panels shown in Figure 1A. Ataxin-3 protein levels were normalized to the respective loading controls and compared to wild type protein levels for each panel.

To investigate whether the observed differences in ataxin-3 protein levels merely reflect dissimilar mRNA levels for the expression constructs, we measured transcription levels by quantitative real time PCR analysis. Plasmids encoding FLAG-AT3Q25(FL) or FLAG-AT3Q22(C14A) were transiently transfected in COS-7 cells, and ataxin-3 mRNA levels were standardized to an endogenous control mRNA (c-Myc). As shown in Figures 3.1.D and 3.4., differences in mRNA levels cannot account for the marked differences in protein levels between catalytically active and inactive ataxin-3. Transfection of 7.5-fold more DNA for active ataxin-3 than for inactive

ataxin-3 led to similar protein levels despite the fact that mRNA levels for active ataxin-3 were much higher than those for inactive ataxin-3 (Figure 3.1.D). On the other hand, transfection of the same amount of DNA encoding active or inactive ataxin-3 produced markedly higher inactive ataxin-3 protein levels, whereas mRNA levels for catalytically inactive ataxin-3 were only about 2 times higher than its active counterpart (Figure 3.4.). These results suggest that the catalytic activity of ataxin-3 regulates steady state levels of ataxin-3, in part, at a post-transcriptional level.

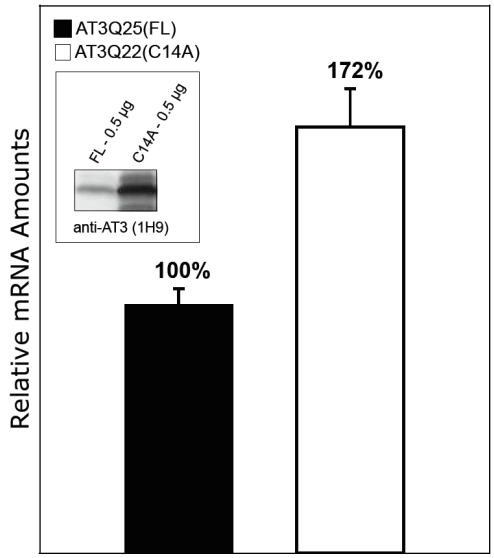

Figure 3.4. - Quantitative real-time PCR analysis complementary to the experiment shown in Figure 3.1.D. COS-7 cells were transiently transfected with the same amount of FLAG-AT3Q25(FL) or FLAG-AT3Q22(C14A) DNA. Shown are means +/- SD (N=3).

3.4.2. Ataxin-3 catalytic activity affects its turnover in cells

Increased steady state levels of a protein often reflect slower degradation. To test this possibility, we conducted pulse-chase labeling experiments to determine whether catalytic activity affects the half-life of ataxin-3. COS-7 cells were transiently transfected with amounts of FLAG-AT3Q25(FL) or FLAG-AT3Q22(C14A) plasmid predetermined to yield comparable steady state ataxin-3 levels. 48 h after transfection,

cells were pulse-labeled with [35S]methionine for 40 min and chased for 0–24 h. FLAG-ataxin-3 was immunoprecipitated with anti-FLAG antibody and assessed by autoradiography. Consistent with its higher steady state levels, ataxin-3 Q22(C14A) is degraded more slowly than ataxin-3 Q25(FL) (Figures 3.5.A and 3.5.B). Densitometry analysis on results from repeated experiments confirmed that protein half-life differed significantly between catalytically active and inactive ataxin-3 (Figures 3.5.B and 3.5.C). Although significant, this difference in degradation rates does not mirror the large dissimilarity in steady state protein levels (Figure 3.1.). Thus, the difference in levels of wild type and catalytically inactive ataxin-3 stems only in part from slower degradation of inactive ataxin-3 protein.

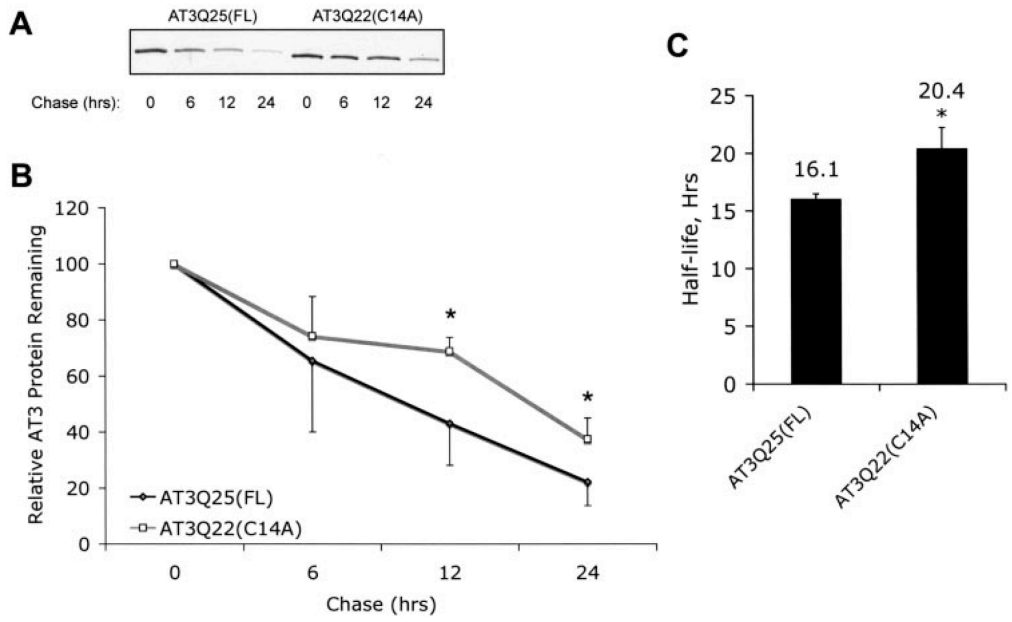

Figure 3.5. - Ataxin-3 catalytic activity enhances its degradation. (**A**) For pulse-chase analysis, transfected COS-7 cells expressing FLAG-AT3Q25(FL) or FLAG-AT3Q22(C14A) for 48 h were pulse-labeled with [35S]methionine for 40 min, chased for 0–24 h, and immunopurified with anti-FLAG antibody beads in RIPA buffer. Functional ataxin-3 is more rapidly degraded than its nonfunctional counterpart. (**B**) Densitometry analysis of autoradiographs from pulse-chase experiments indicates a slower turnover rate for catalytically inactive ataxin-3 in cells. Values are means ± S.D. (n=3). Asterisks indicate significant difference ($p<0.05$). (**C**) Half-lives of AT3Q25(FL) and AT3Q22(C14A) determined from data in B. The calculated half-lives are significantly different ($p<0.05$; means ± S.D. n=3).

3.4.3. Inactive ataxin-3 is more heavily ubiquitinated than its active counterpart

Ataxin-3, which binds to ubiquitin through its UIMs, can also be conjugated to ubiquitin (Chai et al., 2004; Berke et al., 2005). Thus, the slower degradation and higher levels of ataxin-3(C14A) could reflect altered ubiquitination of inactive ataxin-3 compared with ataxin-3(FL). We therefore examined the ubiquitination of active *versus* inactive ataxin-3.

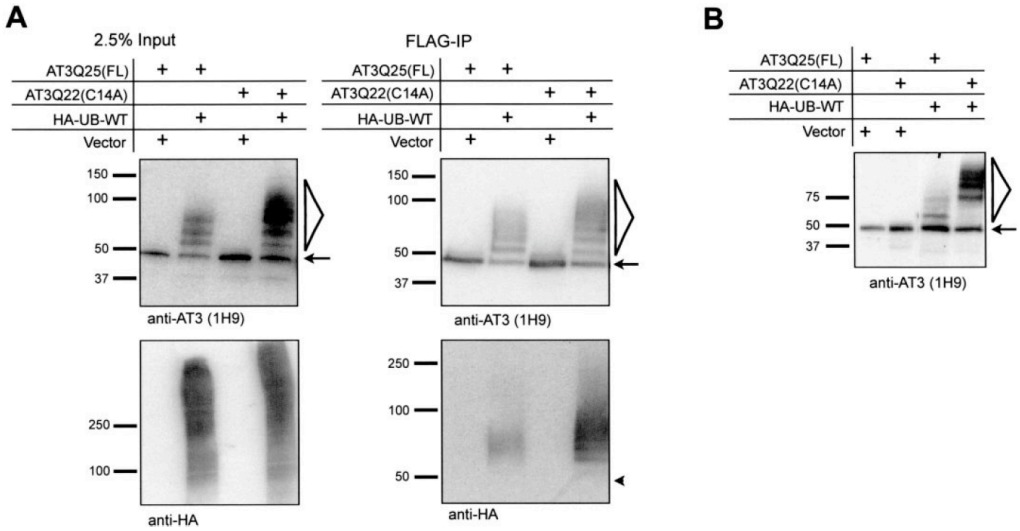

Figure 3.6. - Increased ubiquitination of catalytically inactive ataxin-3. (**A**) Western blot of lysates from COS-7 cells transfected with the indicated constructs. Input (left) and immunoprecipitation (right) results confirm that wild type and catalytically inactive ataxin-3 are both ubiquitinated (triangles). Inactive ataxin-3 is more highly ubiquitinated, shown by the presence of higher molecular weight, ubiquitinated bands. The arrows indicate nonubiquitinated ataxin-3. The arrowhead indicates where nonubiquitinated ataxin-3 migrates in ubiquitin blots. (**B**) A second example from an experiment illustrating a more pronounced difference in ubiquitination of catalytically inactive *versus* active ataxin-3.

In transfected COS-7 cells (Figure 3.6.) or HEK293 (data not shown), we expressed active or inactive ataxin-3 together with HA-tagged ubiquitin, with plasmid DNA levels adjusted to yield similar ataxin-3 protein levels. Cells were harvested 48 h after transfection, and the lysates were subjected to a stringent

denaturation/renaturation step before immunopurification with anti-FLAG antibody to isolate FLAG-ataxin-3 protein. Immunoprecipitated ataxin-3 was then probed with anti-HA antibody to detect ubiquitin. As shown in Figure 3.6.A, ataxin-3 becomes ubiquitinated in cells in the presence of excess ubiquitin, resulting in a ladder of ubiquitinated species, confirming previously published results (Berke et al., 2005). However, we observed that the ubiquitination pattern of ataxin-3 Q22(C14A) differs from that of ataxin-3 Q25(FL), with catalytically inactive ataxin-3 being more heavily ubiquitinated (Figure 3.6.A). This greater ubiquitination of catalytically inactive ataxin-3 was always observed, although the degree of increased ubiquitination of inactive ataxin-3 varied somewhat from experiment to experiment (e.g. see Figure 3.6.B for a marked difference in ubiquitination of active versus inactive ataxin-3). Thus, the catalytic activity of ataxin-3 influences not only the ataxin-3 turnover rate but also its posttranslational modification by ubiquitin.

3.4.4. Ataxin-3 does not deubiquitinate other ataxin-3 proteins *in trans*

Considering that inactive ataxin-3 is more heavily ubiquitinated (Figure 3.6.) and that wild type ataxin-3 can destabilize inactive ataxin-3 (Figure 3.1.B), we investigated whether wild type ataxin-3 can deubiquitinate inactive ataxin-3 and thus affect its turnover rate. FLAG-ataxin-3 Q22(C14A) and wild type HA-ubiquitin were coexpressed in cells, and FLAG-ataxin-3 was then immunopurified from lysates with anti-FLAG antibody. Immunopurified FLAG-ataxin-3 Q22(C14A) was then incubated with recombinant GST-ataxin-3 Q22(FL) or with GST-ataxin-3 Q22(C14A) as a negative control for 0-24 h. As shown in Figure 3.7.A, recombinant ataxin-3 could not deubiquitinate ataxin-3 Q22(C14A), since there was no change in the ladder of ubiquitinated ataxin-3 species (Figure 3.7.A, top). As a positive control, GST-ataxin-3 Q22(FL) readily cleaved hexaubiquitin chains (Figure 3.7.A, bottom), indicating that the recombinant ataxin-3 used here displays catalytic activity against ubiquitin chains.

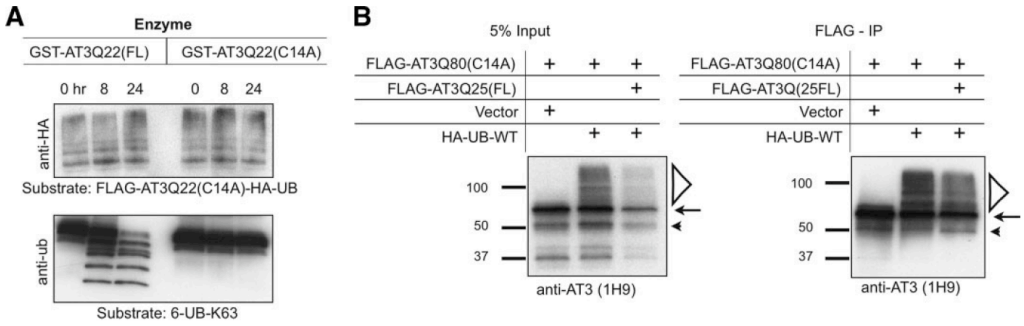

Figure 3.7. - Ataxin-3 does not deubiquitinate other ataxin-3 proteins *in trans*. (**A**) *In vitro* analysis showing the inability of recombinant ataxin-3 (6 μM) to deubiquitinate FLAG-AT3Q22(C14A) (0.5 μM) immunopurified from cells. Results are representative of five experiments. Positive control showing that recombinant ataxin-3 does cleave hexaubiquitin chains (0.25 μM), whereas, as expected, catalytically inactive ataxin-3 does not (bottom). (**B**) Western blots from lysates of COS-7 cells expressing AT3Q80(C14A) (black arrow) and HA-ubiquitin, in the presence or absence of AT3Q25(FL). Although AT3Q25(FL) lowers overall levels of AT3Q80(C14A) (third lane), it does not alter the steady-state ubiquitination pattern of AT3Q80(C14A) (triangles). Arrowheads, nonexpanded, catalytically active AT3Q25(FL) runs similarly to a by-product of expanded, catalytically inactive AT3Q80(C14A).

We extended these *in vitro* results with cell-based studies in which ataxin-3 Q80(C14A) was coexpressed with ataxin-3 Q25(FL) or empty vector (Figure 3.7.B). We used ataxin-3 Q80(C14A) in this experiment so that we could differentiate wild type (normal repeat) and catalytically inactive (expanded repeat) ataxin-3 based on protein size. Although there was an overall reduction in ataxin-3 Q80(C14A) levels when functional ataxin-3 Q25(FL) was coexpressed, the ubiquitination pattern of catalytically inactive ataxin-3 remained unchanged (Figure 3.7.B). This finding further suggests that ataxin-3 cannot deubiquitinate other ataxin-3 proteins *in trans*. Thus, some other mechanism must account for the modulatory effect that active ataxin-3 has on its inactive counterpart's protein levels.

3.4.5. Ataxin-3 catalytic activity affects its proteasomal degradation rate *in vitro*

To investigate whether the observed difference in degradation of ataxin-3 Q25(FL) versus ataxin-3 Q22(C14) (Figure 3.5.) depended on ataxin-3 ubiquitination, we incubated recombinant GST-ataxin-3 Q22(FL) or GST-ataxin-3 Q22(C14A) with 26 S proteasomal fractions and an ATP regeneration system and then assessed degradation over time. As shown in Figure 3.8.A, ataxin-3 Q22(C14A) was degraded more slowly than ataxin-3 Q22(FL). This indicates that the rate of proteasomal degradation of ataxin-3 depends, in part, on the catalytic site of ataxin-3 and suggests that ataxin-3 does not need to be ubiquitinated to be degraded by the proteasome *in vitro*.

Next, we sought to determine how ubiquitinated ataxin-3 was handled by 26 S proteasomal fractions *in vitro*. For this experiment, we used ubiquitinated ataxin-3 (FL) or ataxin-3 (C14A) that had been immunopurified from transfected cells. As shown in Figure 3.8.B, both active and inactive ataxin-3 were quickly deubiquitinated by the proteasomal fraction (Figure 3.8.B, compare 0 with 20 min); ubiquitinated ataxin-3 bands (Figure 3.8.B, triangle) were rapidly converted to non-ubiquitinated ataxin-3 species. This deubiquitination of ataxin-3 was prevented by the inhibitor ubiquitin-aldehyde, which blocks most proteasome-associated DUB activity (Figure 3.8.C). These data indicate that one or more DUBs present in 26S proteasomal fractions can efficiently deubiquitinate ataxin-3.

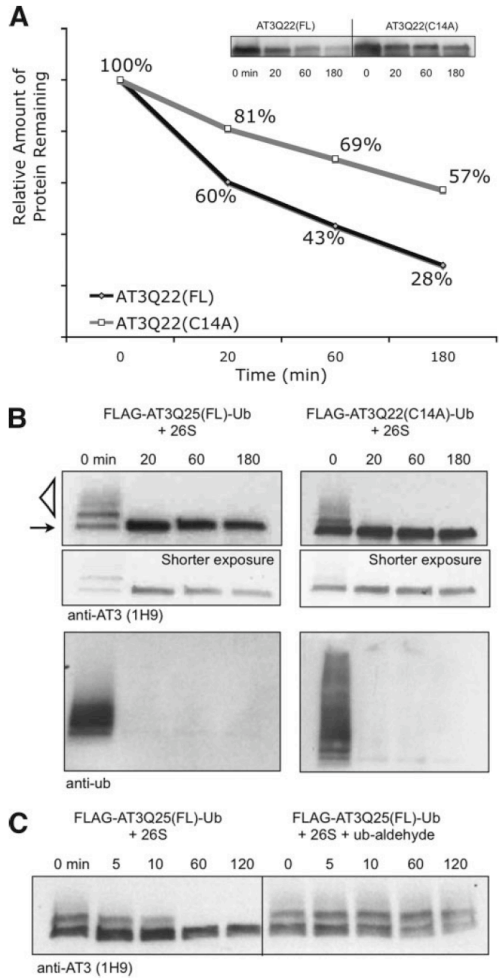

Figure 3.8. - Ataxin-3 catalytic activity affects its proteasomal degradation rate *in vitro*. (**A**) *In vitro* degradation of wild type or catalytically inactive recombinant ataxin-3 by 26S proteasomal fractions. Plotted are the means from four independent experiments. The inset shows a representative Western blot used for densitometry. (**B**) Ubiquitinated ataxin-3 was immunopurified from transfected cells, incubated for 0–180 min with 26S proteasomal fractions and then probed on blots with the indicated antibodies. Within 20 min, the ubiquitinated forms of ataxin-3 (triangle) are reduced to nonubiquitinated ataxin-3 (arrow). (**C**) The addition of ubiquitin-aldehyde inhibits deubiquitination of ataxin-3 by proteasomal fractions.

3.4.6. Ataxin-3 catalytic activity affects both its interaction with VCP/p97 and its subcellular distribution

Ataxin-3 has previously been reported to interact with the proteasome (Doss-Pepe et al., 2003). Therefore, we decided to investigate whether interaction of ataxin-3 with proteasomal subunits and proteasome-associated proteins was influenced by its catalytic site. Recombinant GST-ataxin-3 Q22(FL) or GST-ataxin-3 Q22(C14A) was incubated with 26S proteasomal fractions that had been pretreated with proteasome inhibitors to inhibit proteolysis. We tested the ability of ataxin-3 to interact with various proteasomal subunits, including 19S non-AAA ATPases RPN2 and RPN10; AAA ATPases RPT1, RPT2, RPT3, RPT4, RPT5, and RPT6; and various 20S core subunits. These tests for interaction employing GST pull-downs, together with IPs from cell lysates, or nuclear extracts using mild buffers (see "3.3. Material and methods") did not identify specific interactions of ataxin-3 with any of the 19S and 20S subunits tested (data not shown).

However, when ataxin-3 was expressed in COS-7 cells, we did notice colocalization of ataxin-3 with the endogenous proteasome in the nucleus (Figure 3.9.A). Together, these results suggest that exogenous ataxin-3 does not directly interact with the proteasome or does so only transiently or with low affinity.

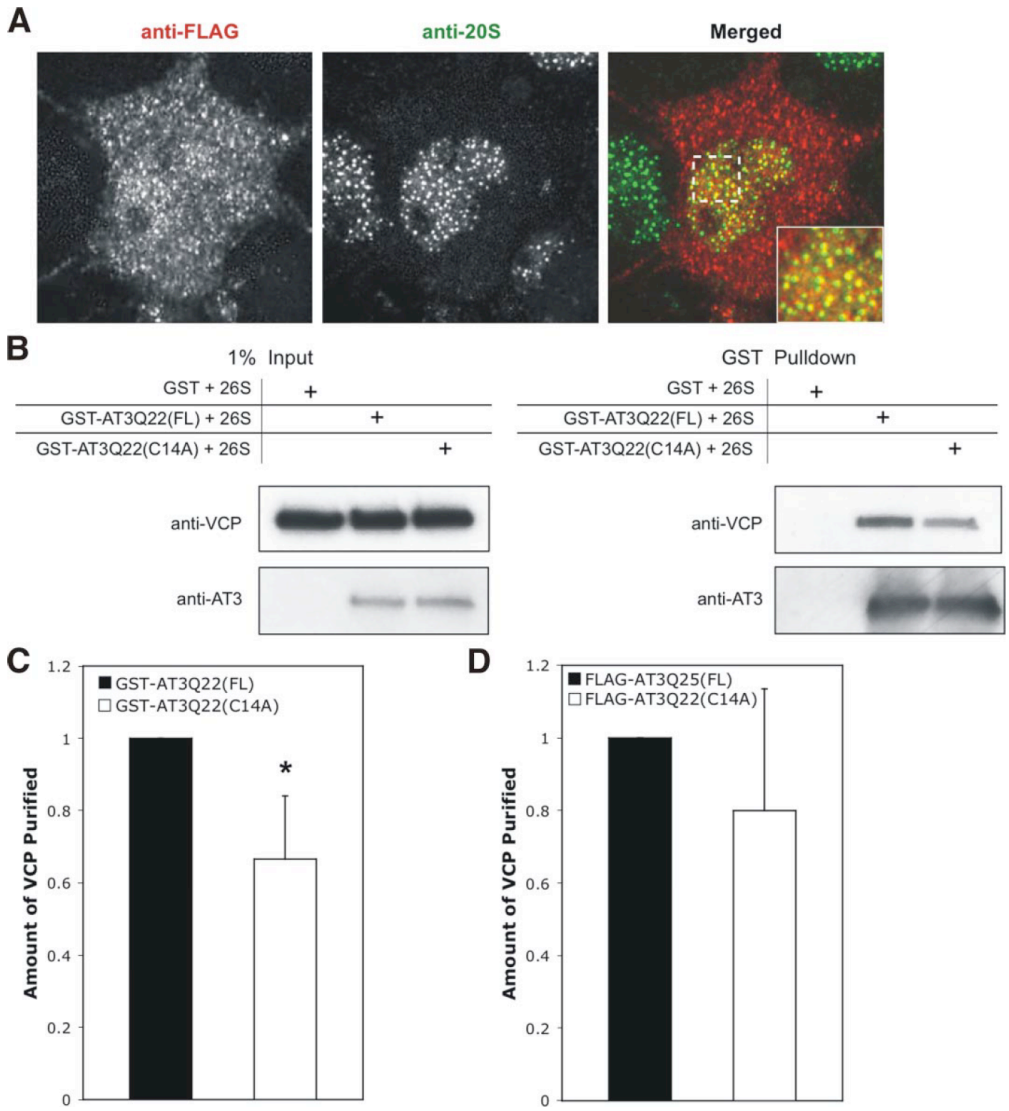

Figure 3.9. - Ataxin-3 subcellular distribution and interaction with VCP/p97 are modulated by catalytic activity. (**A**) Ataxin-3 colocalizes with the 20S proteasome. COS-7 cells were transiently transfected with FLAG-AT3Q25(FL), probed with anti-FLAG (red) and anti-20S (green) antibodies, and imaged using confocal microscopy. Magnification of the boxed area shows colocalization of ataxin-3 and 20S to subnuclear foci (inset). (**B**) GST pull-downs of GST-AT3Q22(FL), GSTAT3Q22(C14A), or GST, incubated with 26S proteasomal fractions in the presence of proteasome inhibitors (lactacystin or MG-132), and ATPγS. VCP/p97 co-purifying with ataxin-3 was detected by anti-VCP/p97 antibody. Less VCP/p97 co-purified with AT3Q22(C14A) than with AT3Q22(FL). (**C**) Quantification of results from (**B**). Mean ± S.D. (n = 13). $p < 0.01$. (**D**) Quantification of VCP/p97 subjected to co-IP with ataxin-3 from COS-7 cell lysates (Mean ± S.D.; n = 9; $p < 0.01$).

In the GST pull-down assays, we noticed that catalytically inactive ataxin-3 associated less avidly with a known ataxin-3-interacting protein, the AAA protein VCP/p97, which is present in the proteasomal fractions (Figures 3.9.B and 3.9.C). VCP/p97 participates in diverse cellular processes, including the shuttling of substrates to the proteasome (Zhang et al., 1994; Rabouille et al., 1995; Dai e al., 1998; Ghislain et al., 1996; Roy et al., 2000; Dai and Li, 2001; Ye et al., 2001; Jarosch et al., 2002). This prompted us to test whether the ability of ataxin-3 to co-precipitate endogenous VCP/p97 from cells is also affected by its catalytic site. Although there was a trend toward reduced interaction of catalytically inactive ataxin-3 with VCP/p97 in cells, this did not reach significant statistical difference (Figure 3.9.D). Based on these data, one reason for reduced ataxin-3 Q22(C14A) degradation by the 26S proteasome *in vitro* may be reduced shuttling or presentation of ataxin-3 to the proteasome by VCP/p97.

Differences in steady state levels of active versus inactive ataxin-3 could also reflect differences in subcellular distribution. When conducting confocal microscopy analyses, we observed a difference in the subcellular distribution between non-expanded, catalytically active and inactive ataxin-3. Catalytically active ataxin-3 preferentially localized to the nucleus, whereas inactive ataxin-3 often distributed similarly in the cytoplasm and nucleus or preferentially in the cytoplasm (Figure 3.10.A). In these experiments, we used ataxin-3 Q25(FL) and ataxin-3 Q22(C14A) plasmid DNA amounts that had been determined to yield similar protein levels on western blots (for an example, see Figure 3.1.D). These data suggest that ataxin-3 catalytic activity modulates its distribution in the cell.

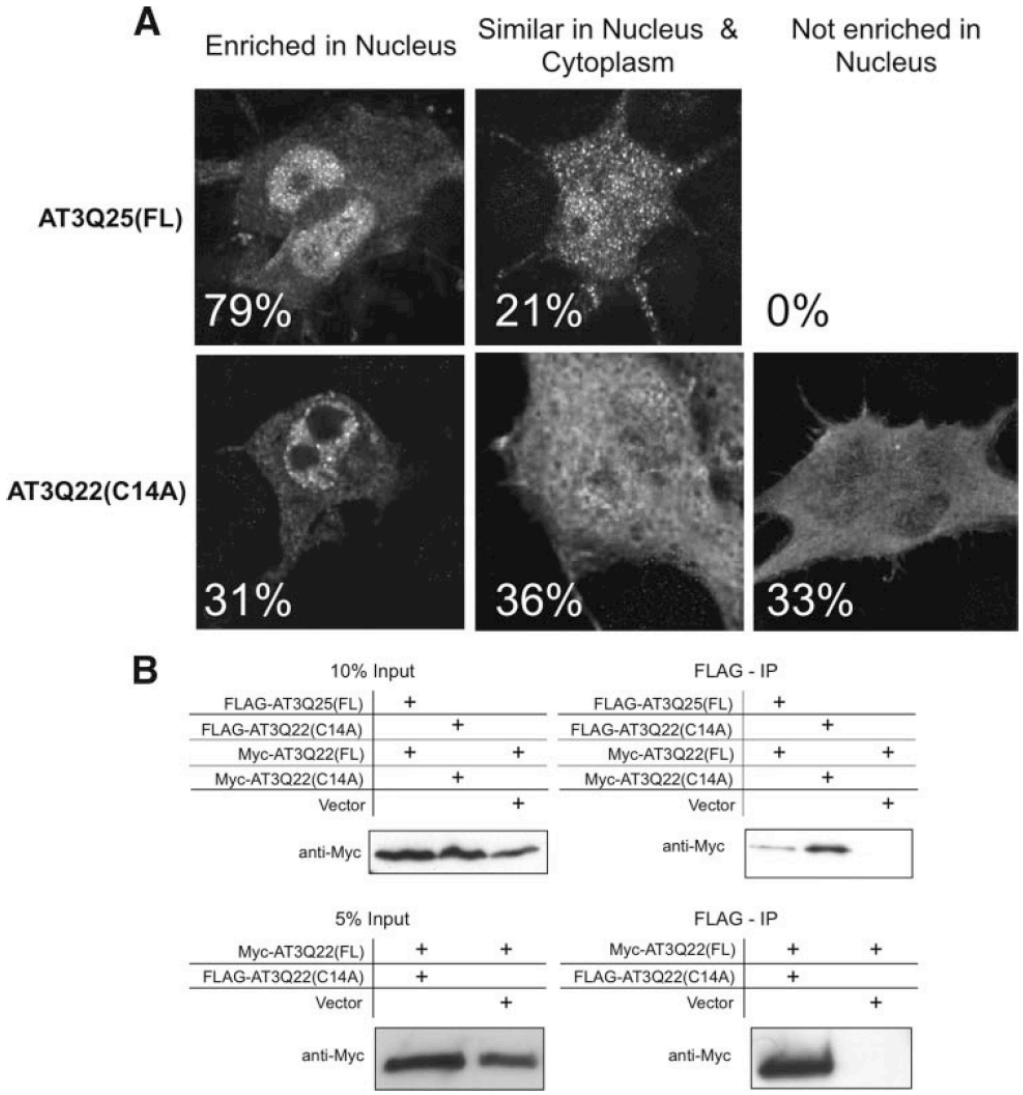

Figure 3.10. - Catalytically inactive ataxin-3 displays altered subcellular distribution. (**A**) COS-7 cells were transiently transfected with FLAG-AT3Q25(FL) or FLAG-AT3Q22(C14A), fixed 48 h later, and probed with anti-FLAG antibody. Cells were imaged with confocal microscopy and scored by a blinded observer. N = 24cells for AT3Q25(FL) and n = 36 for AT3Q22(C14A). (**B**) Ataxin-3 interacts with other ataxin-3 proteins. FLAG- and Myc-tagged ataxin-3 constructs were coexpressed transiently in COS-7 cells and immunopurified using FLAG-antibody beads in FLAG lysis buffer or Buffer A. Self-interaction of active or inactive ataxin-3 (top). Interaction of active ataxin-3 with inactive ataxin-3 (bottom).

Finally, we sought to understand how functional ataxin-3 modifies the protein levels of catalytically inactive ataxin-3, as shown earlier (Figure 3.1.). We conducted immunoprecipitation experiments in which separately epitope-tagged active and inactive ataxin-3 were coexpressed in cells, and ataxin-3 was then immunoprecipitated from the lysate using bead-bound antibody. We noticed that ataxin-3 can interact with other ataxin-3 molecules (Figure 3.10.B). Thus, wild type ataxin-3 may reduce levels of catalytically inactive ataxin-3 through a mechanism involving physical interaction between ataxin-3 molecules (Figure 3.11.).

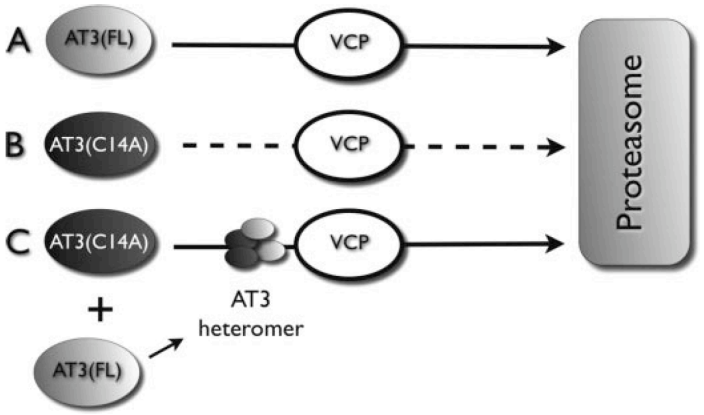

Figure 3.11. - Proposed model of ataxin-3 degradation. (**A**) Catalytically active ataxin-3 (light gray) is shuttled to the proteasome as a monomer (shown) or oligomer (not shown) and degraded. (**B**) Catalytically inactive ataxin-3 (dark gray) is less readily shuttled to the proteasome through decreased binding to VCP/p97 (and perhaps other proteasome-associated proteins), and thus is degraded more slowly. (**C**) In the presence of additional functional ataxin-3, inactive ataxin-3 is more readily degraded, due in part to interactions with functional ataxin-3 that facilitate shuttling to the proteasome.

3.5. Discussion

Here we have presented evidence that the catalytic activity of the deubiquitinating enzyme ataxin-3 affects its own protein levels, ubiquitination pattern, and subcellular localization. Ataxin-3 has been implicated to function in protein quality control pathways (Fujigasaki et al., 2000; Takahashi et al., 2001;Donaldson et al., 2003; Chai et al., 2004; Seilhean et al., 2004; Warrick et al., 2005; Zhong and Pittman, 2006). Regulation of ataxin-3 by its catalytic activity may be an important component to the normal biological function of this protein; determining the precise catalytic activity of ataxin-3, including its possible specificity for cleavage of certain types of ubiquitin linkages, is an ongoing point of investigation. Our findings may also provide insight into MJD/SCA3 pathogenesis, since evidence links polyQ toxicity to various non-polyQ domains in disease proteins. Nuclear localization of the disease polyQ protein is required for pathogenesis in some polyQ diseases (Cummings et al., 1998; Klement et al., 1998; Saudou et al., 1998; Kordasiewicz et al., 2006), and in MJD/SCA3 patients, expanded ataxin-3 accumulates in neuronal nuclei (Paulson et al., 1997a; Schmidt et al., 1998). Additionally, recent data provide strong evidence that nuclear localization of polyQ-expanded ataxin-3 enhances MJD phenotype manifestation in mouse models (Bichelmeier et al., 2007). Therefore, our finding that ataxin-3 subcellular localization is activity-dependent deserves further attention, since it may help lead to a better understanding of MJD/SCA3 pathogenesis.

Considering the slower turnover rate of catalytically inactive, expanded ataxin-3 in cells (ataxin-3 Q80(C14A); Figure 3.1.), it will be interesting to compare the pathogenicity of this protein in the mouse brain to that of the expanded, catalytically active ataxin-3. Our data would suggest that the catalytically inactive form of expanded ataxin-3 may accumulate more readily in neurons and therefore prove more neurotoxic. Expression of expanded, catalytically inactive ataxin-3 is indeed more toxic in *Drosophila* (Warrick et al., 2005); thus, extending this analysis to a mammalian nervous system will be important.

Ataxin-3 cleaves polyubiquitin chains via its N-terminal Josephin domain

(Burnett et al., 2003; Chai et al., 2004; Mao et al., 2005). In our studies employing ataxin-3 mutated in its active site cysteine residue (C14A), the catalytically inactive protein was consistently expressed at higher steady state levels (Figures 3.1.; 3.2. and 3.3.) and was more heavily ubiquitinated than its active counterpart (Figure 3.6.). The higher levels of inactive ataxin-3 could be reduced by co-expression of active ataxin-3 in transiently or stably transfected cells (Figures 3.1.B and 3.1.C), without altering the ubiquitination pattern of inactive ataxin-3 (Figure 3.7.). The mechanism behind our observation that active ataxin-3 reduces levels of inactive ataxin-3 may rely on the ability of ataxin-3 molecules to interact together (Figure 3.10.B) and with the proteasome shuttle protein VCP/p97 (Figure 3.9.). In this view, active ataxin-3 can aid in bringing catalytically inactive ataxin-3 proteins in closer proximity to the proteasome, where degradation then can occur (Figure 3.11.).

Ataxin-3 has many lysine residues interspersed throughout the protein. The presence of multiple lysine residues in ataxin-3, the increased ubiquitination of ataxin-3 when it is catalytically inactive, and the fact that ataxin-3 is itself a DUB together suggest thatataxin-3 could be a substrate for itself. Although we cannot rule out this possibility, in our deubiquitination experiments employing immunopurified ataxin-3, we have not noticed a change in the levels or migration pattern of functional or catalytically inactive ataxin-3, even after overnight incubations (data not shown).

Ataxin-3 Q22(C14A) is ubiquitinated more heavily than its fully functioning counterpart (Figure 3.6.) yet is less rapidly degraded (Figures 3.5. and 3.8.A). This may seem surprising, since ubiquitination is often associated with proteasomal targeting of proteins. However, increased ubiquitination does not necessarily specify a higher proteasomal degradation rate. Indeed, we presented *in vitro* evidence that ataxin-3 can be degraded by the proteasome independently of ubiquitin (Figure 3.8.A) and observed a marked temporal discrepancy between the rapid deubiquitination of ataxin-3 by 26S proteasomal fractions and its subsequent, slower degradation (Figures 3.8.B and 3.8.C). Other proteins are targeted for proteasomal degradation independent of ubiquitination by virtue of their association with proteasome-interacting proteins (Hoyt and Coffino, 2004; Hosoda et al., 2005). We suggest that ataxin-3, as an enzyme directly involved in ubiquitin pathways, may be "handled" by the proteasome differently than typical

substrates.

Our immunoprecipitation studies suggest that the influence of the catalytic activity on ataxin-3 degradation includes activity-modulated interaction of ataxin-3 with the proteasomal shuttling factor, VCP/p97 (Figures 3.9. and 3.11.). VCP/p97 has been linked to a diverse array of cellular processes, including endoplasmic reticulum-associated protein degradation, proteasomal degradation, and organelle formation (Zhang et al., 1994; Rabouille et al., 1995; Dai e al., 1998; Ghislain et al., 1996; Roy et al., 2000; Dai and Li, 2001; Ye et al., 2001; Jarosch et al., 2002). VCP/p97 interaction with ataxin-3 has been previously reported *in vitro* and *in vivo* (Doss-Pepe et al., 2003; Boeddrich et al., 2006; Zhong and Pittman, 2006). An earlier report indicated that the VCP/p97-ataxin-3 interaction in cells was not affected by the catalytic site of ataxin-3 (Zhong and Pittman, 2006). The discrepancy between this earlier study and our current findings may reflect the different conditions used. In our hands, we observe a modest, but statistically significant, decrease in VCP/p97 interaction with ataxin-3 (C14A) *in vitro* and a similar trend in cells (Figure 3.9.) using a variety of buffers and incubation times (see "3.3. Material and methods").

Another report described ataxin-3 interaction with the proteasome (Doss-Pepe et al., 2003). Despite extensive testing using mild buffer conditions, we did not confirm a physical interaction between ataxin-3 however, observe colocalization of ataxin-3 with the proteasome in subnuclear foci, consistent with a functional interaction (Figure 3.9.A). It may be that ataxin-3-proteasome interactions are transient, highly dynamic, and observable by immunopurification only under certain circumstances.

Interestingly, we did not observe a difference in steady state ataxin-3 protein levels in stably transfected cell lines expressing ataxin-3 Q22(FL) *versus* ataxin-3 Q22(C14A) (Figure 3.1.C, gray arrow). There are several possible reasons for this. FLP-in cells integrate a single plasmid copy, leading to nearly physiological expression of the transfected gene product. As such, endogenous (fully active) ataxin-3 may be able to modulate the levels of stably expressed ataxin-3 Q22(C14A) to lower levels than when the construct is overexpressed transiently. Alternatively, feedback mechanisms that come into play in stable cell lines could alter the half-life of ataxin-3 protein in a manner different from the behavior observed in transiently transfected cells. Another

possibility is that the ataxin-3 Q22(FL) cell line expresses more RNA from its integrated plasmid than does the ataxin-3 Q22(C14A) line, leading to similar protein levels.

Finally, it deserves mentioning that although our pulse-chase analysis (Figure 3.5.) and *in vitro* experiments (Figure 3.8.A) demonstrated a difference between the half-lives of active and inactive ataxin-3, they do not fully account for the markedly dissimilar protein levels observed in transfection experiments (Figure 3.1.). Collectively, our findings suggest that differences in protein degradation rates between active and inactive ataxin-3 (Figure 3.11.) comprise only part of the mechanism underlying the large differences in steady state protein levels.

The finding that ataxin-3 levels are autoregulated in a catalytic activity-dependent manner adds to the growing list of routes by which deubiquitinating enzymes can be regulated. DUB function can be regulated through many mechanisms, including transcription, proteasomal degradation, caspase cleavage, phosphorylation, ubiquitin-dependent activation, incorporation into higher order complexes, and autocleavage (Nijman et al., 2005). To our knowledge, ataxin-3 is the first reported DUB whose catalytic activity affects its cellular turnover in a manner apparently independent of its ubiquitination. This finding suggests that other DUBs should be investigated for activity-dependent actions on DUB cellular fate.

In conclusion, we have presented evidence that ataxin-3 regulates its own levels, ubiquitination pattern, and subcellular localization in a catalytic activity-dependent manner. These findings provide clues to the cellular fate of ataxin-3 in cells and provide insights into the cellular function of ataxin-3, both as a DUB and as a pathogenic protein when its polyQ domain is expanded.

Chapter 4

Compromised mitochondrial complex II in models of Machado-Joseph disease

4.1. Abstract

Machado-Joseph disease (MJD), also known as Spinocerebellar Ataxia type 3, is an inherited dominant autosomal neurodegenerative disorder. An expansion of CAG repeats in the *ATXN3* gene is translated as an expanded polyglutamine domain in the disease protein, ataxin-3. Selective neurodegeneration in MJD is evident in several subcortical brain regions including the cerebellum. Mitochondrial dysfunction has been proposed as a mechanism of neurodegeneration in polyglutamine disorders. In this study, we used different cell models and transgenic mice to assess the importance of mitochondria on cytotoxicity observed in MJD. Transiently transfected HEK cell lines with expanded (Q84) ataxin-3 exhibited a higher susceptibility to 3-nitropropionic acid (3-NP), an irreversible inhibitor of mitochondrial complex II. Increased susceptibility to 3-NP was also detected in stably transfected PC6-3 cells that inducibly express expanded (Q108) ataxin-3 in a tetracycline-regulated manner. Moreover, cerebellar granule cells from MJD transgenic mice were more sensitive to 3-NP inhibition than wild-type cerebellar neurons. PC6-3 (Q108) cells differentiated into a neuronal-like phenotype with nerve growth factor (NGF) exhibited a significant decrease in mitochondrial complex II activity. Mitochondria from MJD transgenic mouse model and lymphoblast cell lines derived from MJD patients also showed a trend towards reduced complex II activity. Our results suggest that mitochondrial complex II activity is moderately compromised in MJD, which may designate a common feature in polyglutamine toxicity.

4.2. Introduction

Machado-Joseph disease (MJD), also known as spinocerebellar ataxia type 3, is an inherited autosomal dominant neurodegenerative disorder. MJD is the most common hereditary ataxia in the world, accounting for 21-28% of the autosomal-dominant inherited cerebellar ataxias (Albrecht et al., 2003; Rüb et al., 2003a). Worldwide, it affects 1 or 2 individuals per 100 000 people, but its prevalence can increase to 1% of the population in some regions of the globe. Clinically, MJD is characterized by progressive gait and limb ataxia, dysarthria and a variable combination of other symptoms including pyramidal signs, dystonia, oculomotor disorders, faciolingual weakness, neuropathy, progressive sensory loss and parkinsonian features (Rüb et al., 2002). The first symptoms usually become apparent in adulthood (third or fourth decade of life), although they can manifest earlier in life in severe cases. Symptoms and neurological deficits progressively worsen over time, culminating in patients' death 20 to 30 years later. In MJD, neurodegeneration and astrogliosis are restricted to subcortical brain regions and are particularly prevalent in the pontine nuclei, the dentate nucleus, subthalamic nucleus and spinal cord (Rüb et al., 2002). The mechanisms leading to neuronal dysfunction and cell death are still poorly understood.

MJD belongs to the polyglutamine (polyQ) expansion disorders, a group of ten diseases that share the same genetic alteration, a pathological increase in the number of CAG codon repeats. In MJD, the CAG expansion is present in exon 10 of *ATXN3* gene, located on chromosome 14 (14q32.1) (Kawagushi et al., 1994; Riess et al., 2008). Normal individuals have 12 to 42 CAG repeats, but in MJD carriers, the repeat range extends from 52 to 84 (Rüb et al., 2003). The *ATXN3* gene codes for the ubiquitously expressed 42 kDa protein ataxin-3, and thus, the pathological CAG-expanded gene is translated into ataxin-3 with an extended polyQ tract in its C-terminus (Paulson et al., 1997a; Trottier et al.,

1998; Ichikawa et al., 2001; Schmitt et al., 2003). Although its full biological role remains elusive, several studies have demonstrated that ataxin-3 binds and cleaves polyubiquitin chains, exhibiting a deubiquitinating-like activity (Berke et al., 2003; Burnett et al., 2003; Donaldson et al., 2003; Chai et al., 2004; Winborn et al., 2008). The presence of an expanded polyQ region promotes protein misfolding and destabilization of the expanded ataxin-3 structure, leading to protein deposition and formation of intracellular inclusions (Bevivino and Loll, 2001; Cemal et al., 2002; Evert et al., 2003; Masino et al., 2004). Intracellular aggregates are found in the nuclei of neurons from degenerated areas of MJD patient brains, as well as in nuclei and cytoplasm of cell lines expressing expanded ataxin-3 (Paulson et al., 1997b; Chai et al., 1999; Evert et al., 1999; Chai et al., 2002). Ataxin-3 localizes to the cytoplasm and nucleus, but the presence of expanded ataxin-3 in the nucleus seems to be important for the manifestation of disease in MJD transgenic mice (Bichelmeier et al., 2007).

Several studies have reported altered mitochondrial structure and a consistent deregulation of mitochondrial activity and function in polyQ disorders. Mitochondria from Huntington's disease (HD) patients and transgenic mice show a decrease in membrane potential and in the ability to retain Ca^{2+} (Panov et al., 2002; Panov et al., 2003). Severe defects in mitochondrial complex II and III activities and deficiency in complex IV have also been reported to be correlated to neuronal death in HD (Gu et al., 1996; Benchoa et al., 2006; Solans et al., 2006). PolyQ proteins also impair mitochondrial transport in neuronal processes and induce caspase activation through mitochondrial pathways (Choo et al., 2004; Trushina et al., 2004; Tsai et al., 2004). Moreover, polyQ disease proteins and polyQ-containing protein fragments are able to induce mitochondrial dysfunction and mitochondrial swelling *in vitro* (Choo et al., 2004). Although much data has been gathered for other polyQ disorders (Solans et al., 2006; Oliveira et al., 2007), there is a lack of information regarding altered mitochondrial activity in MJD and the role of mitochondria in the progress of this pathology. Thus, in this study we determined the susceptibility of

cells expressing expanded ataxin-3 to selective mitochondrial inhibitors and assessed the activity of mitochondrial complexes in MJD transgenic mouse brain and human lymphoblasts. The results show a significant trend towards impairment in complex II in different models of MJD and human MJD peripheral cells.

4.3. Material and methods

4.3.1. Materials

Dulbecco's modified Eagle's medium (DMEM) and Roswell Park Memorial Institute's medium (RPMI) were acquired from Sigma-Aldrich Chemical Co. (St. Louis, MO, USA). Neurobasal medium and B-27 supplement, fetal bovine serum (FBS), horse serum were purchased from GIBCO (Paisley, UK). Hygromycin, blasticidin were from Invitrogen (Paisley, UK). Nerve growth factor (NGF) was purchased from Alomone Labs (Jerusalem, Israel). Primary antibodies against ataxin-3 1H9 (1:1000; Chemicon, USA) and microtubule associated protein 2 (MAP-2) were obtained from Chemicon (Temecula, CA, USA). Anti-coilin was from BD biosciences (San Jose, CA, USA) and anti-promyelocytic leukemia protein (PML) was from Santa Cruz Biotechology (Santa Cruz, CA, USA). Secondary antibodies for immmunocytochemistry anti-mouse Alexa-fluor 594, anti-rabbit Alexa-fluor 488 and Hoechst 33342 were from Molecular Probes (Eugene, OR, USA), while secondary antibodies for western blotting were acquired from GE healthcare (Uppsala, Sweden). Superfect reagent was purchased from Qiagen (Hilden, Germany). Unless otherwise stated, all other reagents were from Sigma-Aldrich Chemical Co. (St. Louis, MO, USA) and were of analytical grade.

4.3.2. Constructs, cell lines culture and transfections

Enhanced green fluorescent protein (EGFP)-ataxin-3 (Q28) and EGFP-ataxin-3 (Q84) plasmids encode a fluorescent fusion-protein composed of full-length human ataxin-3 (*MJD1a* isoform) with EGFP attached to its N-terminus (Chai et al., 2002). These constructs were transfected into HEK 293 cells with Superfect reagent, according to manufacturer's instructions. HEK 293 cells were

maintained in DMEM supplemented with 10% (vol/vol) fetal bovine serum (FBS) and 1% (vol/vol) streptomycin/penicillin. Stably transfected, doxycycline-inducible PC6-3 wild type (Q28) or expanded (Q108) cell lines were kept in RPMI supplemented with 5% (vol/vol) FBS, 10% (vol/vol) horse serum, hygromycin, blasticidin and 1% (vol/vol) streptomycin/penicillin. To induce neural differentiation, PC6-3 cells were plated on poly-L-lysine-coated multiwell plates and incubated with 100 ng/ml NGF for 7 days, in low serum-containing medium (1% (vol/vol) FBS) to reduce cell proliferation. Expression of human ataxin-3 was controlled through the addition of doxycycline to the media. Normal and 2 MJD (JMMA and JMJW have 28/68 and 27/78 repeat alleles, respectively) lymphoblastic cell lines were grown in RPMI supplemented with 10% (vol/vol) FBS, 250 mg/L glucose, 10 mM HEPES, 1 mM sodium pyruvate and 1% (vol/vol) streptomycin/penicillin. All cell lines were kept in a 95% air and 5% CO_2 atmosphere at 37ºC.

4.3.3. Culture of cerebellar granule cells isolated from MJD transgenic mice

Cerebellar granule cells from 6-7 day-old MJD transgenic mouse (Goti et al., 2004) pups or wild-type littermates were prepared according to the protocol for the isolation of cerebellar granule cells from rat pups previously described (Courtney et al., 1990), with slight modifications attending to the different species of origin. Cells were plated on poly-L-lysine-coated multiwell plates or glass coverslips. Cells were maintained in Neurobasal medium supplemented with 2% (vol/vol) B-27, 0.2 mM glutamine, 100 U/mL penicillin, 0.1 mg/mL streptomycin and 24 mM KCl. After the first day in culture, 10 μM cytosine arabinose was added to the media to prevent glial cell proliferation. Old medium was partially removed and new medium was added to granule cells every fourth day. Cerebellar granule cells were kept in a humidified atmosphere of 95% air and 5% CO_2, at 37°C, and used after 7-8 days *in vitro*. Isolated

granule cells from expanded ataxin-3 transgenic mice were as healthy in culture as the neurons from the wild-type littermates.

4.3.4. Cytochemistry and immunocytochemistry

Transfected HEK 293 cells expressing EGFP-human ataxin-3 for 24 or 48 hours had their media removed and were washed 2 times with phosphate buffered solution (PBS, in mM: 137 NaCl, 2.7 KCl, 1.4 K_2HPO_4, 4.3 Na_2HPO_4, pH 7.4). The cells then were fixed with methanol:acetone (1:1) solution for 15 minutes in ice. After 3 washes with PBS cells were incubated with Hoechst 33342 (1 μg/μl) in PBS, for 5 minutes. The coverslips were further washed with PBS and mounted in DAKO solution.

PC6-3 cells and murine cerebellar granule cells were also washed 2 times with PBS before fixation with 4% (wt/vol) paraformaldehyde (PFA) in PBS, for 15 minutes. Then, cells were rinsed 3 times with PBS and opsonized with 5% (vol/vol) goat serum in PBT (phosphate-buffered saline plus 0.1% (vol/vol) Triton X-100) for 1 hour at room temperature. Cells were stained with the primary antibodies: anti-ataxin-3 1H9 (1:1000), anti-coilin (1:350), anti-PML protein (1:350) and anti-MAP-2 (1:200) diluted in 5% (vol/vol) goat serum in PBT, for one hour at room temperature. Cells were then washed 2 times with PBS and incubated with the secondary antibodies: anti-mouse Alexa-fluor 594 (1:250) and anti-rabbit Alexa-fluor 488 (1:250) in 5% (vol/vol) goat serum in PBT for one hour at room temperature. The cells were stained with Hoechst 33342 (1 μg/μl) in PBS for 5 minutes before being mounted in DAKO solution.

Immunofluorescence was visualized with an Axioplan fluorescence microscope (Zeiss, Thornwood, NY) using 20, 40, and 63x objectives. Images were captured digitally with a Zeiss MRM AxioCam camera and assembled in Photoshop 7.0 (Adobe Systems, Mountain View, CA). For each antibody, fluorescence intensity was controlled using identical capture time between genotypes, and images were captured on a linear scale.

4.3.5. Cell viability assay

HEK293 cells transfected with EGFP-ataxin-3 (Q28) or (Q84) for 48 hours and transgenic or wild-type cerebellar granule cells after 7 days in culture were incubated with mitochondrial inhibitors for a 24 hour-period. A large concentration range was tested for each of two inhibitors: rotenone (10 nM - 20 μM), an inhibitor of complex I, and 3-nitropropionic acid (3-NP, 10 μM - 10 mM), an irreversible inhibitor of succinate dehydrogenate. Cell viability was evaluated by following the reduction of (3-[4-5-dimethylthiazol-2-]-2,5-diphenyltetrazolium bromide (MTT). MTT (0.5 μg/ml) diluted in Krebs buffer (in mM: 120.9 NaCl, 4.8 KCl, 1.2 KH_2PO_4, 25.5 $NaHCO_3$, 13 glucose, 10 HEPES, pH 7.4) was added to the cell cultures and MTT reduction was carried on for 2 hours. The resultant formazan crystals were dissolved in a HCl-containing solution (0.04 M in isopropanol). The optical density was measured at 570 nm.

4.3.6. Evaluation of cell membrane integrity

Extracellular medium and intracellular samples of HEK 293 cell lines expressing EGFP-ataxin-3 for 48 hours and undifferentiated PC6-3 neural cell lines expressing human ataxin-3 were collected and stored at -80°C. Intracellular extracts were obtained through a double cycle of cell freezing and thawing in a HEPES-buffered solution (10 mM HEPES + 1% (vol/vol) Triton), followed by cell scraping. Intracellular and extracellular samples were centrifuged at 20800 x g for 10 minutes, at 4°C to eliminate cell debris and the resulting supernatant was used for the determination of lactate dehydrogenase (LDH) activity. LDH activity was assessed spectrophotometrically by following the conversion rate of NADH to NAD^+ at 340 nm in a Perkin Elmer lambda 2 UV/VIS spectrophotometer. LDH leakage was expressed as percentage of the total activity (% of LDH released = extracellular LDH/extracellular LDH + intracellular LDH) (Rego et al., 1999).

4.3.7. Mitochondrial fractionation

Mitochondrial crude fractions of PC6-3 and lymphoblastic cell lines were prepared in a sucrose medium (250 mM sucrose, 20 mM HEPES, 10 mM KCl, 1.5 mM $MgCl_2$, 1 mM EDTA, 1 mM EGTA, pH 7.4), at 4ºC. Briefly, cells were washed twice and scraped in ice-cold sucrose medium, followed by homogenization in a potter (120 strokes). The homogenates were centrifuged in a refrigerated table-top centrifuge at 2300 rpm for 12 minutes at 4 ºC to precipitate cell debris and nuclei. The resulting supernatants were collected and stored at -80ºC.

Brain mitochondria were isolated from wild-type and MJD homozygous transgenic mice with 4-5 months according to a method previously described (Rosenthal et al., 1987), with the slight modifications, using 0.02% (wt/vol) digitonin to free mitochondria from the synaptosomal fraction. In brief, mice were euthanized with a ketamine/xylazine solution, followed by a brain perfusion with PBS to reduce blood contamination. The whole brain was rapidly removed, washed, minced, and homogenized at 4ºC in 10 ml of isolation medium (225 mM mannitol, 75 mM sucrose, 5 mM Hepes, 1 mM EGTA, 1 mg/ml bovine serum albumin, pH 7.4) containing 5 mg of the bacterial protease. Single brain homogenates were brought to 30 ml and then centrifuged at 750 x g (Beckman Coulter Avanti J-26 XP1 Centrifuge) for 5 minutes. Mitochondria were recovered from the supernatant by centrifugation at 12 000 x g for 8 minutes. The pellet, including the fluffy synaptosomal layer, was resuspended in 10 ml of the isolation medium containing 0.02 (wt/vol) % digitonin and centrifuged at 12 000 x g for 8 min. The brown mitochondrial pellet without the synaptosomal layer was then resuspended again in 10 ml of medium and re-centrifuged at 12 000 x g for 10 minutes. The mitochondrial pellet was resuspended in 300 ml of resuspension medium (225 mM mannitol, 75 mM sucrose, 5 mM Hepes, pH 7.4) and stored at -80ºC.

4.3.8. Mitochondrial respiratory chain complex activities

NADH–ubiquinone oxidoreductase assay – Complex I activity was determined at 340 nm by following the decrease in NADH absorbance due to ubiquinone reduction to ubiquinol (Ragan et al., 1987). Complex I activity was expressed in nanomoles/minute/milligram protein and corresponds to the rotenone sensitive rate. The enzyme activity was corrected for citrate synthase activity.

Succinate–ubiquinone oxidoreductase assay – Complex II activity was monitored at 600 nm by following the reduction of 6,6-dichlorophenolindophenol (DCPIP) by the ubiquinol resulting from this reaction (Hatefi and Stiggall, 1978). Complex II activity was expressed in nanomoles/minute/milligram protein and corresponds to the thenoyltrifluoroaceton (TTFA) sensitive rate. The enzyme activity was corrected for citrate synthase activity.

Ubiquinol–cytochrome c reductase assay – Complex III activity was monitored at 550 nm by following the ubiquinol reduction of cytochrome c. The assay was started by adding the sample to the reaction mixture (in mM: 35 K_2HPO_4, pH 7.2, 1 EDTA, 5 $MgCl_2$, 1 KCN, 5 μM rotenone) containing 15 μM cytochrome c and 15 μM ubiquinol, at 30ºC. Complex III activity was expressed in rate constant (k) per minute per milligram of protein and corrected for citrate synthase activity.

Cytochrome c oxidase assay – Complex IV activity was determined at 550 nm by measuring the oxidation of reduced cytochrome c by cytochrome c oxidase (Wharton and Tzagotoff, 1967). Complex IV activity was expressed in rate constant (k) per minute per milligram of protein and corrected for citrate synthase activity.

Citrate synthase assay - Citrate synthase (CS) activity was performed at 412 nm following the reduction of 5,5'-dithio-bis(2-nitrobenzoic acid) in the presence of acetyl-CoA and oxaloacetate (Coore et al., 1971). CS activity was expressed in nanomoles/minute/milligram of protein.

4.3.9. SDS-PAGE and immunoblotting

Total extracts from transfected HEK 293 cells, PC6-3 cell lines or primary cerebellar granule cells were collected and SDS-PAGE was performed in 10% polyacrylamide gels. Next, the proteins were transferred onto polyvinylidene difluoride membranes (Hybond-P, GE healthcare), which were further blocked in a 5% (wt/vol) non-fat milk solution for 60 minutes. Membranes were incubated with anti-ataxin-3 monoclonal (1H9, 1:1000) overnight at 4ºC with agitation. After washing, the blots were incubated with alkaline phosphatase-conjugated anti-mouse secondary antibody and developed with enhanced chemifluorescence. The membranes were scanned in a Biorad VersaDoc Imaging System Model 3000.

4.3.10. Statistical analysis

Data were expressed as mean ± SEM of the number of experiments indicated in the figure legends. Comparisons among multiple groups were analyzed with two-way analysis of variance (ANOVA) followed by the Bonferroni post-hoc test, as indicated in the figure legends. Comparisons between two groups/conditions were performed with two-tailed unpaired Student's *t*-test. Significance was defined as $p<0.05$.

4.4. Results

4.4.1. EGFP-ataxin-3 protein aggregation in a transient expression cell model

We initiated our study in a transient expression cell model expressing wild-type or expanded ataxin-3. HEK 293 cells were transfected with mammalian expression vector encoding EGFP fusion protein of wild-type (Q28) or expanded (Q84) ataxin-3 (Figure 4.1.A). EGFP was located at the N-terminus of ataxin-3, near the globular Josephin domain containing the catalytic site. The expression of ataxin-3 fusions was confirmed by western blotting (Figure 4.1.B) and fluorescence microscopy. Both expression vectors were highly expressed with similar transfection efficiency (Figure 4.1.D). Transfected cells displayed a strong EGFP signal 24 hours after transfection (Figures 4.1.Ca and 4.1.Cc). Confocal microscopy revealed different patterns of intracellular localization for wild-type and expanded ataxin-3 (Figure 4.1.C). EGFP-ataxin-3 (Q28) was distributed homogenously throughout the cell (although more abundant in the cytoplasm), regardless of the length of time (24 or 48 hours) after transfection or the expression levels in the cell (Figures 4.1.Ca and 4.1.Cb). In contrast, EGFP-ataxin-3 (Q84) was initially diffusely distributed in the cytoplasm and nucleus of most cells (Figure 4.1.Cc). However, in a small number of cells and at a higher magnification, small sites of EGFP-ataxin-3 (Q84) accumulation with a perinuclear distribution were already detectable (Figure 4.1.Ce). At 48 hours of expression, EGFP-ataxin-3 (Q84) formed readily detectable cytoplasmic and perinuclear aggregates (Figure 4.1.Cd). The aggregates were not present in all transfected cells, and were more frequent in the cells exhibiting higher levels of ataxin-3 expression. Interestingly, in cells exhibiting protein aggregates, nearly all of the intracellular pool of expanded ataxin-3 localized to the aggregate.

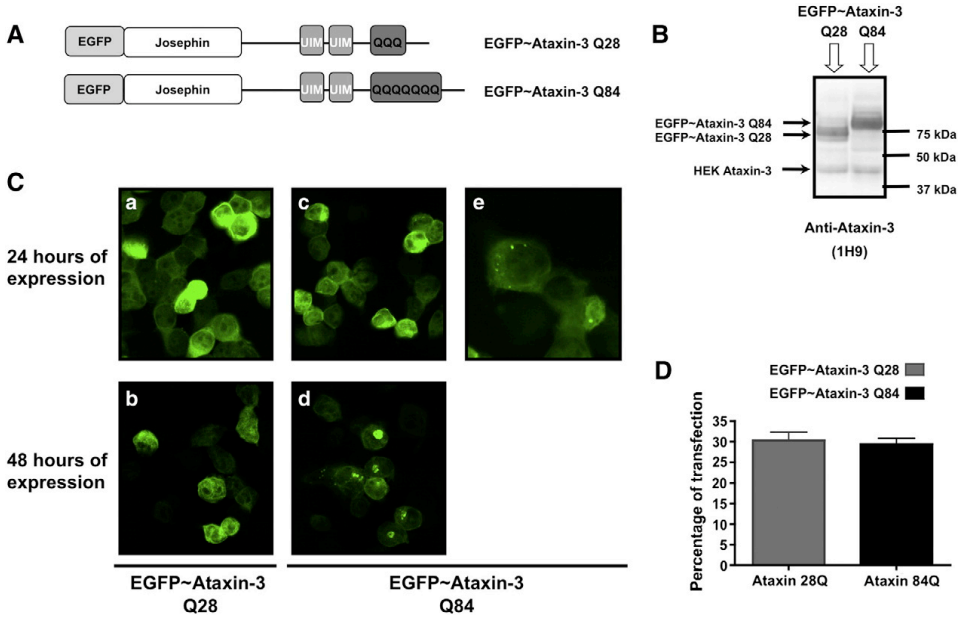

Figure 4.1. - EGFP-ataxin-3 Q84 fusion protein aggregates in a transiently expressed MJD cell model. HEK 293 cells were transfected with EGFP-ataxin-3 Q28 or EGFP-ataxin-3 Q84 plasmid constructs and their expression was carried out for 24 or 48 hours. (**A**) Representative schemes of the wild-type (Q28) and expanded (Q84) ataxin-3 fusion protein being expressed. (**B**) Total extracts prepared from HEK293 cells transfected with EGFP-ataxin-3 (Q28) or (Q84) were analysed through western blotting for ataxin-3 to assess the expression of the plasmid constructs. (**C**) Representative confocal fluorescent microscopy images of HEK293 cells expressing EGFP-ataxin-3 Q28 (a, b) or EGFP-ataxin-3 Q84 (c, d, e) for 24 (a, c, e) or 48 (b, d) hours. (e) Higher magnification of HEK cells transfected with EGFP-ataxin-3 Q84 for 24 hours. (**D**) HEK293 cells expressing EGFP-ataxin-3 Q28 or EGFP-ataxin-3 Q84 fusion proteins were fixed, nuclear stained with Hoechst 33342 and quantified through fluorescent microscopy. The graph plots the percentage of cells expressing wild-type (Q28) or expanded (Q84) ataxin-3 fluorescent fusion proteins in three independent transfections.

The aggregates were not SDS-insoluble, consistent with earlier reports (Ellisdon et al., 2006; Wong et al., 2008). The characteristic high molecular weight bands of SDS-resistant aggregates immunopositive for ataxin-3 or

retention of aggregates in the stacking gel or in the interface between the stacking and the running gels were not detected by western blotting (data not shown). Moreover, longer periods of expression of EGFP-ataxin-3 (Q84) (72, 96 hours) did not result in an increase in the number or size of aggregates (data not shown). For this reason, all other experiments using this cell model were carried out at 48 hours of expression.

4.4.2. Inducibly expressed expanded ataxin-3 accumulates in subnuclear compartments

To compare the formation of ataxin-3 aggregates between dividing cells and neuronal-like cells in the same cellular environment, we used stably transfected PC6-3 cell lines (a PC12 sub-clone (Pittman et al., 1993) expressing wild-type (Q28) or expanded (Q108) ataxin-3 under a tetracycline-regulated promoter (Figure 4.2.). These cell lines stably overexpress human wild-type or expanded ataxin-3 when doxycycline is administered to the culture media. Moreover, after NGF treatment, PC6-3 cells lose their normal growth round shape to develop long cellular processes resembling neurites, assuming a neuronal-like morphology. After differentiation, they exhibit an excitable polarized cell membrane sensitive to depolarization with potassium, not responding to glutamate or acetylcholine stimuli (not shown). Low concentrations of doxycycline (0.1 μg/ml) were efficient at inducing maximal expression of ataxin-3 in these cell lines with no further increase in expression observed for higher dosages of the antibiotic (Figure 4.2.A). There were also no significant differences in the ataxin-3 levels produced in PC6-3 cells expressing wild-type or expanded ataxin-3. To study the ataxin-3 distribution in cells with a neuronal-like phenotype, PC6-3 cells were incubated with NGF for 7 days in culture, before induction of wild-type or expanded human ataxin-3 expression for 24, 48, 72 and 96 hours. Fluorescent microscopic images of PC6-3 cells immunostained for ataxin-3 revealed that the cellular distribution of wild-type ataxin-3 did not alter over time and no aggregation was detected along the time

of expression tested (Figure 4.2.B), as previously observed in HEK293 cells (Figures 4.1.Ca and 4.1.Cb). However, in PC6-3 cells, wild-type ataxin-3 (Q28) had more affinity for the nuclear compartment than the EGFP-ataxin-3 Q28 fusion protein. On the other hand, the expanded form of ataxin-3 (Q108) exhibited a propensity to aggregate in PC6-3 cells, which was visible already at 24 hours after the induction of expression (Figure 4.2.B). Some PC6-3 cells expressing expanded ataxin-3 (Q108) developed visible ataxin-3 positive aggregates, primarily nuclear. These aggregates were SDS-soluble, as no higher molecular weight bands or aggregates in the stacking gel were observed on western blots (data not shown). Interestingly, the formation of intranuclear ataxin-3 aggregates was observed only in PC6-3 cells differentiated with NGF and therefore committed to a neuronal intracellular environment; protein aggregates were not visible in dividing cells (not shown). In cells without visible aggregates, expanded ataxin-3 displayed a nuclear-enriched distribution, similar to wild-type ataxin-3. When present, aggregates condensed almost all ataxin-3 fluorescent signal into a discrete intranuclear distribution, resembling the localization of some subnuclear compartments. In order to investigate this possibility, we co-immunostained PC6-3 cells for ataxin-3 and various signature proteins of subnuclear structures. The aggregates co-localized with promyelocytic leukemia protein (PML) and were often juxtaposed to coilin-positive bodies (Figures 4.2.C and 4.2.D). Nuclear PML-enriched bodies are known to co-localize with aggregates of polyQ proteins and the specific association between the Cajal (coiled) bodies and expanded ataxin-3 has been previously observed (Sun et al., 2007).

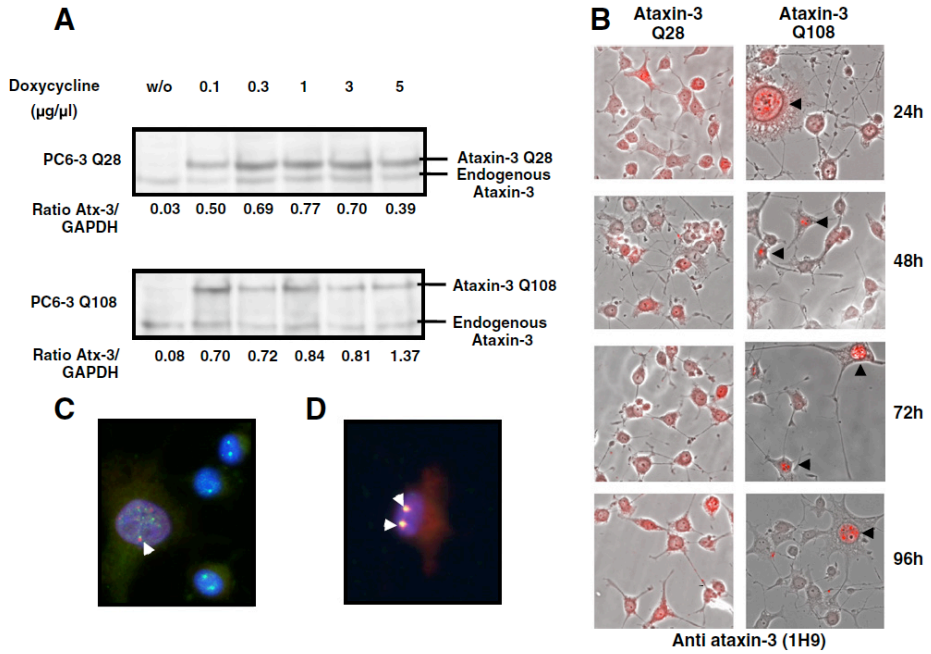

Figure 4.2. - Aggregates of human expanded ataxin-3 in PC6-3 ataxin-3 Q108 cells are primarily nuclear. (**A**) Total extracts were prepared from PC6-3 ataxin-3 Q28 cells or PC6-3 ataxin-3 Q108 cells incubated in the absence or presence of increasing concentrations (0.1, 0.3, 1, 3 and 5 µg/µl) of doxycycline for 24 hours and subsequently probed for ataxin-3 on a western blot. (**B**) Merged representative images of fluorescent and optical differential interference contrast microscopy of PC6-3 cells incubated with doxycycline (1 µg/µl) for expression of human ataxin-3 Q28 or human ataxin-3 Q108 during 24, 48, 72 or 96 hours and immunostained for ataxin-3 (in red). (**C**, **D**) Representative images of PC6-3 ataxin-3 Q108 cells expressing human expanded ataxin-3 for 48 hours, which were fixed and immunostained for ataxin-3 (in red) and coilin (in green) (**C**) or PML protein (in green) (**D**). Yellow shows co-localization between proteins. Nuclei were stained with Hoechst 33342 (1 µg/ml).

4.4.3. Ataxin-3 aggregation in neuronal cultures from a transgenic mouse model

We also investigated the intracellular localization of expanded ataxin-3 in a neuronal context, using primary cultures of cerebellar granule cells isolated from a human expanded ataxin-3 transgenic mouse model (Goti et al. 2004). This MJD transgenic mouse model mimics several pathological features of MJD in humans (Goti et al. 2004). In this model, the expression of the human expanded ataxin-3 (Q71) is under the control of the mouse prion promoter, which drives expression of the transgene throughout the brain. Intranuclear inclusions immune-positive for ataxin-3 are detected in several subthalamic regions of the brain and in the spinal cord of the adult mouse (Goti et al. 2004).

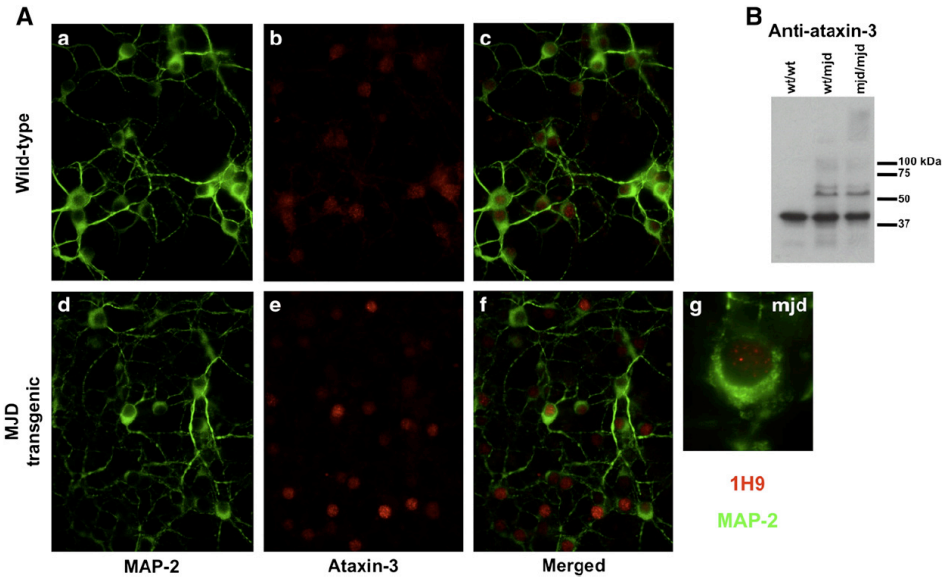

Figure 4.3. - Aggregation in the human expanded ataxin-3 transgenic mouse. (**A**) Cerebellar granule cells were isolated from 7 days wild-type (a, b, c) or transgenic (d, e, f) pups and kept in culture for 7 days. Cells were stained for MAP-2 (a, c, d, f - in green) and ataxin-3 (b, c, e, f - in red) and visualised through fluorescence microscopy. (g) Higher magnification of transgenic cerebellar granule cell immunostained for MAP-2 (in green) and ataxin-3 (in red). (**B**) Western blotting for ataxin-3 was performed in total brain extracts of wild-type (wt/wt), or transgenic (one

copy (wt/mjd) or two copies (mjd/mjd) of the transgene) 4 month old mice to evaluate the expression of the transgene and the aggregation of human expanded ataxin-3.

Western blotting of both wild-type and transgenic total brain extracts was performed to characterize expanded ataxin-3 expression (Figure 4.3.B). Immunostaining for ataxin-3 was higher in the nucleus both for cultured neurons derived from non-transgenic and transgenic mice, however, there were differences in the intranuclear distribution of wild-type murine ataxin-3 and expanded human ataxin-3 (Figure 4.3.A). Fluorescent microscopy images revealed intranuclear foci of expanded ataxin-3 similar to what we observed in the previous cell models. In wild-type neurons, nuclear ataxin-3 had a diffuse and homogeneous disposition, but in the nucleus of transgenic neurons, several discrete foci were easily detectable in almost all cells. The small size and the lack of higher molecular weight bands on western blots suggest that these ataxin-3 positive nuclear foci are not mature, SDS-insoluble aggregates. No differences in nuclear distribution of expanded ataxin-3 were observed in cultured neurons carrying one *versus* two copies of the transgene (i.e. hemizygous versus homozygous transgenic mice; data not shown). However, both homozygous and hemizygous transgenic mice at a later age develop intranuclear inclusions in the adult mouse brain (Goti et al. 2004).

4.4.4. Overexpression of expanded ataxin-3 enhances cell death upon mitochondrial complex II inhibition

Non-transfected HEK cells and cells expressing EGFP-ataxin-3 (Q28) or EGFP-ataxin-3 (Q84) for 48 hours were exposed to increasing concentrations of inhibitors of mitochondrial respiratory chain complexes I and II, rotenone and 3-NP respectively, for 24 hours. Incubation with rotenone or 3-NP induced a dose-dependent decrease in MTT reduction in HEK cells (Figure 4.5.A). Similar levels of cell death were observed for ataxin-3 (Q28) and ataxin-3 (Q84)

expressing HEK cell lines subjected to rotenone treatment (Figure 4.5.A), suggesting that expression of expanded ataxin-3 does not affect cellular susceptibility to inhibition of mitochondrial complex I. In contrast, a statistically significant difference between the survival of the two ataxin-3 expressing HEK cell lines was detected in the presence of 3-NP (Figure 4.5.A). For the lower concentrations of 3-NP (100 μM and 1 mM) tested, cells expressing EGFP-ataxin-3 (Q84) were more vulnerable than cells expressing EGFP-ataxin-3 (Q28) cells, although statistical significance was only detected in the presence of 100 μM 3-NP. Untransfected cells had a similar response to 3-NP exposure as EGFP-ataxin-3 (Q28) cell line, indicating that the differences in cell viability observed at low 3-NP concentrations were not due to transfection procedures, nor to the overexpression of ataxin-3 per se (Figure 4.5.A). Antimycin A, an inhibitor of complex III, was also tested in the HEK cell lines, but there were no differences in cell survival between wild-type and expanded ataxin-3 expressing cells (Figure 4.4.).

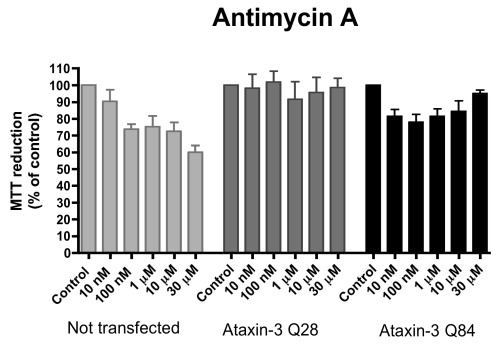

Figure 4.4. - Cell susceptibility to antimycin A is not altered by human expanded ataxin-3 expression. Untransfected HEK293 cells and HEK293 cells transfected with EGFP-ataxin-3 (Q28) or (Q84) were exposed to increasing concentrations of antimycin A (10 nM – 30 μM) for 24 hours, before cell viability assessment through MTT (0.5 μg/ml) assay. Graph summarizes the mean ±

SEM of the percentage of control for each cell type of 4 independent experiments, run in duplicates.

Cerebellar granule neurons from MJD transgenic or non-transgenic mice were also exposed to inhibitors of mitochondrial complexes I and II, rotenone and 3-NP respectively, for 24 hours. In comparison to HEK 293 cells, the cerebellar granule neurons were more susceptible to rotenone or 3-NP (Figure 4.5.). At 1 mM 3-NP, around 25% of the cerebellar granule cells survived, in contrast to 75% survival of HEK cells. Non-transgenic and MJD neurons responded similarly to rotenone inhibition (Figure 4.5.B). On the contrary, transgenic cerebellar granule cells exhibited a higher susceptibility for 30 μM 3-NP, when compared to wild-type neurons (Figure 4.5.B).

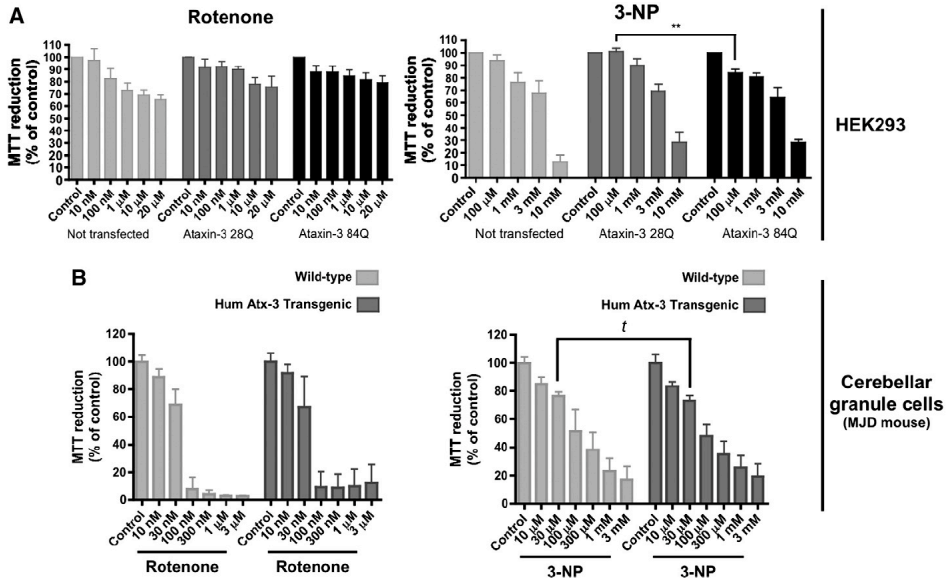

Figure 4.5. - Overexpression of expanded ataxin-3 (Q84) increases cell susceptibility to low concentrations of 3-nitropropionic acid (3-NP). HEK 293 cells transfected with EGFP-ataxin-3 (Q28) or (Q84) (**A**) or cerebellar granule cells from wild-type or transgenic mice pups (**B**) were

incubated with rotenone (10 nM - 20 μM) or 3-NP (10 μM - 10 mM), for 24 hours. After this incubation period, cell viability was assessed by MTT (0.5 μg/ml) reduction. Graphs summarize the mean ± SEM of the percentage of control for each cell type of 4-8 independent experiments, run in duplicates. Statistical analysis: ** $p<0.01$, compared to HEK 293 EGFP-ataxin-3 Q28 treated with 100 μM 3-NP, two-way ANOVA followed by Bonferroni multiple comparison test; *t* $p<0.05$, compared to wild-type cerebellar granule cells treated with 30 μM 3-NP (Student's t-test).

4.4.5. Transient expression of expanded ataxin-3 promotes loss of membrane integrity

3-NP-induced cell death was also analysed by following LDH leakage in transfected HEK cells. Increasing 3-NP dosage induced higher levels of extracellular LDH. Statistically significant differences between these two transfected cell lines were observed for low 3-NP concentrations (Figure 4.6.A). At 100 μM 3-NP, the EGFP-ataxin-3 (Q84) line showed higher extracellular LDH levels than EGFP-ataxin-3 (Q28) expressing cells, supporting the lower cell viability at this concentration, as observed before. Interestingly, the EGFP-ataxin-3 (Q84) cell line exhibited a tendency towards a higher basal LDH release, which was statistically different from the EGFP-ataxin-3 (Q28) expressing cells (Figure 4.6.A), suggesting that expression of expanded ataxin-3 might decrease membrane integrity. Adenosine triphosphate (ATP) levels, adenosine diphosphate (ADP) levels and caspase-3-like activity were also measured in HEK cells expressing ataxin-3 under the same experimental conditions described above. Neither the incubation with 3-NP nor the expression of expanded ataxin-3 altered any of these parameters in these cells (data not shown). The increased loss of membrane integrity (LDH release) and the absence of activated caspase-3 in western blotting and fluorimetric assays suggested that EGFP-ataxin-3 cell lines were most certainly dying through necrosis or a caspase-3 independent pathway.

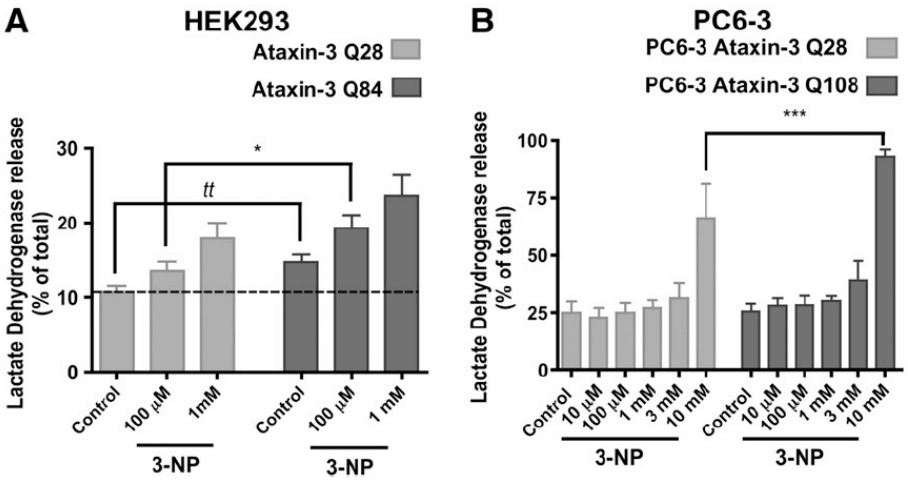

Figure 4.6. - Expanded ataxin-3 induces higher levels of cell death. HEK 293 cells expressing EGFP-ataxin-3 Q28 or Q84 (A) and PC6-3 cells expressing wild-type (Q28) or expanded (Q108) human ataxin-3 (B) were exposed to increasing concentrations of 3-NP (100 μM and 1 mM for HEK cells (A); 10 μM - 10 mM for PC6-3 cells (B)), for 24 hours. Total extracts and the extracellular media of every sample were collected and analysed for LDH activity to evaluate the degree of cell death. Graphs plot the mean ± SEM of the percentage of extracellular LDH activity of the total LDH activity, for each sample. 4-15 independent experiments were conducted. Statistical analysis: (A) *tt* $p<0.01$ compared to HEK 293 EGFP-ataxin-3 Q28 (Student's t-test); * $p<0.05$ compared to HEK 293 EGFP-ataxin-3 Q28 treated with 100 μM 3-NP, two-way ANOVA followed by Bonferroni multiple comparison test. (B) *** $p<0.001$ compared to PC6-3 Ataxin-3 Q28 treated with 10 mM 3-NP, two-way ANOVA followed by Bonferroni multiple comparison test.

We also examined the susceptibility to complex II inhibition in NGF-differentiated PC6-3 cells expressing wild-type (Q28) or expanded (Q108) ataxin-3. Figure 4.6.B shows that concentrations of 3-NP from 10 μM to 3 mM do not change significantly the release of LDH. However, there was a strong increase in the LDH release for both cell lines in the presence of 10 mM 3-NP (Figure 4.6.B). The expanded ataxin-3 PC6-3 cells displayed statistically significant

higher levels of extracellular LDH for this concentration, compared to wild-type ataxin-3 (Q28).

4.4.6. Expression of expanded ataxin-3 affects mitochondrial complex II activity

The increased susceptibility to 3-NP observed in different MJD cell models led us to hypothesise that expanded ataxin-3 overexpression could affect the mitochondria at the level of mitochondrial complex II. Therefore, we next determined the activities of all the mitochondrial respiratory complexes in several MJD models with the purpose of detecting any other effects expanded ataxin-3 might have on mitochondrial electron transport chain. To accomplish this, we collected mitochondrial crude samples from undifferentiated and NGF-differentiated PC6-3 cell lines expressing human ataxin-3, wild-type and MJD transgenic adult mouse brains, and three human lymphoblastic cell lines. Mitochondria from whole mouse brain were obtained from non-transgenic or homozygous transgenic mice at 4-5 months of age. At this age, homozygous MJD mice manifest clear symptoms of abnormal phenotype characteristic of MJD (Goti et al., 2004). Three human lymphoblast cell lines were established after immortalization of lymphoblasts collected from two MJD patients and one healthy individual (Paulson et al. 1997a), with the two MJD lymphoblastic cell lines containing 27/78 (JMJW) and 28/68 (JMMA) CAG repeat alleles.

Measurement of the activity of individual mitochondrial complexes revealed a common trend throughout the three MJD models tested (Figure 4.7.). In all models, no alterations were detected in the activities of complexes I, III and IV in the presence of expanded ataxin-3. Nevertheless, strong tendencies, and in some cases significant differences, were observed for the activity of mitochondrial complex II (Figure 4.7.). Statistically significant differences were observed in NGF-differentiated PC6-3 cell lines expressing expanded *versus* wild-type human ataxin-3 (Figure 4.7.A). PC6-3 ataxin-3 (Q108) cells exhibited an approximately 25% reduction in complex II activity, compared to PC6-3 ataxin-

3 (Q28). A decrease in complex II activity was also determined for the MJD human lymphoblastic cell lines, although statistically significance was not achieved. Accordingly, the protein levels of complex II subunits (ShdA and ShdB) were not altered in mitochondrial extracts of MJD lymphoblastic cell lines (Figure 4.8.).

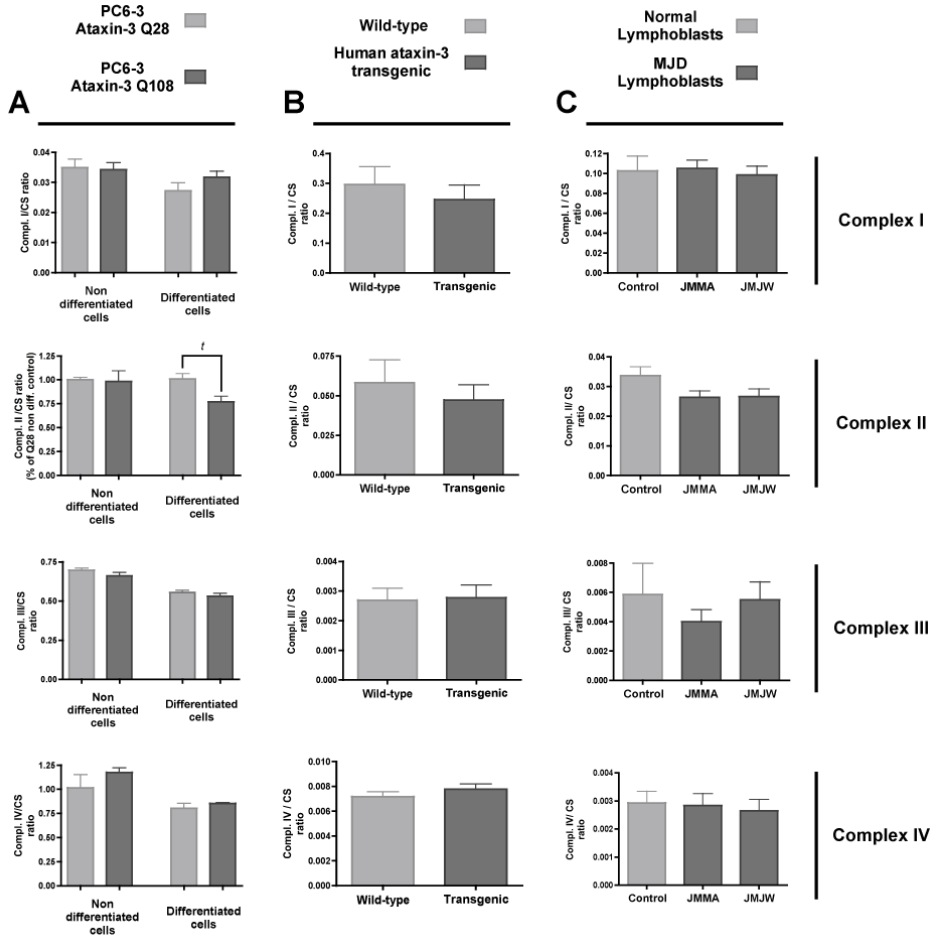

Figure 4.7. - Expanded ataxin-3 expression impairs mitochondrial complex II activity. The activities of complexes I, II, III and IV of the mitochondrial respiratory chain were determined

spectrophotometrically in (**A**) mitochondrial extracts from undifferentiated and NGF-differentiated PC6-3 ataxin-3 Q28 and Q108 cell lines, (**B**) isolated brain mitochondria of 4-5 months wild-type or MJD homozygous transgenic mice, and (**C**) human lymphoblastic cell lines derived from MJD patients (JMMA, JMJW) or control individuals. Graph shows the mean ± SEM of 4-9 independent measurements of the mitochondrial complexes activities. The activities of mitochondrial complexes were normalised for citrate synthase activity. Statistical analysis: *t* $p<0.05$, compared to NGF-differentiated PC6-3 Ataxin-3 Q28 (Student's *t*-test).

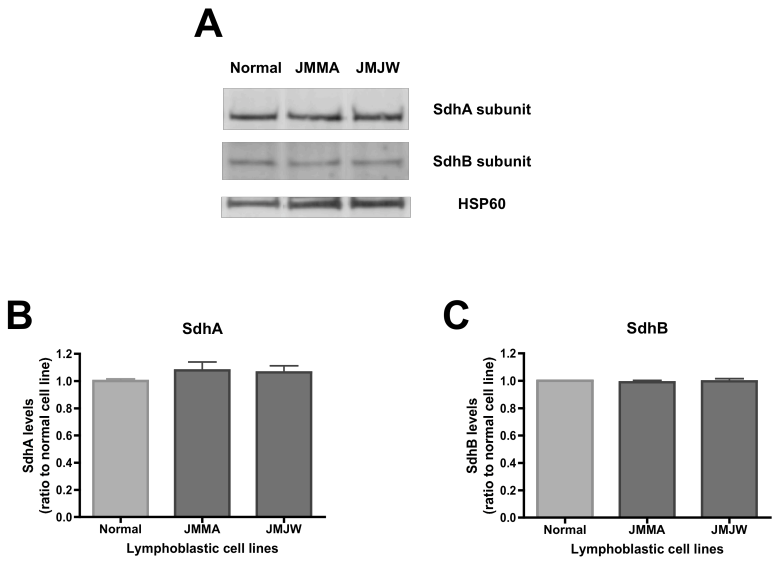

Figure 4.8. - Protein levels of mitochondrial complex II subunits are not changed in MJD lymphoblastic cell lines. (**A**) 40 μg of protein from mitochondrial extracts of normal and MJD (JMMA, JMJW) lymphoblastic cell lines were run in SDS-PAGE and mitochondrial complex II (succinate dehydrogenase) subunits (SdhA and SdhB) were detected through immunoblotting with anti-SdhA and anti-SdhB antibodies. Quantification of SdhA (**B**) and SdhB (**C**) protein levels in MJD lymphoblastic cell lines relatively to the control line in 3 independent experiments, run in triplicates.

4.5. Discussion

Human ataxin-3 has been shown to have an inherent capacity to self-aggregate, even the wild-type variant (Gales et al., 2005). The presence of a pathological polyQ tract in the ataxin-3, however, introduces an additional step in the aggregation process, resulting in the formation of highly stable and SDS-insoluble aggregates (Ellisdon et al., 2006). The presence of protein aggregates containing expanded ataxin-3 and other proteins in specific areas of the brain of MJD patients is a pathological hallmark of this neurological disease (Paulson et al., 1997b; Schmidt et al., 1998; Yamada et al., 2001). In agreement with this, ataxin-3 protein aggregation was observed in the cell and animal models used in this study and occurred selectively in the expanded ataxin-3-expressing models. Analysis of mitochondrial susceptibility in ataxin-3 expressing models revealed that the mitochondrial inhibitor producing the strongest response throughout the different models was 3-NP, an irreversible complex II inhibitor. Indeed, most of the MJD cell models showed a tendency towards increased susceptibility to 3-NP treatment and decreased activity of complex II.

Higher levels of protein and the expression of a more aggregation-proned isoform (*MJD1a*) of expanded ataxin-3 may account for the larger aggregates observed in HEK EGFP-ataxin-3 (Q84) cells. Although in some *in vitro* studies wild-type ataxin-3 has been shown to aggregate (Gales et al., 2005; Ellisdon et al., 2006), in cells we only observed aggregation of expanded ataxin-3.

Aggregation of expanded EGFP-ataxin-3 (Q84) in HEK 293 cell lines was associated with deleterious effects, increasing the susceptibility to mitochondrial complex II inhibitor (3-NP) treatment. Indeed, expression of expanded ataxin-3 alone was sufficient to increase cell death in this model. Aggregation of expanded ataxin-3 in PC6-3 ataxin-3 (Q108) cells decreased cell survival only in the presence of high 3-NP concentrations, compared to HEK

EGFP-ataxin-3 (Q84) cells or MJD cerebellar granule cells, which may account for a lower expression of the transgene in these cells. The aggregates in PC6-3 cells and transgenic cerebellar granule cells are discrete nuclear structures and smaller than the bulky clumps observed in HEK 293 cells. Steric interference caused by the larger aggregates in HEK 293 cells over intracellular movement of proteins and organelles, might contribute for the increased cytotoxicity in these cells. The nuclear localization of aggregates in PC6-3 ataxin-3 (Q108) cells was not random. They were intimately associated with PML bodies and closely juxtaposed to coiled or Cajal bodies. PML bodies have been described as sites of protein degradation in the nucleus, while Cajal bodies are part of a subnuclear organelle implicated in RNA splicing (Wojcik and DeMartino, 2003; Morris, 2008; St-Germain et al., 2008). The close location of expanded ataxin-3 aggregates to nuclear sites of protein degradation may represent a cellular effort to degrade the accumulated protein. Additionally, these specific nuclear sites may gather specific proteins or factors that trigger the seeding stages of expanded ataxin-3 deposition.

Although expanded ataxin-3 is expressed throughout the body, only neurons of some subcortical regions of the brain degenerate in MJD patients. Interestingly, the cells from these regions also represent some of the main sites of ataxin-3 aggregation (Schmidt et al., 1998). In accordance, the formation of aggregates selectively occurs in PC6-3 (Q108) cells committed to a neuronal phenotype (i.e., upon differentiation with NGF) and is associated with increased susceptibility to high concentrations of the mitochondrial complex II inhibitor, 3-NP.

Accumulation of human expanded ataxin-3 in discrete subnuclear sites was also observed in neuronal cultures derived from MJD transgenic mice. Even though the cerebellar granule cells were collected from 7 day-old mouse pups, nuclear foci of accumulated ataxin-3 were already detectable, suggesting that at least the subnuclear localization of expanded ataxin-3, may start early in development, well before the first signs of neuropathology. These early stages of

expanded ataxin-3 accumulation were accompanied by a mild mitochondrial susceptibility of cerebellar MJD neurons. Expanded ataxin-3 inclusions in this mouse model have only been reported in adulthood, starting at 2.5 months of age (Goti et al., 2004). Therefore, the expanded ataxin-3 nuclear foci detected in 7 day-old transgenic neurons may represent the initial stages of ataxin-3 accumulation not yet capable of exerting a full toxic effect. Although the discussion regarding the protective *versus* pathological role of polyQ aggregates is not fully resolved (Uchihara et al., 2002), in our experimental models, aggregates of expanded ataxin-3, which may be dimers, oligomers, or higher order aggregates, were associated with increased cell death.

Activation of mitochondrial apoptotic pathways and reduction in antioxidant enzymes activity followed by increased mitochondrial DNA damage have been reported for cellular models of MJD, establishing a mitochondrial role in MJD pathology (Wong et al., 2008; Yu et al., 2009). We have not observed apoptotic events or energy deficits upon expression of expanded ataxin-3 in HEK293 cells. However, expanded ataxin-3 may exert its pathological effects by interfering and disrupting additional biochemical pathways. Notably, mitochondrial complex II or succinate dehydrogenase is a biochemical converging point between the mitochondrial electron chain and the citric acid or Krebs cycle. Interestingly, we observed that complex II was the only mitochondrial complex to exhibit a consistent tendency towards decreased activity in the presence of expanded ataxin-3, particularly in differentiated PC6-3 cells expressing ataxin-3 (Q108) and in lymphoblastic cell lines derived from MJD patients. Complex II activity in brain mitochondria from MJD transgenic mice showed to be more resilient to human expanded ataxin-3 toxicity. The capacity to sustain a satisfactory complex II activity may be associated to an absence of major neurodegeneration, previously described in this MJD transgenic model (Goti et al., 2004). On the other hand, the mild decrease in complex II activity in dividing, peripheral cells such as MJD lymphoblastic cell lines is a rather interesting result. Indeed, more studies need to be carried out to

verify this direct relationship between expression of expanded ataxin-3 and the drop in complex II activity. Inhibition of complex II was previously linked to production of reactive oxygen species (ROS) (Rodríguez et al., 2010; Sandhir et al., 2010). Thus, increased oxidative stress in cells expressing expanded ataxin-3 would explain the increased susceptibility to ROS induced by the extra complex II inhibition provided by 3-NP treatment. Nevertheless, complex I and complex III inhibitions did not increase cell susceptibility of expanded ataxin-3 expressing cells, suggesting the possibility that oxidative stress should not be the only mechanism underlying ataxin-3 toxicity. Although complex II does not contribute to the mitochondrial proton gradient, disruption of normal mitochondrial calcium handling might be another mechanism involved in ataxin-3 pathology. It is worth noting that a significant decrease in complex II activity was observed in a cell model committed to a neuronal phenotype, the NGF-treated PC6-3 ataxin-3 (Q108) cells.

These cells show aggregates of expanded ataxin-3 occurring primarily in the nucleus, despite the low levels of expanded ataxin-3 expression. Although, complex II is the only mitochondrial complex of the respiratory chain that is exclusively nuclear-encoded and expanded ataxin-3 has been reported to interfere with gene expression in the nucleus (Evert et al., 2003), we have not found alterations in protein levels of complex II subunits in MJD lymphoblasts (Figure 4.8.). Nevertheless, the activity of complex II is not solely determined by changes in the expression of its subunits. Alterations in regulatory proteins involved in phosphorylation and acetylation of complex II (Rutter et al., 2010), mitochondrial import of subunits and/or the activity of chaperones responsible for complex II assembly could also interfere with its activity, without altering the protein levels. One or more of these phenomena may contribute to mitochondrial dysfunction in MJD.

Ataxin-3 is a deubiquitinating enzyme that has been implicated in the ubiquitin-proteasome pathway and in cellular protein quality control. Recent studies have described a crosstalk between the mitochondria and the proteasome

(Fukui and Moraes, 2007). Expression of expanded ataxin-3 may impair the ubiquitin-proteasome system or disrupt the crosstalk between the proteasome and mitochondria. Similarly to what was found upon expression of mutant huntingtin (Martinez-Vicente et al., 2010), macroautophagy malfunction may also occur in the context of expanded ataxin-3 expression due to a failure on the engulfment of cytosolic components in autophagosomes, precluding an adequate elimination of aggregated proteins and/or dysfunctional mitochondria. Indeed, impaired protein degradation pathways may delay protein turnover, promoting the accumulation of altered mitochondrial complexes with reduced activity. An impairment of mitochondrial complex II in MJD cell and animal models is particularly intriguing considering that selective vulnerability to complex II inhibitors and defects in complex II activity have been reported for other polyQ diseases, especially HD (Ryan et al., 2004; Benchoa et al., 2006). Mitochondrial complex II impairment might be central to some of the biochemical changes elicited by various polyQ expanded proteins, making this mitochondrial complex an important target in polyQ toxicity.

Chapter 5

Final conclusions

and future perspectives

5. Final conclusions and future perspectives

In this thesis, we investigated the influence of well-established ataxin-3 interactors on its deubiquitinating activity, the impact of catalytic activity of ataxin-3 over cellular turnover, protein-protein interactions and intracellular distribution of ataxin-3 and the pathological effect of expanded ataxin-3 expression on mitochondrial function.

The first part of this project was focused on *in vitro* studies of ataxin-3 interactions with other intracellular proteins and to which extent these protein-protein interactions modulate the ubiquitin protease activity of ataxin-3. DUBs are highly regulated proteins and their activity is regulated through several mechanisms including phosphorylation, ubiquitination, sumoylation and protein-protein interactions (Reyes-Turcu et al., 2009). In a growing number of recent reports ataxin-3 has been shown to be subjected to similar mechanisms of regulation (Haacke et al., 2007; Mueller et al., 2009; Todi et al., 2009; Todi et al., 2010). Ataxin-3 activity and its cellular distribution can be modulated through ubiquitination and phophorylation of certain residues. The results from this part of the work support the hypothesis that protein interactions represent another regulatory level of ataxin-3 deubiquitinating activity. Indeed, VCP/p97 was able to increase deubiquitination through a direct interaction with ataxin-3. The increase in ataxin-3 activity is a particular feature of VCP/p97 interaction, as other well-established interactors, such as hHR23A do not exert the same effect. Indeed, the selective activation of ataxin-3 by VCP/p97 and the lack of stimulation or even a competition effect by hHR23A might be essential for the unidirectionality of protein degradation pathways, where the ubiquitinated substrates would sequentially be handled by VCP/p97, ataxin-3, progressively delivered to hHR23A, and finally sent to degradation in the proteasomal complex. This VCP/p97-dependent and selective activation of wild-type ataxin-3 is a progress in our knowledge on the diversity of interactions and sequential steps occurring in protein degradation. More so because VCP/p97 and ataxin-3 have been previously shown to work together

in diverse and progressively growing number of cellular pathways, as in the retrotranslocation of misfolded proteins from the ER, cellular stress responses and longevity pathways in *Caenorhabditis elegans* (Zhong and Pittman, 2006; Kuhlbrodt et al., 2011). Interesting results will certainly emerge from future studies on the effect of other recently discovered interactions, namely parkin, which is also associated with the UPP, and the cellular role of ataxin-3 (Durcan et al., 2011; 2012).

On the contrary, VCP/p97 has no stimulating effect on the deubiquitinating activity of expanded ataxin-3, as the ability of expanded ataxin-3 to cleave ubiquitin chains is similar in the presence or absence of VCP/p97. This finding is in favor of a loss of function component for the pathophysiology of MJD. The proportional contribution of the gain of function conferred by the poly Q domain and the loss of function of the normal protein to the pathology of polyQ diseases is still not clear. MJD is no exception and recent reports have even suggested an unsuspected RNA toxicity component in this disorder (Li et al. 2008; Shieh and Bonini, 2011).

Aggregation of the expanded ataxin-3 protein can lead to a decrease in deubiquitinating activity through precipitation of expanded catalytically active enzyme out of solution. However, our data indicate that the expanded polyQ domain blocks the activation of expanded ataxin-3 by VCP/p97, without disrupting the interaction between these two proteins, which may occur before or in absence of any aggregation of expanded ataxin-3. Future studies on the structural alterations promoted by the polyQ domain in the ataxin-3 tridimensional shape will clarify the impact of these architectural modifications on protein-protein interactions and the molecular rearrangements required for the activation of catalysis. Further work on the normal function of ataxin-3 will increase our knowledge on the protein degradation pathways, ubiquitin proteasome pathway in particular, which seem to play a center role in the pathogenesis of MJD and polyQ diseases, in general.

The maintenance of a fully functional enzymatic activity is not only important to overcome the loss of function in the MJD context. The second part of this work demonstrates that the catalytic activity of ataxin-3 influences its protein levels, ubiquitination and protein turnover, its subcellular distribution and protein-protein interactions. Apart from being heavily ubiquitinated, inactive ataxin-3 exhibits a slower

degradation rate and accumulates in the cell. Moreover, the non-catalytic form is less present in the nucleus and has a diminished affinity for VCP/p97. In an unexpected feedback mechanism, active ataxin-3 is able to control its own protein levels, increasing its degradation at the proteasome through a pathway independent of ataxin-3 auto-deubiquitination.

Once more, we show that VCP/p97 interaction and functional ataxin-3 are intimately associated. Monomeric ataxin-3 is able to cleave long ubiquitin chains *in vitro* however, as more protein interactions are being discovered, the concept of ataxin-3 being part of a multimeric complex is increasingly gaining strength. Many of ataxin-3 characteristics in the cell will be dictated by these interactions, and currently, VCP/p97 is one of the most important known modulators of ataxin-3. A functional and active enzyme may be required for the correct assembly into these multimeric complexes, which consequently may determine its subcellular localization and the future cellular role of ataxin-3. On the other hand, non-functional ataxin-3, unable to perform catalysis and to establish normal interactions exhibits an altered intracellular localization and accumulates in the cell.

Surprisingly, the catalytic activity of ataxin-3 influences also the protein location in the cell. Besides allowing the establishment of appropriate interactions, a correct intracellular localization will be necessary to assure that ataxin-3 finds the adequate ubiquitinated substrates, allowing the enzyme to perform its proper function. In all the models used in this work, ataxin-3 is present throughout the cell but exhibits a preference for the nuclear compartment. Nuclear localization of ataxin-3 is probably critical for the proposed function in gene expression. Moreover, the nucleus is a major intracellular site of expanded ataxin-3 aggregation and nuclear expanded ataxin-3 is required for the manifestation of MJD symptoms. Therefore, understanding the correlation between ataxin-3 activity and its import to the nucleus will be valuable to pinpoint therapeutic targets for MJD.

As previously described, the deubiquitinating *in vitro* assays did not find any differences between wild-type and expanded ataxin-3 ability to cleave ubiquitin chains (e.g. Winborn et al., 2008). However, a correspondence can be made between the nonexistent deubiquitinating capacity in catalytically-inactive ataxin-3 and the absence

of VCP/p97-mediated activation of expanded ataxin-3. In the cell these two forms of ataxin-3 may not reach adequate levels of deubiquitinating activity to perform their normal cellular role. Indeed, both inactive and expanded ataxin-3 are harmful to cells and MJD animal models. As both forms of ataxin-3 are less degradable, toxicity might be based in the loss of function component and in the accumulation of intracellular protein levels of these toxic species. However, inactive ataxin-3 does not form aggregates, which may justify its reduced toxicity in comparison to expanded ataxin-3. Future projects on expanded ataxin-3 deubiquitinating activity, its putative loss of function, inability to form regular protein interactions and/or the establishment of new interactions will most certainly increase our knowledge on the toxicity of expanded ataxin-3.

Taking the results of the first and second parts of this work, an apparent and interesting correlation can be established between functional deubiquitinating activity, VCP/p97 interaction and normal cellular performance of ataxin-3 in the cell. All these variables may regulate the neurotoxicity of expanded ataxin-3 toxicity in MJD.

The pathogenic or harmless by-product nature of protein aggregation in polyQ disease is another debate still unsolved. In the third part of this work, expanded ataxin-3 aggregation was present in some models of MJD and it was always associated with a deleterious effect. The expression of the more aggregation-prone variant of expanded ataxin-3 alone was toxic in the MJD models analyzed. In MJD models revealing less extensive aggregation, expanded ataxin-3 exhibits a distinct pattern of nuclear accumulation in close association to subnuclear organelles, Cajal and PML bodies. Since the nucleus is a major intracellular localization of the normal protein, nuclear aggregation of expanded ataxin-3 may add dysfunctional deubiquitinating activity or even loss-of-function to the mechanisms of cytotoxicity through depletion of active enzyme into the aggregates. A decrease in ataxin-3 activity in the nucleus may promote alterations in gene expression, previously reported in MJD models. The main focus of this last part of the project was centered in the evaluation of mitochondrial dysfunction under the expression of expanded ataxin-3. Mitochondrial dysfunction has been observed in other polyQ diseases and its role on the neurodegeneration has been continuously highlighted in these disorders, most notably in HD (Grunewald and Beal,

1999; Panov et al., 2002; Browne, 2008). Alterations in mitochondrial function centered in a reduced activity or higher susceptibility to mitochondrial complex II inhibition are constant tendencies throughout the MJD cell and animal models investigated. No similar correlation is found for other mitochondrial complexes, indicating a directed effect of expanded ataxin-3 on complex II, instead of general deleterious effect over the mitochondrial respiratory chain. Interestingly, complex II is the only mitochondrial complex with all subunits being encoded by nuclear DNA. The alterations in gene expression promoted by expanded ataxin-3 may have a function in this selectivity towards mitochondrial complex II dysfunction, establishing a mitochondria-nuclear crosstalk. Studies on the expression of mitochondrial complex subunits in a MJD context would contribute to understand if complex II dysfunction is mediated through deregulation of gene expression or through a direct effect in the mitochondria. Expanded ataxin-3 has been found inside mitochondria, therefore a direct harmful action in the mitochondria is feasible (Pozzi et al., 2008). Moreover, data on the influence of ataxin-3 in the degradation of mitochondrial proteins is scarce. Finally, expanded ataxin-3 may disrupt regulatory pathways of complex II, influencing mitochondrial complex activity without a direct effect on the protein levels of complex II subunits.

The determination of mitochondrial complex II activity in peripheral blood cells from MJD patients would be of great significance to assess if a similar reduction in its function is observed in affected individuals. Furthermore, horizontal clinical studies involving MJD patients would clarify at what disease stage the reduction of complex II activity would be detectable and if it progresses with the aggravation of symptoms, which would be very useful as a biomarker of MJD progression.

As part of the polyQ disorders, MJD shares similar characteristics with these neurodegenerative diseases. All share the same pathological mutation, thus, some of the disease mechanisms discovered in MJD models may be extrapolated and occur in other polyQ diseases. Protein aggregation and dysfunction in protein degradation pathways are a common trend in all these neurodegenerative conditions. Mitochondrial dysfunction is gaining a major and central role as a common pathophysiologic mechanism of these diseases and, as other polyQ-shared features, its further study may

be of great value in an attempt to design a comprehensive therapeutics for all polyQ disorders. However, a common trinucleotide dynamic mutation does not account for the particularities in each polyQ disease, possessing different clinical symptoms, and distinct patterns of neurodegeneration. Indeed, a variety of phenotypes and manifestations are observed and described even for a unique nosological entity, as MJD. Therefore, one global pathological mechanism may not suffice at explaining all the questions regarding polyQ toxicity. Thus, more data have to be gathered about the particular aspects of each disease, the mechanisms behind each particular symptom, the normal function, interactions and regulation of each expanded protein. In the era of individually patient-designed medical practice, the study of particular aspects of each polyQ disease, and even each polyQ patient, might leads us to provision of a better healthcare. As our comprehension of ataxin-3' normal function and how it is affected by the polyQ stretch increases, the identification of promising therapeutic targets in pathways associated or involved in MJD pathology becomes more efficient. On the other hand, a more detailed and profound knowledge of deubiquitination, expanded ataxin-3 and protein degradation pathways may pave the way for a broader understanding of neurodegeneration as a whole. In the singular differences of each polyQ disease, one might find a common ground.

References

References

Abele M, Minnerop M, Urbach H, Specht K, Klockgether T. (2007) Sporadic adult onset ataxia of unknown aetiology: a clinical, electrophysiological and imaging study. *J Neurol* 254:1384–1389.

Adhikari A., Xu M., Chen Z.J. (2007) Ubiquitin-mediated activation of TAK1 and IKK. *Oncogene* 26:3214–3226.

Albrecht M., Golatta M., Wullner U., Lengauer T. (2004) Structural and functional analysis of ataxin-2 and ataxin-3. *Eur. J. Biochem.* 271:3155-3170.

Albrecht M., Hoffman D., Evert B.O., Scmitt I., Wullner U., Lengauer T. (2003) Structural modelling of ataxin-3 reveals distant homology to adaptins. *Proteins* 50:355-370.

Alves S., Nascimento-Ferreira I., Auregan G., Hassig R., Dufour N., Brouillet E., Pedroso de Lima M.C., Hantraye P., Pereira de Almeida L., Deglon N. (2008) Allele-specific RNA silencing of mutant ataxin-3 mediates neuroprotection in a rat model of Machado-Joseph disease. *PLoS One* 3:e3341.

Alves S., Regulier E., Nascimento-Ferreira I., Hassig R., Dufour N., Koeppen A., Carvalho A.L., Simões S., de Lima M.C., Brouillet E., Gould V.C., Deglon N., de Almeida L.P. (2008) Striatal and nigral pathology in a lentiviral rat model of Machado–Joseph disease. *Hum. Mol. Genet.* 17:2071–2083.

Alves S., Nascimento-Ferreira I., Dufour N., Hassig R., Auregan G., Nóbrega C., Brouillet E., Hantraye P., Pedroso de Lima M.C., Déglon N., de Almeida L.P. (2010) Silencing ataxin-3 mitigates degeneration in a rat model of Machado-Joseph disease: no roel for wild-type ataxin-3? *Hum. Mol. Genet.* 19:2380-2394.

Amerik A.Y., Hochstrasser M. (2004) Mechanism and function of deubiquitinating enzymes. *Biochim. Biophys. Acta.* 1695:189-207.

Antony, P.M., Mantele, S., Mollenkopf, P., Boy, J., Kehlenbach, R.H., Riess, O., Schmidt,T. (2009) Identification and functional dissection of localization signals within ataxin-3. *Neurobiol. Dis.* 36:280–292.

Arrasate M., Mitra S., Schweitzer E.S., Segal M.R., Finkbeiner S. (2004) Inclusion body formation reduces levels of mutant huntingtin and the risk of neuronal death. *Nature* 431:805-810.

Azulay J.P., Blin O., Mestre D., Sangla I., Serratrice G. (1994) Contrast sensitivity improvement with sulfamethoxazole and trimethoprim in a patient with Machado-Joseph disease without spasticity. *J. Neurol. Sci.* 123:95-99.

Baker R.T., Board P.G. (1987) The human ubiquitin gene family: structure of a gene and pseudogenes from the Ub B subfamily. *Nucleic Acids Res.* 15:443–463.

Bauer P.O., Nukina N. (2009) The pathogenic mechanisms of polyglutamine diseases and current therapeutic strategies. *J. Neurochem.* 110:1737-1765.

Beal M.F., Brouillet E., Jenkins B., Henshaw R., Rosen B., Hyman B.T. (1993) Age-dependent striatal excitotoxic lesions produced by the endogenous mitochondrial inhibitor malonate. *J. Neurochem.* 61:1147-1150.

Bence N.F., Sampat R.M., Kopito R.R. (2001) Impairment of the ubiquitin-proteasome system by protein aggregation. *Science* 292:1552-1555.

Benchoua A., Trioulier Y., Zala D., Gaillard M.C., Lefort N., Dufour N., Saudou F., Elalouf J.M., Hirsch E., Hantraye P., Déglon N., Brouillet E. (2006) Involvement of mitochondrial complex II defects in neuronal death produced by N-terminus fragment of mutated huntingtin. *Mol. Biol. Ce*ll 17:1652-1663.

Bennett E.J., Shaler T.A., Woodman B., Ryu K.Y. Zaitseva T.S., Becker C.H., Bates G.P., Schulman H., Koito R.R. (2007) Global changes to the ubiquitin system in Huntington's dsease. *Nature* 448:704-708.

Berke S.J., Chai Y., Marrs G.L., Wen H., Paulson H.L. (2005) Defining the role of ubiquitin-interacting motifs in the polyglutamine disease protein, ataxin-3. *J. Biol. Chem.* 280:32026–32034.

Berke S.J., Paulson H.L. (2003) Protein aggregation and the ubiquitin protesome pathway: gaining the UPPer hand on neurodegeneration. *Curr. Opin. Genet.* Dev. 13:253-261.

Berke, S.J., Schmied, F.A., Brunt, E.R., Ellerby, L.M., Paulson, H.L. (2004) Caspase-mediated proteolysis of the polyglutamine disease protein ataxin-3. *J. Neurochem.* 89:908–918.

Bettencourt C., Lima M. (2011) Machado-Joseph Disease: from first descriptions to new perspectives.*Orphanet J. Rare Dis.* 6: 35.

Bettencourt C., Santos C., Kay T., Vasconcelos J., Lima M. (2008) Analysis of segregation patterns in Machado-Joseph disease pedigrees. *J. Hum. Genet.* 53:920-923.

Bettencourt C., Santos C., Montiel R., Costa M.C., Cruz-Morales P., Santos L.R., Simões N., Kay T., Vasconcelos J., Maciel P., Lima M. (2010) Increased transcript diversity: novel splicing variants of Machado-Joseph Disease gene (ATXN3). *Neurogenetics* 11:193-202.

Bettencourt C., Santos C., Montiel R., Kay T., Vasconcelos J., Maciel P., Lima M. (2010) The (CAG)(n) tract of Machado-Joseph Disease gene (ATXN3): a comparison between DNA and mRNA in patients and controls. *Eur. J. Hum. Genet.* 11:193-202.

Beuron F., Dreveny I., Yuan X., Pye V.E., McKeown C., Briggs L.C., Cliff M.J., Kaneko Y., Wallis R., Isaacson R.L., Ladbury J.E., Matthews S.J., Kondo H., Zhang X., Freemont P.S. (2006) Conformational changes in the AAA ATPase p97-p47 adaptor complex. *EMBO J.* 25:1967-1976.

Bevivino A.E., Loll P.J. (2001) An expanded glutamine repeat destabilizes native ataxin-3 structure and mediates formation of parallel beta-fibrils. *Proc. Natl. Acad. Sci. U.S.A.*

98:11955–11960.

Bezprozvanny I., Hayden M. R. (2004) Deranged neuronal calcium signaling and Huntington disease. *Biochem. Biophys. Res. Commun.* 322:1310-1317.

Bichelmeier U., Schmidt T., Hubener J., Boy J., Ruttiger L., Habig K., Poths S., Bonin M., Knipper M., Schmidt W.J., Wilbertz J., Wolburg H., Laccone F., Riess O. (2007) Nuclear localization of ataxin-3 is required for the manifestation of symptoms in SCA3: in vivo evidence. *J. Neurosci.* 27:7418–7428.

Bilen J., Bonini N.M. (2007) Genome-wide screen for modifiers of ataxin-3 neurodegeneration in *Drosophila*.*PLoS Genet.* 3:1950:1964.

Bilen J., Liu N., Brunett B.G., Pittman R.N., Bonini N.M. (2006) MicroRNA pathways modulate polyglutamine-induced neurodegeneration. *Mol. Cell* 24:157-163.

Boeddrich A., Gaumer S., Haacke A., Tzvetkov N., Albrecht M., Evert B.O., Muller E.C., Lurz R., Breuer P., Schugardt N., Plassmann S., Xu K., Warrick J.M., Suopanki J., Wullner U., Frank R., Hartl U.F., Bonini N.M., Wanker E.E. (2006) An arginine/lysine-rich motif is crucial for VCP/p97-mediated modulation of ataxin-3 fibrillogenesis. *EMBO J.* 25:1547–1558.

Boland B., Kumar A., Lee S., Platt F.M., Wegiel J., Yu W.H., Nixon R.A. (2008) Autophagy induction and autophagosome clearance in neurons: relationship to autophagic pathology in Alzheimer's disease. *J. Neurosci.* 28:6926-6937.

Boy J., Schmidt T., Schumann U., Grasshoff U., Unser S., Holzmann C., Schmitt I., Karl T., Laccone F., Wolburg H., Ibrahim S., Riess O. (2010) A transgenic mouse model of spinocerebellar ataxia type 3 resembling late disease onset and gender-specific instability of CAG repeats. *Neurobiol. Dis.* 37:284–293.

Boy J., Schmidt T., Wolburg H., Mack A., Nuber S., Bottcher M., Schmitt I., Holzmann C., Zimmermann F., Servadio A., Riess O. (2009) Reversibility of symptoms in a conditional mouse model of spinocerebellar ataxia type 3. *Hum. Mol. Genet.* 18:4282–4295.

Breuer P., Haacke A., Evert B.O., Wullner U. (2010) Nuclear aggregation of polyglutamine-expanded ataxin-3: fragments escape the cytoplasmic quality control. *J. Biol. Chem.* 285:6532–6537.

Brooks B.P., Fischbeck K.H. (1995) Spinal and bulbar muscular atrophy: a trinucleotide-repeat expansion neurodegenerative disease. *Trends Neurosci.* 18:459-461.

Brouillet E., Hantraye P., Ferrante R.J., Dolan R., Leroy-Willig A., Kowall N.W., Beal M.F. (1995) Chronic mitochondrial energy impairment produces selective striatal degeneration and abnormal choreiform movements in primates. *Proc. Natl. Acad. Sci. USA* 92:7105-7109.

Browne S.E. (2008) Mitochondria and Huntington's disease pathogenesis. Insight from Genetic and Chemical Models. *Ann. N.Y. Acad. Sci.* 1147:358-382.

Browne S.E., Beal M.F. (2004) The energetics of Huntington's disease. *Neurochem. Res.* 29:531-546.

Browne S.E., Beal M.F. (2006) Oxidative damage in Huntington's disease pathogenesis. *Antioxid. Redox Signal.* 8:2061-2073.

Buhmann C., Bussopulos A., Oechsner M. (2003) Dopaminergic response in Parkinsonian phenotype of Machado-Joseph disease. *Mov. Disord.* 18:219–21.

Burnett B., Li F., Pittman R.N. (2003) The polyglutamine neurodegenerative protein ataxin-3 binds polyubiquitylated proteins and has ubiquitin protease activity. *Hum. Mol. Genet.* 12:3195–3205.

Burnett B.G., Pittman R.N. (2005) The polyglutamine neurodegenerative protein ataxin 3 regulates aggresome formation. *Proc. Natl. Acad. Sci. U.S.A.* 102:4330–4335.

Carvalho D.R., La Rocque-Ferreira A., Rizzo I.M., Imamura E.U., Speck-Martins C.E. (2008) Homozygosity enhances severity in spinocerebellar ataxia type 3. *Pediatr. Neurol.* 38:296–299.

Cemal C.K., Carroll C.J., Lawrence L., Lowrie M.B., Ruddle P., Al-Mahdawi S., King R.H., Pook M.A., Huxley C., Chamberlain S. (2002) YAC transgenic mice carrying pathological alleles of the MJD1 locus exhibit a mild and slowly progressive cerebellar deficit. *Hum. Mol. Genet.* 11:1075–1094.

Cecchin C.R., Pires A.P., Rieder C.R., Monte T.L., Silveira I., Carvalho T., Saraiva-Pereira M.L., Sequeiros J., Jardim L.B. (2007) Depressive symptoms in Machado-Joseph disease (SCA3) patients and their relatives. *Community Genet.* 10:19–26.

Chai Y., Berke S. S., Cohen R. E., Paulson H. L. (2004) Poly-ubiquitin binding by the polyglutamine disease protein ataxin-3 links its normal function to protein surveillance pathways. *J. Biol. Chem.* 279: 3605-3611.

Chai Y., Koppenhafer S.L., Shoesmith S.J., Perez M.K., Paulson H.L. (1999) Evidence for proteasome involvement in polyglutamine disease: localizations to nuclear inclusions in SCA3/MJD and suppression of polyglutamine aggregation *in vitro*. *Hum. Mol. Genet.* 8:673-682.

Chai Y., Shao J., Miller V.M., Williams A., Paulson H.L. (2002) Live-cell imaging reveals divergent intracellular dynamics of polyglutamine disease proteins and supports a sequestration model of pathogenesis. *Proc. Natl. Acad. Sci. U.S.A.* 99:9310–9315.

Chan E.Y., Luthi-Carter R., Strand A., Solano S.M., Hanson S.A., DeJohn M.M., Kooperberg C., Chase K.O., DiFiglia M., Young A.B., Leavitt B.R., Cha J.H., Aronin N., Hayden M.R., Olson J.M. (2002) Increased huntingtin protein length reduces the number of polyglutamine-induced gene expression changes in mouse models of Huntington's disease. *Hum. Mol. Genet.* 11:1939-1951.

Chang W.H., Tien C.L., Chen T.J., Nukina N., Hsieh M. (2009) Decreased protein synthesis of Hsp27 associated with cellular toxicity in a cell model of Machado-Joseph disease. *Neurosci. Lett.* 454:152-156.

Chen L., Madura K. (2006) Evidence for distinct functions for human DNA repair factors hHR23A and hHR23B. *FEBS Lett.* 580:3401-3408.

Chen, S., Berthelier, V., Hamilton, J.B., O'Nuallain, B., Wetzel, R. (2002) Amyloid-like features of polyglutamine aggregates and their assembly kinetics. *Biochemistry* 41:7391–7399.

Chen X., Tang T. S., Tu H., Nelson O., Pook M., Hammer R., Nukina N., Bezprozvanny I. (2008) Deranged calcium signaling and neurodegeneration in spinocerebellar ataxia type 3. *J. Neurosc.* 28:12713-12724.

Chen Z.J., Sun L.J. (2009) Nonproteolytic functions of ubiquitin in cell signaling. *Mol. Cell* 33:275-286.

Choo Y.S., Johnson G.V., MacDonald M., Detloff P.J., Lesort M. (2004) Mutant huntingtin directly increases susceptibility of mitochondria to the calcium-induced permeability transition and cytochrome c release. *Hum. Mol. Genet.* 13:1407-1420.

Chou A.H., Chen S.Y., Yeh T.H., Weng Y.H., Wang H.L. (2011) HDAC inhibitor sodium butyrate reverses transcriptional downregulation and ameliorates ataxic symptoms in a transgenic mouse model of SCA3. *Neurobiol. Dis.* 41:481–488.

Chou A.H., Yeh T. H., Kuo Y. L., Kao Y. C., Jou M. J. Hsu C. Y., Tsai S. R., Kakizuka A., Wang H. L. (2006) Polyglutamine-expanded ataxin-3 activates mitochondrial apoptotic pathway by upregulating BAx and downregulating Bcl-xL. *Neurobiol. Dis.* 21:333-345.

Chou A.H., Yeh T.H., Ouyang P., Chen Y.L., Chen S.Y., Wang H.L. (2008) Polyglutamine-expanded ataxin-3 causes cerebellar dysfunction of SCA3 transgenic mice by inducing transcriptional dysregulation. *Neurobiol. Dis.* 31:89–101.

Chow M.K., Ellisdon A.M., Cabrita L.D., Bottomley S.P. (2004a) Polyglutamine expansion in ataxin-3 does not affect protein stability: implications for misfolding and disease. *J. Biol. Chem.* 279:47643–47651.

Chow M.K., Mackay J.P., Whisstock J.C., Scanlon M.J., Bottomley S.P. (2004b) Structural and functional analysis of the Josephin domain of the polyglutamine protein ataxin-3. *Biochem. Biophys. Res. Commun.* 322:387–394.

Chow M.K., Paulson H.L., Bottomley S.P. (2004c) Destabilization of a non-pathological variant of ataxin-3 results in fibrillogenesis via a partially folded intermediate: a model for misfolding in polyglutamine disease. *J. Mol. Biol.* 335:333–341.

Ciechanover A. (2003) The ubiquitin proteolytic system and pathogenesis of human diseases: a novel platform for mechanism-based drug targeting. *Biochem. Soc. Trans.* 31:474-481.

Coffee B., Zhang F., Warren S.T., Reines D. (1999) Acetylated histones are associated with FMR1 in normal but not fragile X-syndrome cells. *Nat. Genet.* 22:98-101.

Cohn M.A., Kowal P., Yang K.,Haas W., Huang T.T., Gygi S.P., D'Andrea A.D. (2007) A UAF1-containing multisubunit complex regulates the Faconi anemia pathway. *Mol. Cell* 28:786-797.

Colomer Gould, V.F., Goti, D., Pearce, D., Gonzalez, G.A., Gao, H., Bermudez de Leon, M., Jenkins, N.A., Copeland, N.G., Ross, C.A., Brown, D.R. (2007) A mutant ataxin-3 fragment

results from processing at a site N-terminal to amino acid 190 in brain of Machado–Joseph disease-like transgenic mice. *Neurobiol. Dis.* 27:362–369.

Coo Y.S., Johnson G.V., MacDonald M., Detloff P.J., Lesort M. (2004) Mutant huntingtin directly increases susceptibility of mitochondria to the calcium-induced permeability transition and cytochormoe c release. *Hum. Mol. Genet.* 13:1407-1420.

Cooper J.K., Schilling G., Peters M.F., Herring W.J., Sharp A.H., Kaminsky Z., Masone J., Khan F.A., Delanoy M., Borchelt D.R., Dawson V.L., Dawson T.M., Ross C.A. (1998) Truncated N-terminal fragments of huntingtin with expanded glutamine repeats form nuclear and cytoplasmic aggregates in cell culture. *Hum. Mol. Genet.* 7:783-790.

Coore H.G., Denton R.M., Martin B.R., Randle P.J. (1971) Regulation of adipose tissue pyruvate dehydrogenase by insulin and others hormones. *Biochem. J.* 125:115–127.

Correia M., Coutinho P., Silva M.C., Guimarães J., Amado J., Matos E. (1995) Evaluation of the effect of sulphametoxazole and trimethoprim in patients with Machado-Joseph disease. *Rev. Neurol.* 23:632-634.

Courtney M.J., Lambert J.J., Nicholls D.G. (1990) The interactions between plasma membrane depolarization and glutamate receptor activation in the regulation of cytoplasmic free calcium in cultured cerebellar granule cells. *J Neurosci* 10:3873-3879.

Coutinho P. (1994) Doença de Machado-Joseph: Estudo Clínico, Patológico e Epidemiologico de uma
Doença Neurológica de Origem Portuguesa. Porto, Portugal: Tipografia Nunes Ltda.

Coutinho P., Andrade C. (1978) Autosomal dominant system degeneration in Portuguese families of the Azores Islands. A new genetic disorder involving cerebellar, pyramidal, extrapyramidal and spinal cord motor functions. *Neurology* 28:703-709.

Cuervo A.M. (2004) Autophagy: in sickness and in health. *Trends Cell Biol.* 14:70-77.

Cui L., Jeong H., Borovecki F., Parkhurst C.N., Tanese N., Krainc D. (2006) Transcriptional repression of PGC-1alpha by muntant huntingtin leads to mitochondrial dysfunction and neurodegeneration. *Cell* 127:59-69.

Cummings C.J., Mancini M.A., Antalffy B., DeFranco D.B., Orr H.T., Zoghbi H.Y. (1998) Chaperon supression of aggregation and altered subcellular proteasome localization imply protein misfolding in SCA1. *Nat. Genet.* 19:148-154.

Cummings C.J., Zoghbi H.Y. (2000) Trinucleotide repeats: mechanisms and pathophysiology. *Ann. Rev. Genomics Hum. Genet.* 8:1185-1193.

de Chiara C., Menon R.P., Dal Piaz F., Calder L., Pastore A. (2005) Polyglutamine is not all: the functional role of the AXH domain in the ataxin-1 protein. *J. Mol. Biol.* 354:883-893.

D'Abreu A., Franca M.C., Paulson H.L., Lopes-Cendes I. (2010) Caring for Machado-Joseph disease: current understanding and how to help patients. *Parkinsonism Relat. Disord.* 16:2-7.

D'Abreu A., Franca M.C. Jr, Conz L., Friedman J.H., Nucci A., Lopes-Cendes I. (2009) Sleep

symptoms and their clinical correlates in Machado-Joseph Disease. *Acta Neurol. Scand.* 119:277–280.

D'Abreu A., França M. Jr. , Appenzeller S., Lopes-Cendes I., Cendes F. (2009) Axonal dysfunction in the deep white matter in Machado-Joseph disease. *J. Neuroimaging* 19:9-12.

Dai R.M., Chen E., Longo D.L., Gorbea C.M., Li C.C. (1998) Involvement of valosin-containing protein, an ATPase Co-purified with IkappaBalpha and 26 S proteasome, in ubiquitin-proteasome-mediated degradation of IkappaBalpha. *J. Biol. Chem.* 273:3562-3573.

Dai R.M., Li C.C. (2001) Valosin-containing protein is a multi-ubiquitin chain-targeting factor required in ubiquitin-proteasome degradation. *Nat. Cell Biol.* 3:740-744.

Dalal S., Hanson P.I. (2001) Membrane traffic: what drives the AAA motor? *Cell* 104:5-8.

Dantuma NP, Heinen C, Hoogstraten D (2009) The ubiquitin receptor Rad23: at the crossroads of nucleotide excision repair and proteasomal degradation. *DNA repair (Amst)* 8:449-460.

Davies J.E., Sarkar S., Rubinsztein D.C. (2007) The ubiquitin proteasome system in Huntington's disease and the spinocerebellar ataxias. *BMC Biochem.* 8(Suppl.1), S2.

Dawson T.M., Dawson V.L. (2003) Molecular pathways of neurodegeneration in Parkinson's disease. *Science* 302:819-822.

DeStefano A.L., Cupples L.A., Maciel P., Gaspar C., Radvany J., Dawson D.M., Sudarsky L., Corwin L., Coutinho P., MacLeod P., *et al.* (1996) A familial factor independent of CAG repeat length influences age at onset of Machado-Joseph disease. *Am. J. Hum. Genet.* 59:119-127.

Díaz-Hernández M., Valera A.G., Morán M.A., Gómez-Ramos P., Alvarez-Castelao B., Castaño J.G., Hernández F., Lucas J.J. (2006) Inhibition of 26S proteasome activity by huntingtin filaments but not inclusion bodies isolated from mouse and human brain. *J. Neurochem.* 9:1585-1596.

DiFiglia M., Sapp E., Chase K., Schwarz C., Meloni A., Young C., Martin E., Vonsattel J.P., Carraway R., Reeves S.A. *et al.* (1995) Huntingtin is a cytoplasmic protein associated with vesicles in human and rat brain neurons. *Neuron* 14:1075-1081.

DiFiglia M., Sapp E., Chase K.O., Davies S.W., Bates G.P., Vonsattel J.P., Aronin N. (1997) Aggregation of huntingtin in neuronal intranuclear inclusions and dystrophic neurites in brain. *Science* 277:1990-1993.

do Carmo Costa M., Bajanca F., Rodrigues A.J., Tome R.J., Corthals G., Macedo-Ribeiro S., Paulson H.L., Logarinho E., Maciel P. (2010) Ataxin-3 plays a role in mouse myogenic differentiation through regulation of integrin subunit levels. *PLoS One* 5:e11728.

Doi H., Mitsui K., Kurosawa M., Machida Y., Kuroiwa Y., Nukina N. (2004) Identification of ubiquitin-interacting proteins in purifed polyglutamine aggregates. *FEBS Lett.* 571:171-176.

Donaldson K.M., Li W., Ching K.A., Batalov S., Tsai C.C., Joazeiro C.A. (2003)

Ubiquitin-mediated sequestration of normal cellular proteins into polyglutamine aggregates. *Proc. Natl. Acad. Sci. U.S.A.* 100:8892–8897.

Doss-Pepe E.W., Stenroos E.S., Johnson W.G., Madura K. (2003) Ataxin-3 interactions with rad23 and valosin-containing protein and its associations with ubiquitin chains and the proteasome are consistent with a role in ubiquitinmediated proteolysis. *Mol. Cell. Biol.* 23:6469–6483.

Dunah A.W., Jeong H., Griffin A., Kim Y.M., Standaert D.G., Hersh S.M.,Mouradian M.M., Young A.B., Tanese N., Krainc D. (2002) Sp1 and TAFII130 transcriptional activity disrupted in early Huntington's disease. *Science* 296:2238-2243.

Durcan T.M., Fon E.A. (2011) Mutant ataxin-3 promotes the autophagic degradation of parkin. *Autophagy* 7:233-234.

Durcan T.M., Kontogiannea M., Bedard N., Wing S.S., Fon E.A. (2012) Ataxin-3 deubiquitination is coupled to Parkin ubiquitination via E2 ubiquitin-conjugating enzyme. *J. Biol. Chem.* 287:531-541.

Durcan T.M., Kontogiannea M., Thorarinsdottir T., Fallon L., Williams A.J., Djarmati A., Fantaneanu T., Paulson H.L., Fon E.A. (2011) The Machado–Joseph disease-associated mutant form of ataxin-3 regulates parkin ubiquitination and stability. *Hum. Mol. Genet.* 20:141–154.

Dürr A. (2010) Autosomal dominant cerebellar ataxias: polyglutamine expansions and beyond. *Lancet Neurol.* 9:885-894.

Dürr A., Stevanin G., Cancel G., Abbas N., Chneiweiss H., Agid Y., Feingold J., Brice A. (1995) Gender equality in Machado-Joseph disease. *Nat. Genet.* 11:118–9.

Dürr A., Stevanin G., Cancel G., Duyckaerts C., Abbas N., Didierjean O., Chneiweiss H., Benomar A., Lyon-Caen O., Julien J., Serdaru M., Penet C., Agid Y., Brice A. (1996) Spinocerebellar ataxia 3 and Machado-Joseph disease: clinical, molecular and neuroathological features. *Ann. Neurol.* 39:490-499.

Ellerby L. M., Andrusiak R.L., Wellington C.L., Hackam A.S., Propp S.S., Wood J.D., Sharp A.H., Margolis R.L., Ross C.A., Salvesen G.S., Hayden M.R., Bredesen D.E. (1999) Cleavage of atrophin-1 at caspase site aspartic acid 109 modulates cytotoxicity. *J. Biol. Chem.* 274:8730-8736.

Ellisdon A.M., Pearce M.C., Bottomley S.P. (2007) Mechanisms of ataxin-3 misfolding and fibril formation: kinetic analysis of a disease-associated polyglutamine protein. *J. Mol. Biol.* 368:595–605.

Ellisdon A.M., Thomas B., Bottomley S.P. (2006) The two-stage pathway of ataxin-3 fibrillogenesis involves a polyglutamine-independent step. *J. Biol. Chem.* 281:16888-16896.

Etchebehere E.C., Cendes F., Lopes-Cendes I., Pereira J.A., Lima M.C., Sansana C.R., Silva C.A., Camargo M.F., Santos A.O., Ramos C.D., Camargo E.E. (2001) Brain single photon emission computed tomography and magnetic resonance imaging in Machado-Joseph disease. *Arch. Neurol.* 58:1257–1263.

Evert B.O., Araujo J., Vieira-Saecker A.M., de Vos R.A., Harendza S., Klockgether T., Wullner U. (2006a) Ataxin-3 represses transcription via chromatin binding, interaction with histone deacetylase 3, and histone deacetylation. *J. Neurosci.* 26:11474–11486.

Evert B.O., Schelhaas J., Fleischer H., de Vos R.A., Brunt E.R., Stenzel W., Klockgether T., Wullner U. (2006b) Neuronal intranuclear inclusions, dysregulation of cytokine expression and cell death in spinocerebellar ataxia type 3. *Clin. Neuropathol.* 25:272–281.

Evert B.O., Vogt I.R., Kindermann C., Ozimek L., de Vos R.A., Brunt E.R., Schmitt I., Klockgether T., Wullner U. (2001) Inflammatory genes are upregulated in expanded ataxin-3-expressing cell lines and spinocerebellar ataxia type 3 brains. *J. Neurosci.* 21:5389–5396.

Evert B.O., Vogt I.R., Vieira-Saecker A.M., Ozimek L., de Vos R.A., Brunt E.R., Klockgether T., Wullner U. (2003) Gene expression profiling in ataxin-3 expressing cell lines reveals distinct effects of normal and mutant ataxin-3. *J. Neuropathol. Exp. Neurol.* 62:1006–1018.

Evert B., Wüllner U., Schulz J.B., Weller M., Groscurth P., Trottier Y., Brice A., Klockgether T. (1999) High level expression of expanded full-length ataxin-3 *in vitro* causes cell death and formation of intracellular inclusions in neuronal cells. *Hum. Mol. Genet.* 8:1169-1176.

Everett C.M., Wood N.W. (2004) Trinucleotide repeats and neurodegenerative disease. *Brain* 127:2385-2405.

Fang S., Weissman A.M. (2004) A field guide to ubiquitylation. *Cell Mol. Life Sci.* 61:1546–61.

Fei E, Jia N, Zhang T, Ma X, Wang H, Liu C., Zhang W., Ding L., Nukina N., Wang G. (2007) Phosphorylation of ataxin-3 by glycogen synthase kinase 3beta at serine 256 regulates the aggregation of ataxin-3. Biochem. Biophys. Res. Commun. 357:487-492

Ferro A., Carvalho A.L., Teixeira-Castro A., Almeida C., Tome R.J., Cortes L., Rodrigues A.J., Logarinho E., Sequeiros J., Macedo-Ribeiro S., Maciel P. (2007) NEDD8: a new ataxin-3 interactor. *Biochim. Biophys. Acta* 1773:1619–1627.

Fischer J.A. (2003) Deubiquitinating enzymes: their roles in development, differentiation, and disease. *Int. Rev. Cytol.* 229:43–72.

Franca M.C. Jr, D'Abreu A., Friedman J.H., Nucci A., Lopes-Cendes I. (2007) Chronic pain in Machado-Joseph disease: a frequent and disabling symptom. *Arch. Neurol.* 64:1767–1770.

Friedman J.H. , Fernandez H.H., Sudarsky L.R. (2003) REM behavior disorder and excessive daytime somnolence in Machado-Joseph disease (SCA-3). *Mov. Disord.*18:1520–1522.

Fowler H.L. (1984) Machado-Joseph-Azorean disease. A ten-year study. *Arch. Neurol.* 41:921–925.

Fujigasaki H., Uchihara T., Koyano S., Iwabuchi K., Yagishita S., Makifuchi T., Nakamura A., Ishida K., Toru S., Hirai S., Ishikawa K., Tanabe T., Mizusawa H. (2000) Ataxin-3 is translocated into the nucleus for the formation of intranuclear inclusions in normal and Machado-Joseph disease brains. *Exp. Neurol.* 165:248-256.

Fukui H., Moraes C.T. (2007) Extended polyglutamine repeats trigger a feedback loop involving the mitochondrial complex III, the proteasome and huntingtin aggregates. *Hum. Mol. Genet.* 16:783-797.

Gafni J., Hermel E., Young J. E., Wellington C. L., Hayden M. R., Ellerby L. M. (2004) Inhibition of calpain cleavage of huntingtin reduces toxicity: accumulation of calpain/caspase fragments in the nucleus. *J. Biol. Chem.* 279:20211-20220.

Gales L., Cortes L., Almeida C., Melo C.V., Costa M.C., Maciel P., Clarke D.T., Damas A.M., Macedo-Ribeiro S. (2005) Towards a structural understanding of the fibrillization pathway in Machado–Joseph's disease: trapping early oligomers of non-expanded ataxin-3. *J. Mol. Biol.* 353:642–654.

Gaspar C., Lopes-Cendes I., Hayes S., Goto J., Arvidsson K., Dias A., Silveira I., Maciel P., Coutinho P., Lima M., Zhou Y.X., Soong B.W., Watanabe M., Giunti P., Stevanin G., Riess O., Sasaki H., Hsieh M., Nicholson G.A., Brunt E., Higgins J.J., Lauritzen M., Tranebjaerg L., Volpini V., Wood N., Ranum L., Tsuji S., Brice A., Sequeiros J., Rouleau G.A. (2001) Ancestral origins of the Machado-Joseph disease mutation: a worldwide haplotype study. *Am. J. Hum. Genet.* 68:523-528.

Gauthier L.R., Charrin B.C., Borrell-Pagès M., Dompierre J.P., Rangone H., Cordelières F.P., De Mey J., MacDonald M.E., Lessman V., Humbert S., Saudou F. (2004) Huntingtin controls neurotrophic support and survival of neurons by enhancing BDNF vesicular transport along microtubules. *Cell* 118:127-138.

Gellerich F.N., Gizatullina Z., Nguyen H.P., Trumbeckaite S., ielhaber S., Seppet E., Zierz S., Landwehrmeyer B., Riess O., von Hörsten S., Striggow F. (2008) Impaired regulation of brain mitohondria by extramitochondrial Ca^{2+} in transgenic Huntington disease rats. *J. Biol. Chem.* 283:30715-30724.

Ghislain M., Dohmen R.J., Levy F., Varshavsky A. (1996) Cdc48p interacts with Ufd3p, a WD repeat protein required for ubiquitin-mediated proteolysis in Saccharomyces cerevisiae. *EMBO J.* 15:4884-4899.

Gilman S., Low P.A., Quinn N., Albanese A., Ben Shlomo Y., Fowler C.J., Kaufmann H., Klogether T., Lang A., Lantos P., Litvan I., Mathias C., Oliver E., Robertson D., Schatz I., Wenning G. (1999) Consensus statement on the diagnosis of multiple system atrophy. *J Neurol Sci* 163:94–98.

Glickman M.H., Ciechanover A. (2002) The ubiquitin-proteasome proteolytic pathway: destruction for the sake of construction. *Physiol. Rev.* 82:373-202.

Globas C., du Montcel S.T., Baliko L., Boesch S., Depondt C., DiDonato S., Durr A., Filla A., Klogegether T., Mariotti C., Melegh B., Rakowicz M., Ribai P., Rola R., Schmitz-Hubsch T., Szymanski S., Timmann D., Van de Warrenburg B.P., Bauer P., Schols L. (2008) Early symptoms in spinocerebellar ataxia type 1, 2, 3, and 6. *Mov. Disord.* 23: 2232–2238.

Goldberg A.L. (2003) Protein degradation and protection against misfolded or damaged proteins. *Nature* 426:895-899.

Gordon C.R., Joffe V., Vainstein G., Gadoth N. (2003) Vestibulo-ocular arreflexia in families with spinocerebellar ataxia type 3 (Machado-Joseph disease). *J. Neurol. Neurosurg. Psychiatry* 74:1403–1406.

Goti D., Katzen S.M., Mez J., Kurtis N., Kiluk J., Ben-Haiem L., Jenkins N.A., Copeland N.G., Kakizuka A., Sharp A.H., Ross C.A., Mouton P.R., Colomer V. (2004) A mutant ataxin-3 putative-cleavage fragment in brains of Machado–Joseph disease patients and transgenic mice is cytotoxic above a critical concentration. *J. Neurosci.* 24:10266–10279.

Goto J., Watanabe M., Ichikawa Y., Yee S.B., Ihara N., Endo K., Igarashi S., Takiyama Y., Gaspar C., Maciel P, Tsuji S., Rouleau G.A., Kanazawa I. (1997) Machado-Joseph disease gene products carrying different carboxyl termini. *Neurosci. Res.* 28:373-377.

Graham R.K., Deng Y., Slow E.J., Haigh B., Bissada N., Lu G., Pearson J., Shehadeh J., Bertram L., Murphy Z., Warby S.C., Doty C.N., Roy S., Wellington C.L., Leavitt B.R., Raymond L.A., Nicholson D.W., Hayden M.R. (2006) Cleavage at the caspase-6 site is required for neuronal dysfunction and degeneration due to mutant huntingtin. *Cell* 125:1179-1191.

Green H. (1993) Human genetic diseases due to codon reiteration: relationship to an evolutionary mechanism. *Cell* 74:955-956.

Grunewald T., Beal M.F. (1999) Bioenergetics in Huntington's disease. *Ann. NY Acad. Sci.* 893:203-213.

Gu M., Gash M.T., Mann V.M., Javoy-Agid F., Cooper J.M., Schapira A.H. (1996) Mitochondrial defect in Huntington's disease caudate nucleus. *Ann. Neurol.* 39:385-389.

Guerrini L., Lolli F., Ginestroni A., Belli G., Della Nave R., Tessa C., Foresti S., Cosottini M., Piacentini S., Salvi F., Plasmati R., De Grandis D., Siciliano G., Filla A., Mascalchi M.(2004) Brainstem neurodegeneration correlates with clinical dysfunction in SCA1 but not in SCA2. A quantitative volumetric, diffusion and proton spectroscopy MR study. *Brain* 127: 1785–1795.

Gunawardena, S., Her, L.S., Brusch, R.G., Laymon, R.A., Niesman, I.R., Gordesky-Gold, B., Sintasath, L., Bonini, N.M., Goldstein, L.S. (2003) Disruption of axonal transport by loss of huntingtin or expression of pathogenic polyQ proteins in *Drosophila*. *Neuron* 40:25–40.

Guterman A., Glickman M.H. (2004) Deubiquitinating enzymes are IN/ (trinsic to proteasome function). Curr. Protein Pept. Sci 5:201–211.

Guzik B.W. and Goldstein L.S.B. (2004) Microtubule-dependent transport in neurons: steps towards an understanding of regulation, function and dysfunction. *Curr. Opin. Cell Biol.* 16:443-450.

Haacke A., Broadley S.A., Boteva R., Tzvetkov N., Hartl F.U., Breuer P. (2006) Proteolytic cleavage of polyglutamine-expanded ataxin-3 is critical for aggregation and sequestration of non-expanded ataxin-3. *Hum. Mol. Genet.* 15:555–568.

Haacke A., Hartl F.U., Breuer P. (2007) Calpain inhibition is sufficient to suppress aggregation of polyglutamine-expanded ataxin-3. *J. Biol. Chem.* 282:18851–18856.

Haberhausen G., Damian M.S., Leweke F., Muller U. (1995) Spinocerebellar ataxia, type 3 (SCA3) is genetically identical to Machado-Joseph disease (MJD). *J. Neurol. Sci.* 132:71-75.

Hackam A.S., Singaraja R., Zhang T., Gan L., Hayden M.R. (1999) *In vitro* evidence for both the nucleus and cytoplasm as subcellular sites of pathogenesis in Huntington's disease. *Hum. Mol. Genet.* 8:25-33.

Hackam A. S., Yassa A. S., Singaraja R., Metzler M., Gutkunst C.A., Gan L., Warby S., Wellington C.L., Vaillancourt J., Chen N., Gervais F.G., Raymond L., Nicholson D.W., Hayden M.R. (2000) Huntingtin interacting protein 1 induces apoptosis via a novel caspase-dependent death effector domain. *J. Biol. Chem.* 275:41299-41308.

Hafezparast M., Klocke R., Ruhrberg C., Marquardt A., Ahmad-Annuar A., Bowen S., Lalli G., Witherden A.S., Hummerich H., Nicholson S., Morgan P.J., Oozageer R., Priestley J.V., Averill S., King V.R., Ball S., Peters J., Toda T., Yamamoto A., Hiraoka Y., Augustin M., Korthaus D., Wattler S., Wabnitz P., Dickneite C., Lampel S., Boehme F., Peraus G., Popp A., Rudelis M., Schiegel J., Fuchs H., Hrabe de Angelis M., Schiavo G., Shima D.T., Russ A.P., Stumm G., Martin J.E., Fisher E.M. (2003) Mutations in dynein link motor neuron degeneration to defects in retrograde transport. *Science* 300:808-812.

Hands S., Sinadinos C., Wyttenbach A. (2008) Polyglutamine gene function and dysfunction in the ageing brain. *Biochim. Biophys. Acta* 1779:507-521.

Hands S.L., Wyttenbach A. (2010) Neurotoxic protein oligomerisation associated with polyglutamine diseases. *Acta. Neuropathol.* 120:419-437.

Harris G.M., Dodelzon K., Gong L., Gonzalez-Alegre P., Paulson H.L. (2010) Splice isoforms of the polyglutamine disease protein ataxin-3 exhibit similar enzymatic yet different aggregation properties. *PLoS One* 5, e13695.

Hay D.G., Sathasivam K., Tobaben S., Stahl B., Marber M., Mestril R., Mahal A., Smith D.L., Woodman B., Bates G.P. (2004) Progressive decrease in chaperone protein levels in a mouse model of Huntington's disease and induction of stress proteins as a therapeutic approach. *Hum. Mol. Genet.* 13:1389-1405.

Hashida H., Goto J., Kurisaki H., Mizusawa H., Kanazawa I. (1997) Brain regional differences in the expansion of a CAG repeat in the spinocerebellar ataxias: Dentatorubral-pallidoluysian atrophy, Machado-Joseph disease, and spinocerebellar ataxia type 1. *Ann. Neurol.* 41:505–511.

Hatakeyama S., Yada M., Matsumoto M., Ishida N., Nakayama K.I. (2001) U-box proteins as a new family of ubiquitin-protein ligases. *J. Biol. Chem.* 276:33111-33120.

Hatefi Y., Stiggall D.L. (1978) Preparation and properties of succinate: ubiquinone oxidoreductase (complex II). *Methods Enzymol.* 53:21–27.

Hedge A. N. (2010) The ubiquitin proteasome pathway and synaptic plasticity. *Learn. Mem.* 17:314-327.

Hershko A., Ciechanover A. (1998) The ubiquitin system. *Annu. Rev. Biochem.* 67:425–79.

Holmberg M., Duyckaerts C., Dürr A., Cancel G., Gourfinkel-An I., Damier P., Faucheux B., Trottier Y., Hirsch E.C., Agid Y., Brica A. (1998) Spinocerebellar ataxia type 7 (SCA7): a neurodegenerative disorder with neuronal intranuclear inclusions. *Hum. Mol. Genet.* 7:913-918.

Hope A.D., de Silva R., Fischer D.F., Hol E.M., van Leeuwen F.W., Lees A.J. (2003) Alzheimer's associated variant ubiquitin causes inhibition of the 26S proteasome and chaperone expression. *J. Neurochem.* 86:394-404.

Horimoto Y., Matsumoto M., Akatsu H., Kojima A., Yoshida M., Nokura K., Yuasa H., Katada E., Yamamoto T., Kosaka K., Hashizume Y., Yamamoto H., Mitake S. (2011) Longitudinal study on MRI intensity changes of Machado-Joseph disease: correlation between MRI findings and neuropathological changes. *J. Neurol.*

Hosoda M., Ozaki T., Miyazaki K., Hayashi S., Furuya K., Watanabe K., Nakagawa T., Hanamoto T., Todo S., Nakagawara A. (2005) UFD2a mediates the proteasomal turnover of p73 without promoting p73 ubiquitination. *Oncogene.* 24:7156-7169.

Hoyt M.A., Coffino P. (2004) Ubiquitin-free routes into the proteasome. *Cell Mol. Life Sci.* 61:1596-1600.

Hsieh H.C., Hsieh Y.H., Huang Y.H., Shen F.C., Tsai H.N., Tsai J.H., Lai Y.T., Wang Y.T., Chuang W.J., Huang W. (2005) HHR23A, a human homolog of Saccharomyces cerevisiae Rad23, regulates xeroderma pigmentosum C protein and is required for nucleotide excision repair. *Biochem. Biophys. Res. Commun.* 335:181-187.

Huang Q., Figueiredo-Pereira M.E. (2010) Ubiquitin/proteasome pathway impairment in neurodegeneration: therapeutic implications. *Apoptosis* 15:1292-1311.

Hubener J., Riess O. (2010) Polyglutamine-induced neurodegeneration in SCA3 is not mitigated by non-expanded ataxin-3: conclusions from double-transgenic mouse models. *Neurobiol. Dis.* 38:116-124.

Huen N.Y., Chan H.Y. (2005) Dynamic regulation of molecular chaperone gene expression in polyglutamine disease. *Biochem. Biophys. Res. Commun.* 334:1074-1084.

Humbert S., Bryson E. A., Cordelieres F. P., Connors N. C., Datta S. R., Finkbeiner S., Greenberg M. E., Saudou F. (2002) The IGF-1/Akt pathway is neuroprotective in Huntington's disease and involves Huntingtin phosphorylation by Akt. *Dev. Cell* 2:831-837.

Huynh D. P., Yang H. T., Vakharia H., Nguyen D., Pulst S. M. (2003) Expansion of the polyQ repeat in ataxin-2 alters its Golgi localization, disrupts the Golgi complex and causes cell death. *Hum. Mol. Genet.* 12:1485-1496.

Hu J., Matsui M., Gagnon K.T., Schwartz J.C., Gabillet S., Arar K., Wu J., Bezprozvanny I., Corey D.R. (2009) Allele-specific silencing of mutant huntingtin and ataxin-3genes by targeting expanded CAG repeats in mRNAs. *Nat. Biotechnol.* 27:478-484.

Ichikawa Y., Goto J., Hattori M., Toyoda A., Ishii K., Jeong S.Y., Hashida H., Masuda N., Ogata K., Kasai F., Hirai M., Maciel P., Rouleau G.A., Sakaki Y., Kanazawa I. (2001) The

genomic structure and expression of MJD, the Machado-Joseph disease gene. *J. Hum. Genet.* 46:413-422.

Igarashi S., Takiyama Y., Cancel G., Rogaeva E.A., Sasaki H., Wakisaka A., Zhou Y.X., Takano H., Endo K., Sanpei K., Oyake M., Tanaka H., Stevanin G., Abbas N., Dürr A., Rogaev E.I., Sherrington R., Tsuda T., Ikeda M., Cassa E., Nishizawa M., Benomar A., Julien J., Weissenbach J., Wang G.X., Agid Y., St George-Hyslop P.H., Brice A., Tsuji S. (1996) Intergenerational instability of the CAG repeat of the gene for Machado-Joseph disease (MJD1) is affected by the genotype of the normal chromosome: implications for the molecular mechanisms of the instability of the CAG repeat. *Hum. Mol. Genet.* 5:923-932.

Ikeda F., Dikic I. (2008) Atypical ubiquitin chains: new molecular signals. "Protein Modifications: beyond the Usual Suspects" review series. *EMBO Rep.* 9:536-542.

Ikeda H., Yamaguchi M., Sugai S., Aze Y., Narumiya S., Kakizuka A. (1996) Expanded polyglutamine in the Machado-Joseph disease protein induces cell death *in vitro* and *in vivo*. *Nat. Genet.* 13: 196-202.

Iwabuchi K., Tsuchiya K., Uchihara T., Yagishita S. (1999) Autosomal dominant spinocerebellar degenerations. Clinical, pathological, and genetic correlations. *Rev.Neurol. (Paris)*155:255–270.

Jana N.R., Dikshit P., Goswami A., Kotliarova S., Murata S., Tanaka K., Nukina N. (2005) Co-chaperone CHIP associates with expanded polyglutamine protein and promotes their degradation by proteasomes. *J. Biol. Chem.* 280:11635–11640.

Jana N.R., Tanaka M., Wang G., Nukina N. (2000) Polyglutamine length-dependent interaction of Hsp40 and Hsp70 family chaperones with truncated N-terminal huntingtin: their role in supression og aggregation and cellular toxicity. *Hum. Mol. Genet.* 9:2009-2018.

Jana N.R., Zemskov E.A., Wang Gh., Nukina N. (2001) Altered proteasomal function due to the expression of polyglutamine-expanded truncated N-terminal huntingtin induces apoptosis by caspase activation through mitochondril cytochrome c release. *Hum. Mol. Genet.* 10:1049-1059.

Jardim L.B., Pereira M.L., Silveira I., Ferro A., Sequeiros J., Giugliani R. (2001) Neurologic findings in Machado-Joseph disease: relation with disease duration, subtypes, and (CAG)n. *Arch. Neurol.* 58:899–904.

Jardim L., Silveira I., Pereira M.L., do Ceu Moreira M., Mendonca P., Sequeiros J., Giugliani R. (2003) Searching for modulating effects of SCA2, SCA6 and DRPLA CAG tracts on the Machado-Joseph disease (SCA3) phenotype. *Acta Neurol. Scand.* 107:211-214.

Jarosch E., Taxis C., Volkwein C., Bordallo J., Finley D., Wolf D.H., Sommer T. (2002) Protein dislocation from the ER requires polyubiquitination and the AAA-ATPase Cdc48. *Nat. Cell Biol.* 4:134-139.

Jia K., Hart A.C., Levine B. (2007) Autophagy genes protect against disease caused by polyglutamine expansion proteins in Caenorhabditis elegans. *Autophagy* 3:21-25.

Jiang Y.H., Beaudet A.L. (2004) Human disorders of ubiquitination and proteasomal

degradation. *Curr. Opin. Pediatr.* 16:419–426.

Johnson E.S., Ma P.C., Ota I.M., Varshavsky A. (1995) A proteolytic pathway that recognizes ubiquitin as a degradation signal. *J. Biol. Chem.* 270:17442-17456.

Jung J., Xu K., Lessing D., Bonini N.M. (2009) Preventing ataxin-3 protein cleavage mitigates degeneration in a *Drosophila* model of SCA3. *Hum. Mol. Genet.* 18:4843-4852.

Kahlem P., Terré C., Green H., Djian P. (1996) Peptides containing glutamine repeats as substrates for transglutaminase-catalyzed cross-linking: relevace to diseases for the nervous system. *Proc. Natl. Acad. Sci. USA* 93:14580-14585.

Kanai K., Kuwabara S., Arai K., Sung J.Y., Ogawara K., Hattori T. (2003) Muscle cramp in Machado-Joseph disease: Altered motor axonal excitability properties and mexiletine treatment. *Brain* 126:965–73.

Kang Y., Chen X., Lary J.W., Cole J.L., Walters K.J. (2007) Defining how ubiquitin receptors hHR23A and S5a bind polyubiquitin. *J. Mol. Biol.* 369:168-76.

Katsuno M., Adachi H., Kume A., Li M., Nakagomi Y., Niwa H., Sang C., Kobayashi Y., Doyu M., Sobue G. (2002) Testosterone reduction prevents phenotypic expression in a transgenic mouce model of spinal and bulbar muscular atrophy. *Neuron* 35:843-854.

Katsuno M., Adachi H., Waza M., Banno H., Suzuki K., Tanaka F., Doyu M., Sobue G. (2006) Pathogenesis, animal models and therapeutics in spinal and bulbar muscular atrophy (SBMA). *Exp. Neurol.* 200:8-18.

Kawaguchi Y., Okamoto T., Taniwaki M., Aizawa M., Inoue M., Katayama S., Kawakami H., Nakamura S., Nishimura M., Akiguchi I., *et al.* (1994) CAG expansions in a novel gene for Machado-Joseph disease at chromosome 14q32.1. *Nat. Genet.* 8:221-228.

Kawakami H., Maruyama H., Nakamura S., Kawaguchi Y., Kakizuka A., Doyu M., Sobue G.(1995) Unique features of the CAG repeats in Machado-Joseph disease. *Nat. Genet.* 9:344-345.

Kaytor M.D., Duvick L.A., Skinner P.J., Koob M.D., Ranum L.P., Orr H.T. (1999) Nuclear localization of the spinocerebellar ataxia type 7 protein, ataxin-7. *Hum. Mol. Genet.* 8:1657-1664.

Kazemi-Esfarjani P., Benzer S. (2000) Genetic suppression of polyglutamine toxicity in *Drosophila*. *Science* 287:1837-1840.

Kegel K.B., Kim M., Sapp E., McIntyre C., Castano J.G., Aronin N., DiFiglia M. (2000) Huntingtin expression stimulates endosomal-lysosomal activity, endosome tubulation, and autophagy. *J. Neurosci.* 20:7268-7278.

Khan L.A., Bauer P.O., Miyazaki H., Lindenberg K.S., Landwehrmeyer B.G., Nukina N. (2006) Expanded polyglutamines impair synapic transmission and ubiquitin-proteasome system in *Caenorhabditis elegans*. *J. Neurohem.* 98:576-587.

Kieling C., Prestes P.R., Saraiva-Pereira M.L., Jardim L.B. (2007) Survival estimates for patients

with Machado-Joseph disease (SCA3). *Clin. Genet.* 72:543-545.

Kim H.T., Kim K.P., lledias F., Kisselev A.F., Scaglione K.M., Skowyra D., Gygi S.P., Goldberg A.L. (2007) Certain pairs of ubiquitin-cojugating enzymes (E2s) and ubiquitin-protein ligases (e3s) synthesize nondegradable forked ubiquitin chains containing all possible isopeptide linkages. *J. Biol. Chem.* 282:17375-17386.

Kim Y.T., Shin S.M., Lee W.Y., Kim G.M., Jin D.K. (2004) Expression of expanded polyglutamine protein induces behavioral changes in *Drosophila* (polyglutamine-induced changes in *Drosophila*). *Cell Mol. Neurobiol.* 24:109-122.

Kirkpatrick D.S., Hathaway N.A., Hanna J., Elsasser S., Rsh J., Fnley D., King R.W., Gygi S.P. (2006) Quantitative analysis of *in vitro* ubiquitinated cyclin B1 revelas complex chain topology. *Nat. Cell Biol.* 8:700-710.

Klement I.A., Skinner P.J., Kaytor M.D., Yi H., Hersch S.M., Clark H.B., Zoghbi H.Y., Orr H.T. (1998) Ataxin-1 nuclear localization and aggregation: role in polyglutamine-induced disease in SCA1 transgenic mice. *Cell* 95:41-53.

Klockgether T. (2007) Ataxias. *Parkinsonism Relat. Disord.* 13 Suppl 3:S391-394.

Klockgether T. (2008) The clinical diagnosis of autosomal dominant spinocerebellar ataxias. *Cerebellum* 7:101–105.

Klockgether T., Skalej M., Wedekind D., Luft A.R., Welte D., Schulz J.B., Abele M., Burk K., Laccone F., Brice A., Dichgans J. (1998) Autosomal dominant cerebellar ataxia type I. MRI-based volumetry of posterior fossa structures and basal ganglia in spinocerebellar ataxia types 1, 2 and 3. Brain 121:1687-1693.

Kobayashi Y., Kume A., Li M., Doyu M., Hata M., Ohtsuka K., Sobue G. (2000) Chaperones Hsp70 and Hsp40 suppress aggregate formation and apoptosis in cultured neuronal cells expressing truncated androgen receptor protein with expanded polygutamine. *J. Biol. Chem.* 275:8772-8778.

Koeppen AH. (2005) The pathogenesis of spinocerebellar ataxia. *Cerebellum.* 4:62-73.

Komada M. (2008) Controlling receptor downregulation by ubiquitination and deubiquitination. *Curr. Drug Discov. Technol.* 5:78–84.

Kordasiewicz H.B., Thompson R.M., Clark H.B., Gomez C.M. (2006) C-termini of P/Q-type Ca2+ channel alpha1A subunits translocate to nuclei and promote polyglutamine-mediated toxicity. *Hum. Mol. Genet.* 15:1587-1599.

Kotliarova S., Jana N.R., Sakamoto N., Kurosawa M., Miyazaki H., Nekooki M., Doi H., Machida Y., Wong H.K., Suzuki T., Uchikawa C., Kotliarov Y., Uchida K., Nagao Y., Nagaoka U., Tamaoka A., Oyanagi K., Oyama F., Nukina N. (2005) Decreased expression of hypothalamic neuroeptides in Huntington disease transgenic mice with expanded polyglutamine-EGFP fluorescent aggregates. *J. Neurochem.* 93:641-653.

Koyano S.. Uchihara T., Fujigasaki H., Nakamura A., Yagishita S., Iwabuchi K. (1999) Neuronal intranuclear inclusions in spinocerebellar ataxia type 2: triple-labeling

immunofluorescent study. *Neurosci. Lett.* 273:117-120.

Kremer E.J., Pritchard M., Lynch M., Yu S., Holman K., Baker E., Warren S.T., Schlessinger D., Sutherland G.R., Richards R.I. (1991) Mapping of DNA instability at the fragile X to a trinucleotide repeat sequence p(CCG)n. *Science* 252:1711-1714.

Kuemmerle S., Gutekunst C.A., Klein A.M., Li X.J., Li S.H., Beal M.F., Herch S.M., Ferrante R.J. (1999) Huntington aggregates may not predict neuronal death in Huntington's disease. *Ann. Neurol.* 46:842-849.

Kuhlbrodt K., Janiesch P.C., Kevei E., Segref A., Barikbin R., Hoppe T. (2011) The Machado–Joseph disease deubiquitylase ATX-3 couples longevity and proteostasis. *Nat. Cell Biol.* 13:273–281.

Kuhn A., Goldstein D.R., Hodges A., Strand A.D., Sengstag T., kooperberg C., Becanovic K., Puladi M.A., Sathasivam K., Cha J.H., Hannan A.J., Hydem M.R., Leavitt B.R., Dunnett S.B., Ferrante R.J., Albin R., Shelbourne P., Delorenzi M., Augod S.J., Faull R.L., Olson J.M., Bates G.P., Jones L., Luthi-Carter R. (2007) Mutant huntingtin's effects on striatal gene expression in mice recapitulate changes observed in human Huntington's disease brain and do not differ with mutant huntingtin length or wild-type huntingtin dosage. *Hum. Mol. Genet.* 16:1845-1861.

Kuyumcu-Martinez N.M., Wang G.S., Cooper T.A.(2007) Increased steady-state levels of CUGBP1 in myotonic dystrophy type 1 are due to PKC-mediated hyperphosphorylation. *Mol. Cell* 28:68-78.

La Spada A.R., Wilson E.M., Lubahn D.B., Harding A.E., Fischbeck K.H. (1991) Androgen receptor gene mutations in X-linked spinal and bulbar muscular atrophy. *Nature* 352:77-79.

Lam Y.A., Lawson T.G., Velayutham M., Zweier J.L., Pickart C.M. (2002) A proteasomal ATPase subunit recognizes the polyubiquitin degradation signal. *Nature* 416:763-767.

Lee Y., Samaco R.C., Gatchel J.R., Thaller C., Orr H.T., Zoghbi H.Y. (2008) miR-19, miR-101 and miR-130 co-regulate ATXN1 levels to potentially modulate SCA1 pathogenesis. *Nat. Neurosci.* 11:1137-1139.

Levine B., Klionsky D.J. (2004) Development by self-digestion: molecular mechanisms and biological functions of autophagy. *Dev. Cell* 6:463-477.

Levine B., Kroemer G. (2009) Autophagy in aging, disease and death: the true identity of a cell death impostor. *Cell Death Differ.* 16:1-2.

Li F., Macfarlan T., Pittman R.N., Chakravarti D. (2002) Ataxin-3 is a histone binding protein with two independent transcriptional corepressor activities. *J. Biol. Chem.* 277:45004–45012.

Li H., Li S.H., Yu Z.X., Shelbourne P., Li X.J. (2001) Huntingtin aggregate-associated axonal degeneration is an early pathological event in Huntington's disease mice. *J. Neurosci.* 21:8473-8481.

Li L.B., Bonini N.M. (2010) Roles of trinucleotide-repeat RNA in neurological disease and degeneration. *Trends Neurosci.* 33:292-298.

Li L.B., Yu Z., Teng X., Bonini N.M. (2008) RNA toxicity is a component of ataxin-3 degeneration in Drosophila. *Nature* 453:1107-1111.

Li S.H., Cheng A.L., Zhou H., Lam S., Rao M., Li H., Li X.J. (2002) Interaction of Huntington disease protein with trascriptional activator sp1. *Mol. Cell. Biol.* 22:1277-1287.

Li S.H., Lam S., Cheng A.L., Li X.J. (2000) Intranuclear huntingtin increases the expression of caspase-1 and induces apoptosis. *Hum. Mol. Gen.* 9:2859-2867.

Li X., Li H., Li X.J. (2008) Intracellular degradation of misfolded proteins in polyglutamine neurodegenerative diseases. *Brain Res. Rev.* 59:245-252.

Lima M., Costa M.C., Montiel R., Ferro A., Santos C., Silva C., Bettencourt C., Sousa A., Sequeiros J., Coutinho P., Maciel P. (2005) Population genetics of wild-type CAG repeats in the Machado-Joseph disease gene in Portugal. *Hum. Hered.* 60:156-163.

Limprasert P., Nouri N., Heyman R.A., Nopparatana C., Kamonsilp M., Deininger P.L., Keats B.J. (1996) Analysis of CAG repeat of the Machado-Joseph gene in human, chimpanzee and monkey populations: A variant nucleotide is associated with the number of CAG repeats. *Hum. Mol. Genet.* 5:207–213.

Lindner H.A. (2007) Deubiquitination in virus infection. *Virology* 362:245–256.

Liu C.S., Hsu H.M., Cheng W.L., Hsieh M. (2005) Clinical and molecular events in patients with Machado-Joseph disease under lamotrigine therapy. *Acta Neurol. Scand.* 111:385-390.

Liz M.A., Sousa M.M. (2005) Deciphering cryptic proteases. *Cell Mol. Life Sci.* 62:989–1002.

Lopes-Cendes I., Maciel P., Kish S., Gaspar C., Robitaille Y., Clark H.B., Koeppen A.H., Nance M., Schut L., Silveira I., Coutinho P., Sequeiros J., Rouleau G.A. (1996) Somatic mosaicism in the central nervous system in spinocerebellar ataxia type 1 and Machado-Joseph disease. *Ann. Neurol.* 40:199–206.

Luo S., Vacher C., Davies J. E., Rubinsztein D. C. (2005) Cdk5 phosphorylation of huntingtin reduces its cleavage by caspases: implicatioins for mutant huntingtin toxicity. *J. Cell Biol.* 169:647-656.

Luthi-Carter R., Strand A.D., Hanson S.A., Kooperberg C., Schilling G., La Spada A.R., Merry D.E., Young A.B., Ross C.A., Borcjelt D.R., Olson J.M. (2002) Polyglutamine and transcription: gene expression changes shared by DRPLA and Huntington's disease mouse models reveal context-independent effects. *Hum. Mol. Genet.* 11:1927-1937.

Lunkes A., Lindenberg K.S., Ben-Haïem L., Weber C., Devys D., Landwehrmeyer G.B., Mandel J.L., Trottier Y. (2002) Proteases acting on mutant huntingtin generate cleave products that differentially build up cytoplasmic and nuclear inclusions. *Mol. Cell* 10:259-269.

Macedo-Ribeiro S., Cortes L., Maciel P., Carvalho A.L. (2009) Nucleocytoplasmic shuttling activity of ataxin-3. *PLoS One* 4:e5834.

Maciel P., Costa M.C., Ferro A., Rousseau M., Santos C.S., Gaspar C., Barros J., Rouleau

G.A., Coutinho P., Sequeiros J. (2001) Improvement in the molecular diagnosis of Machado-Joseph disease. *Arch. Neurol.* 58:1821-1827.

Maciel P., Gaspar C., DeStefano A.L., Silveira I., Coutinho P., Radvany J., Dawson D.M., Sudarsky L., Guimaraes J., Loureiro J.E., *et al.*(1995) Correlation between CAG repeat length and clinical features in Machado-Joseph disease. Am. J. Hum. Genet. 57:54-61.

Madsen L, Seeger M, Semple CA, Hartmann-Petersen R (2009) New ATPase regulators - p97 goes to the PUB. *Int. J. Biochem. Cell Biol.* 41:2380-2388.

Mao Y., Senic-Matuglia F., Di Fiore P.P., Polo S., Hodsdon M.E., De Camilli P. (2005) Deubiquitinating function of ataxin-3: insights from the solution structure of the Josephin domain. *Proc. Natl. Acad. Sci. U.S.A.* 102:12700–12705.

Markossian, K.A., Kurganov, B.I. (2004) Protein folding, misfolding, and aggregation. Formation of inclusion bodies and aggresomes. Biochemistry (Mosc.) 69:971–984.

Martinez-Vicente M., Talloczy Z., Wong E., Tang G., Koga H., Kaushik S., de Vries R., Arias E., Harris S., Sulzer D., Cuervo A.M. (2010) Cargo recognition failure is responsible for inefficient autophagy in Huntington's disease. *Nat. Neurosci.* 13:567-576.

Martins S., Calafell F., Gaspar C., Wong V.C., Silveira I., Nicholson G.A., Brunt E.R., Tranebjaerg L., Stevanin G., Hsieh M., Soong B.W., Loureiro L., Dürr A., Tsuji S., Watanabe M., Jardim L.B., Giunti P., Riess O., Ranum L.P., Brice A., Rouleau G.A., Coutinho P., Amorim A., Sequeiros J. (2007) Asian origin for the worldwidespread mutational event in Machado-Joseph disease. *Arch. Neurol.* 64:1502-1508.

Martins S., Calafell F., Gaspar C., Wong V.C., Silveira I., Nicholson G.A., Brunt E.R., Tranebjaerg L., Stevanin G., Hsieh M., Soong B.W., Loureiro L., Dürr A., Tsuji S., Watanabe M., Jardim L.B., Giunti P., Riess O., Ranum L.P., Brice A., Rouleau G.A., Coutinho P., Amorim A., Sequeiros J. (2007) Asian origin for the worldwidespread mutational event in Machado-Joseph disease. *Arch. Neurol.* 64:1502-1508.

Martins S., Calafell F., Wong V.C., Sequeiros J., Amorim A. (2006) A multistep mutation mechanism drives the evolution of the CAG repeat at MJD/SCA3 locus. *Eur. J. Hum. Genet.* 2006, 14:932-940.

Maruyama H., Nakamura S., Matsuyama Z., Sakai T., Doyu M., Sobue G., Seto M., Tsujihata M., Oh-i T., Nishio T., *et al.* (1995) Molecular features of the CAG repeats and clinical manifestation of Machado-Joseph disease. *Hum. Mol. Genet.* 4:807-812.

Masino L., Musi V., Menon R.P., Fusi P., Kelly G., Frenkiel T.A., Trottier Y., Pastore A. (2003) Domain architecture of the polyglutamine protein ataxin-3: a globular domain followed by a flexible tail. *FEBS Lett.* 549:21–25.

Masino L., Nicastro G., Menon R.P., Dal Piaz F., Calder L., Pastore A. (2004) Characterization of the structure and the amyloidogenic properties of the Josephin domain of the polyglutamine-containing protein ataxin-3. *J. Mol. Biol.* 344:1021-1035.

Matsumoto M., Yada M., Hatakeyama S., Ishimoto H., Tanimura T., Tsuji S., Kakizuka A., Kitagawa M., Nakayama K.I. (2004) Molecular clearance of ataxin-3 is regulated by a

mammalian E4. *EMBO J.* 23:659–669.

Mazzucchelli S., De Palma A., Riva M., D'Urzo A., Pozzi C., Pastori V., Comelli F., Fusi P., Vanoni M., Tortora P., Mauri P., Regonesi M.E. (2009) Proteomic and biochemical analyses unveil tight interaction of ataxin-3 with tubulin. *Int. J. Biochem. Cell Biol.* 41:2485–2492.

McCampbell A., Taylor J.P., Taye A.A., Robitshek J., Li M., Walcott J., Merry D., Chai Y., Paulson H., Sobue G., Fischbeck K.H. (2000) CREB-binding protein equestration by expanded polyglutamine. *Hum. Mol. Genet.* 9:2197-2202.

McGurk L., Bonini N.M. (2011) Protein interacting with C kinase (PICK1) is a suppressor of spinocerebellar ataxin 3-associated neurodegeneration in *Drosophila*. *Hum. Mol. Genet.* [Epub ahead of print].

Mello K.A., Abbott B.P. (1988) Effect of sulfamethoxazole and trimethoprim on neurologic dysfunction in a patient with Joseph's disease. *Arch. Neurol.* 45:210-213.

Milakovic T., Johnson G.V. (2005) Mitochondrial respiration and ATP production are significantly impaired in striatal cells expressing mutant huntingtin. *J. Biol. Chem.* 280:30773-30782.

Milakovic T., Quintanilla R.A., Johnson G.V. (2006) Mutant huntingtin expression induces mitochondria calcium handling defects in clonal striatal cells: functional consequences. *J. Biol. Chem.* 281:34785-34795.

Mizushima N., Levine B., Cuervo A.M., Klionsky D.J. (2008) Autophagy fights disease through cellular self-digestion. *Nature* 451:1069-1075.

Monte T.L., Rieder C.R., Tort A.B., Rockenback I., Pereira M.L., Silveira I., Ferro A., Sequeiros J., Jardim L.B. (2003) Use of fluoxetine for treatment of Machado- Joseph disease: an open-label study. *Acta Neurol. Scand.* 107:207-210.

Morfini G., Pigino G., Brady S.T. (2005) Polyglutamine expansion diseases: failing to deliver. *Trends Mol. Med.* 11:64-70.

Morfini G., Szebenyi G., Richards B., Brady S.T. (2001) Regulation of kinesin: implications for neuronal development. *Dev. Neurosci.* 23:364-376.

Mori-Konya C., Kato N., Maeda R., Yasuda K., Higashimae N., Noguchi M., Koike M., Kimura Y., Ohizumi H., Hori S., Kakizuka A. (2009) p97/valosin-containing protein (VCP/p97) is highly modulated by phosphorylation and acetylation. *Genes Cells* 14:483-497.

Morris G.E. (2008) The Cajal Body. *Biochim. Biophys. Acta* 1783:2108-2115.

Moseley M.L., Zu T., Ikeda Y., Gao W., Mosemiller A.K., Daughters R.S., Chen G., Weatherspoon M.R., Clark H.B., Ebner T.J., Day J.W., Ranum L.P. (2006) Bidirectional expression of CUG and CAG expansion transcripts and intranuclear polyglutamine inclusions in spinocerebelar ataxia type 8. *Nat. Genet.* 38:758-769.

Muchowski P.J. (2002) Protein misfolding, amyloid formation, and neurodegeneration: a critical

role for molecular chaperones? *Neuron* 35:9-12.

Muchowski P.J., Schaffar G., Sittler A., Wanker E.E., Hayer-Hartl M.K., Hartl F.U. (2000) Hsp70 and hsp40 chaperons can inhibit self-assembly of polyglutamine proteins into amyloid-like fibrils. *Proc. Natl. Acad. Sci. USA* 97:7841-7846.

Mueller T., Breuer P., Schmitt I., Walter J., Evert B.O., Wullner U. (2009) CK2-dependent phosphorylation determines cellular localization and stability of ataxin-3. *Hum. Mol. Genet.* 18:3334–3343.

Nakano K.K., Dawson D.M., Spence A. (1972) Machado disease. A hereditary ataxia in Portuguese emigrants to Massachusetts. *Neurology* 22: 49-55.

Nicastro G., Masino L., Esposito V., Menon R.P., De Simone A., Fraternali F., Pastore A. (2009) Josephin domain of ataxin-3 contains two distinct ubiquitinbinding sites. *Biopolymers* 91:1203–1214.

Nicastro G., Menon R.P., Masino L., Knowles P.P., McDonald N.Q., Pastore A. (2005) The solution structure of the Josephin domain of ataxin-3: structural determinants for molecular recognition. *Proc. Natl. Acad. Sci. U.S.A.* 102:10493–10498.

Nicastro G., Todi S.V., Karaca E., Bonvin A.M., Paulson H.L., Pastore A. (2010) Understanding the role of the Josephin domain in the PolyUb binding and cleavage properties of ataxin-3. *PLoS One* 5:e12430.

Nijman S.M., Luna-Vargas M.P., Velds A., Brummelkamp T.R., Dirac A.M., Sixma T.K., Bernards R. (2005) A genomic and functional inventory of deubiquitinating enzymes. *Cell* 123:773–786.

Nishiyama K., Murayama S., Goto J., Watanabe M., Hashida H., Katayama S., Nomura Y., Nakamura S., Kanazawa I. (1996) Regional and cellular expression of the Machado-Joseph disease gene in brains of normal and affected individuals. *Ann. Neurol.* 40:776–81.

Nishikawa H., Ooka S., Sato K., Arima K., Okamoto J., Klevit R.E., Fukuda M., Ohta T. (2004) Mass spectrometric and muational analyses reveal Lys-6-linked polyubiquitin chains catalyzed by BRCA1-BARD1 ubiquitin ligase. *J. Biol. Chem.* 279:3916-3924.

Nishitoh H., Matsuzawa A., Tobiume K., Saegusa K., Takeda K., Inoue K., Hori S., Kakizuka A., Ichijo H. (2002) ASK1 is essential for endoplasmic reticulum stress-induced neuronal cell death triggered by expanded polyglutamine repeats. *Genes Dev.* 16:1345-1355.

Nozaki K., Onodera O., Takano H., Tsuji S. (2001) Amino acid sequences flanking polyglutamine stretches influence their potential for aggregate formation. *Neuroreport* 12:3357-3364.

Nucifora F.C. Jr, Sasaki M., Peters M.F., Huang H., Cooper J.K., Yamada M., Takahashi H., Tsuji S., Troncoso J., Dawson V.L., Dawson T.M., Ross C.A. (2001) Interference by huntingtin and atrophin-1 with CBP-mediated transcription leading to cellular toxicity. *Science* 291:2423-2428.

Okazawa H. (2003) Polyglutamine diseases: a transcription disorder? *Cell. Mol. Life Sci.* 60:1427-1439.

Oliveira J.M., Chen S., Almeida S., Riley R., Gonçalves J., Oliveira C.R., Hayden M.R., Nicholls D.G., Ellerby L.M., Rego A.C. (2006) Mitochondrial-dependent Ca^{2+} handling in Huntington's disease striatlal cells: effect of histone deacetylase inhibitors. *J. Neurosci.* 26:11174-11186.

Oliveira J.M., Jekabsons M.B., Chen S., Lin A., Rego A.C., Gonçalves J., Ellerby L.M., Nicholls D.G. (2007) MItochondrial dysfunction in Huntington's disease: the bioenergetics of isolated and in situ mitochondria from transgenic mice. *J. Neurochem.* 101:241-249.

Onodera O., Idezuka J., Igarashi S., Takiyama Y., Endo K., Takano H., Oyake M., Tanaka H., Inuzuka T., Hayashi T., Yuasa T., Ito J., Miyatake T., Tsuji S. (1998) Progressive atrophy of cerebellum and brainstem as a function of age and the size of the expanded CAG repeats in the MJD1 gene in Machado-Joseph disease. *Ann. Neurol.* 43:288–296.

Orr A. L., Li S., Wang C.E., Li H., Wang J., Rong J., Xu X., Mastroberardino P.G., Greenamyre J.T., Li X.J. (2008) N-terminal mutant huntingtin associates with mitochondria and impairs mitochondria trafficking. *J. Neurosci.* 28:2783-2792.

Orr H.T. (2001) Qs in the nucleus. *Neuron* 31:875-876.

Orr H.T., Zoghbi H.Y. (2007) Trinucleotide repeat disorders. *Annu. Rev. Neurosci.* 30:575-621.

Ozkaynak E., Finley D., Varshavsky A. (1984) The yeast ubiquitin gene: head-to-tail repeats encoding a polyubiquitin precursor protein. *Nature* 312:663-666.

Padiath Q.S., Srivastava A.K., Roy S., Jain S., Brahmachari S.K. (2005) Identification of a novel 45 repeat unstable allele associated with a disease phenotype at the MJD1/SCA3 locus. *Am. J. Med. Genet. B. Neuropsychiatr. Genet.* 133:124–126.

Panov A.V., Burke J.R., Strittmatter W.J., Greenamyre J.T. (2003) *In vitro* effect of polyglutamine tracts on Ca^{2+}-dependent depolarization of rat and human mitochondria: relevance to Huntington's disease. *Arch. Biochem. Biophys.* 410:1-6.

Panov A.V., Gutekunst C.A., Leavittt B.R., Hayden M.R., Burke J.R., Strittmatter W.J., Greenamyre J.T. (2002) Early mitochondrial calcium defects in Huntington's disease are a direct effect of polyglutamines. *Nat. Neurosci.* 5:731-736.

Paulson H.L. (1999) Protein fate in neurodegenerative proteinopathies:polyglutamine diseases join the (mis)fold. *Am. J. Hum. Genet.* 64:339-345.

Paulson H.L., Bonini N.M., Roth K.A. (2000) Polyglutamine disease and neuronal cell death. *Proc. Natl. Acad. Sci. U S A.* 97(24):12957-12958.

Paulson H.L. (2007) Dominantly inherited ataxias: lessons learned from Machado-Joseph disease/spinocerebellar ataxia type 3. *Semin. Neurol.* 27:133-142.

Paulson H.L. (2009) The Spinocerebellar ataxias. *J. Neuro-Ophtalmol.* 29:227-237.

Paulson H.L., Das S.S., Crino P.B., Perez M.K., Patel S.C., Gotsdiner D., Fischbeck K.H., Pittman R.N. (1997) Machado–Joseph disease gene product is a cytoplasmic protein widely

expressed in brain. *Ann. Neurol.* 41:453–462.

Paulson H.L., Perez M.K., Trottier Y., Trojanowski J.Q., Subramony S.H., Das S.S., Vig P., Mandel J.L., Fischbeck K.H., Pittman R.N. (1997) Intranuclear inclusions of expanded polyglutamine protein in spinocerebellar ataxia type 3. *Neuron* 19:333-344.

Pandey U.B., Nie Z., Batlevi Y., McCray B.A., Ritson G.P., Nedelsky N.B., Schwartz S.L., DiProspero N.A., Knight M.A., Schuldiner O., Padmanabhan R., Hild M., Berry D.L., Garza D., Hubbert C.C., Yao T.P., Baehrecke E.H., Taylor J.P. (2007) HDAC6 rescues neurodegeneration and provides an essential link between autophagy and the UPS. *Nature* 447:859-863.

Pearson C.E., Nichol Edamura K., Cleary J.D. (2005) Repeat instability: Mechanisms of dynamic mutations. *Nat. Rev. Genet.* 6:729-742.

Perez M.K., Paulson H.L., Pendse S.J., Salonz S.J., Bonini N.M., Pittman R.N. (1998) Recruitment andthe role of nuclear localization in polyglutamine-mediated aggregation. *J. Cell Biol.* 143:1457-1470.

Perutz M. F., Johnson T., Suzuki M., Finch J.T. (1994) Glutamine repeats as polar zippers: their possible role in inhirited neurodegenerative diseases. *Proc. Natl. Acad. Sci. USA* 91:5355-5358.

Perutz M.F., Pope B.J., Owen D., Wanker E.E., Scherzinger E. (2002) Aggregation of proteins with expanded glutamine and alanine repeats of the glutamine-rich and asparagine-rich domains of Sup35 and of the amyloid beta-peptide of amyloid plaques. *Proc. Natl. Acad. Sci. USA* 99:5596-5600.

Peters M.F., Nucifora F.C. Jr, Kushi J., Seaman H.C., Cooper J.K., Herring W.J., Dawson V.L., Dawson T.M., Ross C.A. (1999) Nuclear trageting of mutant huntingtin increases toxicity. *Mol. Cell. Neurosci.* 14:121-128.

Pickart C.M. (1997) Targeting of substrates to the 26S proteasome. *FASEB J.* 11:1055-1066.
Pickart C.M. (2001) Mechanisms underlying ubiquitination. *Annu. Rev. Biochem.* 70:503-533.

Pickart C.M., Cohen R.E. (2004) Proteasomes and their kin: proteases in the machine age. *Nat. Rev. Mol. Cell Biol.* 5:177-187.

Pickart C.M., Eddins M.J. (2004) Ubiquitin: structures, functions, mechanisms. *Biochim. Biophys. Acta* 1695:55–72.

Pickart C.M., Fushman D. (2004) Polyubiquitin chains: polymeric protein signals. *Curr. Opin. Chem. Biol.*8:610–6.

Pickart C.M., Rose I.A. (1985) Ubiquitin carboxyl-terminal hydrolase acts on ubiquitin carboxyl-terminal amides. *J. Biol. Chem.* 260:7903–7910.

Pigino G., Morfini G., Pelsman A., Mattson M.P., Brady S.T., Busciglio J. (2003) Alzheimer's presenilin 1 mutations impair kinesin-based axonal transport. *J. Neurosci,* 23:4499-4508.

Pinsky L., Trifiro M., Kaufman M., Beitel L.K., Mhatre A., Kazemi-Esfarjani P., Sabbaghian N., Lumbroso R., Alvarado C., Vasiliou M. (1992) Androgen resistance due to mutation of

the androgen receptor. *Clin. Invest. Med.* 15:456-472.

Piotrowski J., Beal R., Hoffman L., Wilkinson K.D., Cohen R.E., Pickart C.M. (1997) Inhibition of the 26 S proteasome by polyubiquitin chains synthesized to have defined lengths. *J. Biol. Chem.* 272:23712–23721.

Pittman R.N., Wang S., DiBenedetto A.J., Mills J.C. (1993) A system for characterizing cellular and molecular events in programmed neuronal cell death. *J. Neurosci.* 13:3669-3680.

Poirier M. A., Jiang H., Ross C.A. (2005) A structure-based analysis of huntingtin mutant polyglutamine aggregation and toxicity: evidence for a compact beta-sheet structure. *Hum. Mol. Genet.* 14:765-774.

Pozzi C., Valtorta M., Tedeschi G., Galbusera E., Pastori V., Bigi A., Nonnis S., Grassi E., Fusi P. (2008) Study of subcellular localization and proteolysis of ataxin-3. *Neurobiol. Dis.* 30:190-200.

Puranam K.L., Wu G., Strittmatter W.J., Burke J.R. (2006) Polyglutamine expansion inhibits respiration by increasing reactive oxygen species in isolated mitochondria. *Biochem. Biophys. Res. Commun.* 341:607-613.

Quintanilla R.A., Johnson G.V. (2009) Role of mitochondrial dysfunction in the pathogenesis of Huntington's disease, *Brain Res. Bull.* 80:242-247.

Raasi S., Orlov I., Fleming K.G., Pickart C.M. (2004) Binding of polyubiquitin chains to ubiquitin-associated (UBA) domains of hHR23A. *J. Mol. Biol.* 341:1367-1379.

Rabouille C., Levine T.P., Peters J.M., Warren G. (1995) An NSF-like ATPase, p97, and NSF mediate cisternal regrowth from mitotic Golgi fragments. *Cell.* 82:905-914.

Ragan C.I., Wilson M.T., Darley-Usmar V.M., Lowe, P.N. (1987) Subfractionation of mitochondria, and isolation of the proteins of oxidative phosphorylation, in Mitochondria, a practical approach. (Darley-Usmar V.M., Rickwood D., Wilson M.T., eds), IRL Press., London, 79–112.

Ranganathan S., Harrison G.G., Meyertholen K., Pennuto M., Burnett B.G., Fischbeck K.H. (2009) Mitochondrial abnormalities in spinal and bulbar muscular atrophy. *Hum. Mol. Genet.* 18:27-42.

Rangone H., Poizat G., Troncoso J., Ross C. A., MacDonald M. E., Saudou F., Humbert S. (2004) The serum- and glucocorticoid-induced kinase SGK inhibits mutant huntingtin-induced toxicity by phosphorylating serine 421 of huntingtin. *Eur. J. Neurosci.* 19:273-279.

Ravikumar B., Imarisio S., Sarkar S., O'Kane C.J., Rubinsztein D.C. (2008) Rab5 modulates aggregation and toxicity of mutant huntingtin through macroautophagy in cell and fly models of Huntington disease. *J. Cell Sci.* 121:1649-1660.

Ravikumar B., Vacher C., Berger Z., Davies J.E., Luo S., Oroz L.G., Scaravilli F., Easton D.F., Duden R., O'Kane C.J., Rubinsztein D.C. (2004) Inhibition of mTOR induces autophagy and reduces toxicity of polyglutamine expansions in fly and mouse models of Huntington

disease. *Nat. Genet.* 36:585-595.

Rego A. C., Santos M.S., Oliveira C.R. (1999) Influence of the antioxidants vitamin E and idebenone on retinal cell injury mediated by chemical ischemia, hypoglycemia or oxidative stress. *Free Radic. Biol. Med.* 26:1405-1417.

Regulier E., Trottier Y., Perrin V., Aebischer P., Deglon N. (2003) Early and reversible neuropathology induced by tetracycline-regulated lentiviral overexpression of mutant huntingtin in rat striatum. *Hum. Mol. Genet.* 12:2827-2836.

Reid E., Koos M., Ashley-Koch A., Hughes L., Bevan S., Svenson I.K., Graham F.L., Gaskell P.C., Dearlove A., Pericak-Vance M.A., Rubinsztein D.C., Mauchuk D.A. (2002) A kinesin heavy chain (KIF5A) mutation in hereditary spastic paraplegia (SPG10). *Am. J. Hum. Genet.* 71:1189-1194.

Reina C.P., Zhong X., Pittman R.N., 2010. Proteotoxic stress increases nuclear localization of ataxin-3. *Hum. Mol. Genet.* 19:235–249.

Reyes-Turcu F.E., Ventii K.H., Wilkinson K.D. (2009) Regulation and cellular roles of ubiquitin-specific deubiquitinating enzymes. *Annu. Rev. Biochem.* 78:363–397.

Reyes-Turcu F.E., Wilkinson K.D. (2009) Polyubiquitin binding and disassembly by deubiquitinating enzymes. *Chemical Reviews.* 109:1495-1508.

Ribaï P., Pousset F., Tanguy M.L., Rivaud-Pechoux S., Le Ber I., Gasparini F., Charles P., Béraud A.S., Schmitt M., Koening M., Mallet A., Brice A., Dürr A. (2007) Neurological, cardiological, and oculomotor progression in 104 patients with Friedreich ataxia during long-term follow-up. *Arch Neurol* 64:558–564.

Riess O., Rüb U., Pastore A., Bauer P., Schöls, L. (2008) SCA3: Neurological features, pathogenesis and animal models. *The Cerebellum* 7:125-137.

Riley B. E., Zoghbi H. Y., Orr H. T. (2005) SUMOylation of the polyglutamine repeat protein, ataxin-1, is dependent on functional nuclear localization signal. *J. Biol. Chem.* 280:21942-21948.

Rockel T.D., Stuhlmann D., von Mikecz A. (2005) Proteasomes degrade proteins in focal subdomains of the human cell nucleus. *J. Cell Sci.* 118:5231-5242.

Rodrigues A.J., Coppola G., Santos C., Costa Mdo C., Ailion M., Sequeiros J., Geschwind D.H., Maciel P. (2007) Functional genomics and biochemical characterization of the C. elegans orthologue of the Machado–Joseph disease protein ataxin-3. *FASEB J.* 21:1126–1136.

Rodrigues A.J., do Carmo Costa M., Silva T.L., Ferreira D., Bajanca F., Logarinho E., Maciel P. (2010) Absence of ataxin-3 leads to cytoskeletal disorganization and increased cell death. *Biochim. Biophys. Acta* 1803:1154–1163.

Rodrigues A.J., Neves-Carvalho A., Ferro A., Rokka A., Corthals G., Logarinho E., Maciel P. (2009) ATX-3, CDC-48 and UBXN-5: a new trimolecular complex in *Caenorhabditis elegans*. *Biochem. Biophys. Res. Commun.* 386:575-581.

Rodrigues A.J., Neves-Carvalho A., Teixeira-Castro A., Rokka A., Corthals G., Logarinho E., Maciel P. (2011) Absence of ataxin-3 leads to enhanced stress response in *C. elegans*. *PLoS One* 19:e18512.

Rodríguez E., Rivera I., Astorga S., Mendoza E., García F., Hernández-Echeagaray E. (2010) Uncoupling oxidative/energy metabolism with low sub chronic doses of 3-mitropropionic acid or iodoacetate in vivo produces striatal cell damage. *Int. J. Biol. Sci.* 22:199-212.

Romanul F.C., Fowler H.L., Radvany J., Feldman R.G., Feingold M. (1977) Azorean disease of the nervous system. *N. Engl. J. Med.* 296:1505-1508.

Rosenberg R.N. (1992) Machado-Joseph disease: an autosomal dominant motor system degeneration. *Mov. Disord.*7:193–203.

Rosenberg R.N., Nyhan W.L., Bay C., Shore P. (1976) Autosomal dominant striatonigral degeneration. A clinical, pathologic, and biochemical study of a new genetic disorder. *Neurology* 26:703-714.

Rosenthal R.E., Hamud F., Fiskum G., Varghese P.J., Sharpe S. (1987) Cerebral ischemia and reperfusion: prevention of brain mitochondrial injury by lidoflazine. *J. Cereb. Blood Flow Metab.* 7:752–758.

Ross C.A., Poirier M.A. (2004) Protein aggregation and neurodegenerative disease. *Nat. Med.* 10(Suppl.) S10-S17.

Roy L., Bergeron J.J., Lavoie C., Hendriks R., Gushue J., Fazel A., Pelletier A., Morré D.J., Subramaniam V.N., Hong W., Paiement J. (2000) Role of p97 and syntaxin 5 in the assembly of transitional endoplasmic reticulum. *Mol. Biol. Cell.* 11:2529-2542.

Ruan Q., Lesort M., MacDonald M.E., Johnson G.V. (2004) Striatal cells from huntingtin knock-in mice are selectively vulnerable to mitochondrial complex II inhibitor-induced cell death trough a non-apoptotic pathway. *Hum. Mol. Genet.* 13**:**669-681.

Rüb U., Brunt E.R., Deller T. (2008) New insights into the pathoanatomy of spinocerebellar ataxia type 3 (Machado-Joseph disease). *Curr. Opin. Neurol.* 21:111-116.

Rüb U., Brunt E.R., Del Turco D., de Vos R.A., Gierga K., Paulson H., Braak H. (2003a) The nucleus raphe interpositus in spinocerebellar ataxia type 3 (Machado-Joseph disease). *J. Chem. Neuroanat.* 25:115-127.

Rüb U., Brunt E.R., Gierga K., Schultz C., Paulson H., de Vos R.A., Braak H. (2003b) The nucleus raphe interpositus in spinocerebellar ataxia type 3 (Machado-Joseph disease). *J. Chem. Neuroanat.* 25:115-127.

Rüb U., Brunt E.R., Petrasch-Parwez E., Schols L., Theegarten D., Auburger G., Seidel K., Schultz C., Gierga K., Paulson H., van Broeckhoven C., Deller T., de Vos R.A. (2006a) Degeneration of ingestion-related brainstem nuclei in spinocerebellar ataxia type 2, 3, 6 and 7. *Neuropathol. Appl. Neurobiol.* 32:635–649.

Rüb U., de Vos R.A., Brunt E.R., Sebesteny T., Schols L., Auburger G., Bohl J.,

Ghebremedhin E., Gierga K., Seidel K., den Dunnen W., Heinsen H., Paulson H., Deller T. (2006b) Spinocerebellar ataxia type 3 (SCA3):thalamic neurodegeneration occurs independently from thalamic ataxin-3 immunopositive neuronal intranuclear inclusions. *Brain Pathol.* 16:218–227.

Rüb U., de Vos R.A., Schultz C., Brunt E.R., Paulson H., Braak H. (2002) Spinocerebellar ataxia type 3 (Machado-Joseph disease): severe destruction of the lateral reticular nucleus. *Brain* 125:2115-2124.

Rüb U., Gierga K., Brunt E.R., de Vos R.A., Bauer M., Schöls L., Bürk K., Auburger G., Bohl J., Schultz C., Vuksic M., Burbach G.J., Braak H., Deller T. (2005) Spinocerebellar ataxias types 2 and 3: Degeneration of the pre-cerebellar nuclei isolates the three phylogenetically defined regions of the cerebellum. *J. Neural Transm.* 112:1523–1545.

Rüb U., Seidel K., Ozerden I., Gierga K., Brunt E.R., Schöls L., de Vos R.A., den Dunnen W., Schultz C., Auburger G., Deller T. (2007) Consistent affection of the central somatosensory system in spinocerebellar ataxia type 2 and type 3 and its significance for clinical symptoms and rehabilitative therapy. *Brain Res. Rev.* 53:235–249.

Rubinsztein D.C., Gestwicki J.E., Murphy L.O., Klionsky D.J. (2007) Potential therapeutic applications of autophagy. *Nat. Rev. Drug Discov.* 6:304-312.

Rutter J., Winge D.R., Schiffman J.D. (2010) Succinate dehydrogenase - Assembly, regulation and role in human disease. *Mitochondrion* 10:393-401.

Saeki Y., Kudo T., Sone T., Kikuchi Y., Yokosawa H., Toh-e A., Tanaka K. (2009) Lysine 63-linked polyubiquitin chain may serve as a targeting signal for the 26S proteasome. *EMBO J.* 28:359-371.

Sakai T., Kawakami H. (1996) Machado-Joseph disease: A proposal of spastic paraplegic subtype. *Neurology* 46:846–847.

Sakai T., Matsuishi T., Yamada S., Komori H., Iwashita H. (1995) Sulfamethoxazoletrimethoprim double-blind, placebo-controlled, crossover trial in Machado-Joseph disease: sulfamethoxazole-trimethoprim increases cerebrospinal fluid level of biopterin. *J. Neural Transm. Gen. Sect.* 102:159-172.

Sanchez I., Xu C. J., Juo P., Kakizaka A., Blenis J., Yuan J. (1999) Caspase-8 is required for cell death induced by expanded polyglutamine repeats. *Neuron* 22:623-633.

Sandhir R., Mehtora A., Kamboj S. S. (2010) Lycopene prevents 3-nitropropionic acid-induced mitochondrial oxidative stress and dysfunctions in nervous system. *Neurochem. Int.* 57:579-587.

Sapp E., Schwarz C., Chase K., Bhide P.G., Young A.B., Penney J., Vonsattel J.P., Aronin N., DiFiglia M. (1997) Huntingtin localization in brains of normal and Huntington's disease patients.

Sarge K. D., Park-Sarge O. K. (2009) Sumoylation and human disease pathogenesis. *Trends Biochem. Sci.* 34:200-205.

Saudou F., Finkbeiner S., Devys D., Greenberg M.E. (1998) Huntingtin acts in nucleus to induce apoptosis but death does not correlate with the formation of intranuclear inclusions. *Cell* 95:55-66.

Saunders H.M., Bottomley S.P. (2009) Multi-domain misfolding: understanding the aggregation pathway of polyglutamine proteins. *Protein Eng. Des. Sel.* 22:447-451.

Scharf A., Rockel T.D., von Mikecz A. (2007) Localization of proteasomes and proteasomal proteolysis in the mammalian interphase cell nucleus by systematic application of immunocytochemistry. *Histochem. Cell Biol.* 127:591-601.

Scheel H., Tomiuk S., Hofmann K. (2003) Elucidation of ataxin-3 and ataxin-7 function by integrative bioinformatics. *Hum. Mol. Genet.* 12:2845–2852.

Schilling G., Wood J.D., Duan K., Slunt H.H., Gonzales V., Yamada M., Cooper J.K., Margolis R.L., Jenkins N.A., Copeland N.G., Takahashi H., Tsuji S., Price D.L., Borchelt D.R., Ross C.A. (1999) Nuclear accumulation of truncated atrophin-1 fragments in a transgenic mouse model of DRPLA. *Neuron* 24:275-286.

Schmidt B.J., Greenberg C.R., Allingham-Hawkins D.J., Spriggs E.L. (2002) Expression of X-linked bulbospinal muscular atrophy (Kennedy disease) in two homozygous women. *Neurology.* 59:770-772.

Schmidt M., Hanna J., Elsasser S., Finley D. (2005) Proteasome-associated proteins: regulation of a proteolytic machine. *Biol. Chem.* 386:725–737.

Schmidt T., Landwehrmeyer G.B., Schmitt I., Trottier Y., Auburger G., Laccone F., Klockgether T., Volpel M., Epplen J.T., Schols L., Riess O. (1998) An isoform of ataxin-3 accumulates in the nucleus of neuronal cells in affected brain regions of SCA3 patients. *Brain Pathol.* 8:669–679.

Schmidt T., Lindenberg K.S., Krebs A., Schöls L., Laccone F., Herms J., Rechsteiner M., Riess O., Landwehrmeyer G.B. (2002) Protein surveillance machinery in brains with spinocerebellar ataxia type 3: redistribution and differential recruitment of 26S proteasome subunits and chaperons to neuronal intranuclear inclusions. *Ann. Neurol.* 51:302-310.

Schmitt I., Evert B.O., Khazneh H., Klockgether T., Wüellner U. (2003) The human MJD gene: genomic structure and functional characterization of the promoter region. *Gene* 314:81-88.

Schmitt I., Linden M., Khazneh H., Evert B.O., Breuer P., Klockgether T., Wuellner U. (2007) Inactivation of the mouse Atxn3 (ataxin-3) gene increases protein ubiquitination. *Biochem. Biophys. Res. Commun.* 362:734–739.

Schöls L., Bauer P., Schmidt T., Schulte T., Riess O. (2004) Autosomal dominant cerebellar ataxias: clinical features, genetics, and pathogenesis. *Lancet Neurol* 3: 291–304.

Schöls L., Haan J., Riess O., Amoiridis G., Przuntek H. (1998) Sleep disturbance in spinocerebellar ataxias: Is the SCA3 mutation a cause of restless legs syndrome? *Neurology* 51:1603–7.

Schöls L., Vieira-Saecker A.M., Schöls S., Przuntek H., Epplen J.T., Riess O. (1995) Trinucleotide expansion within the MJD1 gene presents clinically as spinocerebellar ataxia and occurs most frequently in German SCA patients. *Hum. Mol. Genet.* 4:1001–1005.

Schulte T., Mattern R., Berger K., Szymanski S., Klotz P., Kraus P.H., Przuntek H., Schols L. (2001) Double-blind crossover trial of trimethoprim-sulfamethoxazole in spinocerebellar ataxia type 3/Machado-Joseph disease. *Arch. Neurol.* 58:1451-1457.

Schulz J.B., Borkert J., Wolf S., Schmitz-Hübsch T., Rakowicz M., Mariotti C., Schöls L., Timmann D., van de Warrenburg B., Dürr A., Pandolfo M., Kang J.S., Mandly A.G., Nägele T., Grisoli M., Boguslawska R., Bauer P., Klockgether T., Hauser T.K. (2010) Visualization, quantifi cation and correlation of brain atrophy with clinical symptoms in spinocerebellar ataxia types 1, 3 and 6. *Neuroimage* 49: 158–168.

Seidel K., den Dunnen W.F., Schultz C., Paulson H., Frank S., de Vos R.A., Brunt E.R., Deller T., Kampinga H.H., Rub U. (2010) Axonal inclusions in spinocerebellar ataxia type 3. *Acta Neuropathol.* 120:449–460.

Seidel K., Siswanto S., Brunt E.R., den Dunnen W., Korf H.W., Rub U. (2012) Brain pathology of spinocerebellar ataxias. *Acta Neuropathol.* 124:1-21.

Seilhean D., Takahashi J., El Hachimi K.H., Fujigasaki H., Lebre A.S., Biancalana V., Dürr A., Salachas F., Hogenhuis J., de Thé H., Hauw J.J., Meininger V., Brice A., Duyckaerts C. (2004) Amyotrophic lateral sclerosis with neuronal intranuclear protein inclusions. *Acta Neuropathol.* 108:81-87.

Shams'ili S., Grefkens J., de Leeuw B., van den Bent M., Hooijkaas H., van der Holt B., Vecht C., Sillevis Smitt P. (2003) Paraneoplastic cerebellar degeneration associated with antinueronal antibodies: analysis of 50 patients. *Brain* 126:1409-1418.

Shanmugham A., Ovaa H. (2008) DUBs and disease: activity assays for inhibitor development. *Curr. Opin. Drug Discov. Devel.* 11:688–696.

Shieh S.Y. and Bonini N.M. (2011) Genes and pathways affected by CAG-repeat RNA-based toxicity in Drosophila. *Hum. Mol. Genet.* 20:4810:4821.

Shirasaki H., Ishida C., Nakajima T., Kamei H., Koide T., Fukuhara N. (2003) A quantitative evaluation of spinocerebellar degeneration by an acoustic analysis–the effect of taltirelin hydrate on patients with Machado- Joseph disease. *Rinsho Shinkeigaku* 43:143-148.

Sickles D.W., Brady S.T., Testino A., Friedman M.A., Wrenn R.W. (1996) Direct effect of the neurotoxicant acrylamide on kinesin-based microtubule motility. *J. Neurosci. Res.* 46:7-17.

Sieradzan K.A., Mechan A.O.,Jones L., Wanker E.E.; Nukina N., Mann D.M. (1999) Huntington's disease intranuclear inclusions contain truncated, ubiquitinated huntingtin protein. *Exp. Neurol.* 156:92-99.

Silva-Fernandes A., Costa M. do C., Duarte-Silva S., Oliveira P., Botelho C.M., Martins L., Mariz J.A., Ferreira T., Ribeiro F., Correia-Neves M., Costa C., Maciel P. (2010) Motor uncoordination and neuropathology in a transgenic mouse model of Machado–Joseph disease lacking intranuclear inclusions and ataxin-3 cleavage products. *Neurobiol. Dis.*

40:163–176.

Slow E.J., Graham R.K., Osmand A.P., Devon R.S., Lu G., Deng Y., Pearson J., Vaid K., Bissada N., Wetzel R., Leavitt B.R., Hayden M.R. (2005) Absence of behavioral abnormalities and neurodegeneration *in vivo* despite widespread neuronal huntingtin inclusions. *Proc. Natl. Acad. Sci. USA* 102:11402-11407.

Sobue G., Doyu M., Nakao N., Shimada N., Mitsuma T., Maruyama H., Kawakami S., Nakamura S. (1996) Homozygosity for Machado-Joseph disease gene enhances phenotypic severity. *J. Neurol. Neurosurg. Psychiatry* 60:354-356.

Solans A., Zambrano A., Rodríguez M., Barrientos A. (2006) Cytotoxicity of a mutant huntingtin fragment in yeast involves early alterations in mitochondrial OXPOS complexes II and III. *Hum. Mol. Gen.* 15:3063-3081.

Song A.X., Zhou C.J., Peng Y., Gao X.C., Zhou Z.R., Fu Q.S., Hong J., Lin D.H., Hu H.Y. (2010) Structural transformation of the tandem ubiquitin-interacting motifs in ataxin-3 and their cooperative interactions with ubiquitin chains. *PLoS One* 5:e13202.

Song L., Rape M. (2008) Reverse the curse--the role of deubiquitination in cell cycle control. *Curr. Opin. Cell Biol.* 20:156–163.

Song W., Chen J., Petrilli A., Liot G., Klinglmayr E., Zhou Y., Poquiz P., Tjong J., Pouladi M.A., Hayden M.R., Masliah E., Ellisman M., Rouiller I., Schwarzenbacher R., Bossy B., Perkins G., Bossy-Wetzel E. (2011) Mutant huntingtin binds the mitochondrial fission GTPase dynamin-related protein-1 and increases its enzymatic activity. *Nat. Med.* 17:377-382.

Soong B.W., Liu R.S. (1998) Positron emission tomography in asymptomatic gene carriers of Machado-Joseph disease. *J. Neurol. Neurosurg. Psychiatry* 64:499–504.

Steffan J. S., Agrawal N., Pallos J., Rockabrand E., Trotman L.C., Slepko N., Illes K., Lukacsovich T., Zhu Y.Z., Cattaneo E., Pandolfi P.P., Thompson L.M., Marsh J.L. (2004) SUMO modification of Huntingtin and Huntington's disease pathology. *Science* 304:100-104.

Stenoien D.L., Cummings C.J., Adams H.P., Mancini M.G., Patel K., DeMartino G.N., Marcelli M., Weigel N.L., Mancini M.A. (1999) Polyglutamine-expanded androge receptors form aggregates that sequester heat shock proteins,proteasome components and SRC-1, and are supressed by the HJD-2 chaperone. *Hum. Mol. Genet.* 8:731-741.

Stenoien D.L., Mielke M., Mancini M.A. (2002) Intranuclear ataxin-1 inclusions contain both fast- and slow-exchanging components. *Nat. Cell Biol.* 4:806-810.

Stevanin G., Cassa E., Cancel G., Abbas N., Dürr A., Jardim E., Agid Y., Sousa P.S., Brice A. (1995a) Characterisation of the unstable expanded CAG repeat in the MJD1 gene in four Brazilian families of Portuguese descent with Machado-Joseph disease. *J. Med. Genet.* 32:827-830.

Stevanin G., Cancel G., Didierjean O., Dürr A., Abbas N., Cassa E., Feingold J., Agid Y., Brice A. (1995b) Linkage disequilibrium at the Machado-Joseph disease/spinal cerebellar ataxia 3 locus: evidence for a common founder effect in French and Portuguese-Brazilian families as

well as a second ancestral Portuguese-Azorean mutation. *Am. J. Hum. Genet.* 57:1247-1250.

St-Germain J.R., Chen J., Li Q. (2008) Involvement of PML nuclear bodies in CBP degradation through the ubiquitin-proteasome pathway. *Epigenetics* 3:342-349.

St-Pierre J., Drori S., Uldry M., Silvaggi J.M., Rhee J., Jäger S., Handschin C., Zheng K., Lin J., Yang W., Simon D.K., Bachoo R., Spiegelman B.M. (2006) Suppression of reactive oxygen species and neurodegeneration by the PGC-1 transcriptional coactivators. *Cell* 127:397-408.

Stevanin G., Durr A., Brice A. (2000) Clinical and molecular advances in autosomal dominant cerebellar ataxias: from genotype to phenotype and physiopathology. *Eur J Hum Genet* 8: 4–18.

Strachan T., Read A.P. (2004) Human Molecular Genetics 3, Third edition. Garland Press.

Sugiura A., Yonashiro R., Fukuda T., Matsushita N., Nagashima S., Inatome R., Yanagi S. (2010) A mitochondrial ubiquitin ligase MITOL controls cell toxicity of polyglutamine-expanded protein. *Mitochondrion* 11:139–146.

Suite N.D., Sequeiros J., McKhann G.M. (1986) Machado-Joseph disease in a Sicilian-American family. *J. Neurogenet.* 3:177-182.

Sun J., Xu H., Negi S., Subramony S.H., Hebert M.D. (2007) Differential effects of polyglutamine proteins on nuclear organization and artificial reporter splicing. *J. Neurosci. Res.* 83:2306-2317.

Sun X.M., Butterworth M., MacFarlane M., Dubiel W., Ciechanover A., Cohen G.M. (2004) Caspase activation inhibits proteasome function during apoptosis. *Mol. Cell.* 14:81-93.

Szebenyi G., Morfini G.A., Babcock A., Gould M., Selkoe K., Stenoien .L., Young M., Faber P.W., MacDonald M.E., McPhaul M.J., Brady S.T. (2003) Neuropathogenic forms of huntingtin and androgen receptor inhibit fast axonal transport. *Neuron* 40:41-52.

Tait D., Riccio M., Sittler A., Scerzinger E., Santi S., Ognibene A., Maraldi N.M., Lehrach H., Wanker E.E. (1998) Ataxin-3 is transported into the nucleus and associates with the nuclear matrix. *Hum. Mol. Genet.* 7:991-997.

Takahashi J., Tanaka J., Arai K., Funata N., Hattori T., Fukuda T., Fujigasaki H., Uchihara T. (2001) Recruitment of nonexpanded polyglutamine proteins to intranuclear aggregates in neuronal intranuclear hyaline inclusion disease. *J. Neuropathol. Exp. Neurol.* 60:369–376.

Takei A., Fukazawa T., Hamada T., Sohma H., Yabe I., Sasaki H., Tashiro K. (2004) Effects of tandospirone on **"**5-HT1A receptor-associated symptoms**"** in patients with Machado-Josephe disease: an open-label study. *Clin. Neuropharmacol.* 27:9-13.

Takiyama Y., Igarashi S., Rogaeva E.A., Endo K., Rogaev E.I., Tanaka H., Sherrington R., Sanpei K., Liang Y., Saito M., *et al.* (1995) Evidence for intergenerational instability in the CAG repeat in the MJD1 gene and for conserved haplotypes at flanking markers amongst Japanese and Caucasian subjects with Machado-Joseph disease. *Hum. Mol. Genet.* 4:1137-1146.

Takiyama Y., Nishizawa M., Tanaka H., Kawashima S., Sakamoto H., Karube Y., Shimazaki H., Soutome M., Endo K., Ohta S., *et al.* (1993) The gene for Machado-Joseph disease maps to human chromosome 14q. *Nat. Genet.* 4:300-304.

Tanaka M., Morishima I., Akagi T., Hashikawa T., Nukina N. (2001) Intra- and intermolecular beta-pleated sheet formation in glutamine-repeat inserted myoglobin as a model for polyglutamine diseases. *J. Biol. Chem.* 276:45470-45424.

Tang T.S., Tu H., Chan E. Y., Maximov A., Wang Z., Wellington C. L., Hayden M. R., Bexprozvanny I. (2003) Huntingtin and huntingtin-associated protein 1 influence neuronal calcium signaling mediated by inositol-(1,4,5) triphosphate receptor type 1. *Neuron* 39:227-239.

Taniwaki T., Sakai T., Kobayashi T., Kuwabara Y., Otsuka M., Ichiya Y., Masuda K., Goto I. (1997) Positron emission tomography (PET) in Machado-Joseph disease. *J. Neurol. Sci.* 145:63–67.

Tao R.S., Fei E.K., Ying Z., Wang H.F., Wang G.H. (2008) Casein kinase 2 interacts with and phosporylates ataxin-3. *Neurosci. Bull.* 24:271-7.

Taroni F., DiDonato S. (2004) Pathways to motor incoordination: the inherited ataxias. *Nat Rev Neurosci* 5:641–655.

Teixeira-Castro A., Ailion M., Jalles A., Brignull H.R., Vilaça J.L., Dias N., Rodrigues P., Oliveira J.F., Neces-Carvalho A., Morimoto R.I., Maciel P. (2011) Neuron-specific proteotoxicity of mutant ataxin-3 in *C.* elegans: rescue by the DAF-16 and HSF-1 pathways. *Hum. Mol. Genet.* 20:2996-3009.

Terashima T., Kawai H., Fujitani M., Maeda K., Yasuda H. (2002) SUMO-1 co-localized with mutant atrophin-1 with expnaded polyglutamines accelerates intranuclear aggregation and cell death. *Neuroreport* 13:2359-2364.

Thakur A. K., Jayaraman M., Mishra R., Thakur M., Chellgren V.M., Byeon I.J., Anjum D.H., Kodali R., Creamer T.P., Conway J.F., Gronenborn A.M., Wetzel R. (2009) Polyglutamine disruption of the huntingtin exon 1N terminus triggers a complex aggregation mechanism. *Nat. Struct. Mol. Biol.* 16:380-389.

Todd P.K., Paulson H.L. (2010) RNA-mediated neurodegeneration in repeat expansion disorders. *Ann Neurol* 67: 291–300.

Todi S.V., Laco M.N., Winborn B.L., Travis S.M., Wem H.M., Paulson H.L. (2007) Cellular turnover of the polyglutamine disease protein ataxin-3 is regulated by its catalytic activity. *J. Biol. Chem.* 282:29348-29358.

Todi S.V., Scaglione K.M., Blount J.R., Basrur V., Conlon K.P., Pastore A., Elenitoba-Johnson K., Paulson H.L. (2010) Activity and cellular functions of the deubiquitinating enzyme and polyglutamine disease protein ataxin-3 are regulated by ubiquitination at lysine 117. *J. Biol. Chem.* 285:39303-39313.

Todi S.V., Winborn B.J., Scaglione K.M., Blount J.R., Travis S.M., Paulson H.L. (2009)

Ubiquitination directly enhances activity of the deubiquitinating enzyme ataxin-3. *EMBO J.* 28:372–382.

Trettel F., Rigamonti D., Hilditch-Maguire P., Wheeler V.C., Sharp A.H., Persichetti F., Cattaneo E., MacDonald M.E. (2000) Dominant phenotypes produced by the HD mutation in STDdh(Q111) striatal cells. *Hum. Mol. Genet.* 9:2799-2809.

Trottier Y., Cancel G., An-Gourfinkel I., Lutz Y., Weber C., Brice A., Hirsch E., Mandel J.L. (1998) Heterogenous intracellular localization and expression of ataxin-3. *Neurobiol. Dis.* 5:335-347.

Trushina E., Singh R.D., Dyer R.B., Cao S., Shah V.H., Parton R.G., Pagano R.E., McMurray C.T. (2004) Mutant huntingtin impairs axonal trafficking in mammalian neurons in vivo and *in vitro*. *Mol. Cell Biol.* 24:8195-8209.

Tsai H. F., Tsai H. J., Hsieh M. (2004) Full-length expanded ataxin-3 enhances mitochondrial-mediated cell death and decreases Bcl-2 expression in human neuroblastoma cells. *Biochem. Biophys. Res. Commun.* 324:1274-1282.

Tsuji S. (1997) Molecular genetics of triplet repeats: unstable expansion of triplet repeats as a new mechanism for neurodegenerative diseases. *Intern. Med.* 36:3-8.

Tuite P.J., Rogaeva E.A., George-Hyslop P.H., Lang A.E. (1995) Dopa-responsive parkinsonism phenotype of Machado-Joseph disease: Confirmation of 14q CAG expansion. *Ann. Neurol.* 38:684–7.

Tzvetkov N., Breuer P. (2007) Josephin domain-containing proteins from a variety of species are active de-ubiquitination enzymes. *Biol. Chem.* 388:973–978.

Ueda H., Goto J., Hashida H., Lin X., Oyanagi K., Kawano H., Zoghbi H. Y., Kanazawa I., Okazawa H. (2002) Ehnanced SUMOylation in polyglutamine diseases. *Biochem. Biophys. Res. Commun.* 293:307-313.

Uchihara T., Fujigasaki H., Koyano S., Nakamura A., Yagishita S., Iwabuchi K. (2001) Non-expanded polyglutamine proteins in intranuclear inclusions of hereditary ataxias–triple-labeling immunofluorescence study. *Acta Neuropathol. (Berl.)* 102:149–152.

Uchihara T., Iwabuchi K., Funata N., Yagishita S. (2002) Attenuated nuclear shrinkage in neurons with nuclear aggregates - a morphometric study on pontine neurons of Machado-Joseph disease brains. *Exp. Neurol.* 178:124-128.

Uversky, V.N. (2010) Mysterious oligomerization of the amyloidogenic proteins. *FEBS J.* 277:2940–2953.

van Alfen N., Sinke R.J., Zwarts M.J., Gabreels-Festen A., Praamstra P., Kremer B.P., Horstink M.W. (2001) Intermediate CAG repeat lengths (53,54) for MJD/SCA3 are associated with an abnormal phenotype. *Ann. Neurol.* 49:805-807.

Varadan R., Assfalg M., Raasi S., Pickart C., Fushman D. (2005) Structural determinants for selective recognition of a Lys48-linked polyubiquitin chain by a UBA domain. *Mol. Cell* 18:687-698.

Venkatraman P., Wetzel R., Tanaka M., Nukina N., Goldberg A.L. (2004) Eukaryotic proteasomes cannot digest polyglutamine sequences and release them during degradation of polyglutamine-containing proteins. *Mol. Cell* 14:95-104.

Ventii K.H., Wilkinson K.D. (2008) Protein partners of deubiquitinating enzymes. *Biochem. J.* 414:161–175.

Verkerk A.J., Pieretti M., Sutcliffe J.S., Fu Y.H., Kuhl D.P., Pizzuti A., Reiner O., Richards S., Victoria M.F., Zhang F.P., *et al.* (1991) Identification of a gene (FMR-1) containing a CGG repeat coincident with a breakpoint cluster region exhibiting length variation in fragile X syndrome. *Cell* 65:905-914.

Wang, G., Sawai, N., Kotliarova, S., Kanazawa, I., Nukina, N. (2000) Ataxin-3, the MJD1 gene product, interacts with the two human homologs of yeast DNA repair protein RAD23, HHR23A and HHR23B. *Hum. Mol. Genet.* 9:1795–1803.

Wang G. H., Mitsui K., Kotliarova S., Yamashita A., Nagao Y., Tokuhiro S., Iwatsubo T., Kanazawa I., Nukina N. (1999) Caspase activation during apoptotic cell death induced by expanded polyglutamine in N2a cells. *Neuroreport* 10:2435-2438.

Wang H., Lim P.J., Karbowski M., Monteiro M.J. (2009) Effects of overexpression of huntingtin proteins in mitochondrial integrity. *Hum. Mol. Genet.* 18:737-752.

Wang H. L., Yeh T. H., Chou A. H., Kuo Y. L., Luo L. J., He C. Y., Huang P. C., Li A. H. (2006a) Polyglutamine-expanded ataxin-7 activates mitochondrial apoptotic athway of cerebellar neurons by upregulating Bax and downregulating Bcl-x(L). *Cell. Signal.* 18:541-552.

Wang Q., Li L., Ye Y. (2006b) Regulation of retrotranslocation by p97-associated deubiquitinating enzyme ataxin-3. *J. Cell Biol.* 174:963–971.

Wang Q., Li L., Ye Y. (2008) Inhibition of p97-dependent protein degradation by Eeyarestatin I. *J. Biol. Chem.* 283:7445-7454.

Wang Q., Song C., Li C.C. (2004) Molecular perspectives on p97-VCP: progress in understanding its structure and diverse biological functions. *J. Struct. Biol.* 146:44–57.

Warby S.C., Doty C.N., Graham R.K., Carroll J.B., Yang Y.Z., Singaraja R.R., Overall C.M., Hayden M.R. (2008) Activated caspase-6 and caspase-6-cleaved fragments of huntingtin specifically colocalize in the nucleus. *Hum. Mol. Genet.* 17:2390-2404.

Warby S. C., Doty C. N., Graham R. K., Shively J., Singaraja R. R., Hayden M. R. (2009) Phosphorylation of huntingtin reduces the accumulation of its nuclear fragments. *Mol. Cell. Neurosci.* 40:121-127.

Warrick J.M., Paulson H.L., Gray-Board G.L., Bui Q.T., Fischbeck K.H., Pittman R.N., Bonini N.M. (1998) Expanded polyglutamine protein forms nuclear inclusions and causes neural degeneration in *Drosophila*. *Cell* 93:939-949.

Warrick J.M., Chan H.Y., Gray-Board G.L., Chai Y., Paulson H.L., Bonini N.M. (1999)

Suppression of polyglutamine-mediated neurodegeneration in *Drosophila* by the molecular chaperone HSP70. *Nat. Genet.* 23:425–428.

Warrick J.M., Morabito L.M., Bilen J., Gordesky-Gold B., Faust L.Z., Paulson H.L., Bonini N.M. (2005) Ataxin-3 suppresses polyglutamine neurodegeneration in *Drosophila* by a ubiquitin-associated mechanism. *Mol. Cell* 18:37–48.

Wharton D.C., Tzagotoff A. (1967) Cytochrome oxidase from beef heart mitochondria. *Methods Enzymol.* 10:245–250.

Weissman A.M. (2001) Themes and variations on ubiquitylation. *Nat. Rev. Mol. Cell Biol.* 2:169–178.

Welchman R.L., Gordon C., Mayer R.J. (2005) Ubiquitin and ubiquitin-like proteins as multifunctional signals. *Nat. Rev. Mol. Cell Biol.* 6:599-609.

Wellington C.L., Ellerby L.M., Hackam A.S., Margolis R.L., Trifiro M.A., Singaraja R., McCutcheon K., Salvesen G.S., Propp S.S., Bromm M., Rowland K.J., Zhang T., Rasper D., Roy S., Thornberry N., Pinsky L., Kakizuka A., Ross C.A., Nicholson D.W., Bredesen D.E., Hayden M.R. (1998) Caspase cleavage of gene products associated with triplet expansion disorders generates truncated fragments containing the polyglutamine tract. *J. Biol. Chem.* 273:9158-9167.

Wen F.C., Li Y.H., Tsai H.F., Lin C.H., Li C., Liu C.S., Lii C.K., Nukina N., Hsieh M. (2003) Down-regulation of heat shock protein 27 in neuronal cells and non-neuronal cells expressing mutant ataxin-3. *FEBS Lett.* 546:301-314.

Weydt P., Pineda V.V., Torrence A.E., Libby R.T., Satterfield T.F., Lazarowski E.R., Gilbert M.L., Morton G.J., Bammler T.K., Strand A.D., Cui L., Beyer R.P., Easley C.N., Smith A.C., Krainc D., Luquet S., Sweet I.R., Schwartz M.W., La Spada A.R. (2006) Thermoregulatory and metabolic defects in Huntington's disease transgenic mice implicate PGC-1alpha in Huntington's disease neurodegeneration. *Cell Metab.* 4:349-362.

Wiborg O., Pedersen M.S., Wind A., Berglund L.E., Marcker K.A., Vuust J. (1985) The human ubiquitin multigene family: some genes contain multiple directly repeated ubiquitin coding sequences. *EMBO J.* 4:755–759.

Wilkinson K.D. (1997) Regulation of ubiquitin-dependent processes by deubiquitinating enzymes. *FASEB J.* 11:1245–1256.

Wilkinson K.D., Tashayev V.L., O'Connor L.B., Larsen C.N., Kasperek E., Pickart C.M. (1995) Metabolism of the polyubiquitin degradation signal: structure, mechanism, and role of isopeptidase *T. Biochemistry* 34:14535–14546.

Williams A.J., Paulson H.L. (2008) Polyglutamine neurodegeneration: protein misfolding revisited. *Trends Neurosci.* 31:521-528.

Winborn B.J., Travis S.M., Todi S.V., Scaglione K.M., Xu P., Williams A.J., Cohen R.E., Peng J., Paulson H.L. (2008) The deubiquitinating enzyme ataxin-3, a polyglutamine disease protein, edits Lys63 linkages in mixed linkage ubiquitin chains. *J. Biol. Chem.* 283:26436–26443.

Wojcik C., DeMartino G.N. (2003) Intracellular localization of proteasomes. *Int. J. Biochem. Cell. Biol.* 35:579-589.

Wong E., Cuervo A.M. (2010a) Autophagy gone awry in neurodegenerative diseases. *Nat. Neurosci.* 13:805-811.

Wong E., Cuervo A.M. (2010b) Integration of clearence mechanisms: the proteasome and autophagy. *Cold Spring Harb. Perspect. Biol.* 2:a006734.

Wong S.L., Chan W.M., Chan H.Y. (2008) Sodium dodecyl sulfate-insoluble oligomers are involved in polyglutamine degeneration. *FASEB J.* 22:3348-3357.

Woods B.T., Schaumburg H.H. (1972) Nigro-spino-dentatal degeneration with nuclear ophthalmoplegia. A unique and partially treatable clinicopathological entity. J. Neurol. Sci. 17:149-166.

Wyttenbach A., Carmichael J., Swartz J., Furlong R.A., Narain Y., Rankin J., Rubinsztein D.C. (2000) Effects of heat shock, heat shock protein 40 (HDJ-2), and proteasome inhibition on protein aggregation in cellular models of Huntington's disease. *Proc. Natl. Acad. Sci. USA* 97:2898-2903.

Wyttenbach A., Swartz J., Kita H., Thykjaer T., Carmichael J., Bradley J., Brown R., Maxwell M., Schapira A., Orntoft T.F., Kato K., Rubinsztein D.C. (2001) Polyglutamine expansions cause decreased CRE-mediated transcription and early gene expression changes prior to cell death in an inducible cell model of Huntington's disease. *Hum. Mol. Genet.* 10:1829-1845.

Xia H., Mao Q., Eliason S.L., Harper S.Q., Martins I.H., Orr H.T., Paulson H.L., Yang L., Kotin R.M., Davidson B.L. (2004) RNAi suppresses polyglutamine-induced neurodegeneration in a model of spinocerebellar ataxia. *Nat. Med.* 10:816-820.

Xu P., Duong D.M., Seyfried N.T., Cheng D., Xie Y., Robert J., Rush J., Hochstrasser M., Finley D., Peng J. (2009) Quantitative proteomics revelas the function of unconventional ubiquitin chains in proteasomal degradation. *Cell* 137:133-145.

Yamada, M., Hayashi, S., Tsuji, S., Takahashi, H. (2001) Involvement of the cerebral cortex and autonomic ganglia in Machado–Joseph disease. *Acta Neuropathol.* 101:140–144.

Yeh T.H., Lu C.S., Chou Y.H., Chong C.C., Wu T., Han N.H., Chen R.S. (2005) Autonomic dysfunction in Machado-Joseph disease. *Arch. Neurol.* 62:630–636.

Ying Z., Wang H., Fan H., Zhu X., Zhou J., Fei E., Wang G. (2009) Gp78, an ER associated E3, promotes SOD1 and ataxin-3 degradation. *Hum. Mol. Genet.* 18:4268–4281.

Yamamoto A., Lucas J.J., Hen R. (2000) Reversal of neuropathology and motor dysfunction in a conditional model of Huntington's disease. *Cell* 101:57-66.

Yao T., Song L., Xu W., DeMartino G.N., Florens L., Swanson S.K., Washburn M.P., Conaway R.C., Conaway J.W., Cohen R.E. (2006) Proteasome recruitment and activation of the Ucn37 deubiquitinating enzyme by Adrm1. *Nat. Cell Biol.* 8:994-1002.

Ye Y., Meyer H.H., Rapoport T.A. (2001) The AAA ATPase Cdc48/p97 and its partners transport proteins from the ER into the cytosol. *Nature.* 414:652-656.

Yoshizawa T., Yoshida H., Shoji S. (2001) Differential susceptibility of cultured cell lines to aggregate formation and cell death produced by the truncated Machado-Joseph disease gene product with an expanded polyglutamine stretch. *Brain Res. Bull.* 56:346-352.

Yvert G., Lindenberg K.S., Picaud S., Landwehrmeyer G.B., Sahel J.A., Mandel J.L. (2000) Expanded polyglutamines induce neurodegeneration and trans-neuronal alterations in cerebellum and retina of SCA7 transgenic mice. *Hum. Mol. Genet.* 9:2491-2506.

Yu Y.C., Kuo C.L., Cheng W.L., Liu C.S., Hsieh M. (2009) Decreased antioxidant enzyme activity an increased mitochondrial DNA damage in cellular models of Machado-Joseph disease. *J. Neurosci. Res.* 87:1884-1891.

Zander C., Takahashi J., El Hachimi K.H., Fujigasaki H., Albanese V., Lebre A.S., Stevanin G., Duyckaerts C., Brice A. (2001) Similarities between spinocerebellar ataxia type 7 (SCA7) cell models and human brain: proteins recruited in inclusions and activation of caspase-3. *Hum. Mol. Genet.* 10:2569-2579.

Zoghbi H.Y., Orr, H.T. (2000) Glutamine repeats and neurodegeneration. *Annu. Rev. Neurosci.* 23:217-247.

Zhang L., Ashendel C.L., Becker G.W., Morré D.J. (1994) Isolation and characterization of the principal ATPase associated with transitional endoplasmic reticulum of rat liver. *J. Cell Biol.* 127:1871-1883.

Zhong X., Pittman R.N. (2006) Ataxin-3 binds VCP/p97 and regulates retrotranslocation of ERAD substrates. *Hum. Mol. Genet.* 15:2409–2420.